Population dynamics of microbiota bacteria lead morphogenetic variations, phenotypic pathogenesis shifts and antimicrobial resistance expression

by

Elisa Pierella

A thesis submitted in partial fulfilment for the requirements for the degree of Doctor of Philosophy at the University of Central Lancashire

May 2023

Student Declaration

Type of Award PhD

School Medicine

1. Concurrent registration for two or more academic awards

I declare that while registered as a candidate for the research degree, I have not been a registered candidate or enrolled student for another award of the University or other academic or professional institution

2. Material submitted for another award

I declare that no material contained in the thesis has been used in any other submission for an academic award and is solely my own work

3. Collaboration

The research programme per se was not part of a collaborative project. However, an *in silico* experimental section of the project consisting on the development of a mathematical model applied to microbiological system has been conducted by Jaroslav Čepl (University of Live Sciences, Prague, Czech Republic), Vladimir Scholtz (University of Chemistry and Technology, Prague, Czech Republic) and Jirina Scholtzova (Czech Technical University, Prague, Czech Republic). Elisa Pierella (myself) have conducted all the *in vitro* experiments required for the model to be developed and attended a dedicated workshop on programming language organized by Jaroslav Čepl.

4. Use of a Proof-reader

No proof-reading service was used in the compilation of this thesis.

Signature of Candidate	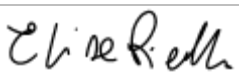

Print name: Elisa Pierella

Abstract

The wide and essential role of the gut microbiota includes fending off pathogens, enabling nutrient generation, metabolism and absorption, participating in the development of immune and nervous system and more. Although correlational research has given us an insight on the microbiota composition, a mechanistic understanding of microbial population coordination and dynamics and its impact on the host health remains a key challenge. For example, the process that leads commensal microbiota players to become pathogens, and the factors that limit the establishment of incoming healthy bacteria (probiotics) have not been fully elucidated. Likewise, the critical involvement of micronutrients on microbial selection is at its infancy.

The primary aim of this PhD Thesis was to investigate the differential prevalence of a subset of bacterial species commonly encountered in the gut as commensal or as pathogens to better understand bacterial population dynamics and competition. Specifically, we aimed to elucidate bacterial population dynamics in response to an underrated but emerging potential pathogen, *Serratia marcescens*, and external factors such as the micronutrient zinc.

To study such a complex ecosystem, we used a bottom-up approach of *in vitro* co-culture competition experiments with pairs of bacterial species (*Escherichia coli*, *Serratia marcescens*, *Pseudomonas aeruginosa, Proteus vulgaris*, *Klebsiella aerogenes*, *Staphylococcus aureus*, *Enterococcus faecalis*, *Lactobacillus plantarum* and *Streptococcus salivarius*). A rich microbiological media was used as a surrogate for the postprandial intestine.

While no difference in prevalence was observed in pairwise competitions between strains of *E. coli* and *S. marcescens*, we have identified a novel phenomenon where *S. marcescens* in co-culture with *E. coli* exhibited a differential spatial geometric distribution on solid media with the appearance of a “bull’s eye” pattern. The pattern only and consistently appeared in well-defined conditions (cell density, temperature, nutrients). This morphogenetic pattern was accompanied by phenotypic changes that affected virulence and antimicrobial resistance, a novel and cutting-edge finding that may help to design effective intervention tools to treat infectious diseases and tackle antibiotic resistance. The phenomenon was mathematically modelled, and the outcome suggested the need to increase model complexity thus informing biological research going forward. We also observed that *P. aeruginosa* prevailed over some Gram-positive cocci (*S. aureus* and *S. streptococcus*) and *S. marcescens,* and that *Lactobacillus plantarum* inhibited the growth of selected Gram-negatives.

Our results established proof of concept regarding bacterial behaviours and morphogenetic variations that can be harnessed to explore genome-wide changes and related virulence and pathogenesis mechanisms, and may enrich the microbiota-linked prevention and infections management.

Table of contents

Acknowledgements

I would like to express my gratitude to my supervisors Dr Jorge Garcia-Lara, Dr Katja Vogt and Professor Nicola Lowe for assessing my progress constantly and for providing outstanding feedbacks and steady support during the course of these years.

I want to thank our collaborators in Prague universities, Jaroslav, Jirina and Vladimir, for contributing to the development of part of my PhD project and for being extremely welcoming during my visit in Prague.

A special thanks to Matthew Allott, an exceptional peer on the bench, friend at the pub and chef at home since the first day I have landed in Preston.

Also, it has been amazing to work with all the students, undergrads, postgrads, medical and Erasmus ones, who have joined, even if fort short periods, the *HoMe-SuRE* research group led by Dr Jorge Garcia-Lara and Dr Katja Vogt.

Thank you to all the staff of the School of Medicine and the Biomedical Research Facility who have enabled the success of my research programme.

It has been a privilege being awarded by the Marie Skłodowska-Curie/DTA3 fellowship, and I am extremely grateful to all the PhD students from all over the world that I have met. Particularly, I must thank you Marta, Cristina, Spyros, Udit, Maria and Tanya who have been one of the reasons why I have never given up.

Thank you of course to my parents, sister, boyfriend and friends of life, who have been supporting me and celebrating my achievements despite the distance, made even more difficult by a global pandemic.

Finally, thank you to the members of my acquired family in Preston, Swarnim and Ranbir, and the Larder family, particularly Bill, a life mentor for me.

List of tables

List of figures

List of abbreviations

°C	degrees Celsius
µ	growth rate
µg	microgram
µl	microliter
µm	micrometre
µM	micromolar
16s rRNA	16S ribosomal RNA
AA/AAs	amino acid/amino acids
AHL	N-Acyl homoserine lactones
AI	autoinducer
AMR	antimicrobial resistance
approx.	approximately
Asn	asparagine
Arg	arginine
B. subtilis	*Bacillus subtilis*
BHI	Brain Heart Infusion
BHIA	Brain Heart Infusion Agar
BMRF	Biomedical Research Facilities
bp	base pairs
CDI	contact-dependent growth inhibition
CFU	colony forming unit
CLED	Cystine–lactose–electrolyte-deficient agar
CF	cystic fibrosis
CM	Conditioned medium
cm	centimetre
cm^2	square centimetre
CV	Crystal violet
Cys	Cysteine
DMEM	Eagle Medium
dNTPs	Deoxyribonucleotide
E. coli	*Escherichia coli*
E. faecalis	*Enterococcus faecalis*
EBA	Esculin Bile agar
EP	Elisa Pierella
EPS	Extracellular polymeric substances
EU	European Union EU
F	forward
FBS	foetal bovine serum

g	gram
GI tract	Gastrointestinal tract
H_2O	Water
H_2O_2	Hydrogen peroxide
HCl	Hydrochloric acid
Ile	Isoleucine
K. aerogenes	*Klebsiella aerogenes*
KCl	Potassium chloride
KH_2PO_4	Potassium phosphate monobasic
L. plantarum	*Lactobacillus plantarum*
LB	Luria Bertani
LB++	Luria Bertani with glucose and buffer
LBA	Luria Bertani Agar
LBbuff	Luria Bertani with buffer(K_2HPO_4)
LB-NaCl	LB with no NaCl
Levofloxacin	LFX
Lys	Lysine
m^2	square meter
MA	Matthew Allott
MCA	MacConkey agar
MDCK	Madin-Darby canine kidney
Met	Methionine
MIC	minimum inhibitory concentration
mg	milligram
ml	millilitre
mm	millimetre
mM	millimolar
mm^2	square millimetre
mq H_2O	MilliQ ultrapure water
MRS	De Man, Rogosa and Sharpe
MSA	Mannitol salt agar
Na_2HPO_4	sodium phosphate dibasic
NaOH	Sodium hydroxide
NB	Nutrient broth
NBA	Nutrient Agar
NBglu	Nutrient broth with glucose
o/n	overnight
OD_{600}	optical density measured at an absorbance of 600 nm
P. aerogenes	*Pseudomonas aerogenes*
P. mirabilis	*Proteus mirabilis*

P. vulgaris	*Proteus vulgaris*
PBS	Phosphate saline buffer
PCR	polymerase chain reaction
qPCR	quantitative polymerase chain reaction
QS	Quorum sensing
R	reverse
RDI	recommended daily intake
ROS	reactive oxygen species
rpoS	RNA polymerase sigma factor
RT	room temperature
S. aureus	*Staphylococcus aureus*
S. enterica	*Salmonella enterica*
S. marcescens	*Serratia marcescens*
S. salivarius	*Streptococcus salivarius*
S. typhimurium	*Salmonella typhimurium*
SCFAs	short chain fatty acids
SD	standard deviation
SEM	standard srror of measurement
Ser	serine
sp./spp.	species (singular/plural)
Ta	Annealing temperature
Thr	Threonine
Tm	Melting temperature
TSA	Tryptone Soy Agar
TSB	Tryptone Soy Broth
UCLan	University of Central Lancashire
UK	United Kingdom
USA	United States of America
Val	valine
WHO	World Health Organization
Zn	zinc
ZnCl2	zinc chloride
Zur	Zinc Uptake Regulator

INTRODUCTION

1.1 Background and context of the research project

The research project was initially designed as a bench-based research programme which consisted on the study of the role of the micronutrient zinc (Zn) at physiologically relevant concentration in bacterial gut population selection and dynamics. Our initial programme was designed to harness faecal samples from in collaboration in a University Hospital in Pakistan. The human loss of our co-supervisor in Pakistan, who died from cancer, was accompanied by the inability to provide with the samples. As a mitigation strategy, alternative source of samples from the UK National Health Service (NHS) was identified in agreement with collaborators from Blackpool Teaching Hospitals NHS Foundation Trust. However, with the advent of COVID ethical approval and collection of NHS-connected faecal samples became non-viable options. The programme was then planned to run in collaboration with the UCLan Dental clinic. However, the collection of samples from non-NHS dental patients from the UCLan Dental clinic was not possible because the clinic was closed due to COVID. In addition, the Biomedical Research Facilities (BMRF) at UCLan were shut down for 1st and 2nd years PhD students following National guidelines from March until October 2020, and for an additional year the number of individuals allowed to access the laboratories concomitantly was limited, delaying research activities. Ultimately, the project was based on bacterial gut microbiota laboratory strains, to be assessed upon Zn challenge.

The set of strains selected for our investigations was based on their presence within the human gut microbiota as potential pathogens, or probiotics, and, likewise, based on their availability in the BMRF. Among Gram-negative bacteria, *Escherichia coli* (*E. coli)* is a commensal bacterium in the human GI tract, actually one of the first at colonizing the intestine in neonates at birth[1]; besides its contribution in digestion, vitamin production and fending off pathogens[2,3], some *E. coli* species can lead to GI, urinary and respiratory tract infections[4]. Although normally not considered in the context of the human gut microbiota, but rather for being leading causes of respiratory tract infections[5,6], *Klebsiella aerogenes* (*K. aerogenes*) and *Pseudomonas aeruginosa* (*P. aeruginosa)* also reside in the GI tract. Similarly, *Proteus vulgaris* (*P. vulgaris*) is a leading cause of urinary tract infections and normally present in the intestine as well. The main representative in the human gut microbiota among Gram-positive cocci is *Enterococcus faecalis* (*E. faecalis*), a foremost player in multidrug resiststance[7] and infections[8]. Ultimately, we have selected a couple of strains known to be probiotic species[9], *Lactobacillus plantarum* (*L. plantarum)* and *Streptococcus salivarius (S. salivarius)*, intended to have health benefits in the gut physiology mediated by their ability to fend off pathogens competing with niches and nutrients, to produce short chain fatty acids (SCFAs) and to enhance epithelial cells proliferation[10]. As described in the following introduction, the enterobacterium *Serratia marcescens* (*S. marcescens)* is an underrated opportunistic pathogen, normally residing in the human intestine besides soil, plant and water, which has been only recently brought to the attention of health services and strategic health programme.

1.2 The impact of infectious diseases and the threat of antibiotic resistance

Infectious disease is a leading cause of mortality worldwide, on the top four causes of death in high-income countries in 2019[11] with respiratory and bloodstream infections being the deadliest. in 2019,

13.7 million people worldwide died from infections, with 3 million occurring in children. In 2019 infectious diseases have been estimated to contribute to 10% of all deaths in the United Kingdom (UK), 7% of potential life years lost, 8% of hospital bed days contributing up to £30 billion of costs annually in the country[12–15]. The full impact of infectious diseases expands beyond mortality into infection-related long-term consequences, i.e. increase in morbidity, length of stay in hospital and consequent healthcare cost, and the potential and likely aftermath of antimicrobial resistance (AMR)[16,17].

Vaccinations, antimicrobial drugs and improved hygiene offer an opportunity for non-communicable diseases to overtake infectious disease as the main cause of death globally. However, the rising threat of AMR, driven by the use and abuse of antibiotics, threatens the effective prevention and treatment of an ever-increasing range of infections caused by bacteria, parasites, viruses and fungi, and it is compounded by a failure in the discovery of new effective antimicrobials and vaccines[18,19]. In 2013, over 70% of clinically-relevant pathogens were found resistant to at least one drug used for treatment[20] and typically also responsible for most of the high severity clinical presentations. Of note, many bacteria were also multidrug-resistant, upon which the development of new antimicrobials is critical to combat the threat of AMR[21]. Over 33.000 deaths in 2015 were a result of antibiotic resistant bacteria in Europe with over 870.000 cases causing disability-adjusted life years for patients[22]. In the United States it is estimated that AMR results per annum in as much as $20 billion in excess direct costs, with $35 billion in societal costs for lost productivity. In the European Union (EU), AMR is associated with extra healthcare costs and lost productivity amounting to €1.1–1.5 billion yearly[23]. In 2017, 2 million people became infected with antibiotic-resistant bacterial strains per year; actually, by 2050 AMR is predicted to result in 10 million death per year with further economic costs if action is not taken[24]. Recently, the WHO has published a list of antibiotic-resistant "priority pathogens", classified based on their "critical, high, and medium" antibiotic resistance published on 2017[25]. Among Gram-negative bacteria, characterized by a thin peptidoglycan cell wall and a further outer membrane containing lipopolysaccharides, *P. aeruginosa* and *Acinetobacter baumannii* were reported as carbapenem-resistant, resistance mediated by the production of hydrolysing enzymes, efflux pumps and porin mutations[26]. Notable, *Klebsiella pneumoniae*, *E. coli*, *Enterobacter* species (spp)., *Serratia* spp., *Proteus* spp. were all pathogens found in the third-generation cephalosporin-resistance sub-group, and not surprisingly known to be responsible for severe infections in a wide range of human sites. Despite political prioritisation of AMR as a health threat and guidance for antimicrobial stewardship and infection prevention and control, high levels of resistance remain**.** In addition to measures to limit the spread of AMR in animal settings, food chain and sanitary systems, such as diminishing the abuse and misuse of antibiotics in both humans and animals[18,27], emerging strategies would need to be considered. The modulation of the human microbiota, the complex microbial system residing within our body, that may outcompete potentially invading pathogens is an incipient strategy, yet at the forefront of innovation to tackle the AMR threat.

1.3 *Serratia marcescens*, an emerging infectious agent that has always been there

Serratia spp. are Gram-negative bacteria known to cause severe human infections and listed by the WHO among antibiotic-resistant "priority pathogens" in 2017[25]. In particular, the species *Serratia*

marcescens is the most important, based on its frequent occurrence in hospitals, of medical significance, as discussed in the next sections.

1.3.1 Taxonomy and epidemiology of *Serratia* species

The genus *Serratia* belongs to the family of Enterobacteriaceae and includes at least 14 recognized species, ubiquitous, motile, Gram-negative rod-shaped facultatively anaerobic bacteria [28,29]. Most *Serratia* species are characterized by the red colour, given by the production of prodigiosin, a metabolite with a tripyrrole skeleton. Curiously, to our knowledge, Pythagoras was the first who observed and documented this 'bloody' pigment on food around 600bc; later, in 1264, prodigiosin pigment was most likely responsible for the miracle of blood on Eucharistic bread in Italy. Only in the 19th century, the physicist Serafino Serrati identified and named the bacterium *S. marcescens* [30,31]. Despite it has been firstly described in early 19th century, there is still scarcity of genomic information across the genus[29].

Serratia can be found in a plethora of environmental niches, from water sources to plants. In fact, much of the research have been focusing on *Serratia* species infecting plants or isolated from soil or water [32,33] (Table 1.1). *Serratia* infections can be acquired through contact with contaminated hospital settings or ingestion of contaminated food as a result of poor sanitation and hygiene practice[34]. *Serratia* can cause contamination of food through the ingestion of infected raw meat or cross-contamination of fruit, vegetables and food processing equipment[34]. Nonetheless, *Serratia* foodborne illness is rare as the infectious dose needs to be quite high to cause illness in healthy individuals, and also the contaminated food easily undergoes discoloration and off-flavours, hence preventing its consumption. For these reasons, *Serratia* spp. are not listed among foodborne pathogens yet by the WHO[35], FDA (Food and Drug Administration)[36] or CDC (Centres for Disease Control and Prevention)[37].

Metagenomics studies have revealed the presence of *S. marcescens* among the members of the human gut microbiota[38], therefore indicating that the human gut microbiota is also a likely reservoir of *S. marcescens*.

Table 1.1: ***Serratia* species reservoirs.** Table adapted from Mahlen *et al.*[39].

	Sources						
Bacterial Species	Water	Plants	Soil	Insect	Animals	Nemato-des	Humans
S. entomophyla				✓			
S. ficaria		✓		✓			✓
S. fonticola	✓						
S. glossinae				✓			
S. grimesii	✓		✓				
S. liquefaciens	✓	✓	✓	✓	✓		✓
S. marcescens	✓	✓	✓	✓	✓		✓
S. nematodiphila						✓	
S. odoriphera		✓					✓
S. plymuthica	✓	✓		✓	✓		✓
S. proteamaculans	✓	✓	✓	✓	✓		
S. quinivorans	✓	✓	✓	✓	✓		✓
S. rubidaea	✓	✓					✓
S. ureilytica	✓						

Outbreaks of *Serratia* in hospitals have been reported for decades in UK[40], China[41], USA[42] and other countries[43–45]. The treatment of *Serratia* infections is difficult as clinical isolates have a natural resistance to diverse microbial agents (e.g., ampicillin, cephalosporins, macrolides, nitrofurantoin, and colistin)[46,47] and often exhibit an increased antibiotic resistance acquired thorough horizontal gene transfer or point mutations. In 1998, in China, 32% of patients who reported infections in the a hospital, died of *S. marcescens* bacteremia; all the *Serratia* isolated were moreover resistant to a number of antibiotics [41]. Further epidemiological studies evidenced outbreaks of *Serratia* in hospitals across the UK and Ireland between 2001 and 2011[48]; bacteria isolated showed a high level of genetic variations, contributing to antibiotic resistance, evidence that stresses the needs of further investigation of this opportunistic pathogen to prevent and reduce the outbreaks of *S. marcescens*. Of note, *S. marcescens* have been reported also in regional hospitals in Lancashire, with a weekly-based occurrence among hospitalized patients (personal communication).

Despite those numbers from clinics and hospitals, considering that data often is underreported or unpublished, as well as the occurrence of *S. marcescens* infections and the emergence of AMR *S. marcescens* strains are a stark threat to health and wellbeing, this species is still one of the least well-studied bacteria from a pathogenic and virulence standpoint.

1.3.2 Physiological and pathogenic determinants of *S. marcescens*

1.3.2.1 Prodigiosin

Most *Serratia* species are characterized by a red appearance, resulting from the production of the metabolite prodigiosin. Besides conferring the bright pigmentation of the bacterial cells, prodigiosin

gained interest because of its antimicrobial and immunosuppressive activities[49–51]. For instance, it has been demonstrated that extracted prodigiosin from *S. marcescens* has a bacteriostatic effect on *E. coli* [52] , *P. aeruginosa*[53], *S. typhimurium* and *E. faecalis* biofilm formation[54]; it inhibits multiple bacteria in their growth with minimum inhibitory concentration (MIC) ranging from 4 to 8 µM for different strains, i.e.; *S. aureus, B. subtilis, E. faecalis, E. coli* and *P. aeruginosa* [55], and reduces protease activity for *S. aureus*, *E. coli* and *E. faecalis*[54]. Even parasites, *C. elegans*[56] and *Trypanosoma cruzi*[55] are affected by prodigiosin. Ultimately, prodigiosin limits proliferation, migration and invasion nasopharyngeal cancer cells[57] and induces apoptosis in multiple cell lines, such as in haematopoietic cancer cell lines[58] or lymphoblast cells[59]. Possible mechanisms of action associated with prodigiosin anticancer and immunosuppressive effects are: (i) disruption of pH gradient between various cellular compartments by functioning as sodium-chloride symporter, (ii) interacting in the DNA facilitating DNA fragmentation, (iii) leading to cell cycle arrest interfering with cyclin-dependent kinase inhibitor p27, other cyclins or activating caspase induction[30,57,59].

The physiology, regulation and biochemistry of reactions required for tripyrrole production have been documented[30]. Prodigiosin (molecular formula: $C_{20}H_{25}N_3O$, molecular weight: 323.44 Da)[60] has a tripyrrole structure with three rings synthetized from proline (Pro), serine (Ser), methionine (Met), pyruvate, and 2-octenal. The characteristic structure of prodigiosin derives from the condensation of a 2-methyl-3-n-amyl-pyrrole (MAP), and 4-methoxy-2,2′-bipyrrole-5-carbaldehyde (MBC).

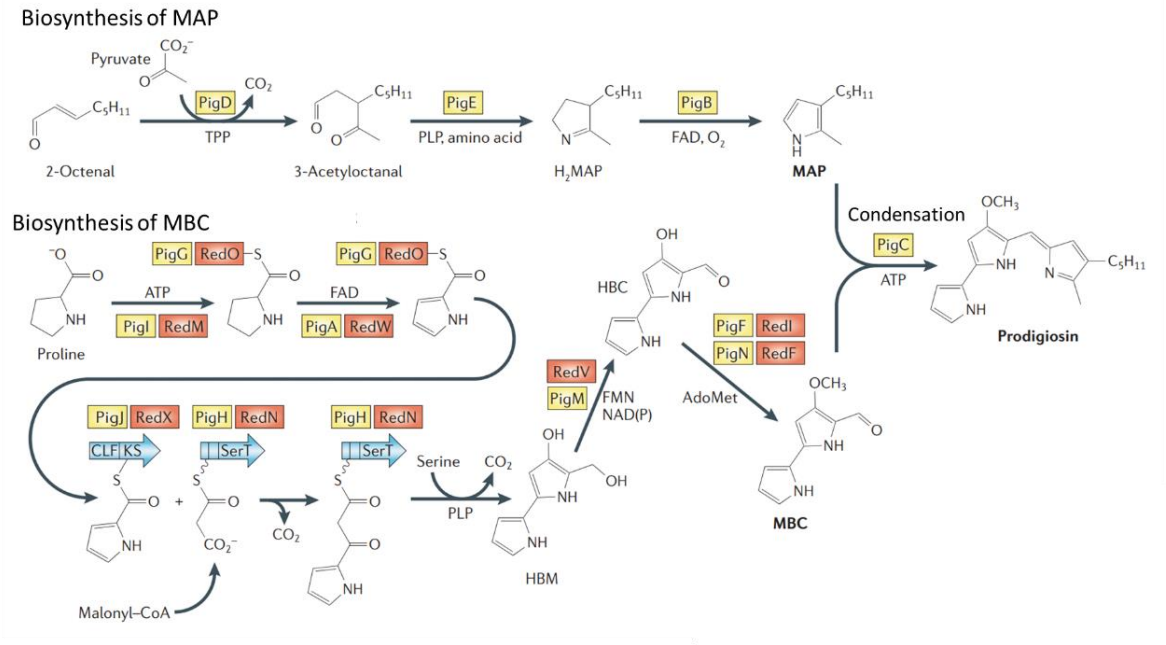

Figure 1.1: **The biosynthetic pathway of prodigiosin in *Serratia*.** The trypirrole structure derives from the independent synthesis of MAP and MBC, followed by a condensation of the terminal products. Figure from Williamson *et al.*[30]

Enzymes involved in prodigiosin production in *Serratia* spp. are located in the *pig* gene cluster, for a total of 14 genes named in order *pigA-pigN*[61,62]. Specifically, *pigB, pigD*, and *pigE* genes are responsible for the production of the monopyrrole fraction, MAP, while *pigA*, *pigF*, *pigG*, *pigH*, *pigI*, *pigJ*, *pigM*, and

pigN genes for the synthesis of the bipyrrole moiety, MBC. *PigC* is instead involved in the condensation of both MAP and MBC[30] (Figure 1.2).

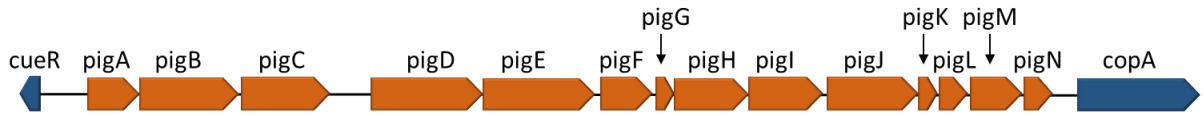

Figure 1.2: **Prodigiosin synthesis gene cluster of *S. marcescens* NCTC12241.** Adapted from Williamson *et al.,* 2006 [30] based on the *S. marcescens* NCTC12241 genome analyses in Geneious®Primer 2021.1.1

Although extensive research around prodigiosin function and metabolism has been conducted, knowledge on its regulatory network is still limited. The major regulators of prodigiosin in *Serratia* spp. seem to be (i) PigP and other downstream six regulatory genes (*pigQ/pigW*)[50,63] that positively regulate the Pig cluster gene expression; and (ii) PigX which is, in contrast, a repressor of the Pig operon. Both PigP and PigX display a highly pleiotropic regulation of other metabolism and virulent genes in *Serratia* spp. For instance, *pigP* mutants of *Serratia* sp. ATCC39006, besides lacking in prodigiosin production, have a reduction in swarming motility and proteolysis activity[64]. Likewise, mutation in *pigX* leads to an expected increase of prodigiosin production, and even an increase in plant virulence[65]. Moreover, Williamson and co-authors have shown that a mutation in a downstream target of *pigX*, *opgG*, significantly reduces swimming motility in *Serratia*. This alteration is mediated by the repression of the motility master regulator FlhC[66].

The interplay between prodigiosin and other physiological and virulent features of *Serratia* have been investigated. It is not a surprise that QS systems have been shown to substantially affect the Pig cluster regulation and prodigiosin production. For example, AHLs, products of SmaI/SmaR (LuxI/LuxR homologs in *Serratia* spp.) can repress prodigiosin production regulating the pig-cluster genes and rap (Regulation of Antibiotic and Pigment), a further regulator of prodigiosin and carbapenem production in *Serratia* ATCC39006[50,67]. Similarly, *luxS* overexpression, and its by-product AI-2, lead to a decrease in prodigiosin synthesis and virulence in both *Serratia* sp. ATCC39006 and *S. marcescens* 274[68].

The surrounding microenvironment also plays a determinant role in prodigiosin production in *Serratia spp.* A number of environmental factors, such as carbon sources, salt concentrations, temperature, oxygen availability[30], mineral availability[69] and phosphate limitation[70] have been found to modulate prodigiosin expression. For instance, it is well known that maximal pigmentation in *S. marcescens* occurs near room temperature, from 22 to 38ºC[71]. Of note, when *S. marcescens* is grown at 37ºC, a number of genes are downregulated compared to an incubation at 28ºC, some of which critical for haemolysis (*shlBA*) and motility (*flhDC*)[71–73], again highlighting the complex and intricate mechanisms underlying of *Serratia* spp. pigmentation. A complex regulatory network involving cell density and environmental features such as temperature, salt and nutrient availability, seems to be emerging in the modulation of prodigiosin production, most likely mediated by the PigP/PigX system[30,74]. Other regulatory systems and transcription factors known to affect prodigiosin production and physiology and/or virulent factors in *Serratia* spp. have been identified and summarized in Table 1.2

Critically, there is evidence that *Serratia* can lose the ability to produce prodigiosin production through spontaneous colour mutants arising after a few generations, suggesting that the white mutants may bear a growth advantage[51]. In fact, it is known that bacterial cells growing in long-term stationary phase can develop spontaneous mutations leading to the appearance of new phenotypes, and characterized by a growth advantage competitive ability[75]. Recently, Qin *et al.* confirmed that non-pigmented mutants of *S. marcescens* survive longer than red pigmentated wild type[76]. Further evidence arises from the clinic, where non-pigmented variants are significantly more frequent than red isolates[77]. Prodigiosin-producing cells were found to promptly accumulate ATP, hence multiplying more rapidly and growing approximately twice the biomass compared to non-pigmented cells – suggesting that prodigiosin may provide a growth advantage[78].

Table 1.2: **Summary table of genes known to regulate prodigiosin in *Serratia spp* and other virulence factors.** Genes (in light blue) whose expression affect prodigiosin expression, motility, proteolysis, haemolysis biofilm formation and other virulence factors, are reported in the table. (+) increased expression/activity, (-) reduced expression/activity, (=) no variation

Reference	Species	Strain	Source	Growth condition	Gene	Prodigiosin Regulation	Swarming motility	Swimming motility	Proteolysis, Haemolysis	Biofilm	Virulence (other)
[79]	*S. marcescens*	K904	Soil	30°C, LB	*cAMP-CRP*	-					
[80]	*S. marcescens*	PIC3611	Insect	30°C, LB	*eepR/eepS*	+	+		+		
[61]	*S .marcescens*	FZSF02	Soil	37°C, LB	*envZ*	+					
[81]	*Serratia spp.*	ATCC39006	Plant	30°C, LB	*floR*	+	-				
[82]	*Serratia spp.*	ATCC39006	Plant	30°C, LB	*fnR*	+					
[83]	*S. marcescens*	K904	Human	30°C, LB	*gumB*	+	+	+	+		
[80]	*S. marcescens*	PIC3611	Insect	30°C, LB	*hexS*	-			-		
[74]	*S. marcescens*	ATCC274	NA	30°C, LB	*luxS*	+			+	-	+
[84]	*S .marcescens*	JNB5-1	Soil	30°C, LB	*metR*	-	+	+		+	
[61]	*S .marcescens*	FZSF02	Soil	37°C, LB	*ompR*	+					
[64]	*S .marcescens*	PIC3611	Insect	30°C, LB	*pigP*	+	+	=	+		

[64]	*S .marcescens*	Nima	NA	30°C, LB	*pigP*	+					
[64]	*S .marcescens*	CHASM	Soil	30°C, LB	*pigP*	+					
[64]	*S .marcescens*	K904	Soil	30°C, LB	*pigP*	+					
[50]	*Serratia spp.*	ATCC39006	Plant	30°C, LB	*pigP*	+					
[50]	*Serratia spp.*	ATCC39006	Plant	30°C, LB	*pigQ*	+					
[50]	*Serratia spp.*	ATCC39006	Plant	30°C, LB	*pigR*	+					
[50]	*Serratia spp.*	ATCC39006	Plant	30°C, LB	*pigS*	+					
[50]	*Serratia spp.*	ATCC39006	Plant	30°C, LB	*pigU*	+					
[50]	*Serratia spp.*	ATCC39006	Plant	30°C, LB	*pigV*	+					
[50]	*Serratia spp.*	ATCC39006	Plant	30°C, LB	*pigW*	+					
[66]	*Serratia spp.*	ATCC39006	Plant	30°C, LB	*pigX*	-	-	=			-
[65]	*Serratia spp.*	ATCC39006	Plant	30°C, LB	*pigX*	-					
[85]	*Serratia spp.*	ATCC39006	Plant	30°C, LB	*RbsR*	+	-	-			+
[76]	*S .marcescens*	1912768R	Soil	30°C, LB	*rpoS*	+	-	-	+	+	
[86]	*S .marcescens*	SS-1	NA	30°C, LB	*rssB/rssa*	-	-		-	+	-

[51]	*S .marcescens*	SCQ1	Insect	30°C, LB	*slyA*	+	-	-
[87]	*S .marcescens*	SS-1	NA	30°C, LB	*spnR*	-	-	

1.3.2.2 Motility, an apparent fitness advantage for bacteria

Bacteria have developed a range of motility systems that can provide critical advantages to the cells, for instance escaping from hostile conditions or to pursue nutrients and exploit available resources. However, as previously described, non-motile *persister* cells in *P. aeruginosa* or *E. coli* biofilms displayed an increased resistance to antibiotics compared with motile phenotypes[88], suggesting an apparent advantage for the non-motile cells rather than for the swarmer cells. Motility mechanisms can be classified into swimming and swarming, both involving the use of flagella[89–92]. Other structural molecules such as type IV pili, adhesins and surfactants are implicated in bacterial motility mechanisms which are less commonly described than swimming and swarming, such as twitching and gliding motility[91]. In all cases, for bacteria to move, intercellular communication and coordination mediated by QS-signalling molecules are essential[93,94].

Serratia spp. are known to exhibit both, swarming and swimming motility. In swarming conditions, the bacteria produce surfactants, mainly serrawettin, a lipopeptide biosurfactant encoded by *waaE* gene**,** which helps to reduce surface tension and allow for movement across the surface, such as an agar gel. In *S*. *liquefaciens* QS activation is associated with an increase in serrawettin production and swarm cell differentiation[93]. Importantly, *waaE* downregulation has been correlated not just with a reduction in swarming, but also in prodigiosin production[95,96].

As described in the Table 1.2 multiple genes are known to regulate prodigiosin production also affect the bacterial motility, again suggesting a complex interplay between phenotypic variants. For instance, *pigP* positively modulates the swarming motility in *Serratia* sp. PIC3611[64], while the negative regulator *pigX* reduces swarming, a process most likely mediated by the *flhC* and *rhlA*, genes that are involved in the repression of surfactant production[65,66]. It has been shown that RpoS inhibits the transcription of the flagellar regulator FliA in *E. coli*[97]. Additionally, in *S. marcescens*, white mutants display mutations in *rpoS* and an increased swimming motility, decreased biofilm formation, and increased lipase and proteinase activity[76]. Further genetic constructs through gene knock-out and gene knock-in displayed that RpoS is a regulator of prodigiosin production in *S. marcescens* and also promotes nutritional competence, and reduces stress resistance, including the resistance to oxidative stress generated by oxygen free radicals[76].

So far, the mechanisms at the interplay between motility and virulence is being elucidated but is not clearly defined. For example, non-motile mutans of *Helicobacter pylori, Campylobacter jejuni, Vibrio cholerae, S. typhimurium, P. aeruginosa, Proteus mirabils, E. coli* and other species display less virulence, mainly associated with reduced invasion and colonization of the host[98]. Furthermore, clinical isolates of *E. coli* with higher motility exhibit a higher rate of infections (peritonitis). It is reasonable to suggest that the higher motility *E. coli* may enhance the inflammatory response in enterocytes and favour the translocation of the bacteria in the intestinal lumen triggering peritonitis[99]. The differentiation into swarmer cells is linked with the expression of some virulence genes encoding urease, haemolysis and protease in *Proteus mirabilis (P. mirabilis)*[100]. Similarly, *P. aeruginosa* in swarming conditions

exhibits the over-expression of a number of genes involved in proteolysis, iron transportation and other virulence secretion systems, hence affecting the bacterial virulence. Moreover, an increased antibiotic resistance against polymyxin B, gentamicin, and ciprofloxacin compared to planktonic cells is observed[101]. Again, swarmer cells of *P. aeruginosa, E. coli, S. marcescens* and *B. subtilis* display higher resistance to most of the classed of antibiotics tested (e.g., fluoroquinolones, beta-lactams, aminoglycosides etc.), than their planktonic counterparts[94] .

1.3.2.3 Proteolysis and haemolysis

The production of prodigiosin and the ability to move in *Serratia* spp. have been also connected to proteolytic and haemolytic activities (Table 1.2).

In plant pathogenic bacteria, bacterial proteases play a crucial role in a range of functions, including obtaining nutrients from the environment and penetrating and colonizing tissues; cleaving host immune molecules and interfering with the host defence response; modulating virulence factors, regulating defence response pathways, suppression of the host immune response, degradation of host tissue; and maintaining homeostasis under stress conditions[102]. Still little is known about the regulatory mechanisms for most of the bacterial extracellular proteases, their structure and specificity[102].

Serratia's proteolytic activity is essential for cytotoxicity and contributes to pathogenesis in both insects and humans[103]. The most characterized proteases in *Serratia* spp. are (i) PrtA, a zinc-dependant extracellular metalloprotease, which correlates with invasion in endothelial cell lines and severity of *Serratia*-keratitis infections[104–106], and (ii) PrtS, a type-I secreted protease known to have broad substrate specificity, including human immunoglobulins and complement components. *PrtA*-mutants of *Serratia* sp. SCBI show reduced rates of proteolytic activity[103]. Also swarming and swimming motility was altered in some *prtA*-mutants, but results are controversial. In fact, only some mutants display reduced rates of swarming when tested at 30°C. At 37°C, mild but not statistically significant changes are also observed in swimming motility. These disputable results may be associated with *prtA* temperature-dependence, which is limited when the temperature decreases from 37°C to 30°C[107]. In *S. marcescens* PIC3611 the EepR response regulator (transcription factor) positively modulates the production of prodigiosin and the PrtS[80]. The latter is also negatively regulated by the *hexS* gene, known to modulate virulence and motility in the plant pathogen *Erwinia carotovora*[108]. A *hexS* mutation in *S. marcescens* suppressed prodigiosin and protease defects induced by *eepR* gene mutation, and, likewise, it reversed associated phenotypes[80].

A crucial virulent feature for bacteria invading hosts is bacterial haemolytic activity, a process by which the bacterium breaks down red blood cells and is of medical significance, as it contributes to the destruction of tissues and the spread of infection. Production of haemolysis by *S. marcescens* is attributed to the presence of various haemolysin genes, such as *shlA*, *shlB*[73,109,110] or the phospholipase-encoding gene *plhA*[111]. The haemolytic process appears to be to be temperature-dependant because when cells where cultured at 30°C they exhibit a 10-fold greater haemolytic capability than cells cultured at 37°C[73]. In the ShlAB system, the haemolysin ShlA is the pore-forming

and contact-dependent protein, whereas ShlB regulates ShlA activation and extracellular transportation[110].

A complex regulatory network between motility and haemolysis mediated by the RssAB two-component system has been described. Lin and co-authors have identified a virulence regulatory pathway in *S. marcescens* that involves the RssAB two-component system, the downstream elements FlhDC and the ShlBA system[112]. FlhDC positively controls the expression of *shlBA*, which is repressed by RssAB signalling. RssAB negatively affect swarming, suppresses haemolysin production, and promotes biofilm formation. In fact, deletion of RssAB increases swarming and haemolysis, evidence supported by *in vivo* experiments: both, cellular and animal models show that the loss of RssAB in *S. marcescens* increases infections rates[112]. Of note, RssAB system has been found to negatively regulate prodigiosin production and other virulence factors in *S. marcescens*[86].

To summarise, it is evidenced that the QS-signalling system is not limited to the cell-to-cell communication but often modulates the regulation of multiple physiological functions in *S. marcescens*. However, the complex regulatory mechanisms underlying the genome-wide changes and related outcomes have not yet been fully elucidated.

1.3.3 AMR in *Serratia* species

Serratia spp. are naturally or intrinsically resistant to some antibiotics[46,47,113–115]. Specifically, the *ampC* gene, encoding for AmpC β-lactamases, confers the intrinsic resistance to a few antibiotics, i.e., penicillin, third- generation cephalosporins and cephamycin, binding to the targets substrates for the antibiotics (e.g., penicillin-binding-site) in *Serratia* , *Pseudomonas, Acinetobacter, Citrobacter* and *Enterobacter* species[116,117]. Other intrinsic mechanism limiting the effect of certain drugs comprises the slow uptake or rapid extrusion of the antibiotics[118]. For instance, the ABC-type efflux pump MacAB has been linked to resistance towards macrolides in *E. coli* and *Salmonella enterica* (*S. enterica)* and to aminoglycoside antibiotics and polymyxins in *S. marcescens*[119]. Furthermore, the efflux pump SdeAB and a TolC-like outer-membrane protein (HasF) conferred resistance to ciprofloxacin in *S. marcescens*[120]. Differently, acquired-resistance to antibiotics is developed through gene mutations or acquisition of antibiotic resistant genes, most frequently carried by plasmids[121]. For instance, *gyrA* point mutation in *S. marcescens* conferring resistance to fluoroquinolones[122]. Contrary to intrinsic or acquired resistance, phenotypic or adaptive resistance is a non-inheritable feature triggered by an environmental signal[123,124]; upon environmental stressor(s) removal the resistant phenotype is normally reversed into the non-resistant one.

Begic *et al.* have shown that the susceptibility of *S. marcescens* to norfloxacin (hydrophilic fluoroquinolone) and nalidixic acid (hydrophobic fluoroquinolone), is influenced by a chemical compound (salicylate), nutrient availability (sucrose), temperature and pH. This is most likely to be due to changes in the membrane permeability[125]. So far, adaptive phenotypes conferring a transient, reversible resistance and driven by signals affecting the bacterial physiology, have been scarcely described in the context of antibiotic resistance. An understanding of the mechanisms of phenotypic resistance is crucial to address the challenge of increasing AMR.

1.3.4 Fluoroquinolones, a broad-spectrum antibiotic used to treat enterobacteria infections

Serratia spp, and other enterobacteria infections are commonly treated with cefepime, carbapenems[126], chloramphenicol[127] and fluoroquinolones[128,129]. Fluoroquinolones are a group of synthetic antibiotics widely used in the clinics due to their efficacy, broad activity spectrum – in fact, they work both Gram-negative and Gram-positive bacteria and are characterised by bioavailability as well as good safety profile[130].

Table 1.3: **Fluoroquinolones antibiotics.** Nalidixic acid was the first fluoroquinolone, reported in 1962. Successive generations of antibiotics have been synthesised years later, with improvements in terms of spectrum of activity and serum concentration; ciprofloxacin and levofloxacin remain the most widely used in the clinics[131]

Generation	Antibiotics	
1st	Nalidixic acid	
2nd	Ciprofloxacin	Norfloxacin
3rd	Levofloxacin	Sparfloxacin
4th	Moxifloxacin	Delafloxacin

Fluoroquinolones act by inhibiting DNA topoisomerases involved in bacterial DNA topology, specifically, DNA gyrase and topoisomerase IV. DNA gyrase plays a crucial role in the initiation of DNA replication, introducing a negative supercoil in DNA double-strand and allowing the binding of initiation proteins[130,132,133]. Topoisomerase IV, on the other hand, disentangles daughter chromosomes[134]. The antibiotics interfere with the cleavage-binding site forming an enzyme- cleaved DNA - fluoroquinolone complex, inhibiting the DNA coiling and relaxation and interrupting the DNA synthesis, leading to cell death[130]. Hence, the contributions of agents/factors which can cause DNA damages, may potentiate the bactericidal effect of the antibiotics[135].

Part of the DNA damage indirectly caused by the exposure to fluoroquinolones, can be repaired through the activation of the SOS response system. The SOS response is a global and inducible DNA repair system activated in response to triggers that may lead to DNA damage, such as exposure to antibiotics or oxidative stress. It is regulated by LexA and RecA[136]. DNA damage triggers RecA protein activation, which in turn promotes the cleavage of LexA, a repressor that binds to the promoter region of the SOS response. LexA cleavage promotes the SOS response pathways and therefore the recruitment of DNA repair machinery. Although is known that LexA is a repressor, while RecA is a promoter of the SOS downstream pathways, considerable variations in its regulation and functions are still under debate[137].

1.3.4.1 Mechanisms leading to fluoroquinolone resistance

Fluoroquinolone resistance has been associated with different mechanisms:

i) mutations in genes encoding for DNA gyrase or topoisomerase IV, specifically, for the first enzyme mutations normally occur in the so-called fluoroquinolone resistance-determining region; while for topoisomerase alterations may occur in one of subunit ParC or, less frequently ParE[137].

ii) a reduction of drug diffusion into the cell resulted from an increased expression of AMR membrane-associated efflux pumps, for instance, *acrAB-tolC* in enterobacteria, including *S. marcescens*[120,138,139] or decreased levels of outer membrane proteins responsible for drug diffusion such as porins, protein channels that facilitate the entrance of the drugs through the outer membrane of Gram-negative bacteria[132,139]

iii) Plasmid-mediated resistance[132,140] carrying the following genes:

a) ***aac(6')-Ib-cr*** encoding-gene, a variant of an aminoglycoside acetyltransferase which reduces the drug activity through acetylation[141].

b) *oqxAB, qepA1*, and *qepA2* genes that encode for efflux plumps facilitating the expulsion of the internalized antibiotic[142,143]

c) *qnr* genes encoding-pentapeptide-repeated-proteins known to confer fluoroquinolone resistance in Enterobacteriaceae through the binding to DNA gyrase and topoisomerase IV, consequently lowering the number of available target enzymes for fluoroquinolone on the chromosome[144,145].

It is worth further describing the *qnr* -mediated resistance because this is fairly common among bacterial strains of medical significance. Initially, multiple plasmid-encoded genes (*qnrA, qnrB, qnrS, qnrC* and *qnrD*) were identified in *E. coli* and *K. pneumonia*[143,146,147]. Captivatingly, subsequent studies have demonstrated the existence *qnr* genes on bacterial chromosomes. For instance, almost 70% of clinical isolated of *E. coli* and *Klebsiella spp*. that displayed resistance to a number of antibiotics were *qnr* gene carriers[148] . Velasco *et al.* have identified a *qnr* sequence in *S. marcescens*, named *Smaqnr*, sharing 80% amino acid (AAs) sequence identity with the plasmid-encoded sequence *qnrB*; they have demonstrated that when the gene is transferred to *E. coli*, the latter acquired resistance to fluoroquinolone[149]. *Qnr* genes flank an upstream LexA binding site, which is well conserved among proteobacteria and where essential conserved sequences are --CTGT--------ACAG--[150–153]. *Qnr* expression is indeed regulated through the SOS response in a LexA/RecA-dependent manner, a pathway that can be induced by the exposure to fluoroquinolone. In *E. coli*, the LexA regulon has been found to regulated up to 31 genes[154]. There is evidence that *recA* can be activated by fluoroquinolone[155,156]. The underlying mechanism suggests that *recA* upregulation leads to the inactivation of LexA, and consequently to the expression of *qnr* – as it is negatively regulated by LexA – which may consequently confer resistance to the fluoroquinolone.

1.3.5 Phenotypic changes associated with antibiotic resistance

The understanding of environmental signals and/or stressors and underlying mechanisms leading to phenotypic resistance have been poorly studied. It is conceivable that physiological changes in antibiotic susceptibility may be linked to phenotypic variability resulting from genome-wide changes in response to an environmental signal or to the antibiotic exposure itself.

In support of this, the existence of a link between phenotypic resistance and bacterial growth has been shown[123]. Bacteria normally grow as a biofilm, a complex biological structure established on surfaces and consisting of a biotic (bacterial) component, and embedded abiotic components[157,158]. The latter actually constitutes 90% of the biofilm mass and is made of microbial extracellular polymeric substances

(EPS), including polysaccharides, proteins, DNA, lipids and organic molecules which facilitate adhesion between cells and the surface and enable the architectural organisation[159,160]. Bacteria in biofilms adhere and colonize surfaces using secreted proteins, cell surface adhesins and flagella and/or pili [161]. Bacteria growing as biofilm, rather than as planktonic cells, have evolutionary advantages, for instance an increased resistance to antibiotics[162–165]. Critically, bacterial biofilms are responsible for up to 80% of all infections[166–168]. Resistance may be mediated, by released DNA (extracellular DNA) which can chelate cationic antimicrobial peptides and some antibiotics[169,170], or by facilitating horizontal gene transfer of genetic materials encoding for antimicrobial resistance[171]. It has been showed that sub-inhibitory concentrations of antibiotics may trigger the formation of biofilm[172] and the development of *persister* cells, dormant variants which are more resistant to drugs in *E. coli* [173] or *P. aeruginosa*[174]. They comprise about 1% of biofilms mass[175], representing a serious challenge for treating infections. For example, antibiotic-resistance variants of *P. aeruginosa* display enhanced ability to form a biofilm and to colonise the lungs of cystic fibrosis patients[176].

Dorr *et al.* have showed that the majority of *persister* cells resistant to ciprofloxacin were formed in a manner dependent on the SOS response[173], hence promoting *recA* expression. In *S. enterica* and *E. coli* , RecA has been shown to also be essential for motility, most probably through the involvement in flagellar rotation, affecting swarming and swimming[177]. In fact, swarming motility is described as a collective and coordinated flagella-dependant bacterial movement on semi-solid surfaces, mainly through flagellar rotation. In swimming, flagella are used by the single cell to move into liquid surfaces[89–92]. In *Salmonella typhimurium (S. typhimurium)*[177] and in *E. coli* K-12[178] the lack of RecA reduced swimming ability. RecA directly interacts with chemoreceptors signalling proteins, CheW and CheA, hence regulating the recognition of specific chemical signals and subsequent responses. Connected to this, it has been shown that the overexpression of *recA* disturbed the chemoreceptor complex formation, inhibiting swarming ability in *S. enterica*[179]. Moreover, swarmer cells of *P. aeruginosa* are less resistant to multiple antibiotics compared to cells undergoing surfing motility, a change that can be attributed to transcriptomic alterations, as several genes involved in metabolism and energy production are dysregulated in surfing cells[88].

1.4 Bacteria as a multicellular organism: communication and coordination mechanisms

Bacteria are traditionally considered unicellular organisms. However, research has shown that in reality, bacteria normally co-exist as multicellular bodies, blurring the line between unicellularity and multicellularity. Examples of bacterial multicellularity is observed in species of myxobacteria, soil-dwelling bacteria, or cyanobacteria, photosynthetic bacteria, both able to form multicellular structures[180]. Ultimately, bacterial biofilms likewise represent an example of a multicellular structure, able to harness bacterial establishment and survival more efficiently that planktonic cells[181]. Intercellular communication and coordination and the interplay with the environment and the host are crucial for (i) community assembly, establishment and survival, (ii) determination of the community's biogeography/spatial organization, and (iii) the bacterial populations relative fitness. Intercellular communication is governed by quorum sensing (QS) signalling molecules and/or direct physical contact on a population-wide

scale[182]. QS systems involve the production, secretion, sensing of specific chemical signal molecules, as well as their subsequent import and processing. These signals, when above certain threshold concentrations, can induce changes at the gene expression level, thereby altering phenotypic adaptations[183]. In a biofilm, QS regulates the production of extracellular components to form and maintain the bacterial population architecture as well as allowing the flow of nutrients for survival[184,185]. It modulates the production of surface lectins, which mediate bacterial adherence to epithelial cells initiating infection processes, and of siderophores which sequester iron from the environment[186,187].

Notably, QS mechanisms are also critical to bacterial antibiotic resistance: QS signalling molecules can upregulate the expression of multi-drug resistance pumps favouring the intracellular removal of toxic substances, and affect membrane permeation, hence preventing or delaying the penetration of certain antibiotics[188]. Targeting QS mechanisms in the context of antimicrobial resistance may unveil a new strategy for the treatment of drug-resistant bacteria.

1.4.1 The interplay between QS systems, bacterial physiology and pathogenesis

The simplest and earliest identified QS system involved in the regulation of QS-signalling molecules, was found in *Vibrio fischeri* and consisted of the LuxI/LuxR paired system[189], regulating the bioluminescence of the bacteria. The identified molecules were N-Acyl homoserine lactones (AHL), synthesised by the LuxI protein and regulated by LuxR. In 1994, the 'autoinducer' signal was recognized in *Vibrio harveyi* and characterized as autoinducer-2 (AI-2). Successively, both AHL and AI-2 systems have been identified and studied in a plethora of bacteria, both Gram-negative and Gram-positive[190].

Generally for QS, Gram-negative bacteria use both autoinducer systems, AHL and AI-2, while Gram-positives preferentially use oligopeptides[191,192]. The only communication mechanisms shared by both Gram-positive and Gram-negative bacteria are AI-2 molecules and regulatory small RNAs (sRNAs)[193].

Table 1.4: **Quorum-sensing system in Gram-negative and Gram-positive bacteria.** Table adapted from Fala *et al.*[183].

System	Molecules	Gene(s)	Producer
Autoinducer 1 (AI-1)	Acylated-homoserine lactones (AHL)	*luxR/luxI* (or homologous)	Gram-negative
Autoinducer 2 (AI-2)	tetrahydroxytetrahydro-furan	*luxS* (or homologous)	Gram-negative and Gram-positive
Autoinducer peptides	Post-translationally modified peptides		Gram-positive
Small RNAs	miRNAs and siRNAs		Gram-negative and Gram-positive

Environmental sensing and signalling is also mediated by second nucleotide messengers, for example the global bacteria second messenger c-di-GMP, c-AMP or ppGpp[194,195]. c-di-GMP is involved in the modulation of exopolysaccharides and adhesins in bacterial biofilm and acts as a negative regulator in bacterial motility, hence promoting biofilm maintenance[194]. Although released QS molecules and second nucleotide messengers have been characterized, little is known about intercellular communication-mediated by cell-to-cell contact, such as the contact-dependent growth inhibition (CDI)

system. Willett *et al.* described bacterial CDI – a mechanism which relies on physical contact with bacterial cells (Gram-negative) and inhibits growth via the translocation of growth inhibitory toxin domains[196]. CDI filamentous exoproteins specifically bind receptors into the targeted bacterial cells for releasing toxins. The CDI system also seems to be implicated in the mechanism of the formation of the biofilm: *cdiA* mutations have been associated with decreased biofilm formation in numerous species[197–200].

Besides its critical role in QS for both Gram-negative and Gram-positive bacteria, AI-2 seems to have a metabolic role as well. In fact, it is a by-product of the activated methyl-cycle throughout the recycling of S-adenosyl-l-methionine (SAM)[201]. SAM is indeed converted in S-adenosyl-homocysteine (SAH) which in turn leads to the formation of ribosyl-homocysteine (SRH), a reaction catalysed by the Pfs enzyme. Ultimately, SRH is broken down by the LuxS enzyme to generate homocysteine and 4,5-dihydroxy-2,3-pentanedione (DPD), precursor of AI-2[190,202,203]. SAM is also a substrate for AHL synthase in Gram-negative bacteria, with the formation of acyl-homoserine lactone (AHL)[204].

Crucially, AAs, such as Cysteine (Cys) and Methionine (Met), have been shown to play a role in synchronizing activities within bacterial populations, as either signals or precursors of signalling molecules in QS mechanisms (Figure 1.3). Met metabolism connected to QS has been extensively characterized in Gram-positive bacteria[205–207] and in Gram-negative including enterobacteria[208]. In *E. coli* Met synthesis is catalysed by two enzymes, MetH, a B_{12}-dependent methyltransferase, or *metE* gene, a cobalamin-independent methyltransferase[208,209]. MetR positively regulates *metE* expression, therefore Met synthesis; contrarily, MetJ is a negative regulator of the biosynthetic pathway[210]. SAM also mediates the Met synthesis: it is sensed by MetJ which in turn represses the expression of the synthesis of Met repressing MetR. Moreover, it has been shown that high levels of Met and vitamin B_{12} on the growth media can repress *metE* [211] and *metR*[84] expressions, while in Met depletion, *metR*[84] is upregulated[212]. Remarkably, *luxS* and *pfs* genes are located near genes involved in metabolic pathways linked to the methyl cycles, for example *metB* and *cysK* in *Clostridium* sp., *Helicobacter pylori* and *Enteroccous feacium*, or *gshA* (alpha-glutamate cysteine ligase) in *E. coli* and *S. marcescens*[201].

Of note, MetR has recently been found to act as a pleiotropic regulator in *S. marcescens* (strain isolated from soil), affecting prodigiosin production, swimming and swarming motility, biofilm formation, H_2O_2 and heat tolerance, besides its role in Met synthesis modulation[84].

Virulent mechanisms were also affected in *luxS* mutants for multiple bacteria, both Gram-negative and Gram-positive. In *E. coli* K-12 *luxS* -mutants biofilm formation was substantially decreased[213]. *E. coli* EPEC *luxS* -mutants show decreased adhesion to epithelial cells and flagellin production [214]. Similarly, in *E. coli* EHEC *luxS* -mutants, reduced motility was described[215]. *LuxS* mutants of *H. pylori* show an increased capacity for biofilm formation and display a lower expression of the flagellin-dependent gene than the wild-type[216]. *Streptococcus mutants* lacking *luxS* are more resistant to H_2O_2 and form less biofilm mass[217]. Furthermore, in *P. gingivalis* LuxS mutants, have reduced production of Cys protease and haemagglutinin activities[218]. On the other hand, haemolysis activity significantly increased in *Streptococcus pyogenes*[219] and *V. vulnificus*[220] *luxS* -mutants. More examples of the role of LuxS in

bacterial metabolism and pathogenesis, besides its primary role in QS, are summarized in the review of Vendeville *et al*[203].

The linkage of *luxS* and its gene product AI-2 with metabolic and virulent phenotypes is becoming better understood and may complement important pathways to pathogenesis of infections.

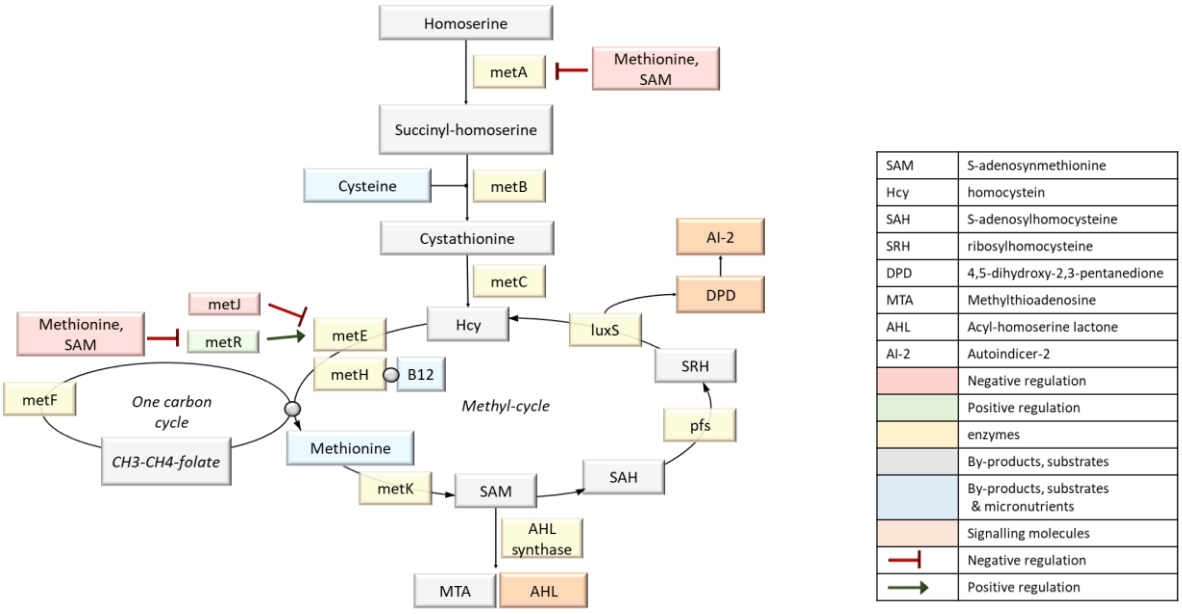

Figure 1.3: **Relationship between the Activated Methyl-cycle and the production of QS-signalling molecules AI-2 and AHL.** Adapted from Hondorp & Matthews, 2006[202].

1.4.2 Bacterial communication in *Serratia*: an interplay between QS-signalling molecules, physiology and virulence

In *Serratia spp*. LuxI/LuxR homologues, i.e., SmaI/SmaR, SwrI/SwrR, SpnI/SpnR, encoding for AI-21 or AHL have been identified[68,221]. *LuxS* gene products, AI-2 molecules, are also involved in *Serratia* spp. intercellular communication, as supported by the non-production of AI-2 when *luxS* genes were knocked-out in both *S. marcescens* NCTC1377 and *Serratia* sp. ATCC39006[68]. Moreover, *luxS* has been found to be involved in virulence functions in *Serratia*. For instance, *luxS* mutants in *S. marcescens* NCTC1377 exhibited a down regulation in prodigiosin production and reduced haemolytic activity[68]. Using *C. elegans* model Coulthurst *et al.* have also showed a minor but reproducible decrease in virulence of *luxS* -mutants of *S. marcescens* NCTC1377. Whether the observed phenotypic changes in *luxS* mutants resulted from a AI-2 shortage or from a complex metabolic derangement is not known[68]. The proposed mechanism was that at low cell density, hence with a low level of QS signals produced, *S. marcescens* represses the putative pleiotropic regulator with a negative effect on swarming motility, pigment production, and secretion of protease and haemolysin. Conversely, at high cell density, so with more signals produced, the expression of a putative pleiotropic regulator and downstream phenotypes is activated[74].

Likewise, the positive regulator of the methyl-cycle MetR, indirectly involved in the production of QS-signalling molecules AI-2 and AHL (Figure 1.3), has been found to be a global regulator in *S. marcescens* JNB5-1 (a soil-isolated strain)[84]. Pan and co-authors have demonstrated that the MetR mutants of *S. marcescens* displayed an overproduction of prodigiosin and a reduction in both swarming and swimming motility, in biofilm formation and in stress tolerance[84].

Therefore, a complex regulatory network in *Serratia* spp. between QS-signalling molecules involved in intercellular communication and virulent and pathogenic factors, e.g., haemolytic and proteolytic activity, or physiological features such as prodigiosin production, seems to be emerging.

1.5 More than just looks: colony variants as a macroscopic manifestation of genome-wide changes

A morphopattern, also known as morphological pattern, refers to the characteristic appearance or arrangement of cells or structures which can provide important information about their functions. Morphopatterns can be used to describe a variety of biological specimens, including cells, tissues, and organisms. For example, in histology, the morphopattern can provide information about the function and organization of the tissue, as well as any abnormalities that may be present. In microbiology, morphopatterns can be used to describe the shape and arrangement of bacterial cells, for instance cocci bacteria which arranged in clusters or chains, arrangements of bacterial cells in biofilm. The relationship between structure and function is considered a crucial and central concept in science and studied in many different disciplines, from biology to chemistry[222].

A pillar of microbial ecology (i.e. the study of microorganisms and their relationships with one another and with their environment) is how the structural interaction among microbes impacts the overall community functions[181]. For example, in co-cultures the presence of certain species of bacteria may facilitate the growth of other species by providing necessary nutrients or creating a suitable environment. Conversely, the presence of some microbes may inhibit the growth of others, either by consuming shared resources or by producing toxic compounds. By studying these interactions, we can gain insight into how microbial communities function and how they respond to changes in their environment. This information can be used to develop strategies for managing microbial communities in a variety of contexts, such as in agriculture, biotechnology, and medicine.

The variety of bacterial cell morphological characteristics (bacterial plasticity) is most likely due to competitive advantages they confer and are modulated by multiple stressors, such as nutrient deprivation, pH or osmotic pressure change and more[223]. Indeed, bacterial plasticity is a hallmark for some pathogenic bacteria, such the filamentous morphology providing a selective advantage for pathogenic *E. coli* [224] and *H. pylori*[225], or the transition from a typically spiral to a coccoid shape in *C. jejuni*[226].

In the context of bacterial pathogenesis and virulence, understanding the mechanisms that lead to the transition from one cell type to another is crucial for elucidating the underlying causes of disease[227]. For example, some bacterial pathogens may undergo a transition from a non-virulent form to a virulent form,

which is associated with changes in the expression of certain genes and the production of specific virulence factors. By studying the mechanisms that regulate these transitions, researchers can develop new strategies for controlling or preventing bacterial infections.

Bacteria mostly live in complex dynamics interspecies communities known as biofilms; the spatial arrangement of bacterial cells and their genotypes within a community impact the cooperative and competitive cell-cell interactions hence determining the bacterial population overall structure, function and the fitness of the individual bacterial species[228]. For instance, interactions between *P. aeruginosa* and *S. aureus* in chronic murine wounds have been characterized[229]: both species co-exist at high densities in the environment, exhibiting a patchy distribution most likely influenced by *P. aeruginosa*-secreted antimicrobial metabolites. Strikingly, they have shown that alteration of the spatial structure in the biofilm enhances *S. aureus* tolerance to some antibiotics, suggesting that the biogeography may impact the infection outcome[229]. The spatial distribution of microbial communities and their ecological influences is studied mainly in soil[230–232]*.* More recently, a characteristic spatial distribution of bacterial communities among physical niches in the intestine has been described, such as colonic mucus layer or colonic crypts. This is in addition to the distinctive bacterial distribution along the longitudinal axis of the gastrointestinal (GI) tract[233]. Likewise, in the periodontal microbiome, a defined biogeography of polymicrobial infections of Streptococcus mutants, is associated with dental caries[234].

Despite significant progress in this field, many aspects of microbial community spatial distribution and environmental influence remain poorly understood. Many questions remain unanswered, such the environmental (physical or chemical) factors that shape microbial community composition and function in different habitats, or the impact of certain microbial community spatial distributions[181]. Studying these processes is important for advancing our understanding of microbial ecology and its relevance to a wide range of fields, including medicine and biotechnology, and required multidisciplinary approaches including integrated computational systems.

1.5.1 Mathematical modelling for describing and predict complex biological system

Cellular automata are mathematical models of computation for describing the evolution of complex systems. The cellular automata were designed in the late 1940s by Stan Ulam and John von Neumann in Los Alamos; initially as simulations of growing crystals on a lattice or to simulate thermodynamic behaviour of liquids as they change states in discrete space and discrete time. A cellular automaton consists of a grid of cells that can be in one of a finite number of states. The state of each cell evolves according to a set of rules that determine how the cell's state is affected by the states of its neighbours. The rules are usually deterministic, meaning that the same state transitions will always occur given the same initial conditions. The basic elements of a cellular automaton are: (i) a regular grid of cells, often arranged in a two-dimensional lattice, (ii) a set of discrete states that each cell can be in, (iii) a set of transition rules that specify how the state of each cell evolves based on the states of its neighbours. Cellular automata can exhibit complex behaviours and patterns emerge from the interactions of individual cells according to the rules. They are used to model a wide variety of phenomena, including physics, chemistry, biology, and social systems[235–237].

The first attempt at mathematical modelling applied to microbial growth was achieved in 1967 with *E. coli* growing on solid surface (nutrient agar). The authors showed that *E. coli* grows with a constant rate of increase in the colony radius, depending on nutrient and oxygen supply [238]. A few decades later, mathematical models designed to simulate the real processes leading to spatial distribution have been documented. Tyson *et al.* have described the high-density aggregates arranged in geometrical patterns in colonies of *E. coli* or *S. typhimurium* which are importantly influenced by the bacterial secretion of aspartate in response to the activation of the tricarboxylic acid cycle [239]. Golding *et al.* studied the patterns forming in growing bacterial colonies on a solid surface, poor in nutrients, including diffusion, food consumption , reproduction and inactivation as features affecting the branching patterns[240]. *B. subtilis* cells are known to produce two types of bacterial cells depending on the substrate softness, nutrient availability and population density[241]*;* a model which may predict the real-life colony pattern considering population density and nutrient availability was proposed[241]. Three soil bacteria, *Azotobacter vinelandii*, *Bacillus licheniformis* and *Paenibacillus curdlanolyticus,* have been used as a model for studying the interspecies interaction among soil microorganisms. The researchers have found that the spatial structure is associated with the competition and interaction within the bacterial community, suggesting that controlling the spatial distribution may enable the manipulation of bacterial species with environmental and biomedical relevance[242]. More recently, Martinez-Rabert *et al.* have proposed a model of three populations including multiple ecological interactions. The researchers have concluded that multiple ecological interactions, such as competition, predation, and mutualism, influence the assembly of the bacterial community. However, they have also found that the environment, including the availability of nutrients, pH, temperature, and moisture, is the main driving force for the spatial distribution of bacteria[181].

1.5.1.1 *Serratia* : a case study

Serratia spp. strains are known to form different colony patterns under diverse conditions. Different morphogenesis of *Serratia* colonies depending on multiple factors, such as the presence of other bacterial body in the vicinity or in close contact, or the nature of the surrounding media, have been investigated by the research group guided by Markos *et al.* over the last two decades[243–247]. Morphological variations of *S. marcescens* CNCTC5965 have been observed and studied from single cells growing in Nutrient Broth agar (NBA) supplemented with 27 mM glucose and incubated at 27^{o}C. A concentric fountain-shaped pattern of *S. marcescens* CNCTC5965, characterized by a red central spot and a red outer edge intercalated by a non-pigmented area, was observed and the pattern described as “fountain-shaped” (Figure 1.4). The main factors affecting the morphogenetic pathways of the bacteria are: (i) the amount, density and distribution pattern of the inoculated cells, (ii) the conformation of the solid surface (growth medium), (iii) the presence of other bacterial cells in the vicinity, and (vi) the signals propagated by the growing bacterial bodies. They have proposed a “embryo-like colony model where multicellular bacterial bodies develop along genuine ontogenetic pathways”[247]. Čepl *et al.* propose a model on colony morphogenesis and inter-colony interactions to understand the process of the formation of well-developed colonies in *S. rubidaea*. from one or more bacterial cells. Bacterial colonies can be shaped by autonomous patterning guided by the self-colony ontology, or by signals generated by physical factors, such as the geometric of the solid growing surface, and biological

factors such as the age of the colony, neighbouring bodies and nutrient availability. Signals propagated by the growing colonies can be volatile airborne signals or close contact agar-borne signals [245]. Morphotypes (i.e., groups of bacterial cells with similar or identical morphology) of *S. rubidaea* and *S. marcescens* in either single or multispecies have been also investigated. They have observed that *Serratia* spp. develop regular and reproducible patterns that can be altered by multiple factors, including the age of the colony, the vicinity of other bacterial bodies – homotypic or heterotypic interactions - , temperature and nutrients availability (e.g., glucose), as well as factors which influence the colony ontology via QS-mediated signals and nutritional signals released in the environment [246]. *S. rubidaea* strains can differ morphologically in the production of the red pigment prodigiosin. A mathematical model of experimental situations of mixed colony of two strains of *S. rubidaea* has been designed for understanding the behaviours of the bacteria in response to environmental factors and related changes in fitness of the bacterial cells during colony growth[243]. Recently, Čepl and co-authors have studied the concentric fountain-shaped pattern of *S. marcescens* CNCTC5965 previously observed [247] characterized by red central spot and a red outer rim intercalated by a non-pigmented area. This spatial distribution of *S. marcescens* CNCTC5965 varied based on the pH, days of growth neighbour cells metabolic activity of growing colonies and the disposition and availability of nutrients (glucose and AAs) on the growing surface[244].

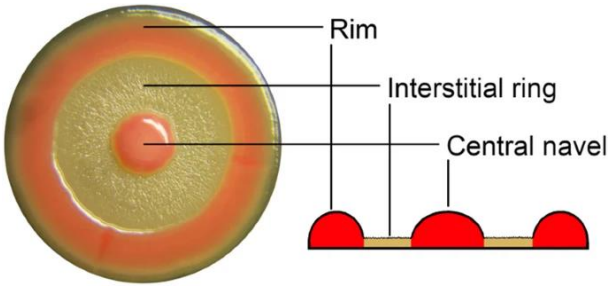

Figure 1.4: ***Serratia marcescens* fountain-morphotype**. Picture from Cepl *et al.*,2019[244]

Studying mathematical modelling in microbial systems is essential for understanding the dynamics of interspecies communities and factors/signals involved in this multi-species crosstalk and has wide ranging applications, including biotechnology and industrial developments or applications of medical significance. In this context, mathematical models may be used to (i) predict bacterial growth in response to different conditions, allowing for more effective control and management of microbial populations; (ii) design and optimize microbial processes for harnessing them for the development of new treatments to combat the infections and AMR threat.

Ultimately, models help us to highlight complex scenarios with multiple variables, such as the polymicrobial populations within the human host. Here we are introducing the concepts and current knowledge of the complex microbial populations living within our bodies.

1.6 In real life: polymicrobial population

1.6.1 Population dynamics in the microbiota community

1.6.1.1 Humans are "superorganisms"

The view of the human body exclusively composed by eukaryotic cells has been replaced by the concept of human as "superorganism". This superorganism includes microbial cells (microbiota) as an integral part of the body. Microbial communities in humans differ among different body sites (gut, oral, nasal, skin, vaginal microbiota), whereby the highest density and taxonomic diversity is reached in the GI tract[248,249]. The GI tract is divided into several compartments, from the oral cavity to the large intestine, whose last portion is the rectum. The review of Hillman *et al.* highlighted the differences in microbiota (Bacteria, Archaea, Virus, Fungi) along the whole GI tract of healthy humans [248]. The microflora reaches its peak in the colon with an estimated number of 10^{14} microorganisms and almost 2000 different species of bacteria[248,250,251]. The collective genome of the gut microbiota (i.e. microbiome) contains over 100 times the number of genes in the human genome, that means ~10-fold more genes in our microbiome than in each human genome – without considering the variability in the composition of the microbiota between individuals[252]. The microbiota of the gut is mainly a 'bacteriobiota' owing to the clear dominance of bacteria respect to Archaea, Virus, Fungi. The GI tract represents a surface area of interaction between the host and the environment ranging from 250 m^2 to 400 m^2 - from the mouth to the rectum - depending on the considerations leading the estimates, approximately 15 to 200 times larger than that of the skin[248,253], with the greatest contribution to this extensive surface given by the small intestine which twists and turns for a length of between 3 and 6 m. The surface area of the small intestine epithelium is further increased for maximal digestion and absorption by the presence of villi and microvilli. A wide range of exogenous organic and inorganic compounds as well as microorganisms from the environment pass continuously through the human GI tract, many which are friends or foe to gut integrity and function[249].

1.6.1.2 The bacteriobiota and host physiology

Owing to its large genomic content and metabolic complement and through a multifaced crosstalk with the host environment, the bacteriobiota provides a range of beneficial properties to the host and impacts organ development and function, in particular the immune system. The intestinal epithelial barrier and mucus layer divide the intestinal lumen and lamina propria region; the lumen of the large intestine is the main site for commensal, symbiotic and pathogenic bacteria, while the lamina propria carries immune cells. The intestinal barrier not simply limit the translocation of harmful exogenous substances or endogenous bacteria, it acts as an active sensor that allows a mutual relationship between the host and the microbiota; different cell types embedded in the intestinal epithelial cells, such as absorptive enterocytes, goblet cells, Paneth cells, and enteroendocrine cells, are involved in maintaining gut homeostasis that is continuously conditioned by the resident microflora[252]. Intestinal epithelial cells promote innate immunity and the secretion of mucus that acts as physical barrier. The Intestinal epithelial cells act as a first line of cellular response by secreting antimicrobial peptides. Furthermore, it expresses receptors which sense specific antigens and trigger the immune system to mount an anti-inflammatory response. The lamina propria carries B and T cells involved in adaptive immune response.

The loss of both, microbiota composition and immune function homeostasis, is one of the main mechanisms that threaten the health of the host [252,254,255]. In addition, the interaction with microbiota is essential for the normal development of both the intestinal mucosal and systemic immune system, as demonstrated by the deficiency in several immune cell types and lymphoid structures exhibited by germ-free animals[252].

Bacteriobiota plays other essential functions *in loco*: specific colonic bacteria strains are able to degrade complex carbohydrates, promoting the breakdown of undigested components and generating metabolites, such as short chain fatty acids (SCFAs), in fermentation processes catalysed by carbohydrate-active enzymes[249]. These SCFAs, propionate, butyrate and acetate, which are rapidly absorbed by epithelial cells in the GI tract where they are involved in the regulation of cellular processes such as gene expression, differentiation, proliferation and apoptosis. Butyrate is known for its anti-inflammatory and anticancer roles, it functions as an energy source for epithelial cells that line the colon, it attenuates bacterial translocation and enhances gut barrier function by affecting tight-junction assembly and mucin production[256]. SCFAs also appear to regulate hepatic lipid and glucose homeostasis via complementary mechanisms. For instance, propionate activates hepatic gluconeogenesis, whilst acetate and butyrate are lipogenic[257]. Besides resistant saccharides, commensal bacteria are also able to metabolise a wide range of different substrates including lipids, peptides but also drugs and toxins[258,259]. In addition, the gut microbiota is crucial to the *de novo* synthesis of essential vitamins, which the host is incapable of producing.

Interspecies interactions within the human microbiota can have significant effects on human health, via, for example, cross-feeding interactions, where one species produces a metabolite that is used as a nutrient by another species, and syntrophic interactions, where two species work together to carry out a metabolic process that neither can carry out alone[260]. Ultimately, the bacteriobiota influences the ability of other commensals or pathogens to colonise, potentially giving some commensal species a competitive advantage in the gut and competing for attachment sites or nutrient sources, and by producing antimicrobial substances, thus influencing the overall composition of the microbiota and its impact on human health.

The human microbiota is a complex and dynamic ecosystem of microorganisms which vary among individuals and during time influenced by a wide range of external factors (e.g. diet, age, geography, medications etc.)[261]. Attempts to identify a stable configuration of healthy microbiota have been undertaken with great anticipation: about a decade ago the concept of ‘enterotype’ was introduced, which aimed to ’stratify’ the gut microbiome across the population, with high representation of taxa from the *Bacteroides*, *Ruminococcus*, or *Prevotella* genera[262,263]. However, the number of stable communities may be quite large and not easily classifiable. More and more projects focus on the role of human bacterial communities in diseases: not surprisingly, dysbiosis, i.e. the disruption of normal balance between the gut microbiota composition and the host, leads to perturbation in gut permeability, increased leakage of microbes and microbial by-products enhancing the host susceptibility to infections and a wide range of disorders[264]: gut-related diseases such as small intestine bacterial overgrowth (SIBO)[265] or irritable bowel syndrome (IBS); autoimmune diseases[266], such as type1-diabetes, Crohn’s

disease, multiple sclerosis and rheumatoid arthritis[267]; colorectal cancer[268]; cardiovascular diseases[269]; neuropsychiatric disorders[270,271] , etc. Larsen *et al.* proposed and applied a model to identify dysbiosis based on the hypothesis that are not just the presence or absence of selected bacteria strains, but the metabolome of the entire community[272]. They demonstrated that the community genotypic and phenotypic profiles, and related functions and produced metabolites of a microbiome, are more predictive of dysbiosis than a simple descriptive of the microbiome community.

1.6.1.3 Bacteriobiota, from the era of description into the age of understanding

The early discovery of natural microbial colonization of human surfaces by Antonie Van Leeuwenhoek was followed a couple of hundred years later by culture-based technologies for the characterization of the microflora. The first studies about the gut microbiota composition relied on culture-based technologies followed by the identification of morphological and biochemical characteristics[273]. The latter were afflicted by technical limitations, such as the inability to detect viable, non-culturable microorganisms. The advent of genomics circumvented some of those restrictions: high-throughput sequencing and next generation technologies, have contributed to the identification and characterization of a wide range of microbial communities[274]. About a decade ago, the first studies using the analyses of sequences of 16S ribosomal RNA (*16s rRNA*) gene to characterise the microbiome were published[275,276]. Targeting of the bacterial *16s rRNA* gene is also a popular approach nowadays since its products - the RNA components of the small subunit of ribosomes - are present in all bacteria and archaea. *16s rRNA* gene contains nine highly variable regions (V1–V9), which reflects the evolutionary divergence of bacteria, and hence, these sequences provide a reliable method for identification and phylogenetic classification of bacterial species[273,277]. More reliable estimates of microbiota composition and diversity may be provided by whole-genome shotgun metagenomics, due to the higher resolution and sensitivity of these techniques[273]. The gut microbial community can be well characterized by various omics technologies including genomics, transcriptomics, metagenomics, metabolomics, proteomics, and thus it offers much promise for data integration within a mechanistic approach. The largest-scale studies to characterize the human microbiome have been the MetaHit[261,278] and the Human Microbiome Project [279]. These works provided an extensive characterization of metagenomic profile of the human microbiome, with the identification of more than 2000 species classified into 12 different phyla. More recently, Almeida *et al.* identified almost 2000 uncultured candidate bacterial species by reconstructing 92,143 metagenome-assembled genomes from 11,850 human gut microbiomes[250], contributing immensely to a broader descriptive understanding of the bacterial communities in the human gut. Despite the large contribution to knowledge of the human microbiome, these projects still carry some limitations, such as (i) the limited availability of reference genomes, (ii) the comparison of limited data types collected from a restricted set of samples, (iii) the use of methodological approaches which are inevitably biased towards the most abundant bacterial species, and (iv) the lack of an understanding of the functional relationship between the microbes and the host.

1.6.1.4 Understanding the gut microbiome: a challenging task

Studying the complex microbial communities that reside in our entangled intestine and analysing their genetic make-up, which is unique for each single human being, through *in vitro* and *in silico* research projects, is a fascinating but demanding challenge. For instance, the need for a (micro)anaerobic environment for most of the commensal bacteria[280], the regional specialization within the intestinal epithelial cells[281] or the spatial distribution of bacteria among the intestinal niches[233] are just a few considerations which exemplify the complexity and the limitations of the study of the human gut microbiota. Novel and innovative methods that sustain the bacterial community establishment in contact with intestinal epithelial cells, in an *in vitro* microenvironment that can resemble the gut ecosystem, have been studied and developed in recent years. Jalili-Firoozinezhad *et al.* have co-cultured epithelial cells with anaerobic and aerobic gut bacteria in a chip that allows a controlled assessment of physiologically relevant oxygen gradients, enabling the study of the functional relationship between intestinal epithelial cells, immune cells, and gut microbes, including anaerobic bacterial species[282]. Even more recent is the method developed by McGrath *et al.*, a microaerobic, mucus-producing vertical diffusion chamber, which allows cell growth in an optimized culture medium of anaerobic gut commensal bacteria, and the underlying intestinal epithelial cells which require oxygen[283]. Those new methods are examples of tools which can enhance the knowledge around the mechanistic understanding of the gut microbiota and tools for the improvement of the design of microbiome investigations applied to human health.

The essential and valuable advances which the literature reports, are mainly descriptive, with a redundant categorization and extensive metagenomic sampling of the gut microbiome, but the whole picture is just a description of how microbial communities vary in response to lifestyle and behavioural changes, physiological impairments and illness[284]. The cellular and molecular processes that drive microbiota shifts and adaptation as well as the resulting impact on the host environment are broadly not understood. We still do not have answers to fundamental questions. What constitutes a healthy gut microbiota? How does bacterial evolution impact host geno-/pheno-/types? How does nutrition and environmental exposure alter gene and population selection? What external determinants may lead the shift from physiological to pathogenic gene expression in the bacteriobiota? What parameters limit the establishment of incoming healthy bacteria or promote the colonization of disease-causing bacteria in an existing microbiota? Answers to these questions are critical to rationally harness the microbiota towards therapeutic and prophylactic applications, to prevent disease or manage its switch to health.

1.6.2 The importance of micronutrients: focus on zinc

1.6.2.1 Zinc: an essential micronutrient for the human body

Macronutrients (recommended daily intake (RDI >1g/day) and micronutrients (vitamins and minerals, RDI <1g/day[285]) shape human physiology, including the microbial community[286]. The total body Zn content has been estimated to be approximately 2 g , 60% of which is stored in skeletal muscle followed by bone mass; plasma Zn represents only 0.1% of the whole Zn content and it is mainly bound to albumin[287,288]. Zn absorption mainly occurs in the small intestine through two mechanisms, a passive diffusion, and a transporter mediated. The transporter mediated process can be upregulated to increase

Zn absorption when dietary intakes are low. The major losses of Zn from the body are through the intestine and urine, by desquamation of epithelial cells, and in sweat depending on Zn intake[289]. Depending on extrinsic and intrinsic factors affecting mineral availability, e.g., mineral competitors such as phytates or Zn release from pancreas or enterocytes, it has been estimated that from the 15-20 mg Zn in a Western diet, 16-50% of the Zn is absorbed in the small intestine, and the rest is excreted[290]. Unavoidably, dietary Zn that reaches the GI tract directly interacts with the microbial community. Post-mortem body tissue and fluid analysis suggest concentrations of 15.7 ± 5.22 (mean ± Standard Deviation (SD.)) µg/g of intestinal tissue[291]. The physiological luminal intestinal concentration of Zn after a meal varies around 6.5 mg/litre (100 µM)[290] in the small intestine, depending on the composition and the size of the meal, a concentration considered not toxic to bacteria, but most likely contributing to protein structure and functions and being involved in gene expression regulation in bacterial cells.

1.6.2.2 Zinc: a multi-talented player: toxic, functional are regulatory roles

Zn is an essential mineral of all forms of life: in eukaryotic cells, Zn has structural and/or catalytic roles in more than 300 enzymes[292,293], it stabilizes the molecular structure of cellular components and membranes maintaining cell integrity, and it is involved in the process of genetic expression[288,294,295]. Remarkably, bacteria require Zn for their survival too, to the point that they have developed strategies to overcome Zn deficiency conditions and keep its intracellular levels within a narrow range. This homeostasis is achieved via transcriptional regulation by metal-sensing proteins and Zn efflux and acquisition across cell membranes[296]. The structural and functional roles of Zn in eukaryotic genes and proteins, and the antimicrobial properties of Zn as a toxicant are well understood and make this mineral a good candidate for industrial and bio-pharmaceutical products (e.g., Zn oxide nanoparticles).

Also, Zn is a key player in oxidative stress and inflammation and, hence, in prevention of related diseases[297]: its deficiency causes oxidative damage to DNA, proteins and lipids, destabilization of membrane structure, dysregulation of Zn-binding protein metallothioneins. On the other hand, Zn overload contributes to augment cellular oxidative stress through different mechanisms, for instance disruption of cellular organelles functions[298]. According to Lee *et al.*, Zn exerts antioxidant functions through the following actions: the catalytic action of Zn-superoxide dismutase (SOD), stabilization of membrane structure, protection of the protein sulfhydryl groups, and regulation of the expression of metallothioneins, which possess metal-binding capacity and also exhibit antioxidant functions. In addition, Zn suppresses anti-inflammatory responses that would otherwise augment oxidative stress[299]. It is well established that viral and bacterial infections trigger the production of radical oxygen species (ROS)[300]. Remarkably, more studies, summarized in the review of Gammoh *et al.*[301], have demonstrated that Zn supplementation may ameliorate infections outcomes.

In bacterial cells, Zn is involved in a range of biological functions, broadly categorised as structural and functional. Structural roles include maintaining protein and membrane integrity and DNA stability[302]. Functional roles include enzymatic roles as a co-factor, and the regulation of gene expression through metalloregulatory proteins, such as the prokaryotic Zur (Zn Uptake Regulator), the latter regulating genes mainly involved in Zn homeostasis[303]. In addition to genes encoding for Zn-transporters to adjust intracellular contents of this micronutrient, Zn also regulates gene expression of ribosomal proteins, a

variety of metabolic enzymes, virulence factors and more. A common bacterial mechanism to mobilize or conserve Zn when it is limiting, consists of the shift from using a Zn-dependent enzyme to an equivalent non-Zn requiring enzyme, highlighting the complex interplay between Zn and bacterial metabolism and physiology[304,305].

Given the considerable amount of Zn in the intestine (estimated to be around 100 µM[290]), and the crucial functions it exerts in bacterial cells, we are now discussing the role that concentration of Zn and other micronutrients may have on the human microbiota populations.

1.6.2.3 Micronutrients shaping the microbial community

The interplay between Zn and microbiota has been superficially investigated in a wide range of contexts from environmental microbiology, and antimicrobial biotechnology to animal models and epidemiology. Most of the available data is derived from animal studies in chicks[306,307], piglets[308–310] or mice[311,312], overall providing a controversial picture.

Some studies have evidenced the pro-inflammatory role of Zn, most likely mediated by a shift towards pathogenic bacterial species and a reduction in richness and diversity in the microbiota composition. For instance, mice fed with high-Zn diet revealed a higher level of inflammation and toxin production, loss of gut barrier function and subsequent bacterial translocation, and an increased susceptibility to *Clostridium difficile* infection[312]. Excessive Zn seems to induce oxidative stress and consequent epithelial damage and inflammation in the intestinal environment through the generation of reactive oxygen species (ROS) [312]. It is reasonable to hypothesise that, in healthy animals, a very high dose of Zn might have a negative effect on the intestine and overall health, but when the mineral is given to mice with a strong inflammatory response, it ameliorates the inflammation and necrosis of epithelial cells[313]. In support of this, in mice infected by *Shigella flexneri*, Zn supplementation has been shown to ameliorate the severity of the disease, including an improvement of the intestinal inflammation[314]. Again, Bolick *et al.* evidenced a better response to pathogenic *E. coli* infection when mice were fed with Zn compared to mice fed a Zn deficient diet[311]. Given the similarity between their metabolism, pigs represent an appropriate model for human metabolic studies, including gut microbiome studies[315]. In line with some studies in murine models[312], the supplementation of Zn in pigs led to an increase in the number of pathogenic bacteria strains, such as *Shigella* or *Klebsiella spp*. and to an overall decrease in bacterial richness and diversity[310,316]. However, controversial results arise from other studies showing a decrease in the number of pathogenic bacterial species in pigs fed with Zn[317].

Overall, there is variability and conflict emerging from the available literature, again highlighting the complexity of studying such a dynamic microenvironment. The contrasting results from the studies suggest that there might be a threshold of Zn above which the mineral may have a pro-inflammatory role rather than anti-inflammatory effects. Whether those effects and mediating or mediated by a shift in the animal gut microbiota is not understood.

The study of the impact of the mineral Zn on the gut microbiota in humans is still at its infancy. Trials in humans reveal that Zn supplementation can have a therapeutic effect, improving gut barrier integrity and immune response functionality: the mineral has been mainly used, with positive outcomes, for the

prevention and treatment of diarrheal conditions in low-income countries[318–320]. Moreover, promising studies demonstrated that Zn could be used for improving gut permeability in inflammatory bowel diseases, such as Crohn's disease, in humans[321]. In support of this, *in vitro* studies in epithelial cells demonstrated that Zn deprivation caused alteration of tight and adherent junctions and disorganization of structural proteins with consequent disruption of gut barrier integrity and inflammation[322,323], reasons that may explain why Zn supplementation improves diarrheal and inflammatory conditions. Up to now, despite the ultimate effect of Zn on gut function and permeability is growing, the role of Zn as a gene regulator in bacterial genomic burden present in the gut, should be further investigated.

1.6.2.4 Zinc, a gene signal in virulence and pathogenesis

As explained in Section 1.6.2.2, Zn is essential for regulating a wide range of cellular functions in bacterial cells, including modulating the expression of some genes. In 2005, Lee *et al.* found that $ZnSO_4$ added to *E. coli* cultures, grown in chemostats leading to a "Zn-stress condition" , induced up-regulation of 64 genes and down-regulation of 58 genes involved in Zn homeostasis, stress responses, QS system and biofilm formation[324]. Other researchers demonstrated that the addition of Zn to *E. coli* influenced the expression of genes also involved in AA metabolism[325] and the RpoE (sigma factor E)-cascade pathway[326]. Similarly, Zn addition to *Enterococcus faecalis* (*E. faecalis*) led to substantial changes at a genome-wide level, with genes involved in bacterial metabolism and stress response displaying an altered expression in response to micromolar concentrations of Zn[327].

Recent studies focused on Zur-regulated genes in pathogenic bacteria have found that Zur can repress genes encoding for virulence, secretory and membrane proteins[328] and haemolysin, a virulence factor studied in uropathogenic *E. coli*[329]. As it is known that calprotectin released by neutrophils in inflammatory conditions can act as a chelator for Zn[330], it reasonable to assume that intestinal Zn limitation due to inflammation could promote the expression of Zur-regulated genes encoding for proteins with an ultimate pathogenic potential in the context of gut microbiota populations. An example of a protein involved in pathogenesis during Zn starvation may be DksA, encoded by a gene part of the Zur regulon[331,332] and involved in the regulation of the transcription of genes involved in (i) motility, (ii) proteolysis, (iii) toxin productions (*Vibrio cholerae*) and (iv) QS-system (*P. aeruginosa*)[333,334].

The impact of Zn limitation in bacterial virulence has been investigated for different bacterial species. Ammendola *et al.* found that Zn was required for *S. enterica* motility, biofilm formation and QS signal production as in Zn deficiency condition these functions were reduced[335,336]. Likewise, motility was inhibited in *P. mirabilis*[337] and ability to form biofilm was reduced in pathogenic *E. coli* [338], and *Staphylococcus spp.*[339,340]. Consistently, the Zn exposure led to the overexpression of genes involved in QS, increased motility and toxin production in *P. aeruginosa,* hence harnessing the commensal-to-pathogen transition of *P. aeruginosa* [341,342]. In contrast, some studies have found that the addition of Zn to growth media, at micromolar concentrations, decreased the formation of biofilm for *E. coli* and *Klebsiell*a, most likely competing for the Fe uptake [343], inhibited toxin release and other virulence mechanisms in pathogenic *E. coli*[344,345]. In co-culture experiments, Zn negatively affected the growth of *Streptococcus sanguinis* in favour of *P. aeruginosa*[346], suggesting that metal homeostasis is a key factor driving population dynamics.

Although a wide range of mechanisms which bacteria use to maintain intracellular Zn homeostasis has been extensively studied and understood, this is not true for the role of Zn in bacterial pathogenesis and virulence, with controversial results arising from the available studies. Promisingly, Zn seems to play a crucial role during pathogen colonization and survival, but more knowledge regarding its cellular and molecular impact on the microbiota and related processes is required.

1.6.3 Bacterial co-culture models: humble but essential

The human gut microbiome is a complex ecosystem of microorganism-host-metabolites interactions which vary according to the ecological contexts. The use of innovative technologies in combination with conventional approaches can harness a better understanding of the mechanisms between the bacterial community and the host. Using models of two or more bacterial strains growing on conventional microbiological growth media is a useful approach to address fundamental questions regarding competitive mechanisms among bacteria inhabiting the human gut microbiota. Integration of multiple approaches, from pairwise and multiple interactions in co-culture experiments to metagenomics and transcriptomics techniques, could provide a broader insight into bacterial population dynamics and represent a promising inception towards further novel exploration in several contexts, including bacterial physiology, ecology and clinical settings. So far, a limited number of studies have addressed the phenomenological and mechanistic understanding of co-cultured bacterial species, especially in the context of the human gut microbiota, here described.

P. aeruginosa represents a leading cause of infections in the clinic. Its interaction with other microorganisms has been studied in co-culture experiments, with controversial results. In co-culture with *Agrobacterium tumefaciens, P. aeruginosa* displayed a considerable growth advantage in both planktonic status and biofilm[347]. More research exists on *P. aeruginosa* and *S. aureus,* two major pathogens often co-existing in respiratory tract infections, however it shows some controversial results [348,349]. It seems that *P. aeruginosa* may show a competitive advantage on *S. aureus*, limiting its growth by disturbing the electron transport chain, competing for micronutrients or producing antimicrobial substances production[350]. On the other hand, *in vitro* studies showed the co-existence of the two bacterial strains, where *P. aeruginosa* could facilitate *S. aureus* growth with molecular mechanisms still unclear[351]. Transcriptomic analyses suggest that the bacteria form an expression pattern as part of their genetic adaptation to co-existence, resulting mainly from adaptation due to the competition for resources and metabolic changes[352,353]. Scott *et al.* have recently suggested that *P. aeruginosa* limits *Streptococcus spp*. growth through iron competition[354]. On the other hand, it seems that *P. aeruginosa* can upregulate the expression of Zn-transporter genes in *Streptococcus sanguinis*, favouring its growth[355]. This suggests there are very specific adaptations at play, rather than generic phenotypical changes due to environmental changes.

Co-culture models of *Staphylococcus epidermidis* and *E. faecalis* have been established to study the use of some antibiotics for ocular infections[356]. Further studies on marine microorganisms, not described here, have been documented[357–359].

The poor description of bacterial co-cultures in the literature, points out the need to study bacterial interactions with humble and conventional microbiological techniques which can lay the foundation to study complex and multispecies interplay among bacterial communities and the host, and which can ultimately provide insights into the mechanisms underlying the switch from health to disease in the context on human microbiota and infection diseases.

1.7 Our project: an innovative and promising tool for harnessing bacterial population dynamics and the influence of human host

Although great improvements have been made on the structure and function of the human microbiota, those advances are mostly descriptive, while functional and mechanistic knowledge is limited. Bacteria have developed multiple strategies to respond to environmental changing conditions, to compete and synergise with their neighbouring microorganisms for nutrients or niches, and mechanisms to optimize their growth pattern to the surrounding microenvironment. Which factors, for instance micronutrients or metabolic signals, may influence microbial selections in niches within the microbiota, and how bacteria respond to those changes, are effectively unexplored at the mechanistic level. We have considered the involvement the micronutrient Zn susceptible to drive microbiota changes on the selection, dynamics and functions of bacterial populations, from a regulatory (i.e., as a signal determining expression of genes) perspective, rather than as a structural or functional protein cofactors.

In addition, our research group has an interest on studying *S. marcescens* behaviours and phenotypes in relation to the gut microbiota context, an enterobacterium which has been only recently brought to the attention due to recurrent outbreaks in the clinics.

1.7.1 Aims of the project

In the light of the knowledge gaps and rationale described above, our project's aims consisted in the elucidation of bacterial population dynamics, competition and selection in response to

a. a potential pathogen, *S. marcescens,*
b. external factors such as the micronutrient Zn

Our project represents a novel view of harnessing bacterial behaviours and morphogenetic variations to explore genome-wide changes and linked phenotypic shifts, pathogenesis and virulence. Moreover, besides unveiling the interplay of microbiota members, our findings my impact the microbiota linked-prevention and disease management, and may enrich the prophylaxis to treat infectious diseases and tackle antibiotic resistance.

2 MATERIALS AND METHODS

To address our research questions, we have strategically planned an experimental design based on conventional methods and techniques aimed to i) establish proof of concepts which may support our hypothesis (Section 1.7), ii) obtain data in a timely fashion in linear with the duration of the PhD timelines (Section 1.1). A summary of the experimental plan is represented in figure 2.1.

We looked into conditions that would have allowed for the easy establishment of a model, i.e., a limited number of bacterial species, pairwise co-cultures, aerobic growth conditions, use of conventional microbiological growth media. Those conditions and obtained results could set the stage towards the future exploration of more complex and demanding experimental settings. Similarly, the mathematical model that have been presented in this PhD Thesis was a simplification of the real-life colony pattern, but may represent a solid outset for further mathematical formula to be tested.

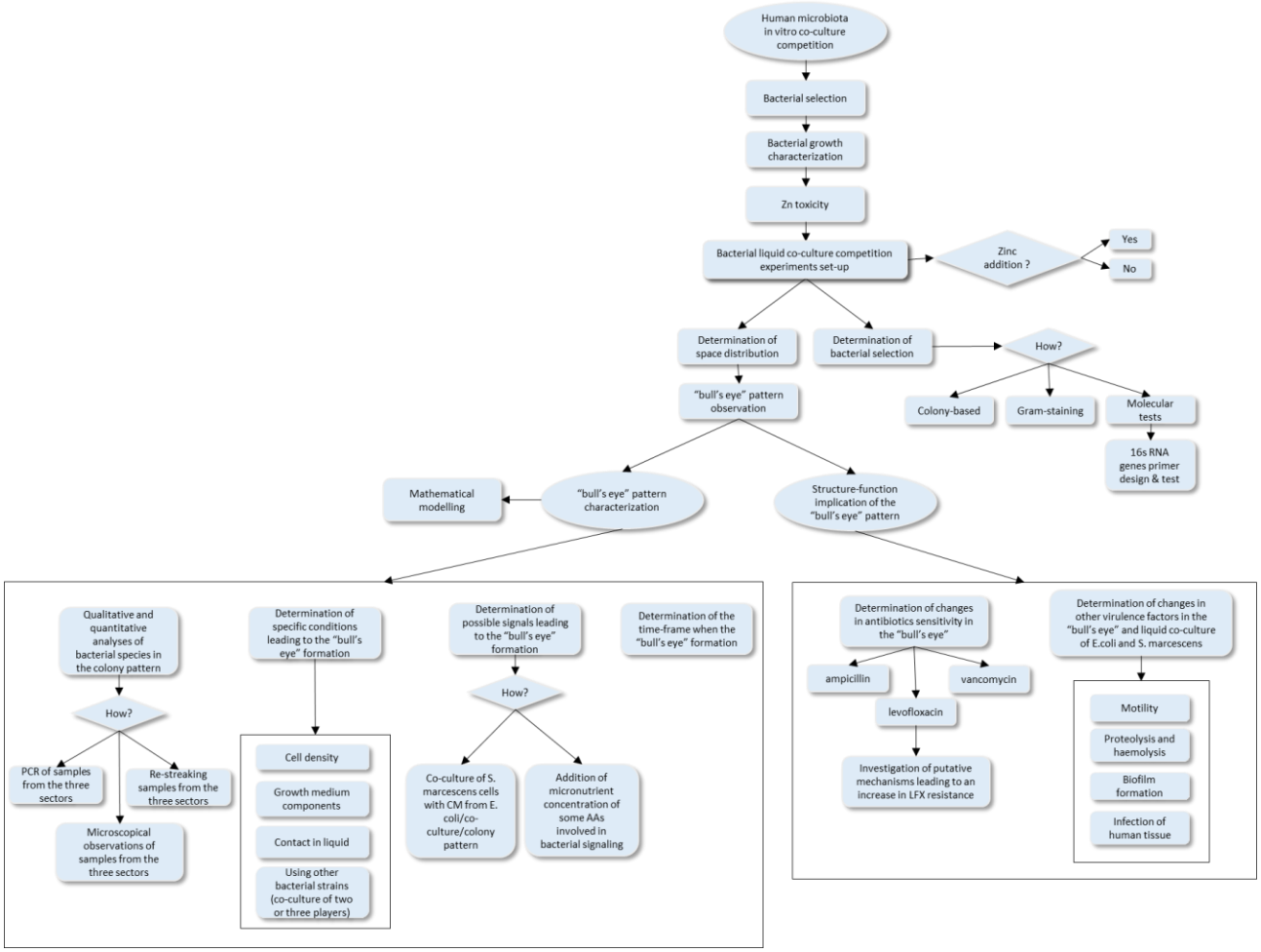

Figure 2.1: **Flowchart summarizing the applied methods during the research progression**.

2.1 General materials

2.1.1 Strains used in this study

Bacterial strains that can be found in the human gut microbiota or as potential pathogens in that system were used in this study and obtained from UCLan Strain Collection (Table 2.1)

Table 2.1: **Bacterial strains used in this study.** Name of the strain, Identification codes, Gram-staining and citations regarding these strains being found in human gut microbiota are indicated.

Name	Identifier	Gram stain	Ref.
Escherichia coli	NCTC12241/ATCC25922	negative	[1]
Escherichia coli	NCTC10418/ATCC10536	negative	[1]
Proteus vulgaris	NCTC4175	negative	[360]
Serratia marcescens	NCTC1377/ATCC274	negative	[38]
Klebsiella aerogenes	NCTC10006	negative	[5,6]
Pseudomonas aeruginosa	PA01	negative	[5,6]
Lactobacillus plantarum	NCTC6376	positive	[9]
Streptococcus salivarius	NCTC8618	positive	[9]
Enterococcus faecalis	NCTC775	positive	[7]
Staphylococcus aureus	NCTC12981/ATCC25923	positive	[361]

2.1.2 Growth media and colony morphology characteristics

Growth media commonly used in basic and clinical bacteriology/microbiology, and which may be considered to resemble the postprandial intestine, have been selected for our study. Each medium was prepared as per manufacturer instructions[362]. Briefly, the corresponding components in powder form indicated in Table 2.2 were resuspended in 1 l of distilled H_2O using a magnetic stirrer. The pH (at 25 °C) was adjusted to 7.4 ± 0.1 for LB medium. The addition of components to the liquid was made progressively, i.e., a component needed to be in suspension before the following component was added. The process rendered a homogenous solution that was subsequently autoclaved at 121^{o}C for 20 minutes. The sterile flasks were kept at room temperature (RT).

Solid medium for TSB, LB, BHI, and NB (named, TSA, LBA, BHIA and NBA, respectively) was prepared by adding bacteriological agar (1.5% w/v, Oxoid, LP0011) to the corresponding liquid media preparations. Selective and differential media were used for species discrimination to complement the data from non-selective/non-differential growth media. Cystine–lactose–electrolyte-deficient agar (CLED) is a differential and non-selective medium used for the isolation of urinary pathogens, such as *Proteus* species, limiting their excessive swarming due to its lack of electrolytes; the presence of bromothymol blue causes the colonies to appear yellow as a result of acid production during lactose fermentation or blue in case of alkalinization[363]. MacConkey agar (MCA) is a differential and selective

media used for isolates Gram-negative bacteria due to the presence of bile salts which are toxic for Gram-positive species[364]. MCA was used for bacterial discrimination in pairwise co-cultures of a Gram-negative and a Gram-positive species. Mannitol salt agar (MSA) is a selective media for isolating staphylococci, thanks to its high concentration of salt which is toxic for most of the bacteria[365]. MSA was used for bacterial discrimination in pairwise co-cultures of *S. aureus* and other strains.

All solid media were autoclaved as described above, except Blood Agar plates that were purchased as ready-to-use from (Oxoid, PB5012A) and used for testing bacterial haemolytic activity. Autoclaved solid media were allowed to cool down to approx. 60ºC before pouring them into 9 cm Petri dishes (approx. 15ml per plate). Freshly poured plates were allowed to cool down on the bench to RT (approx.30 minutes). To prepare skim milk agar plates, used to testing proteolytic activity of bacteria, autoclaved TSA and LBA suspensions, once cooled down to 60°C, were supplemented with skim milk from a 10% w/v stock solution (Oxoid, LP0033B) to a final concentration of 2.5% that was thoroughly resuspended through gentle inversion before distributing it into Petri dishes as above[366]. Unless otherwise indicated solid agar medium plates were stored at 4ºC and used within 3 weeks.

Table 2.2: **Composition (g/L) of growth media used.**

		TSB[367]	Skim-milk TSB[366]	LB[368]	LB-NaCl	LB glu	LB buff	LB ++	Skim-milk LB[366]	BHI[369]	NB[370]	NB glu[244]	CLED[371]	MCA[364]	MSA[365]	Blood Sheep TSA[372]
	Product Brand & code	Neogen NCM0004A	Neogen NCM0004A							Oxoid CM1135	Oxoid CM0001		EOLabs KM0004	Oxoid CM0007	Remel R453902	Oxoid PB5012A
Glucose	FB G/0450/6	2.5	2.5			2.5		2.5	2.5	2		5				2.5
Lactose													10	10		
NaCl	Millipore 1.06400	5	5	10	-	10	10	10	10	5	5	5		5	55	5
K_2HPO_4	FB BP363-1	2.5	2.5				2.5	2.5	2.5	2.5						2.5
Tryptone	Oxoid LP0042			10	10	10	10	10	10							
Peptone										10	5	5		20	11.8	
Yeast Extract	FB J23547-A1			5	5	5	5	5	5		2	2			9	
Enzymatic digest of casein		17	17										4			17
Enzymatic digest of soybean		3	3													3
Enzymatic digest of gelatine													4			
Beef extract											1	1	3			
Beef heart extract										5						
calf brains extract										12.5						
L-cystine													0.128			
Skim milk powder	Oxoid LP0033B		25						25							
Bile salt														5		
Bromothymol blue													0.02			
Mannitol															10	
Lithium Chloride															5	
Aniline Blue															0.2	
Sheep blood																50

TSB, Tryptone Soy Broth; LB, Luria-Bertani; LB-NaCl, Luria-Bertani with no NaCl; LBglu, Luria-Bertani with glucose; LBbuff, Luria-Bertani buffered; LB++, Luria-Bertani with glucose and buffer; BHI, Brain Heart Infusion; NB, Nutrient broth; NBglu, Nutrient Broth with glucose; FB, Fisher Bioreagents.

Colony morphologies on selective and differential media are indicated in Table 4 below. On non-selective/-differential media (i.e., LBA, TSA, NBA and BHIA) the colony characteristics for each species was similar. Because of the importance of those characteristics on the diagnosis of *E. coli* NCTC12241 *and S. marcescens* NCTC1377 in co-cultures from both species it is of value to indicate that *S.*

marcescens NCTC1377 always displayed the production of prodigiosin on non-selective/-differential media of conventional use thus appearing red. Similarly, *E. coli* NCTC12241 always appeared white on those media. To state such stable phenotype for our *Serratia* strain of use, *S. marcescens* NCTC1377 is of particular importance because it is known the mosaic phenomenon of some *S. marcescens* strains and other *Serratia* species, where genetic and/or physiologic variants deprived of prodigiosin expression.

Table 2.3: **Colonies growth and appearance in differential and selective media**. Smears or liquid culture dilutions of exponentially stationary cultures were deposited on agar plates of various nutrient media and incubated at 37°C for 16 hours.

	E. coli	*S. marcescens*	*P. aeruginosa*	*K. aerogenes*	*P. vulgaris*	*E. faecalis*	*S. salivarius*	*S. aureus*	*L. plantarum*
Differential growth Media									
CLED	yellow, opaque, smooth	red, opaque, smooth	green, mucoid	yellow to whitish mucoid	translucent t blue, rough periphery	yellow, punctiform	whitish punctiform, limited growth	yellow, smooth	yellow whitish, minute
Selective & Differential growth media									
MCA	red, opaque, smooth	red, opaque, smooth	green-brown, mucoid	red, mucoid	pale whitish mucoid	NG	NG	NG	NG
Selective growth media									
MSA	NG	NG	NG	NG	NG	NG	NG	Red, opaque, smooth	NG

NG, no growth

2.1.2.1 *Lactobacillus plantarum* growth medium (LBEAP1)

Lactobacillus plantarum is a fastidious organism which requires specific nutrients; in fact, the ideal growth medium for lactobacilli is the selective medium De Man, Rogosa and Sharpe (MRS)[373]. We determined that *L. plantarum* NCTC6376 was unable to grow in LB, the medium generally used for the co-culture experiments in this project. To maximize the opportunity for comparative studies with a similar medium conducive to growth across species, we designed a specific variant of LB, named LBEAP1, which was based on LB supplemented with selected components of MRS. i.e., LB was supplemented with 0.81 mM $MgSO_4$ (Fisher Scientific, M/1050/53) 0.224 mM $MnSO_4$ (Acros Organics, 205905000) and 2% glucose (D-Glucose anhydrous, Fisher Bioreagents, G/0450/60). To determine if and what supplements from MRS added to LB were able to support growth of *L. plantarum* the following media were tested: (i) LB Agar (LBA) (ii) LBA supplemented with $MgSO_4$ (0.81 mM), (iii) LBA supplemented with $MnSO_4$ (0.224mM), (iv) LBA supplemented with both $MgSO_4$ (0.81 mM) and $MnSO_4$ (0.224mM), (v) LBA supplemented with glucose (2%), and, (vi) LBA supplemented with both minerals and glucose. Supplements were added to LBA plates by spreading, thoroughly and homogeneously with a sterile spatula, a total of 200 µl of supplement volume. For diffusion of supplements through the agar plate,

the plates were kept at RT for 1 hour before usage or storage. Roughly 500 cells from an exponential growing culture of *L. plantarum* in BHIA were added on the plates, let the plates dry and incubated at 37°C for 24 hours. Growth in liquid LBEAP1 was also tested applying protocol explain in Section 2.1.5.3. The results (Section 3.1) LBA supplemented with both minerals and glucose (LBEAP1) as a suitable medium to support *L. plantarum* growth in conditions not dissimilar to those for other species and strains. LBEAP1 medium was used in pairwise co-cultures of *L. plantarum* with other strains with appropriate controls, i.e., each strain growing as mono-culture in LBEAP1 medium.

2.1.3 Inorganic solutions and Buffers

Phosphate-buffered saline (PBS) was prepared by progressively mixing in deionized H_2O the components indicated in Table 2.4 until a homogenous solution was obtained. The solution was adjusted to a final pH (at 25°C) of 7.4 ± 0.1 with 1N NaOH and 1M HCl, and was subsequently autoclaved at 121°C for 20 minutes and kept at RT.

Table 2.4: **PBS composition (g/L) used for this study**

Salt	g/L	Product details (Company, Code)
Sodium Chloride (NaCl)	8.0	Millipore, 1.06400
Potassium Chloride (KCl)	0.2	Fisher Bioreagents, P/4240/60
Sodium phosphate dibasic (Na_2HPO_4)	1.42	Fisher Bioreagents, BP332-1
Potassium phosphate monobasic (KH_2PO_4)	0.24	Fisher Bioreagents, BP363-1

Stock solutions in H_2O of 1 N sodium hydroxide (NaOH) and 1 M hydrochloric acid (HCl), were prepared from powder (Acros Organics, 424330010) and a 37% solution in H_2O (source), respectively. A 0.1% crystal violet (CV) solution was prepared in 1:4 methanol:H_2O from CV powder (Sigma, C3886-100G). A sterile 3 M stock of $ZnCl_2$ in H_2O was prepared using zinc chloride anhydrous (98+%, Alfa Aesar, A16281.22). The solution was filtered sterilized through a 0.22 µM sterile filter in polyvinylidene fluoride (Star Lab). The working solution for experiments was obtained through 10-fold dilution of the stock in sterile distilled H_2O to obtain a solution 0.3M of $ZnCl_2$. To prevent the formation of zinc oxychlorides or other precipitates HCl was added to the solution to a final concentration of 6 mM HCl. Ready-made 20% hydrogen peroxide (H_2O_2) (FisherScientific, 11961506), i.e., 9.8 M, was obtained from the UCLan Biomedical Research facility. Sub-stocks of 1 and 0.1 M were prepared diluting the main stock in sterile distilled H_2O and kept at 4°C.

2.1.3.1 Organic solutions

A 50% stock solution of glucose was prepared by adding 50 g of D-glucose anhydrous (Termofisher, G/0450/60) to 100 ml of H_2O, mixed until dissolved and autoclaved at 121°C for 20 minutes. Glycerol (Fisher Bioreagents, BP229-1) was diluted in sterile H_2O for a final 50% stock solution. A 10% (w/v) of skim milk solution was prepared from skim milk powder (Oxoid, LP0033B) in distilled H_2O, first mixing the powder to a smooth paste then gradually adding more H_2O until an opaque withe homogenous mix

was obtained. The solution was autoclaved at 121°C for 5 minutes. Stocks of 200 mM Cys (L-cysteine 98+% Fisher Scientific,11488643) as well as 5 mM Met (L-methionine 98+% Fisher Scientific, 11424083) were prepared in distilled H_2O and autoclaved at 121°C for 20 minutes.

2.1.3.2 Gram-staining reagents

The Gram-staining protocol involved the following solutions that were obtained as a kit from Pro-Lab Diagnostics (Gram Stain Kit Pro-Lab Diagnostics, PL.8055/25) solutions, CV 90%, Gram's iodine, Acetone/ethanol (50:50 v:v), safranin.

2.1.4 Staining and Imaging

To confirm Gram-staining characteristics of each bacterium, Gram-staining, a procedure that discriminate bacteria based on their cell wall, was undertaken. After a smear of a bacterial colony was heat-fixed on a slide, a few drops of CV flooding the smear were added and kept for 1 minute to fix and stain the sample. The slide was then rinsed with distilled H_2O. A few drops of Gram's iodine were added and kept for 1 minute. The slide was subsequently rinsed with distilled H_2O. A few drops of the decoloriser (Acetone/ethanol (50:50 v:v)) were added to the slide for 10 seconds, followed by washing with distilled H_2O, counter-stained with safranin for 40 seconds, rinsed with distilled H_2O, gently dried with absorbent paper, and water-mounted for microscopic observation. Slides observed at the optical microscope (Nikon ECLIPSE E200 Microscope, 40x and 100x objectives). Pictures of colonies on Petri dishes, reaction vials, and any other optical macroscopic pictures were taken with a Xiaomi Redmi Note 10 M2101K7AG; 48 MP, f/1.8, 26 mm (wide), 1/2.0", 0.8µm, phase detection auto focus (PDAF) 8Mpond.

2.1.5 Bacterial growth and maintenance

2.1.5.1 Bacterial manipulation, maintenance and storage

The sterility of bacterial cultures during the manipulations involved in the experiments involving bacterial growth was ensured by being undertaken in an area not larger than 50cm around a Bunsen burner, which was also kept clean, uncluttered and a clear above. Pipettes and micropipette pipette tips, wooden toothpicks, as well as all glass containers used for bacterial growth were autoclaved at 121°C for 20 minutes. Metal Kohle loops (nickel-chromium alloy -nichrome- or platinum) were flamed-sterilized in the Bunsen burner to redness for a few seconds and then allowed to cool down before usage with bacterial cultures. Plastic Kohle loops were also used occasionally, and were purchased sterile from the manufacturer (VWR, United Kingdom). Plastic spectrophotometry cuvettes (VWR, United Kingdom) were not sterile and re-used upon thorough cleaning with soapy water and rinsing with tap water followed by deionized sterile H_2O. A glass spreaders were flame sterilized by dipping the, in ethanol, shaking off the excess alcohol, and igniting the residue. The spreader was allowed to cool before putting in contact with the biological sample.

A permanent stock of bacterial strains was kept at -80°C (**strain collection frozen stock**). It was obtained from exponential grown cultures of each strain prepared as follows. A single colony from

freshly streaked BHIA incubated at 37ºC for 16 hours collected with a sterile Kohle loop was used to inoculate 5 ml of TSB in a 30 ml Universal that was subsequently incubated for 16-hoursat 37ºC and 200rpm. The resulting culture was resuspended in 5 ml of fresh TSB to an initial OD_{600} of 0.01 and incubated at 37ºC, 200rpm until mid-exponential phase was reached, approx. 2 hours. A 1 ml aliquot of the liquid culture was centrifuged (Eppendorf Centrifuge 5424) at 13,000rpm for 1 minute. The supernatant was discarded, and the pellet resuspended in 1 ml of BHI by vortex mixing. A volume of 500ul of a 50% glycerol stock solution was added to the resulting resuspension to reach a final concentration of 15% glycerol (Glycerol (Molecular Biology), Fisher Bioreagents, BP229-1), which is deemed cryoprotectant. The 1.5ml suspension was placed in a 2ml cryovial at -80ºC for permanent storage.

Bacteria for the experiments were obtained from BHIA plates that had been streaked from a scrape from the strain collection frozen stock obtained with a sterile Kohle loop or wooden toothpick. The strain collection frozen stock was never allowed to thaw. The plate was maintained by re-streaking of a single colony on TSA (*E. coli, K. aerogenes, P. vulgaris*), LBA (*P. aeruginosa, S. marcescens*) or BHIA (*S. aureus, E. faecalis, S. salivarius, L. plantarum*) every two weeks (**strain collection plate stock**). Periodically the strain collection plate stock was re-established from the strain collection frozen stock. To activate bacteria out of storage each strain was collected and streaked out on BHI agar (BHIA) plates and grown for 24-48 hours at 37ºC until single colonies appeared on the plates.

2.1.5.2 Preparation of pre-inoculum and inoculum for bacterial growth experiments

Lag or stationary phase bacterial cultures in liquid media or bacteria colonies on solid medium have an inherent heterogeneity in the physiological status of the bacterial cells within the population and in addition there is a variability on those culture across experiments. To maximize the opportunities for a similar physiological status of bacterial populations within an experiment and across experiments involving bacterial growth, exponential cultures were used for the experiments, unless otherwise indicated, that were prepared and standardized as follows., The bacterial inoculum culture stage was preceded by a pre-inoculum culture stage. A 16-hours **pre-inoculum culture** was prepared from a single colony from a strain collection plate stock that was inoculated in 5 ml of LB (or LBEAP1 for *L. plantarum*) and grown at 37ºC, 200rpm. As indicated above, the strain collection plate stock was never older than 2 weeks. Then bacterial cells were diluted in 5 ml of fresh LB to an initial optical density at 600nm (OD_{600}) of 0.01 and was subsequently incubated at 37ºC, 200rpm until exponential phase was reached, generally 2 hours. This culture will be referred to as **inoculum** henceforth.

2.1.5.3 Bacterial growth dynamics and growth rate determination

An inoculum culture (see above) was inoculated in 5 ml of TSB or LB in a 30 ml Universal to a starting OD_{600} of 0.001 and incubated at 37ºC and 200 rpm for 8 hours. This culture would correspond to the **test culture**. The turbidity of the culture was determined measuring OD_{600} every hour with a spectrophotometer (Biochrom, 80-30003-50) using 1 cm path plastic spectrophotometry cuvettes (VWR, United Kingdom). A volume of 700 μl or 1 ml, for narrow or wide volume spectrophotometry cuvettes, respectively, of fresh LB or TSB (depending on the growth medium used in a given

experiment) was used as a blank to adjust the spectrophotometer. Periodically a 1 ml aliquot from the test culture was obtained in sterile conditions (see Bacterial manipulation, maintenance and storage above). The test culture was diluted as necessary (typically 10-fold) in LB or TSB medium, depending on the growth medium of the experiment, for the OD_{600} to be measured not to exceed 0.6, thus staying within the sensitivity range of the technique and the machine.

Simultaneously, the number of viable cells in each sterile aliquot from the test culture was assessed through colony forming unit per ml (CFU/ml) on rich nutrient medium (TSA). The number of viabe cells was measured applying the Miles-Misra method[374]. Briefly, every hour 100 µl of the growing bacterial sample was collected (test culture aliquot) and diluted 1:10 in 900 µl of PBS solution in a microcentrifuge tube. The resulting suspension was then serially diluted in a decimal series in PBS (10-fold dilution in each step) in 1.5 ml microfuge tubes. A drop of 10 µl from each dilution was plated in triplicate on rich nutrient medium, TSA. The culture drops were allowed to dry at RT and were then incubated for 16 hours at 37ºC. The morphological features of the colonies were observed, and the colonies quantified from drops where single colonies were countable and had no more than 40 colonies per 10 µl drop. An average colony count from the three drops for each dilution was calculated and corrected by the dilution factor to establish the number of CFU/ml in the test culture.

The results were plotted as the independent variable (OD_{600} or CFU/ml y-axis) over the dependent variable (time, x-axis). In addition, The CFU/ml were plotted against its corresponding OD_{600} for each hourly timepoint. Such correlation for each bacterial species was harnessed towards an accurate inoculation of bacterial numbers in the pertinent experiments from the OD_{600} values obtained from inoculum cultures. Effectively, OD_{600} was used as an immediate surrogate indicator of the number of cells present within a bacterial culture population. Graphic plots were produced using Prism (GraphPad Software Ltd. vs 9.3.1, 2021, Dotmatics, Boston, United States)

Growth rates (µ) were calculated as per convention (h^{-1}) from values from the exponential phase of bacteria growth, and calculated using the well-established formula $\mu = (\ln N - \ln N_0)/(t - t_0)$, i.e., the natural log of the number of cells at time t minus the natural log of the number of cells at time zero (t_0) divided by that time interval.

2.1.6 Mammalian cells growth and maintenance

Madin-Darby canine kidney (MDCK)[375] cells were kindly gifted by K. Ayscough (University of Sheffield, United Kingdom). MDCK were prepared by and obtained from, Matthew Allott, a member of Dr. Garcia-Lara research group. MDCK cells were grown in Dulbecco's Modified Eagle Medium (DMEM;Corning,15-013-CV) supplemented with penicillin (100 units) streptomycin (100 µg), 4 mM L-glutamine (Sigma, G75-13) and 10% foetal bovine serum (FBS) (Sigma, F7524). MDCK were maintained at 37°C in a 5% CO_2 humidified incubator and passaged at 80% confluency (approx. $3x10^6$ cells/ml). When seeding cells for infection assays, DMEM with all the above described additives, except the antibiotics (penicillin and streptomycin) was used.

2.2 Human microbiota *in vitro* co-culture competition

The project is underpinned by the premise of gaining an understanding of human intestinal microbiota species population dynamics and selection, through competition studies involving a reduced number of species *in vitro*. To that effect the most basic simple to initiate the investigation was to set-up pairwise bacterial co-culture competition experiments, which are described below. Similar, experiments with three different bacterial species were also undertaken.

2.2.1 Bacterial liquid co-culture competition experiments set-up

Pre-inoculum culture and inoculum culture were prepared for two bacterial strains growing independently in LB medium at 37ºC and 200 rpm as described above. A total of 10^5 cells from each of both exponentially growing inoculum cultures were inoculated into 5 ml of LB, corresponding to (t_0) of the experiment. In selected experiments LB was supplemented with $ZnCl_2$ (0.25 mM) to assess possible population switches led by this micronutrient. The cultures were then incubated at 37ºC and 200rpm for 48 hours. Samples were collected and their CFU/ml determined as indicated above at different timepoints (0, 8, 24 and 48 hours from inoculation) evaluating any differential prevalence over time colony properties discrimination. When the latter differentiation between bacterial species was not possible, molecular methods were designed and implemented. All experiments were performed at least in duplicate.

2.2.2 Colony properties and PCR-based bacterial species discrimination in co-cultures

The species used differ on their morphological properties and/or on their ability to differentially grow on differential and/or selective media (Table 2.2 and Table 2.3) . Those differences were used to distinguish between separate colonies from one or another species on growth medium solid plates from co-culture experiments. When colony-based or differential/selective growth medium discrimination was not possible, molecular tools were designed and employed, i.e., polymerase chain reaction (PCR) or quantitative polymerase chain reaction (qPCR) for qualitative and quantitative examination of single species, respectively.

2.2.2.1 *16S rRNA* genes library preparation and species-specific primer design

The 16S ribosomal RNA (*16S rRNA*) is the RNA component of the 30S subunit of prokaryotic ribosomes. Due to its high conservation among bacteria, the *16S rRNA* sequence has been utilized since 1977 for the phylogenetic differentiation of bacterial species[376]. However, the use of such sequence for that purpose is typically accompanied by DNA sequencing of the corresponding sequence. Such approach is particularly necessary when studying rich mixed-species bacterial populations. And especially so, if they include phylogenetically close species (e.g., *Escherichia, Klebsiella* and *Serratia*, or staphylococci and enterococci), as the level of identity of their *16S rRNA* sequences can be as high as 97.4%. However, given the costs entailed by comprehensive DNA sequencing necessary for any subset of colony isolates from co-culture experiments, we considered

and explored the design of specific primer pairs capitalizing on minor differences between the *16S rRNA* genes in the various species to be used in this study.

To identify the *16S rRNA* sequences for the species/strains in this study, 510,000 *16s rRNA* sequences available in the SILVA Reference Non Redundance database[377] were downloaded and stored in DNA/protein sequence manager and analyser Geneious Prime® 2021.1.1 (Biomatters, New Zealand; now Dotmatics, United States). The following *16S rRNA* sequences were found in the SILVA database, *Escherichia coli* NTCT12241 *Pseudomonas aeruginosa* PAO1*, Enterococcus faecalis* NCTC775. For the rest strains, with not identified in the SILVA database (*Serratia marcescens* NCTC1377*, Proteus vulgaris* NCTC4175*, Klebsiella aerogenes* NCTC10006*, Lactobacillus plantarum* NCTC6376, *Streptococcus salivarius* NCTC8618, and *Staphylococcus aureus* NCTC12981) the full genome sequences were downloaded from NCIMB database[378]. As bacterial strains have multiple copies of *16S rRNA* genes, for each full genome sequence, all the *16S rRNA* genes were extracted and aligned using the same Geneious software confirming that the *16S rRNA* genes in a given strain were 100% identical. A randomly selected single *16S rRNA* gene for each strain was used as an exemplar to pursue an species-specific primer design.

First hypervariable regions for every strain were identified and selected as preferred targets for species-specific primer design. Then, with the resulting regions were analysed using several primer design tools to inform the selection of potential primers and primer pairs, namely, Geneious Prime®2021.1.1, GenScript®[379], and IDT® PrimerQuest Tool[380]. The criteria chosen as parameters in the analysis of the sequences based on available literature and experience within the research group were:

- A melting temperature (Tm) in the 50-58°C range
- An oligonucleotide length of 16-24 bp
- Low chance of harpin, self-dimerization of an oligonucleotide, and hetero-dimer formation between different primer pairs in one species, as determined by agreement by more than one tool, including Oligo Analyzer Tool (Sigma-Aldrich®[381]) and PrimerQuest Tool (IDT®)[380].
- Low chance of cross-reactivity between primer pairs, i.e., the capacity of a species-specific primer to bind to a different bacterial sequence (in principle 16S RNA, but it could be any unspecific binding) amongst the strains as determined by Geneious Prime®2021.1.1
- Whenever possible, a GC clamp at the 3' end of the oligonucleotide was preferred, or alternatively a G, a C or combinations of these bases

In addition, I designed an A-T rich sequence tail of 4-5 bases in length non-complementary between the forward (F) and reverse (R) primers was added at the 5' end of each oligo to avoid 5' interactions thus increasing primer binding opportunities at the 3' end, which typically result in a more productive PCR reaction. The primers resulting from the thorough analysis indicated above are listed in Table 2.5. The validity of their application for the intended purpose was determined through PCR. The conditions for the PCR were selected from the information generated by the tools above, but also through refinement in cases of experimental failure.

Table 2.5: **16s rRNA primers designed for each bacterial species used in this study.** Direction of the oligonucleotide - reverse or antisense (R), forward or sense (F) - , Name given to the primers, sequence of the primers with the 5' tail in red, Melting temperature (Tm) , Annealing temperature (Ta) used per set and expected fragment length are indicated.

Bacterial Species	Direction	Name	Sequence (with extension)	Tm (°C)	Ta (°C)	Fragment length (bases)
K. aerogenes NCTC1006	R	aEAP24Ueaer	ATATCCAAAGCATCTCTGCTA	54.2	52.5	951
K. aerogenes NCTC1006	F	sEAP24Jeaer	TAATCAGAGAGCTTGCTCTCG	57.3		
E. faecalis NCTC775	R	aEAP24Vefae	ATATTTCAGTTACTAACGTCCTT	53.3	51	404
E. faecalis NCTC775	F	sEAP24Oefae	ATAAGCACTCAATTGGAAAGAG	54.4		
E. coli NCTC12241	R	aEAP24Lecol	ATAACTCATCTCTGAAAACTTCCG	56.8	53	572
E. coli NCTC12241	F	sEAP24Kecol	TATAAGTAAAGTTAATACCTTTGCTC	53.5		
L. plantarum NCTC6376	R	aEAP24Flpla	ATTACTCAGATATGTTCTTCTTTAAC	53.5	51	401
L. plantarum NCTC6376	F	sEAP24Slpla	ATAAGCATCATGATTTACATTTGAG	54.3		
P. vulgaris NCTC4175	R	aEAP24Gpvul	ATTTTCACTCCTCTATCTCTAAAGG	55.9	51	585
P. vulgaris NCTC4175	F	sEAP24Tpvul	ATTAATGTTAAGATTAATACTCTTAGCA	53.7		
P. aeruginosa PAO1	R	aEAP24Dpaer	ATATCGCCACTAAGATCTCAAGGAT	59.3	56	224
P. aeruginosa PAO1	F	sEAP24Ppaer	ATATAAACTACTGAGCTAGAGTACG	55.4		
S. marcescens NCTC1377	R	aEAP24Nsmar	ATATAGAGTAACGTCAATTGATGAAC	55.5	55	417
S. marcescens NCTC1377	F	sEAP24Msmar	ATATAGAGCTTGCTCCCTGGG	58.7		
S. aureus ATCC25923	R	aEAP24Nsaur	AATAATACACATATGTTCTTCCCTAATAA	55.4	55	266
S. aureus ATCC25923	F	sEAP24Msaur	TTTAACGGTCTTGCTGTCACTTATA	58.5		
S. salivarius NCTC8618	R	aEAP24Lssal	ATATTACTTTCCACTCTCACACTCG	58.4	57	310
S. salivarius NCTC8618	F	sEAP24Wssal	ATTATCCGCATAACAATGGATGACA	59		

R, reverse primer; F, forward primer. Forward or reverse were considered in regard to the *16S rRNA* gene 5' to 3' or 3' to 5' orientation.

2.2.2.2 DNA extraction

DNA extraction from bacterial cultures was required to use the DNA as a template for PCR and qPCR reactions. The use of enzymatic methods (e.g., lysozyme) demands protocol variations between Gram-negative and Gram-positive organisms. As the former has an outer membrane, it requires for instance its chemical-mediated removal (e.g., using EDTA) before using lysozyme. Also, some species, like the staphylococci, are more refractory to lysozyme lysis, and lysostaphin would be a better lytic enzyme. However, there is a particular variability between lysostaphin specific activity across sources/stocks (Prof. Simon Foster, University of Sheffield, personal communication). Alkali lysis of cultures is another common protocol for bacterial DNA extraction but more efficient with Gram-positives than Gram-negatives. In all these case, further DNA purification is required whether through column-mediated adhesion/elution kits traditional chloroform:isopropanol extraction and salt-mediated precipitation.

These protocols may still display heterogeneity in lysis efficacy, extraction and purification for different colony isolates. The variety of reagents and conditions, and the need to ensure proportional lysis from bipartite or tripartite species in co-cultures would introduce the complexity of a significant number of assessments to standardize the enzymatic and chemical protocols per species and combination of species. Consequently, I explored the possibility of using physical methods to enable easier

standardization and high throughput. The protocol of choice was the use of repetitive cycles of freeze-boiling. Different times at -80°C and 100°C were considered with the combination of a cycle of 5 minutes at -80°C and 3 minutes at a 100°C proving the most efficient method. The number of cycles vary based on the bacterial resistance to lysis. A total of 4 cycles for Gram-negative species as well as *E. faecalis* and *S. salivarius*, and 8 cycles for the rest of Gram-positives, *S. aureus* and *L. plantarum*. Estimation of the minimum but sufficient number of cycles for full lysis was important to maximize DNA yield but minimize DNA damage. Full apparent lysis by naked eye observation, productive DNA amplification (reduced number of cycles resulted on no detectable bands), and absence of viable cells after the ideal number of cycles and freezing:boiling treatment indicated above was confirmed. The samples for DNA extraction corresponded to 1ml from the co-culture after 16 hours of cultivation, which was spun down at 13,000rpm for 1 minute at RT, resuspended in 1ml of LB. Subsequently, the freeze:boiling cycles were applied as described above, the sample centrifuged (13,000rpm, 1 minute, RT), and any pellet with debris discarded. The supernatant corresponded to the **DNA template**. The Purity of DNA was measured with a Thermo Scientific, Nanodrop 2000c spectrophotometer.

2.2.2.3 *16S rRNA* amplification: qualitative and semi-quantitative PCR

The *16S rRNA* genes were amplified by PCR in a thermal cycler (Veriti 96 Well Thermal Cycler – Applied Biosystems by Thermo Fisher Scientific, UK). DreamTaq DNA Polymerase, oligonucleotides (Table 2.5)- and dNTPs were purchased from Thermo Fisher Scientific. The PCR reactions were set up according to the DreamTaq manufacturer's recommendation [382] . Briefly, the reaction mixture contained 1 µl of DNA template, 0.5U of DreamTaq, 1x DreamTaq buffer, 200 µM dNTPs and MilliQ (MQ) ultrapure H_2O up to 20 µl final volume. An initial denaturation step was run at 95ºC for 1 minute. Every amplification cycle consisted on thermal denaturation at 95°C for 15 seconds, followed by a variable annealing temperature depending on the primer set for 30 seconds (Table 2.5), and extension at 72°C for a length of determined by the length of the expected amplicon. The latter was calculated based on the DreamTaq DNA polymerase processivity (1 minute/kb). The amplification cycle was run 30 times. A final extension step at 72°C for 5 minutes followed by incubation at 12°C concluded the reactoin. The amplicons were separated in 1.5% agarose gel by electrophoresis (100V for 25-30 minutes) using the Gene Ruler 100bp DNA ladder (ThermoFisher Scientific, 1304158) to size the resulting amplicons. Agarose powder, TAE 1x buffer and GelRed Nucleic acid stain loading buffer -10,000x in H_2O- were purchased from Thermo Fisher Scientific (UK). Bands were observed through Bio-Rad Gel-Doc System.

Species-specificity or cross-reactivity for each of the oligonucleotides was determined using DNA samples from single cultures against heterologous primers from other species. Other genes (i.e., housekeeping genes and prodigiosin genes) and related primers already used and described in literature were adapted to our bacterial sequences and purchased as a back-up plan in case designed 16s rRNA primer would have not worked (Table 2.6 and

Table 2.7). Although not used in this PhD Thesis, the design efforts and production offer an opportunity for immediate downstream experimentation in follow up projects.

The methods above will show the presence or absence of a given amplicon, and in turn of a given bacterial DNA template, therefore indicate the presence of a given bacterial species. However, it would not inform the number of bacteria present in the sample. Two methods were considered and employed for a semi-quantitative and quantitative determination of bacterial cell density within a population using PCR. The semi-quantitative determination of the differential presence of one bacterium versus another in a bacterial co-culture consisted on the use of DNA templates for PCR reactions obtained from serial dilutions of the DNA sample from the test culture. The principle underpinning the technique is that in the co-culture experiment, initially each bacterial species is inoculated at the same cell density. With a certain ratio of amplicons of one species compared to amplicons of another species (run in independent PCR reactions from the same DNA sample). An imbalance in this ratio over co-culture incubation time would suggest the prevalence of one strain compared to the other. The serial dilutions of each DNA sample were made in MQ ultrapure H_2O and amplification of the diluted samples with PCR conditions as indicated above.

Table 2.6: **Prodigiosin primers designed for each bacterial species used in this study.** Direction of the oligonucleotide - reverse or antisense (R), forward or sense (F) - , Name given to the primers, sequence of the primers with the 5' tail in red, Melting temperature (Tm) , Annealing temperature (Ta) used per set and expected fragment length are indicated. Primers adapted from Jia *et al.* [383]

Bacterial Species	Direction	Name	Sequence (with extension)	Tm (°C)	At (°C)	Fragment length (bases)
S. marcescens NCTC1377	R	aEAP165b pigA	AAATAAACAGTGTCGGCTAATGCTC	60.2	58	118
S. marcescens NCTC1377	F	aEAP165d pigB	AATTAAAACCGATCCTCGAACG	57.1		
S. marcescens NCTC1377	R	aEAP165f pigD	ATATAATGATGGATGAATTCAAGGG	55	54	120
S. marcescens NCTC1377	F	aEAP165h pigE	TTTTTATCCGTTCGTCAGCG	56.9		
S. marcescens NCTC1377	R	aEAP165L pigF	AAAATGTCGCTGAACATGCTGG	60.4	55	447
S. marcescens NCTC1377	F	aEAP165N pigG	AAATAGCATATCGCCACCCAGTATC	60.9		
S. marcescens NCTC1377	R	aEAP165p pigI	ATATATCAGCGATACACAACTGAC	56.5	54	145
S. marcescens NCTC1377	F	aEAP165r pigN	TATTTCATGATCTTCGGCGGC	58.9		
S. marcescens NCTC1377	R	sEAP165a pigA	TTAAAACGGCATATTCGGAAATCAAC	59.3	57	136
S. marcescens NCTC1377	F	sEAP165c pigB	ATTTATGATTGTCCATCCAATTGG	55.8		
S. marcescens NCTC1377	R	sEAP165e pigD	ATATAATTCGTCGTCGCTGACC	58.4	59	203
S. marcescens NCTC1377	F	sEAP165g pigE	ATATAGAATTTCCAGGTGGTGTG	56		
S. marcescens NCTC1377	R	sEAP165i pigF	AAATACGATCAGGGTGCGTG	58.3	55	150
S. marcescens NCTC1377	F	sEAP165M pigG	TAAAGCACCAGCGCAACCATC	61.8		
S. marcescens NCTC1377	R	sEAP165o pigI	TAATAAGCCTGGCAATCTTTCTG	56.9	59	194
S. marcescens NCTC1377	F	sEAP165q pigN	TTTTAGCCGCTGTTCAGCAACC	62.2		

Table 2.7: **Housekeeping genes designed for each bacterial species used in this study**. Direction of the oligonucleotide - reverse or antisense (R), forward or sense (F) - , Name given to the primers, sequence of the primers with the 5' tail in red, Melting temperature (Tm) , Annealing temperature (Ta) used per set and expected fragment length are indicated. Primers adapted from Besler *et al.*[384], Duary et al[385]., Sakuraoka *et al.*[386], Zhang *et al.*[387]

Bacterial Species	Direction	Name	Sequence (with extension)	Tm (°C)	At (°C)	Fragment length (bases)
S. marcescens NCTC1377	R	aEAP166b adk	TTTTTGCCGCTTCTTTGCTGTAG	60.8	56	468
S. marcescens NCTC1377	F	aEAP166d gyrB	TATATCAGCGTACGAGTCATC	54.6		
S. marcescens NCTC1377	R	aEAP166f mdh	AATAAAGAGACAGACCGAAACG	56.5	54	525
S. marcescens NCTC1377	F	aEAP166h recA	ATTATTCGCCGTACATGATTTG	55.3		
S. marcescens NCTC1377	R	sEAP166a adk	AAAATGGTAAAGGTACTCAGGC	56.3	54	468
S. marcescens NCTC1377	F	sEAP166c gyrB	ATTTATCGACGACAACTCCTATAAAG	57.2		
S. marcescens NCTC1377	R	sEAP166e mdh	TTTTACGTGGTGCTGATTTCC	57.1	52	465
S. marcescens NCTC1377	F	sEAP166g recA	TTTTGCTGGATCCTATCTATGC	56		
P. aeruginosa PAO1	R	aEAP167b ampC	TATACGGTGAAGGTCTTGCT	56	54	240
P. aeruginosa PAO1	F	aEAP167c fabD	AAATTATCCCTCGCATTCGTCT	57.9		
P. aeruginosa PAO1	R	aEAP167g rpoD	AAAAAAGAAGGAAATGGTCGAGG	57.5	55	128
P. aeruginosa PAO1	F	sEAP167a ampC	TAATTATTCCCCTGCCTGTGC	58.1		
P. aeruginosa PAO1	R	sEAP167d fabD	AAAAAGGCGCTCTTCAGGAC	58.8	54	123
P. aeruginosa PAO1	F	sEAP167h rpoD	ATATTGGAGAACTTGTAGCCG	55.5		
L. plantarum NCTC6376	R	aEAP168b gyrB	ATTTAATCCCACGACCGTTATC	56.3	55	57
L. plantarum NCTC6376	F	aEAP168c ldhL	TATATGATCCTCGTTCCGTTG	55		
L. plantarum NCTC6376	R	aEAP168e recA	TATAAGAACAGATCAAGGAAGGAAC	56.4	53	123
L. plantarum NCTC6376	F	sEAP168a gyrB	TTATAAATTGATGAAGCCCTAGCAG	57.3		
L. plantarum NCTC6376	R	sEAP168d ldhL	AAAAACGAACACCATCTTCTAAC	55.7	53	81
L. plantarum NCTC6376	F	sEAP168f recA	ATATAGATACCTTGACCATACATG	53.3		
E. coli NCTC12241	R	aEAP169a fumC	ATATTCGTCGTTAGGGTGAAC	55.5	55	274
E. coli NCTC12241	F	aEAP169d gyrB	AAAATCCATGTAGGCGTTCAGG	59		
E. coli NCTC12241	R	aEAP169e recA	ATTTTCGCATTCGCTTTACCCTG	60.4	55	743
E. coli NCTC12241	F	sEAP169b fumC	ATATTGGAGCATTTCCGCATTTC	58.1		
E. coli NCTC12241	R	sEAP169c gyrB	TTAAACATGGTATTCGAGGTGG	56.2	57	373
E. coli NCTC12241	F	sEAP169f recA	TTAAACGTATGATGAGCCAGGC	58.8		

2.2.2.4 Quantitative PCR

To further complement the qualitative and semi-quantitative PCR data, real-time PCR was performed using the SYBR® Green PCR Master Mix (Thermo Fisher Scientific, 4368577), designed primers (10 µM each), 1 µl of the DNA template and MQ ultrapure H_2O to reach the desired reaction volume of 10 µl. Amplification was conducted in the QuantStudio™ from Applied Biosytems in a 96-well plate. The mixture was heated at 95°C for 10 minutes (DNA denaturation), then subjected to 40 cycles of thermal cycling at 95°C for 15 seconds, 52ºC (average annealing temperature) set for 30 seconds, and 60°C for 40 seconds (extension). Results were analysed and plotted with the QuantStudio™ associated software. The threshold ct was automatically set based on the amplification curves.

2.3 Characterization of "bull's eye" pattern formation from liquid co-cultures

Co-culture competition experiments between *E. coli* NCTC12241 and *S. marcescens* NCTC1377 revealed the presence of a "bull's eye" pattern (Section 4.1) on TSA incubated at 37ºC for 16 hours, with an apparent differential and regular spatial distribution in the colony of *S. marcescens* (red coloured regions in the centre and edge of the colony) and *E. coli* (white colour region in middle section between the two *S. marcescens* regions). The following sections describe efforts taken towards the characterization of the phenomenon.

2.3.1 Determination of differential species distribution in the "bull's eye" pattern

It was first necessary to determine whether those different sections in the "bull's eye" pattern correspond to absence or decrease of any of the species in each region, or whether the pattern is due to phenotypic pigmentation differences of the species in the sections. Bacterial samples from a circular area of approximately 1 mm in diameter (0.78 mm^2) from the three different sections of the pattern were collected with a Gilson 10P microbiological pipette loaded with a sterile 200μl micropipette "yellow" tip. The colony sample was resuspended in 1ml of PBS. Subsequent dilutions in the same buffer were performed to an approximate concentration of 500 cells/ml. Given the similar growth rates, absorbance values and viable counts during growth in LB of *E. coli* NCTC12241 and *S. marcescens* NCTC1377, the CFU to OD_{600} conversion growth curves obtained in Section 3.1 were used here. The calculated CFU/ml were multiplied by 1.27 (1 ml/0.78 mm^2) to convert to CFU/mm^2. Aliquots of 200 µl aliquot from the resulting dilution were spread on different TSA plates, allowed to dry and incubated at 37ºC for 16 hours. The objective of this "high volume over high area" plating was to maximise the opportunities to recover a sufficient number of colonies from both species to enable at least a two logarithmic units dynamic range difference between both species. The discrimination of *Escherichia* or *Serratia* colonies was based initially on colony morphology, white/cream and red, respectively.

To discriminate whether the white morphology characteristics of the single colonies on TSA plates may be a reversible physiological adaptation, which has been observed in certain strains of *Serratia* or were maintained in subsequent generations, 5 single white colonies and 5 single red colonies from each of the previous plates above, were re-streaked on fresh TSA plate and incubated for 16 hours at 37ºC. As a control to study the colony morphology characteristics of *S. marcescens* NCTC1377 growing as a monoculture on different agar media (Table 2.2) in conditions resembling those of the bipartite species co-culture, 1µl drops containing 10^5 cells from an exponentially growing culture inoculum of *S. marcescens* NCTC1377 in LB were placed on the corresponding media, placed in the 37ºC and 26ºC incubator with controlled humidity (adapted from Čepl *et al.*, 2019[388]) and colony characteristics were monitored and imaged daily for 7 days.

2.3.2 Liquid co-culture growth dependence for *S. marcescens* and *E. coli* for "bull's eye" pattern distribution

The dependence of the formation of the "bull's eye" pattern on TSA from joint growth of *E. coli* NCTC12241 and *S. marcescens* NCTC1377co-cultures in liquid preceding the deposition on solid agar medium was determined as follows. Exponentially growing independent culture inocula of *E. coli*

NCTC12241 and *S. marcescens* NCTC1377 were prepared as previously described (Section 2.1.5.3). The cultures were mixed at a 1:1 ratio to a final combined cell density of 10^8 cells/ml. Immediately, 10ul drops containing 10^6 combined number of total cells from the culture mix were placed on TSA plates, allowed to to dry and then incubated at 37°C for 16 hours.

2.3.3 Mono-/co-culture conditioned medium effect on "bull's eye" pattern formation

The possibility of an extracellular signal released by *E. coli* NCCT12241 in response to growth in the presence of *S. marcescens* NCTC1377 and vice-versa mediating "bull's eye" pattern formation process when in co-culture was considered. To test whether conditioned medium (CM) from the co-culture of *S. marcescens* NCTC1377 and *E. coli* NCTC12241 can lead *S. marcescens* NCTC1377 to form the "bull's eye" pattern, the co-culture was grown from pre-inoculum/inoculum process in TSB (as the pattern was observed in TSA plates but not in LBA) for 24 hours (37°C, 200 rpm). 1 ml samples were collected every hour after inoculation of the test culture and centrifuged at 13,000 rpm for 1 minute. The pellet was discarded. The supernatant, which corresponded to the CM, was collected and filtered sterilized with 0.22 µM pore filter (StarLab). This filtered CM (fCM) added to a PBS-washed pellet of exponentially grown *S. marcescens* NCTC1377 as described above. The *S. marcescens* pellet was gently resuspended in the fCM and plated on TSA plates at a volume and total cell number known to form the pattern, i.e., 10 µl containing 10^6 cells. The drops were dried at RT and incubated at 37°C for 16 hours.

To determine whether the CM from either or both of the mono-cultures of *E. coli* NCTC12241 and *S. marcescens* NCTC1377 may also contain a possible extracellular signal leading "bull's eye" pattern formation, the same protocol was applied to fCM obtained from each of the mono-cultures. As an additional control, the independence from CM on the formation of the "bull's eye" pattern was also assessed as follows. Volumes of 1 ml of exponentially grown *E. coli* NCTC12241 and *S. marcescens* NCTC1377 co-cultures grown as described in Section 2.1.5.2 were washed by centrifugation (13,000 rpm,1 minute, RT), the supernatant (i.e., the CM) was removed, and the remaining pellet was then resuspended in 1ml of PBS. The same wash operation was repeated resulting cell suspension in PBS was plated on TSA at the desired concentration, volumes of 10 µl each containing 10^6 cells.

The possibility that an extracellular signal was produced and released by the co-culture on solid media (sCM), and may still be remain within the "bull's eye"-patterned colony, compared to the potential signal already be present in the preceding CM resulting from liquid co-culture growth was also assessed. Ten "bull's eye" patterned colonies resulting after 24 hours growth on TSA at 37°C of co-cultures setup as previously described (Section 2.3.2) were collected and resuspended in LB, each colony in 1ml, to allow any possible extracellular signal to diffuse into the liquid eluent. After centrifugation (13,000 rpm for 1 min), the pellet was discarded and the liquid filter sterilized through 0.22 µM polyvinylidene fluoride sterile filters (StarLab),and labelled as sCM. PBS-washed pellets isolated from exponentially grown culture inocula of *S. marcescens* NCTC1377 as indicated above were resuspended in a range of dilutions (in LB) of the resulting sCM, and plated in 10µl volumes on TSA plates. Once the drops dried, plates were incubated at 37°C for 16 hours

2.4 Establishment and characterization of the "bull's eye pattern" from independently grown cultures of *S. marcescens* and *E. coli*

2.4.1 Species in-liquid contact dependence for "bull's eye" pattern formation

I have shown the formation of a bull's eye pattern on TSA after 16 hours at 37°C from a 1:1 inoculum with 10^5 to 10^6 cells of *S. marcescens* NCTC1377 and *E. coli* NCTC12241 obtained after growth in LB for 8 hours at 37°C and 200rpm. To determine whether such joint growth in liquid preceding the plating is necessary for the "bull's eye" pattern to form, independent exponentially grown cultures of *E. coli* NCTC12241 and *S. marcescens* NCTC1377 as described in Section 2.1.5.2 were produced. The cultures were then mixed at a 1:1 ratio to a combined cell density of approximately $1x10^8$ cells/ml. Drops of 10 µl, thus containing a combined total from both species of 10^6 cells were immediately plated on TSA, air-dried at RT, and incubated for 16 hours at 37°C

2.4.2 Time-lapse-based determination of "bull's eye" pattern formation onset

To determine the timeframe when the "bull's eye" pattern first forms, the pattern was allowed to generate from independently grown cultures of *S. marcescens* NCTC1377 and *E. coli* NCTC12241 that were subsequently mixed and immediately plated on TSA and allowed to dry at RT, as indicated above. From the time of seeding, periodically for 24 hours a sample was taken from the locations where the sectors were predicted to be. Such prediction was based on the area covered by the dried drop and the experience accumulated on the reproducible location of where the sectors would be. Reasonably, the sectors of the "bull's eye" pattern are not visually recognisable during the early hours after seeding. Samples were generally taken every 1 to 2 hours except the 14 hours overnight interval with restricted access to the laboratory facilities. The analysis of the presence of *S. marcescens* or *E. coli* in a given sector was based on colony morphology, red and white, respectively. Confirmation of the retained phenotype was subsequently obtained by re-streaking of colonies.

2.4.3 Inocula cell density impact on "bull's eye" pattern generation

The "bull's eye" pattern was identified from equal concentration mixtures of *S. marcescens* NCTC1377 and *E. coli* NCTC12241 plated on TSA at combined initial inoculum cell numbers of 10^5 to 10^6 on the plate. To test whether overall cell densities or differential concentrations of either species at inoculum may affect pattern formation or distribution of the sections, exponentially grown populations of both species, were mixed at different cell densities and ratios in a cross-grid that ranged from 10 to 10^7 cells in the 10 µl drop that were seeded on TSA plates. The plates were incubated for 16 hours at 37°C to reproduce the conditions used in equivalent experiments but using exponential co-cultures of both species, as inocula for the plates.

2.5 Identification of extracellular factors influencing "bull's eye" pattern generation

To complement studies on the role of using CM from spent mono- and co-cultures of *S. marcescens* NCTC1337 and *E coli* NCTC12241 on "bull's eye" pattern generation, readily available exogenous reagents that may act as nutrients, waste products or signals could be explored.

2.5.1 Role of growth medium and selected nutrients "bull's eye" pattern production

The "bull's eye" pattern formed by co-cultures of *S. marcescens* NCTC1337 and *E coli* NCTC12241 has thus far been shown on this project as presenting on TSA plates. To determine whether it is a medium-specific and in turn nutrient/component-dependent process, the ability to form on other general purpose rich solid growth media (LBA, BHIA, and NBA) was also studied. In addition, given the heterogeneous composition amongst nutrient media, selected nutrients/components were added to inform specific influences in the process, which may simultaneously contribute towards the future mechanistic understanding of the process. LBA depleted from salt would inform the lack of NaCl in TSA, while LBA supplemented with glucose and/or dipotassium hydrogen phosphate (who may act as a buffering agent) at concentrations equivalent to those in TSA may inform their role in the latter.; NBA supplemented with glucose enable to approximate to conditions reported by Čepl *et al.*[388] who did report the formation of an apparent self-forming similar "bull's eye" pattern in mono-cultures of a different strain of *S. marcescens* (5965). CLED Agar was used as a differential growth media to potentially highlight the differential distribution of the two strains on the agar plate. Inoculation of all these media was done in conditions identical to those previously described for TSA, briefly, 10 µl drops containing 10^6 cells from exponential growing liquid (LB) mono-culture of *S. marcescens NCTC1377* or *E. coli* NCTC12241 or a 10 µl drop of a combined 10^6 cells from a 1:1 mixture of each species; once plates were dried, they were incubated at 37ºC for 16 hours.

2.5.2 Signal-mediated "bull's eye" pattern formation

The strain used in my study, *S. marcescens* NCTC1377, does not form the "bull's eye" pattern when grown by itself on any of the solid growth media assayed. However, the fact that the presence of *E. coli* NCTC12241 in co-culture with *S. marcescens* NCTC1377 on TSA at 37ºC results on the formation of a "red and white" geometric pattern suggests that there must be a mediator or set of mediators produced either or both strains leading the process. It may be a nutrient/s, a waste product/s, or an intra-/inter-species extracellular signal/s. CM experiments suggested that no extracellular signal was involved, that it was labile, or that I may involve close cell-to-cell contact for release and receipt.

AAs, such as methionine (Met) and cysteine (Cys) have been shown to play a role in synchronizing activities within bacterial populations, for instance as either signals or precursors of signalling molecules in QS mechanisms [389]. Therefore, we have considered to determine whether the presence of those AAs on the growth medium may affect the patterning of *S. marcescens* NCTC1377, *E. coli* NCTC12241, *E. coli* NCTC10418 and their respective co-cultures.

Based on the values found in the literature and the concentration present in CLED growth medium, we have supplemented our TSA plates with 2 mM Cys (L-cysteine 98+% Fisher Scientific, 11488643) and 50 µM Met. Co-cultures of *S. marcescens NCTC1377* or *E. coli* NCTC12241 prepared in conditions that lead to the "bull's eye" pattern on the media indicated above fail to generate the same pattern in CLED. CLED is supplemented with 2 mM Cys. Supplementation at the concentrations indicated was provided from filter-sterile liquid stocks of these AAs that were added to warm (60ºC) TSA and gently mixed before pouring into Petri dishes.

2.6 *S. marcescens* NCTC1377 growth partners influencing the formation of the "bull's eye" pattern

The "bull's eye" pattern noticed in *S. marcescens* NCTC1377 on TSA does not occur when this *Serratia* strain grows by itself but when it grows in the presence of *E. coli* NCTC12241. It is important to determine whether other species and strains are able to lead the same pattern development.

2.6.1 Impact of *E. coli* NCTC1224 neighbouring bodies on *S. marcescens* NCTC1377 prodigiosin expression and colony patterning

Liquid cultures of *S. marcescens* NCTC1377 have revealed a reduction of prodigiosin production when *Serratia* is in the presence of *E. coli* NCTC1224 (Section 4.1.7). To inform whether the presence of *E. coli* matrices (well-developed colonies) in the vicinity from *S. marcescens* colonies influence space distribution and/or colony's morphology as well as prodigiosin gene expression in the latter, the following experiment was conducted.

Exponentially growing *E. coli* NCTC12241 in LB at 37ºC (200rpm) was streaked on three TSA plates as a broad streak encompassing the width of the plate, with a 10 µl metal Kohle loop. Simultaneously, a *S. marcescens* NCTC1377 exponential growing LB culture was serially diluted in PBS. Four 10 µl drops, each containing respectively 5, 500, 5.000 and 500.000 cells were seeded in the vicinity of *E. coli* matrices at different distances from 0.5 to 3 cm. Once the drops air-dried, plates were incubated at 37ºC, with controlled humidity, for 6 days. Macroscopic pictures were taken every 24 hours.

2.6.2 *S. marcescens* NCTC1377 in co-coculture with strains other than *E. coli* NCTC12241

As previously described *S. marcescens* NCTC1377 was grown jointly with a set of bacterial strains, including the strain leading the appearance of the "bull's eye" pattern, *E. coli* NCTC12241. Namely, *Proteus vulgaris* NCTC4175, *Klebsiella aerogenes* NCTC10006, *Pseudomonas aeruginosa* PA01, *Lactobacillus plantarum* NCTC6376, *Streptococcus salivarius* NCTC8618 or *Enterococcus faecalis* NCTC775). None of those co-cultures led to the formation of a similar pattern. To see whether the effect was *E. coli*-species specific, we have grown *S. marcescens* NCTC1377 with another *E. coli* strain (*E. coli* NCTC10418) available in the strain collection in conditions that replicate those used for the co-culture and plating of *E. coli* NCTC12241.

2.6.3 Addition of a third strain in the co-culture *S. marcescens* NCTC1377 - *E. coli* NCTC1224

The discovery of the "bull's eye" pattern resulting from a bipartite combination of strains (*S. marcescens NCTC1377* or *E. coli* NCTC12241) and potentially mediated my nutrients, waste products or signalling molecule led the consideration of whether the presence of an additional strain, potentially able to consume those nutrients, release the same or different waste products and/or produce/use signals may interfere with pattern development. Two frequent colonizers of the enteric system were independently added to the bipartite combination the *S. marcescens* NCTC1377 / *E. coli* NCTC1224 to see whether they may alter interplay between these two species, specifically, the Gram-negative, *E. coli* NCTC10418, and a Gram-positive, *E. faecalis* NCTC775.

Following the protocol previously described, a 10 µl drop containing 10^6 bacterial cells of the exponentially grown cultures of *E. coli* NCTC12241 and *S. marcescens* NCTC1377 plus either *E. coli* NCTC10418 or *E. faecalis* NCTC775, at a ratio of 1:1:1, were mixed and immediately plated on TSA. Once air-dried, plates were incubated at 37ºC for 16 hours. Mono-cultures of each of these bacterial species were processed in a similar manner as controls.

2.7 Structure-function implications of the "bull's eye" pattern: virulence

The phenotypic characteristics of bacterial colonies on growth medium can be observed as the macroscopic manifestation of morphogenes and can be accompanied by genome-wide changes. In our case, the formation of the "bull's eye" pattern may grant changes in genes expression in *S. marcescens* NCTC1377 and/or *E. coli* NCTC12241 which may lead an alteration of bacterial physiology, virulence or pathogenesis, as seemingly occurring with prodigiosin expression. Hence, we have assessed, i.e., antibiotic resistance, motility, haemolysis, proteolysis, biofilm formation and infection capacity, to identify any changes on these variables in co-culture cells from a "bull's eye" pattern compared to cells isolated from mono-culture colonies or in conditions which do not lead the formation of such a geometric pattern.

2.7.1 Antibiotic sensitivity and resistance of cells in the "bull's eye" pattern

Serratia marcescens strains are typically multi-resistant to antibiotics, including natural resistance to extended spectrum β-lactamases, macrolides, first generation cephalosporins, and they seem to be displaying increasing resistance to aminoglycosides. Quinolones appear to be highly active against *Serratia* and are the drug of choice in infections due to multidrug-resistant gram-negatives.

Sensitivity to the quinolone levofloxacin (LFX) was evaluated. Samples of approximately $1x10^6$ cells collected from each of the 3 zones of the "bull's eye" pattern (centre, middle and edge) as described in the Section 2.3.1 with the following modifications. The resuspension of the bacterial paste obtained from the colony was done in LB, not in PBS, and the concentration of cells was $1x10^6$ cells/ml (extrapolated from an OD600 measurement of 0.01). Independent 1 ml aliquots of the ultimate bacterial suspension in LB were exposed to a range of LFX concentrations (0-20 µg/ml) that were incubated in microfuge tubes (37ºC, 200rpm, 16 hours). To control for the sensitivity or resistance of the mono-

cultures of both species, an identical protocol was applied, including the selection of bacterial paste samples from the centre, middle and edge of mono-culture colonies. Subsequently, samples were serially diluted in PBS and viability on TSA plates assessed through cell counting (CFU/ml).

Similarly, the sensitivity of these strains in liquid medium was also assessed. Samples were also collected from mono- and co-culture experiments grown in LB for 8 hours at 37^{o}C and 200rpm, which are the conditions used on the bacterial growth dynamics and competition experiments (see above). The cultures were diluted in LB to adjust the cellular concentration to 1x10^{6} cells/ml as above Samples collected from a colony of *S. marcescens* NCTC1377 or *E. coli* NCTC12241 as mono-cultures, grown at identical conditions were used as controls.

The same protocol was applied to evaluate the resistance against ampicillin and vancomycin, to which *Serratia* is expected to be resistant to. To the former because of its natural resistance to β-lactamases and to the latter because of the impermeability of the outer membrane of gram-negatives. The range of concentrations investigated ranged from 0-100 µg/ml for ampicillin and 0-50 µg/ml for vancomycin.

To test whether the increase in antibiotic resistance in the *S. marcescens* NCTC1377 embedded in the centre and edge sections of the "bull's eye" pattern could be explained by a physiological adaptation compared to a genetic change of the strain. The ability of the resistant colonies from cultures exposed to antibiotics to transfer the resistance to subsequent generations was evaluated. Briefly, surviving single colonies on TSA plates coming from liquid cultures that had been exposed to LFX were independently resuspended in PBS. Their sensitivity to LFX was again assessed, by seeding serial dilutions of those cell suspensions on TSA plates containing increasing concentrations of LFX (0-1 µg/ml) and incubated at 37°C for 16 hours. Single colonies isolated from *S. marcescens* NCTC1377 or *E. coli* NCTC12241 mono-cultures followed the same processing and were used as controls. Plates were observed after 16 to 48 hours to establish the number of viable counts.

2.7.2 Oxidative stress-mediated modulation of antibiotic susceptibility and "bull's eye" pattern formation

2.7.3 Motility: swimming and swarming

To test motility of the strains, TSA plates with conventionally accepted 0.3% and 0.7% agar for swimming and swarming motility assays, respectively were used. 1µl drop containing 10^{5} cells from exponential growing LB cultures of *E. coli* NCTC12241, *E. coli* NCTC10418, and *S. marcescens* NCTC1377 as mono- or co-cultures were placed onto the 0.3% and 0.7% agar plates. Plates were allowed to settle at RT to be then incubated at 37°C for 24 hours. After incubation, the diameter of each grown colony was measured to compare the bacterial ability to swim or swam in these conditions. Also, the resulting plates with grown co-cultures were then left at RT (20-22°C) for further 8 hours to enhance red pigmentation due to prodigiosin production. Prodigiosin maximum expression is reached between 22 and 27^{o}C[390,391]. Samples of different colour in the colonised area of the plates were collected and re-streaked on conventional LBA plates followed by 16-hour incubation at 37^{o}C to assign and quantify species-specific bacterial cells grown on the soft agar plates.

2.7.4 Multi-species biofilm

Bacterial biofilm formation relies on a complex cell-to-cell communication system. The putative signalling-mediated space distribution into a “bull’s eye pattern” between *S. marcescens* NCTC1377 and *E. coli* NCTC12241 may be accompanied by an alteration in biofilm formation properties and therefore in the virulence of each species. The ability (or lack thereof) *S. marcescens* NCTC1377 to form a biofilm may be influenced by the presence or absence of *E. coli* NCTC12241.

Bacterial biofilm growth was supported on Nunclon 96-well plates (Termo Fisher Scientific, UK). 200 µl of sterile distilled H_2O was added to the external wells of the 96-well plates to keep humidity constant. The media selected for growing the mono-species bacterial biofilm were LB and LB supplemented with 2% glucose. The growth media with appropriate supplements were added to the wells.

Pre-inoculum and inoculum were prepared as described above in the bacterial dynamics setup protocol. A total of approximately 1,000 cells from exponentially growing bacterial cultures of *S. marcescens* NCTC1377, *E. coli* NCTC 12241, *E. coli* NCTC 10418 and the *S. marcescens* & *E. coli* NCTC12241 co-culture, was placed in the wells in a 96-well plate, except liquid medium alone contamination controls. The 96-well plate was incubated for 24 hours at 37°C in a humidity chamber (Tupperware® box with lid not sealed tight to allow oxygen circulation and wet tissues to keep humidity).

To determine biofilm growth each well was gently rinsed with PBS 3x, then 0.1% CV solution was added to each well and allow to stain for 10 minutes before further washing with sterile distilled H_2O. The remaining liquid was removed by gently tapping the inverted plate on a tissue. Once the plate dried at room temperature for approximately 20 minutes the wells are observed with an optical microscope (Nikon ECLIPSE E200 Microscope, 40x objective). Macroscopic pictures were taken.

Another 96-well plate set up and grown as a above and processed in parallel was used to enumerate the viability counts of the planktonic bacterial suspension and of the biofilm mass. Samples of 100 µl of the liquid suspension were collected for each condition, serially diluted in PBS, and plated on TSA as per the Miles and Misra method. Incubation was carried out at 37°C for 16 hours. To ascertain the viable counts in the biofilm, the LB suspension was transferred to a fresh tube, and each well was gently rinsed 100 µl with PBS buffer once. The biofilm mass was thoroughly scratched in 100 µl of PBS added to each well. The resulting suspensions were collected and again serially diluted in PBS, plated in 3x10 µl drops on TSA plates and incubated at 37°C for 16 hours. The viability test was not done for the co-culture *E. coli* NCTC12241 & *E. coli* NCTC10418 as colonies are not distinguishable based on colony morphology (smooth white round colonies for both strains).

2.7.5 Host-pathogen interactions: infection assay

In the same manner that several features studied above potentially connected to pathogenesis may be altered upon formation of the “bull’s eye” pattern by *S. marcescens* NCTC1377 or *E. coli* NCTC12241 co-cultures, it was of value to explore changes on adherence or invasion of human tissue cells. We have set-up a bacterial/cell culture-based infection model. The following experiments have been

conducted in collaboration with Matthew Allott (MA) in the laboratory, who prepared the cells for the infection assays.

2.7.5.1 Infection assay: adherence

MDCK cells were seeded in a 24-well plate containing 1 ml DMEM supplemented with 4 mM L-glutamine and 10% FBS at cell numbers to obtain 80% confluency and incubated at 37°C, 5%CO_2 for 20 hours. Empty wells were filled with 1x PBS to provide humidity. Supplemented media was removed from MDCK cells 2 hours prior to infection and replaced with non-supplemented DMEM to induce cell starvation to ideally maximize adherence and internalization.

Samples were collected from the outer edge of bacterial colonies on TSA (37oC, 18 hours) of (i) *S. marcescens* NCTC1377, (ii) *E. coli* NCTC12241 and (iii) the "bull's eye" pattern resulting from *S. marcescens* NCTC1377 & *E. coli* NCTC12241 co-cultures. Samples were collected with a Gilson P10 pipette loaded with a 200µl yellow tip, resuspended in 1 ml of LB and washed with 1x PBS (pH 7.4) after harvesting by centrifugation (13,000 rpm, 1 minute). After removal of the supernatant the pellet was resuspended in 1 ml LB, and cell density was standardized to an OD_{600} of 0.5 corresponding to 10^8 CFU/ml. A total of $2x10^5$ bacterial cells of each sample type were put in contact for 30 minutes at 37°C with the MDCK cells in the wells, resulting in a final multiplicity of infection (MOI) of 1. As an exception, given the 1:10 ratio between *E. coli* NCTC12241: *S. marcescens* NCTC1377 at the edge of the co-culture patterned colony, the mono-culture assay control for *E. coli* NCTC12241 was also performed at an MOI of 0.1. Each condition was tested in duplicate. Supernatants were harvested and immediately placed on ice. MDCK-containing wells were washed 3x with 300 µl of PBS. Bacterial cells adhered to the tissue were resuspended via mechanical scraping in fresh 1 ml PBS that was subsequently serially diluted and plated to determine the number of CFU/ml. Viable counts of bacteria in the supernatant were also determined. Scraping and plating on agar plates induced lysis of epithelial cells, with no need of using lysis agents[392].

2.7.5.2 Infection assay: internalization

The determination of the number of bacterial cells internalized by the MDCK cells was accomplished with an experimental setup identical to the adherence assay above, but with the addition of gentamicin (an antibacterial agent unable to penetrate the host membrane). Only bacteria internalized inside of MDCK cells would be protected from the bactericidal activity of gentamicin. After the 30 minutes contact time between the bacteria and the tissue culture cells a 100ug/ml of gentamicin were added to each well and allowed to act for 45 minutes at 37ºC. Bacterial cells were harvested, and supernatants dispose. The pellets were washed 3x with 300 µl PBS and internalized cells resuspended via mechanical scraping in fresh PBS. The viability of bacterial cells was assessed through CFU counting.

2.8 *In silico* tools

2.8.1 Genomic comparison of *E. coli* NCTC12241 and *E. coli* NCTC10418

We have shown that the "bull's' eye" pattern formation only appears with *S. marcescens* NCTC1377 in contact with *E. coli* NCCT12241 and not with *E. coli* NCTC10418. Such disparity offers the opportunity for an *in silico* comparison of both *E. coli* genomes to identify differences that may provide an insight as to the mechanisms underlying the morphogenetic and functional differences in the *S. marcescens* NCTC1377 being in contact with *E. coli* NCCT12241.

Full genomes and annotations of *E. coli* NCTC12241 and *E. coli* NCTC10418 were downloaded from ATCC database[393] and imported in Geneious Prime®2021.1.1. Comparative genome analyses of the two genomes were constructed through a Mauve alignment – a multiple genomic alignment and visualization software based on an algorithm to identify Locally Collinear Blocks (LCB) with conserved segments, to expeditiously study genome-wide evolutionary dynamics clearly illustrating orthologous and xenologous regions recognisable at a glance.

Following the Mauve-identified differences between both genomes, all genes in both species were translated to their AA sequences also using the Geneious Prime®2021.1.1. Sequences were extracted in FASTA format and analysed in Protein BLAST[394]. Our search set in Protein BLAST consisted in non-redundant protein sequences as a database only within the organism *Escherichia coli* ATCC25922. General Algorithm parameters were the following: Max target sequence (100), Expected threshold (0.05), Word size (6), Max matches in a query range (1). Results were downloaded as *.cvs* file. They included: Name of the sequence (Query), Accession codes (or sequence ID) of the matched Subjects, identity (%), Query Coverage(%), Length, Gap, Query start and end, Subject start and end, E-value, score bites. To obtain the descriptions (names) of all access codes, a detailed search in the NCBI website under the section 'Protein' was conducted; NCBI Reference sequences and results including the accession codes protein sequence and related protein name, were collected as FASTA files. Protein names were added to the relative downloaded data resulted from the BLAST analyses. The full translations list was imported and analyses in Geneious Prime®2021.1.1 and Microsoft Excel. The output consisted on the percentage of proteins with a certain degree of conservation for both full genomes.

2.8.2 Translational analysis of methionine-related proteins between *E. coli* strains

The impact of a micromolar concentration of Met on "bull's eye" pattern formation on *S. marcescens* NCTC1377 grown as a mono-culture led to consider the preliminary in silico study of genes/gene products connected to Met metabolism and indirectly to QS regulation (MetR and MetE) we ran a translational comparative analysis of proteins involved in Met metabolism, of both *E. coli* strains.

metR and *metE* from both genomes, *E. coli* NCTC12241, *E. coli* NCTC10418 were identified, extracted, and translated. The translated sequence of MetR and MetE from both *E. coli* were aligned performing a Pairwise Global Geneious alignment (Alignment type: Global alignment with free end gaps; Cost Matrix: Blosum62). Alphafold2[395] (Jumper *et al.*, 2021a) was used to determine the 3D structure of MetR

and MetE proteins. Alphafold2 generates .pdb files which were then visualized in Geneious Prime®2021.1.1 or RCSB PDB. The 3D protein structures were aligned in Geneious Prime® 2022.1.1.1 to search for differences that may potentially underpin differences between both strains able to explain the differential effect they have in the formation of the "bull's eye" pattern by *S. marcescens* NCTC1377. AA sequence conservation across MetR and MetE protein sequences amongst *E. coli* strains using as a template the corresponding proteins in *E. coli* NCTC12241 and *E. coli* NCTC10418 was conducted in BlastP (Organism*: Escherichia coli (ta*xid:562); Max target sequences within Algorithm parameters set at 1000) was undertaking to determine the predictive value of strains that may or not lead to changes in *S. marcescens* NCTC1377 when present within the same organism.

2.8.3 A mathematical model simulating the "bull's eye" pattern

A mathematic model able to explain the formation of a "bull's eye" pattern was performed by Čepl Jaroslav[i], Scholtz Vladimir[ii] and Jirina Scholtzova[iii] and undertaking as part of a collaborative initiative.

Pictures of mixed colonies of *E. coli* NCTC12241 and *S. marcescens* NCTC1377 grown on TSA for 16 hours with different cell density at a ratio 1:1 were used to build a mathematical model for simulating the "bull's eye" pattern formation. The model was based on the reaction–diffusion model used to a bacterial colony growth modelling described by Cepl at al. in a previous study[243]. C-programming language was used. The Petri dish was represented by hexagonal net of cells in which the bacteria proliferation occurred, and the diffusion of nutrients and of signalling substances was considered. The simulation performs on a square dish consisting of net of 200×200 (absolute value used in the programming language) hexagonal cells, where the mixture of *S. marcescens* cells (red) and *E. coli* cells (white) were inoculated at the ratio of 1:1 in the middle of the dish. The growth of each bacterial species was described by the Fisher–Kolmogorov equation:

$$\frac{\mathrm{d}x_\mathrm{i}}{\mathrm{d}t} = \left\lfloor D_x \cdot \nabla^2 x_\mathrm{i} \right\rfloor + \mathrm{a_i} \cdot x_\mathrm{i} \cdot n$$

dx_i/dt is the overall change of number of each bacterial species in time. For indicating the two bacterial populations, x_1 and x_2 were used, where 1 is *E. coli* (white cells) and 2 is *S. marcescens* (red cells). The term $Dx \cdot \nabla^2 x_i$ expresses the bacteria flow between cells of the dish (hexagon), $a_i \cdot x_i \cdot n$ the replication. Bacterial growth/replication was determined considering: (i) replication coefficient of white cells, (ii) replication coefficient of red cells, (iii) diffusion of white cells, (iv) diffusion of red cells. The amount of nutrients subjected to diffusion and consumption proportional to the number of bacteria, was also considered (Petri dish nutrient coefficient) as a factor influencing the bacterial growth and space distribution in the dish and factored in as. Signalling substances (e.g.; metabolites, waste products and other signals) were all factored in a single coefficient. The diffusion simulation was replaced by an analytic function of $\cos^2$ to streamline the process.

[i] University of Live Sciences, Prague, Czech Republic
[ii] University of Chemistry and Technology, Prague, Czech Republic
[iii] Czech Technical University, Prague, Czech Republic

3 CHAPTER 3

Human microbiota *in vitro* co-culture competition experiments

The human gut microbiome is a complex ecosystem of microorganism-host-metabolites interactions. The behaviour of a given bacterial species will vary depending on the ecological context. The microbiota is a complex ecosystem, made up of thousands of bacterial species. Understanding the contribution of each of these species and their members as well as the interplay amongst them using *in vitro* models has inherent limitations. The principle underpinning this doctoral research is to ascertain the population dynamics of combinations of a restricted number of species. Using models of two or more bacterial strains growing on conventional microbiological growth media (*in vitro* co-culture competition experiments) is the first step to approach the fundamental questions regarding competitive mechanisms among bacteria inhabiting the human gut microbiota. These advances could be used in the future as a building block for upscaled ecosystems. To study the properties of bacterial species in co-culture it is essential to first determine their capabilities and fitness growing as single organisms.

3.1 Mono-culture growth in typical bacteriological nutrient media of a range of microbiota and pathogenic bacterial species

The growth dynamics of a range of common bacterial species in the human gut microbiota were determined in conventional bacteriological rich growth media (LB and TSB) in aerobic and anaerobic conditions. All species were able to productively grow in these media (Figure 3.1 and Figure 3.2) as determined by viability and absorbance.

In TSB, while a subset of species, *E. coli* NCTC12241, *E. coli* NCTC10418, *S. marcescens* NCTC1377, *P. aeruginosa* PAO1, *P. vulgaris* NCTC4175, *K. aerogenes* NCTC10006 and *S. aureus* NCTC12981 (Figure 3.1A-G) showed similar dynamics by both detection methods, two of the Gram-positive cocci, *E. faecalis* NCTC377 and *S. salivarius* NCTC8618 seemed to display an initial lag phase by OD_{600} that was not reflected by the apparent exponential growth seen by CFU (Figure 3.1H and I). While most species entered the stationary phase after 6 hours of growth (*E. coli*, *S. marcescens*, *K. aerogenes*, *S. aureus*, and *S. salivarius*), *P. aeruginosa* and *P. vulgaris* reached it a bit later after 8 hours of growth. Oppositely, *E. faecalis* and *L. plantarum* entered the stationary phase earlier, after 5 and 2 hours of growth respectively. All species reached the stationary phase at a cell density of approx. $1x10^8$ cells/ml (Figure 3.1A-I) apart from *L. plantarum* who left exponential growth at approx. $1x10^6$ cells/ml (Figure 3.1J).

Unlike TSB, when growing in LB each strain displayed similar dynamics by both detection methods (Figure 3.2 A-J). However, there were noticeable differences on the time to enter the stationary phase by the various species. It was not until after 8 hours of growth that *P. aeruginosa* reached the stationary phase (Figure 3.2 D). In contrast, both *E. coli* did it after 7 hours, while *S. marcescens*, *K. aerogenes*, *P. vulgaris*, and *S. salivarius* became stationary after 6 hours (Figure 3.2 A,B,E,F,I). Finally, *S. aureus*

and *E. faecalis* left the exponential phase of growth after only 4 hours (Figure 3.2 G,H).. Interestingly, all Gram-positive strains entered the stationary phase at a cell density of $1x10^8$ while the Gram-negative strains entered at a higher density, approx. 10^9 cells/ml. Of note, LB medium did not support the growth of *L. plantarum* NCTC6376, with cell density constant between $1x10^4$ and $1x10^5$ cells/ml (Figure 3.2 J) . In fact, *L. plantarum* is a fastidious organism which requires specific nutrients, glucose and minerals, to support growth. We have therefore developed a specific medium (LBEAP1) rich in glucose, manganese and magnesium, which can support the proficient growth of the *L. plantarum*. The addition of glucose and minerals in conventional LB enabled the growth of *L. plantarum* to achieve similar dynamics to the other strains, reaching a stationary phase 6 hours at a cell density of $1x10^7$ (Figure 3.3).

To define the increase in the number of bacteria in a population, we calculated the growth rate (h^{-1}) during the exponential phase. Growth rates values (Table 3.1), defined as the rate of bacterial population increase per hour, showed, as expected, slightly faster rates for each species in TSB than in LB. This is consistent with TSB being richer growth medium than LB, including the presence of glucose. Gram-negative bacteria grew faster than Gram-positive strains in both growth media, TSB and LB. The average growth rate of Gram-negative bacteria was 1.63 h^{-1} (SD. ± 0.04), with the exception of K. *aerogenes* which grew noticeably more slowly in LB, 1.45 h^{-1} (Table 3.1). The growth rates were similar for each Gram-positive strain whether grown in TSB or LB, and also similar across the strains, with an average growth rate of 1.27 h^{-1}(SD. ± 0.09). These values exclude *L. plantarum* NCTC6376, which although able to grow in TSB, its growth rate was distinctively lower (growth rate of 0.75 h^{-1}) and it was altogether unable to grow in LB. As indicated above, *L. plantarum* was able to grow in modified LB medium (LBEAP1) with a growth rate of 1.19 h^{-1}, not dissimilar from the rest of Gram-positive bacteria. When considering the results from co-cultures of *L. plantarum* with other strains in LBEAP1, it is important to factor in the differences in this medium compared to conventional LB. Nonetheless, we demonstrated that our selected strains reached an OD_{600} after 24 hours of growth in LBEAP1 equivalent to that in LB. However the exponential phase growth rate remains to be determined.

The determination of growth conditions which allowed selected bacterial strains to grow at similar growth dynamics was a critical step to enable population selection for the subsequent co-culture competition experiments, clearly demonstrating that the growth medium was not a limiting or selecting factor.

Ultimately, the study of mono-culture growth in conventional media enabled us to determine the correlation between OD_{600} and CFU/ml, essential step for downstream experiments.

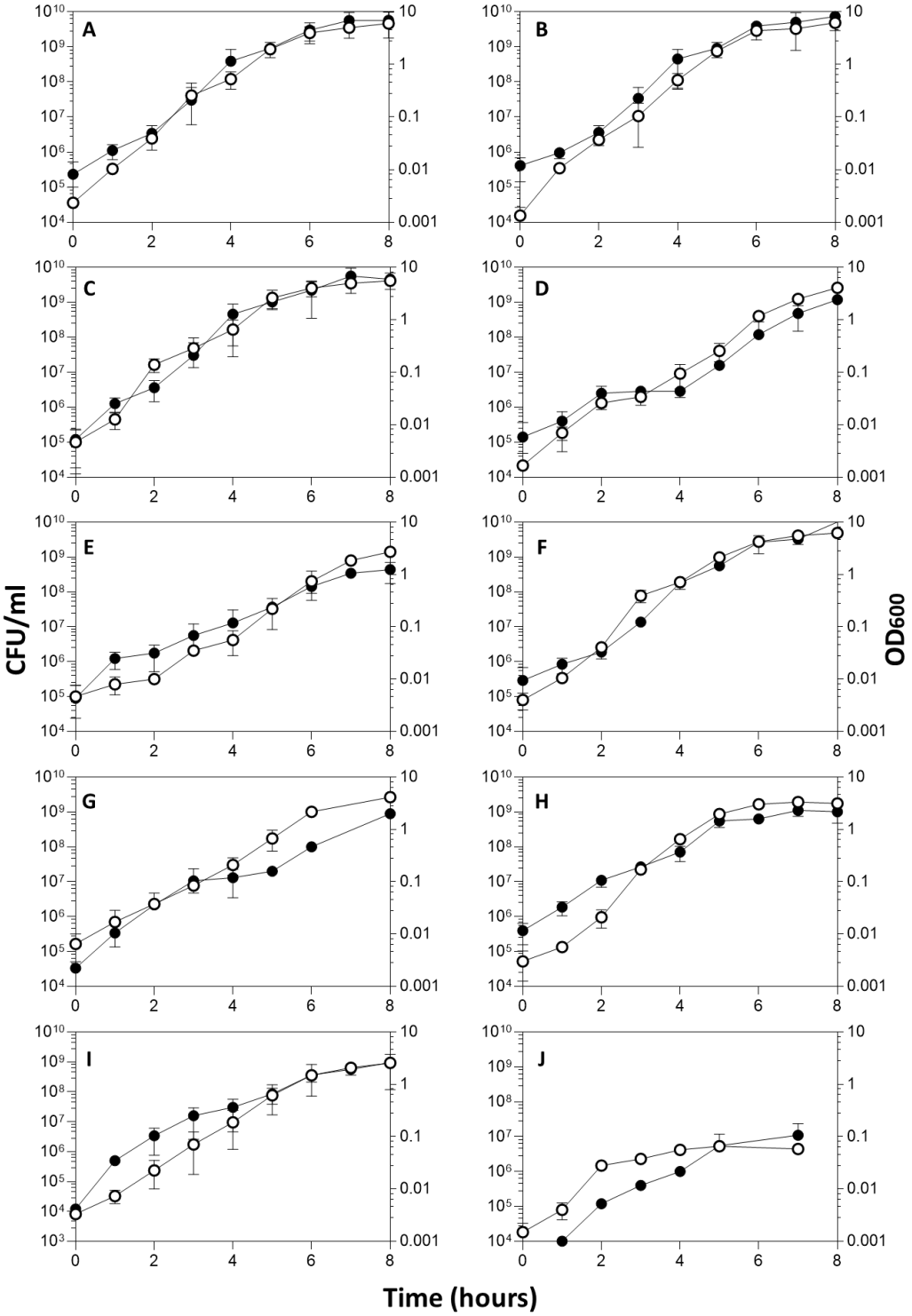

Figure 3.1: **Bacterial growth aerobically in TSB at 37ºC and 200rpm.** A. *Escherichia coli* NCTC12241; B. *Escherichia coli* NCTC1418; C. *Serratia marcescens* NCTC1377; D. *Pseudomonas aeruginosa* PAO1; E. *Proteus vulgaris* NCTC4175; F. *Klebsiella aerogenes* NCTC10006; G. *Staphylococcus aureus* NCTC12981; H. *Enterococcus faecalis* NCTC377; I. *Streptococcus salivarius* NCTC8618; J. *Lactobacillus plantarum* NCTC6376. (●) CFU/ml, (O): OD_{600}. X axis: Hours of growth from the inoculation at t_0; Left Y axis: CFU/ml; Right Y axis: OD_{600}. Results and error bars indicate mean ± SD of three technical replicates.

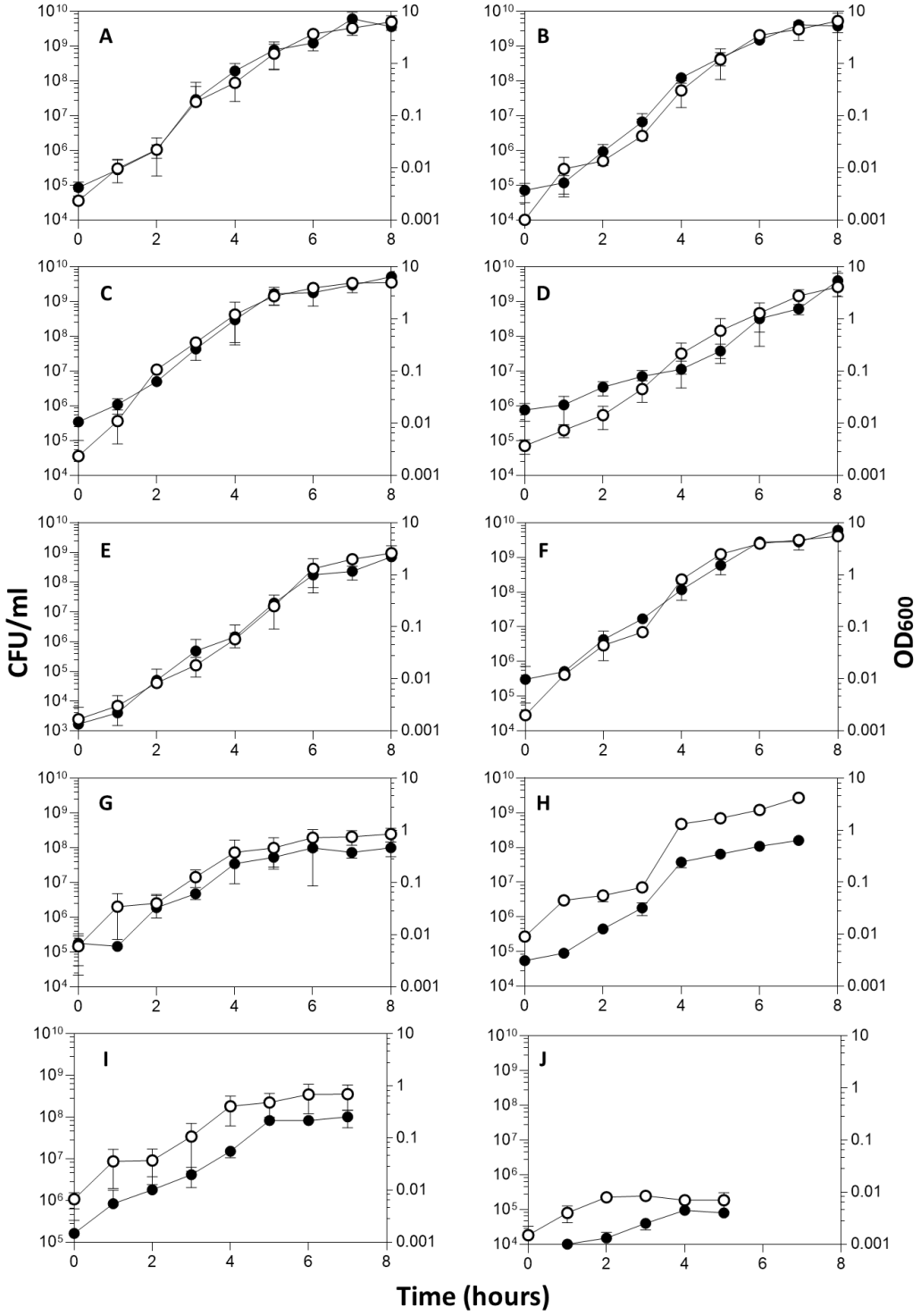

Figure 3.2: **Bacterial growth aerobically in LB at 37°C and 200rpm.** A. *Escherichia coli* NCTC12241; B. *Escherichia coli* NCTC1418; C. *Serratia marcescens* NCTC1377; D. *Pseudomonas aeruginosa* PAO1; E. *Proteus vulgaris* NCTC4175; F. *Klebsiella aerogenes* NCTC10006; G. *Staphylococcus aureus* NCTC12981; H. *Enterococcus faecalis* NCTC377; I. *Streptococcus salivarius* NCTC8618; J. *Lactobacillus plantarum* NCTC6376. (●) CFU/ml, (O) OD_{600}. X axis: Hours of growth from the inoculation at t_0; Left Y axis: CFU/ml; Right Y axis: OD_{600}. Results and error bars indicate mean ± SD of three technical replicates

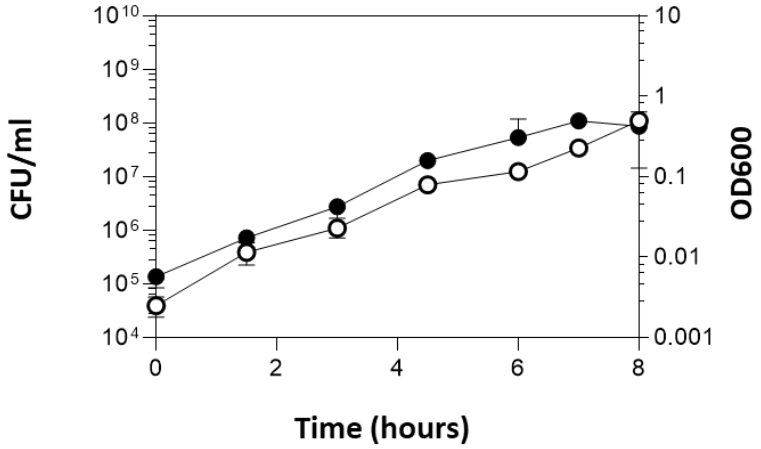

Figure 3.3: ***Lactobacillus plantarum*** **NCTC6376 growth aerobically in LBEAP1 at 37°C and 200rpm.** (●) CFU/ml, (O) OD_{600}. X axis: Hours of growth from the inoculation at t_0; Left Y axis: CFU/ml; Right Y axis: OD_{600}. Results and error bars indicate mean ± SD of three technical replicates.

Table 3.1: **Bacterial growth rates (h^{-1}) determined from growth curves.** The colour gradient in grey stands out the values of the growth rates, from lower values in light grey, to higher values in dark grey. Results indicate mean of three technical replicates.

		Growth rate	
		TSB	LB*
Gram-negative	*Escherichia coli NCTC12241*	1.70	1.60
	Serratia marcescens NCTC1377	1.63	1.59
	Pseudomonas aeruginosa PAO1	1.65	1.63
	Klebsiella aerogenes NCTC10006	1.56	1.45
	Proteus vulgaris NCTC4175	1.62	1.66
Gram-positive	*Enterococcus faecalis NCTC775*	1.21	1.29
	Staphylococcus aureus NCTC12981	1.40	1.35
	Streptococcus salivarius NCTC8618	1.18	1.21
	Lactobacillus plantarum NCTC6376	0.75	1.19

*LBEAP1 was used for *L. plantarum*

Bacterial strains in the gut microbiota are exposed to a (micro)anaerobic environment. Hence, it seemed reasonable to investigate how the microbiota and pathogenic bacterial strains from our selection grow in anaerobic conditions. As a slower growth than in aerobic condition was expected, bacterial growth in anaerobic conditions was monitored over time for three days, measing OD_{600} after 8, 24, 48 and 72 hours. Values reported in Table 3.2 showed that *E. coli* NCTC12241, *S. marcescens* NCTC1377, *K. aerogenes* NCTC10006 and *E. faecalis* NCTC775 reached OD_{600} between 0.4 and 0.7 after 8 hours, corresponding to a late exponential phase, and OD_{600} values between 0.8 and 1.0 after 72 hours of growth, hence indicating a good tolerance for anaerobic conditions. Contrarily *P. vulgaris* NCTC4175 and *L. plantarum* NCTC6376 and *S. salivarius* NCTC8618 displayed a slower growth than the strains

mentioned above, with OD600 between 0.1 and 0.3 after three days. Ultimately, *P. aeruginosa* PAO1 and *S. aureus* NCTC12981 did not show good growth rates in anaerobic conditions, at least within 72 hours, with OD_{600} values no greater than 0.1.

Overall, we showed that the selected bacterial species can grow in bacteriological nutrient media (LB and TSB) in both, aerobic and anaerobic conditions, even if more slowly in the latter.

Table 3.2: **Bacterial growth in anaerobic conditions in LB, at 37°C, static condition**. Optical density values for bacterial species growing anaerobically in liquid LB, statically, for 72 hours. The colour gradient in grey emphasises the values of the growth rates, from lower values in light grey, to higher values in dark grey. LBEAP1 was used for *L. plantarum*. Results indicate mean of three technical replicates.

	Optical density (OD_{600})				
	Time of incubation (hours)				
	0	**8**	**24**	**48**	**72**
Escherichia coli NCTC12241	0.001	0.46	0.86	0.78	0.99
Serratia marcescens NCTC1377	0.002	0.44	1.17	0.97	0.91
Pseudomonas aeruginosa PAO1	0.002	0.004	0.067	0.086	0.115
Klebsiella aerogenes NCTC10006	0.003	0.549	0.76	0.87	0.88
Proteus vulgaris NCTC4175	0.001	0.266	0.45	0.329	0.276
Enterococcus faecalis NCTC775	0.003	0.72	0.88	0.76	0.8
Staphylococcus aureus NCTC12981	0.003	0.017	0.062	0.073	0.09
Streptococcus salivarius NCTC8618	0.002	0.138	0.151	0.173	0.15
Lactobacillus plantarum NCTC6376	0.001	0.275	0.302	0.317	0.411

3.2 Zinc tolerance changes in different growth conditions

The micronutrient Zn was selected as a potential switch, able to shift bacterial population selection and dynamics, an effect most likely mediated by its regulatory role. To ensure that any effect of Zn in our assays was not mediated through its toxic effect, each bacteria species was grown with an increasing concentration of $ZnCl_2$ (0-4 mM) aerobically at 37°C, in LB or TSB, evaluating the impact of Zn on bacterial growth during time (up to 8 hours). While most bacterial strains were not affected by high $ZnCl_2$ concentrations (4mM) when growing in a rich medium (TSB) as shown in Figure 3.5, they were robustly impacted in LB (Figure 3.4). Specifically, 4 mM of Zn had a bactericidal effect for *E. coli* NCTC12241, *K. aerogenes* NCTC10006 and *S. aureus* NCTC12981 (Figure 3.4, A, E, F) after only 1 to 2 hours of growth and for *S. salivarius* NCTC8618 and L. plantarum NCTC6376 after 6 hours (Figure 3.4, H,I), while it displayed a bacteriostatic effect for *S. marcescens* and *P. vulgaris* (Figure 3.4, B, D) Strikingly, *E. faecalis* NCTC775 was able to grow, even if slightly slower, with 4 mM of Zn (Figure 3.4,G). A concentration of 2.5 mM had a bacteriostatic effect for *K. aerogenes, S. aureus*, *S. salivarius* and *L. plantarum*; in contrast, the same concentration resulted in a reduced growth rate in the rest of the strains except for

E. faecalis, which in fact was not affected by any of the tested concentrations of Zn in LB or TSB. Ultimately, we showed that none of the Gram-negative strains were impacted by 1 mM of Zn, while *S. salivarius* and *L. plantarum* seemed to still be able to grow, but more slowly than in the absence of Zn, displaying lower growth rates (Table 3.3).

In TSB with 4 mM Zn, only the Gram-positive *S. aureus* NCTC12981, *S. salivarius* NCTC8618 and *L. plantarum* NCTC6376 displayed a slower growth than in TSB alone.

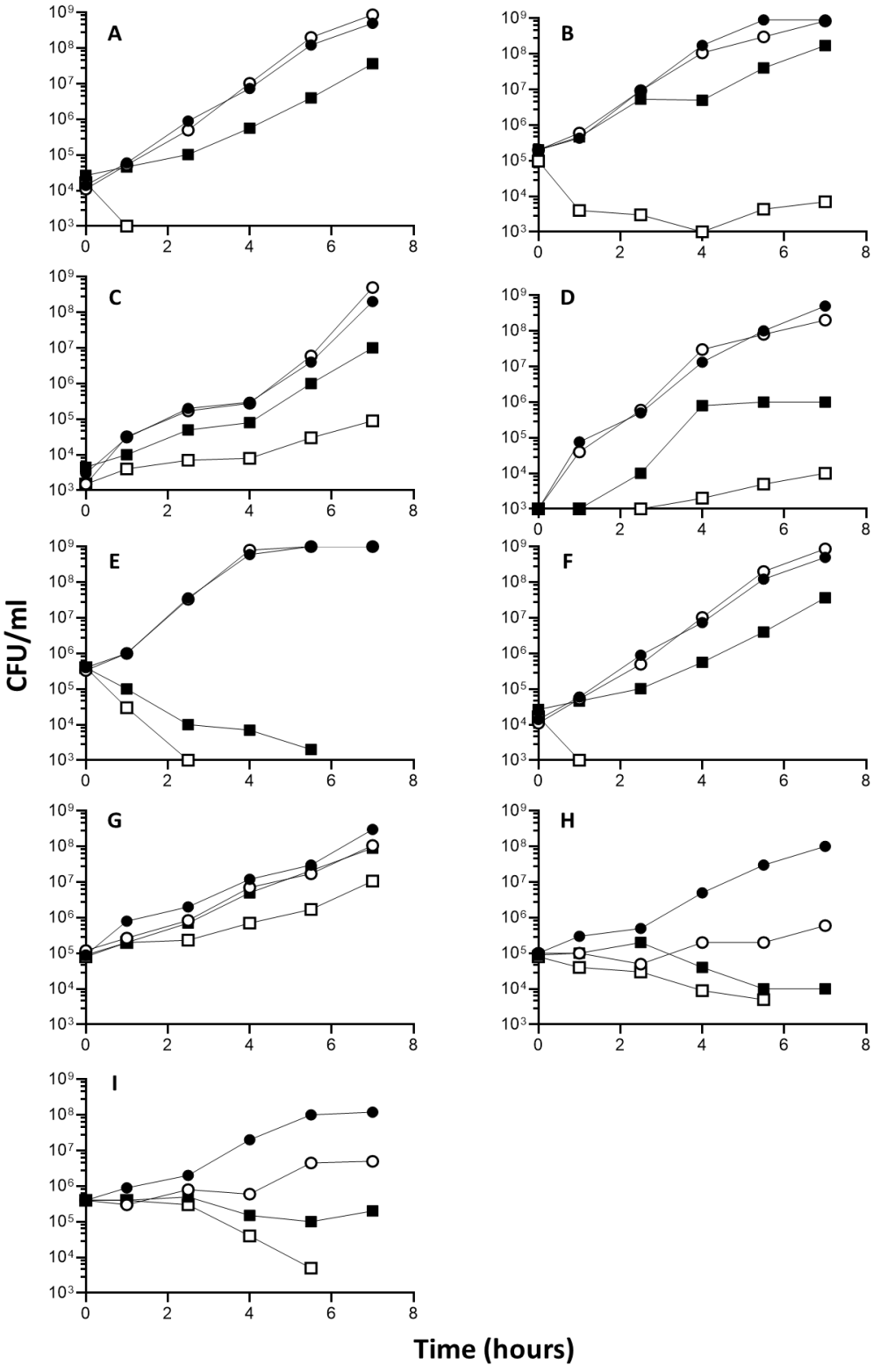

Figure 3.4: **Aerobic bacterial growth in LB at 37ºC and 200rpm with increasing concentrations of $ZnCl_2$.** A. *Escherichia coli* NCTC12241; B. *Serratia marcescens* NCTC1377; C. *Pseudomonas aeruginosa* PAO1; D. *Proteus vulgaris* NCTC4175; E. *Klebsiella aerogenes* NCTC10006; F. *Staphylococcus aureus* NCTC12981; G. *Enterococcus faecalis* NCTC377; H. *Streptococcus salivarius* NCTC8618; I. *Lactobacillus plantarum* NCTC6376. LBEAP1 was used for *L. plantarum* (I). (●) No supplemented Zn; (O) 1mM Zn; (■) 2.5mM Zn; (❑) 4mM Zn. X axis: Hours of growth from the inoculation at t_0; Y axis: CFU/ml.

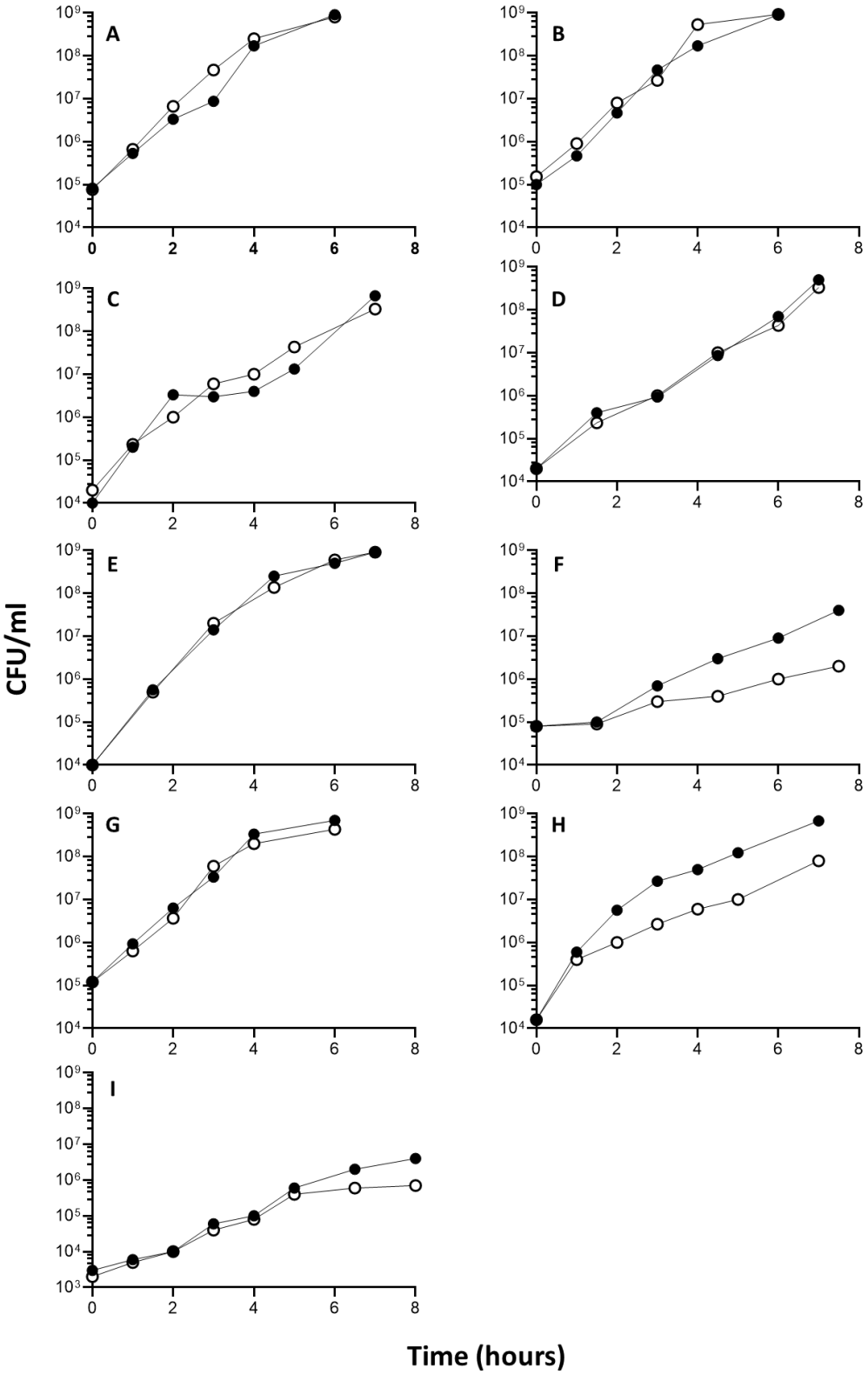

Figure 3.5: **Aerobic bacterial growth in TSB at 37ºC and 200rpm with increasing concentrations of $ZnCl_2$** . A. *Escherichia coli* NCTC12241; B. *Serratia marcescens* NCTC1377; C. *Pseudomonas aeruginosa* PAO1; D. *Proteus vulgaris* NCTC4175; E. *Klebsiella aerogenes* NCTC10006; F. *Staphylococcus aureus* NCTC12981; G. *Enterococcus faecalis* NCTC377; H. *Streptococcus salivarius* NCTC8618; I. *Lactobacillus plantarum* NCTC6376. (●) No supplemented Zn; (O) 4mM Zn. X axis: Hours of growth from the inoculation at t_0; Y axis: CFU/ml

Table 3.3: **Growth rates (h^{-1}) determined from growth curves.** The colour gradient in grey stands out the values of the growth rates, from lower values in light grey, to higher values in dark grey. Results indicate mean of three technical replicates.

	Growth rate					
	TSB		LB*			
Zn concentration (mM)	**0**	**4**	**0**	**1**	**2.5**	**4**
Escherichia coli NCTC12241	1.57	1.85	1.77	1.79	1.48	<0
Serratia marcescens NCTC1377	1.67	1.47	1.71	1.67	0.99	<0
Pseudomonas aeruginosa PAO1	1.62	1.45	1.81	1.76	1.27	0.56
Enterococcus faecalis NCTC775	1.32	1.31	1.07	1.09	1.11	0.72
Proteus vulgaris NCTC4175	1.30	1.32	1.60	1.26	0.41	0.41
Klebsiella aerogenes NCTC10006	1.74	1.63	1.70	1.60	<0	<0
Staphylococcus aureus NCTC12981	1.93	1.69	1.78	1.38	<0	<0
Streptococcus salivarius NCTC8618	1.67	1.29	1.15	0.88	<0	<0
Lactobacillus plantarum NCTC6376	0.36	0.46	0.81	0.36	<0	<0

*LBEAP1 was used for *L. plantarum*

3.3 250 µM Zinc does not affect bacterial growth

Considering that in the intestinal lumen we may have a postprandial Zn concentration of around 100 µM, which varies according to many factors, the ideal micronutrient concentration for our subsequent investigations was set at 250 µM, an amount likely to be high enough to play a role in gene expression. In fact, 200 to 250 µM of Zn have been found to modulate QS-system, motility and biofilm formation in *S. typhimurium*[335,396] and in *E. coli*[397]. To confirm that such a concentration of Zn would not affect bacterial growth, we grew bacterial strains with 250 µM Zn. Growth rates in Table 3.4 displayed that the presence of 250 µM Zn did not affect the bacterial growth for any of the strains tested, hence representing a good concentration to use for downstream experiments.

Table 3.4: **Growth rates determined from bacterial growing in LB with 0 or 0.25 mM of Zn aerobically at 37°C and 200rpm.** The colour gradient in grey stands out the values of the growth rates, from lower values in light grey, to higher values in dark grey. Results indicate mean of three technical replicates.

Growth rate		
	LB*	
Zn concentration (mM)	**0**	**0.25**
Escherichia coli NCTC12241	1.57	1.55
Serratia marcescens NCTC1377	1.58	1.49
Pseudomonas aeruginosa PAO1	1.34	1.32
Enterococcus faecalis NCTC775	1.35	1.37
Proteus vulgaris NCTC4175	1.36	1.30
Klebsiella aerogenes NCTC10006	1.03	1.06
Staphylococcus aureus NCTC12981	1.08	1.01
Streptococcus salivarius NCTC8618	1.14	1.08
Lactobacillus plantarum NCTC6376	1.01	1.03

*LBEAP1 was used for *L. plantarum*

3.4 *In vitro* co-cultures competition experiments

3.4.1 No differential prevalence between most of the bacterial species in co-culture

Having shown that the bacterial strains had similar growth rates under the selected test conditions, we set-up pairwise bacterial co-culture competition experiments to test for any potential differential prevalence over time. We observed that, overall, most of bacterial species can co-habit and grow together, with no differential prevalence or competitive advantage over each other, (in green in Table 3.5) with Zn not influencing the selection of competing bacterial populations. For example, the co-culture between *P. aeruginosa* PAO1 and *E. faecalis* NCTC775 is shown in Figure 3.6D.

3.4.2 *P. aeruginosa* is taking over Gram-positive cocci

A competitive advantage over time was observed for *P. aeruginosa* when growing with two Gram-negative cocci, *S. salivarius* or *S. aureus* (Figure 3.6). *S. salivarius* in mono-culture reached a cell density of 10^7 CFU/ml after 24 hours of liquid growth, less compared to *P. aeruginosa* which reached 10^9 CFU/ml, indicating a better fitness for the latter compared to *S. salivarius*. When they both grew together, a significant decrease of *S. salivarius* after 24 or 48 hours was observed, indicating that *P. aeruginosa* negatively impacted its growth, probably due to competition for nutrients in favour of *P. aeruginosa* or the release of antimicrobial substances which may limit the growth of the Gram-positive (Figure 3.6). Gram-staining observation after 48 hours of liquid growth confirmed that exclusively pink rods (typical of *P. aeruginosa* and other Gram-negative enterobacteria) were present (data not shown as photographs at the microscope not taken). Similarly, we observed this competitive advantage for *P.*

aeruginosa when growing with *S. aureus* (Figure 3.6). The selective medium MSA was used to confirm that *S. aureus* growth was significantly inhibited when growing with *P. aeruginosa*. The mechanisms underpinning the apparent competitive advantages of *P. aeruginosa* on *S. salivarius* or *S. aureus* need to be evaluated.

3.4.3 The micromolar concentration of Zinc seems to mediate bacterial selection in *P. aeruginosa* and *S. marcescens* co-culture

Interestingly, based on colony counts, *S. marcescens* was significantly decreased when growing in co-culture with *P. aeruginosa* for 48 hours in LB supplemented with 250 µM Zn (Figure 3.5), hence indicating that Zn mediates or facilitates the competitive advantage of *P. aeruginosa* on *S. marcescens*. Actually, a slightly decrease of *S. marcescens* was also observed in the absence of Zn after 48 of liquid growth, suggesting that *P. aeruginosa* may be able to prevail on *S. marcescens* even without Zn, but the latter significantly enhanced the bacterial selection. However, semi-quantitative analyses with PCR indicated that both strains co-existed in liquid LB after 48 hours, with or without Zn (discussed later in Section 3.6.2), suggesting that the *S. marcescens* advantage over *P. aeruginosa* may only occur on a solid plate, or even that the absence of *S. marcescens* colonies is only apparent and may be a by-product of *S. marcescens* losing the ability to produce prodigiosin.

3.4.4 The probiotic *L. plantarum* inhibits potential pathogens

Another interesting observation arose from the co-cultures between *L. plantarum* with *E. coli* and *P. aeruginosa (*Figure 3.7). In fact, in those conditions, *L. plantarum* seemed to substantially prevail based on the determined CFU. As *L. plantarum* appears as purple rod-shape long cells at Gram-staining, while *E. coli* and *P. aeruginosa* are pink rod-shape cells, the Gram-stain colouration was used for further evaluate the bacterial prevalence after 24 ad 48 hours of growth in co-culture. In contrast with the colony viability results, the Gram-staining of the liquid co-culture between *L. plantarum* and *E. coli* and likewise the co-culture between *L. plantarum* and *P. aeruginosa*, showed that both strains prevailed after 24 or 48 hours (Appendix I). This suggests that *L. plantarum* may inhibit the ability of the other strains to grow as colonies on the growth media, hence inducing them into a dormient state, but may not kill them. Those data, although very promising, are anyway not conclusive and due to time restriction, we could not further investigate these phenomena.

Table 3.5: **Pairwise bacterial co-cultures competition experiments**. Bacterial strain on top row (blue) combined with bacterial strains in the first column (yellow). Green cells indicates that both strains prevailed over time based on CFU determined by the miles misra method. Blue cells indicates that the bacterial strain in blue (top row) prevailed; yellow cells indicates that the bacterial strain in yellow (left column) prevailed.

	E. coli NCTC12241	*S. marcescens* NCTC1377	*P. aeruginosa* PAO1	*K. aerogenes* NCTC10806	*P. vulgaris* NCTC4175	*E. faecalis* NCTC775	*S. salivarius* NCTC8618	*L. plantarum* NCTC6376
S. marcescens NCTC1377								
P. aeruginosa PAO1								
K. aerogenes NCTC10006								
P. vulgaris NCTC4175			Ndi[i]					
E. faecalis NCTC775								
S. salivarius NCTC8618	ND[ii]			ND[ii]	ND[ii]	ND[ii]		
L. plantarum NCTC6376							Ndi[i]	
S. aureus NCTC12981							Ndi[i]	

[i] Not distinguishable (Nd[i])
[ii] Not determined (ND[ii])

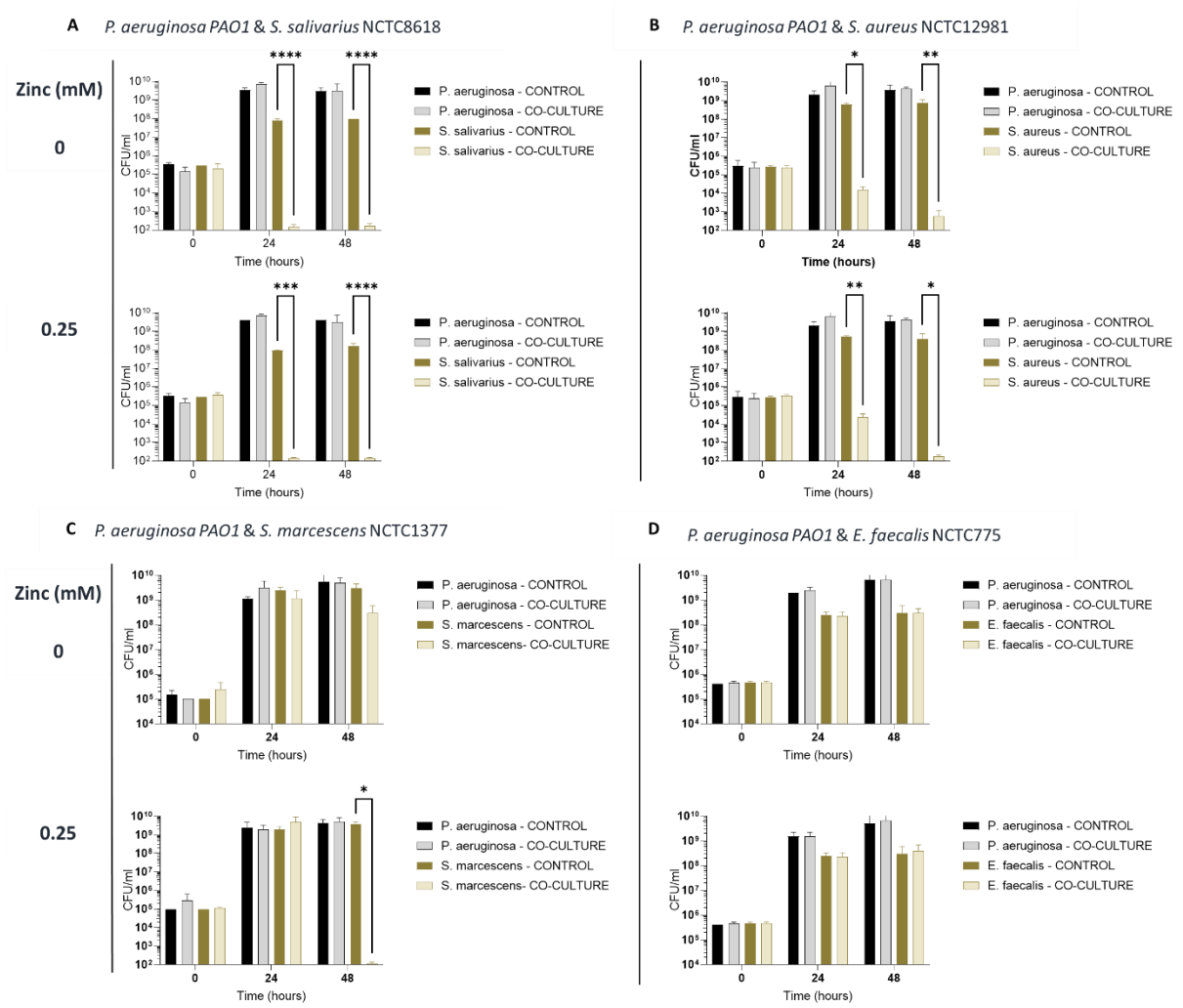

Figure 3.6: **Bacterial liquid co-cultures with or without Zn.** A) Bacterial liquid co-culture between *P. aeruginosa* and *S. salivarius*. B) Bacterial liquid co-culture between *P. aeruginosa* and *S. aureus*. C) Bacterial liquid co-culture between *P. aeruginosa* and *S. marcescens*. D) Bacterial liquid co-culture between *P. aeruginosa* and *E. faecalis*. Bacteria from independent exponential growing culture were co-cultured in LB with 0 (top) or 0.25 mM (bottom) $ZnCl_2$ and incubated at 37ºC, 200rpm. Sample for colony counting were collected at the time of inoculation (time 0), after 24 and 48 hours (X axis). Y axis indicates CFU/ml over time. Results and error bars indicate mean ± SD of three technical replicates. Graphs show representative data from three independent experiments. Data analysis was performed with a two-way analysis of variance (ANOVA) using Prism (GraphPad 9.3.1,2021). P-values less than 0.05 were considered significant and indicated with asterisks. 0.049-0.033(*), 0.032-0.002(**), 0.0019-0.0002(***), 0.0001(****).

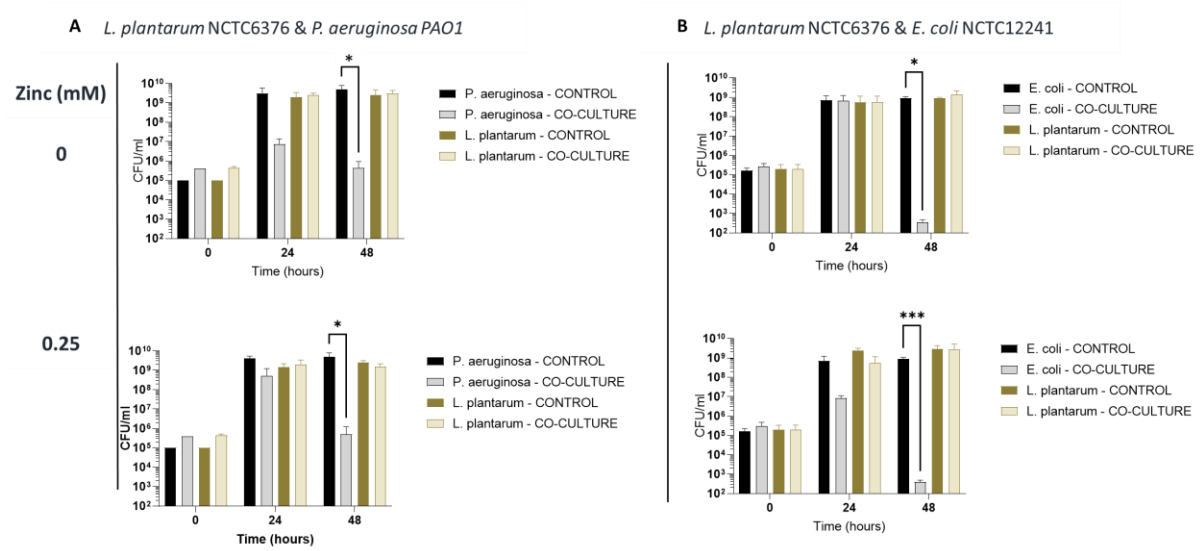

Figure 3.7: **Bacterial liquid co-cultures with or without Zn.** A) Bacterial liquid co-culture between *P. aeruginosa* and *L. plantarum*. B) Bacterial liquid co-culture between *E. coli* and *L. plantarum*. Bacteria from independent exponential growing culture were co-cultured in LB with 0 (top) or 0.25 mM (bottom) $ZnCl_2$ and incubated at 37ºC, 200rpm. Sample for colony counting were collected at the time of inoculation (time 0), after 24 and 48 hours (X axis). Y axis indicates CFU/ml over time. Results and error bars indicate mean ± SD of three technical replicates. Graphs show representative data from three independent experiments. Data analysis was performed with a two-way analysis of variance (ANOVA) using Prism (GraphPad 9.3.1,2021). P-values less than 0.05 were considered significant and indicated with asterisks. 0.049-0.033(*), 0.032-0.002(**), 0.0019-0.0002(***), 0.0001(****).

All the remaining results related to bacterial co-culture competition experiments, with no differences in prevalence over time, are included in Appendix II.

3.5 Molecular tools for species-specific identification

16s rRNA genes represent the most popular target for qualitative and quantitative analyses of bacterial diversity in environments since 1980[398]. Indeed, what makes the *16s rRNA* gene a good target for bacteria identification, is (i) its universality, (ii) poorly affected by horizontal gene transfer, (iii) its abundancy, i.e., the number of copies varies among species, (iv) the presence of variable regions flanking the universal conserved short sequences. In fact, the full 16s rRNA is roughly 1500 bases in length and consists in 9 hypervariable regions separated by the 9 conserved regions[277] (Figure 3.8). Normally, primers for qualitative analyses are built against the constant regions, enabling bacterial amplification of phylogenetically distant species, while the sequencing of hypervariable region through sequencing techniques[399] allows a broad bacterial differentiation and characterization. The *16S rRNA* gene amplification through PCR for qualitative single-species bacterial detection and qPCR for quantitative analyses is not commonly used and may represent an incipient novel technique for single-species bacterial detection and quantification in bacterial population. Hence, for our research, we identified species-specific primer pairs that anneal to the variable regions of 16s rRNA in order to discriminate single bacterial strains through the amplification of a limited region of genes (200-800 bases) for qualitative and semi-quantitative examination for single species.

Figure 3.8: **Graphical representation of the *16s rRNA* gene on *E. coli* genome.** V1-V9 represent variable regions (grey), C1-C8 represent constant regions (blue) and *E. coli* genomic DNA (orange)/ Built based on the sequenced identified in Geneious Prime on *E. coli* NCCT12241

3.6 *16s rRNA* genes library preparation and species-specific primers design

As it was difficult to identify appropriate primer pairs identification, we needed to undertake an in-depth bioinformatics analysis. Table 3.6 shows that the 16S rRNA sequences are extremely similar between various species and pairwise identity percentage among all strains were calculated with Geneious Prime® 2021.1.1 varied from 73 to 97%. As a result of an iterative process of analysis, primer pairs were identified (Section 2.2.2.1).

Species	Identity (%)							
	S. marcescens	*P. aeruginosa*.	*P. vulgaris*	*K. aerogenes*	*E. faecalis*	*L. plantarum*	*S. salivarius*	*S. aureus*
E. coli	96.25	84.83	92.98	95.93	76.16	75.87	76.07	76.08
S. marcescens		85.22	94.11	97.41	76.35	75.54	76.09	76.71
P. aeruginosa.			83.62	85.02	75.71	75.42	75.88	76.62
P. vulgaris				93.91	75.67	74.66	75.12	76.05
K. aerogenes					75.52	74.9	75.32	75.88
E. faecalis						88.32	87.75	89
L. plantarum							85.02	85.35
S. salivarius								84.12

Table 3.6: **Identity percentage calculated from pairwise alignment in Geneious Prime® 2021.1.1.** Colour gradient, from light grey to dark grey, is an indication of the increasing percentage identity.

3.6.1 Qualitative examination: most of the designed 16s rRNA primers may represent an innovative tool for bacterial detection

First, we wanted to test whether the designed primers can be used to amplify the DNA. The use of all the 16s rRNA primer pairs, except oligonucleotides for *Klebsiella aerogenes*, resulted specific DNA products of expected length indicating that they bound specifically. Of note, *S. aureus* and *L. plantarum* both required three cycles of freeze-boiling for DNA extraction. Moreover, *L. plantarum* primer pairs specifically bind to *L. plantarum* when annealing temperature was decreased from 50 to 48°C.

Once showed that each designed 16s rRNA primer pairs amplified a region of expected length for each bacterial strains, except for *K. aerogenes* (Figure 3.9), we wanted to test whether each primer primers annealing was effectively species-specific, as expected from the *in silico* analyses conducted to the primers designed. Results showed that primers designed for *S. marcescens* NCTC12241 and *P. aeruginosa* PAO1 were not binding exclusively to the expected species (Figure 3.10). In fact, the following results were observed: *(i) S. marcescens* primers specifically bound to *S. marcescens 16s rRNA gene* as expected, but also resulted in an amplicon from *K. aerogenes* DNA. When those primers were tested on *K. aerogenes* NCTC1006 genome on Geneious Prime® *2021.1.1*, they did not bind, hence predicting a specificity only for *S. marcescens 16s rRNA* gene among the selected ones. Considering that *K. aerogenes* NCTC1006 primer pairs did not bind to our *K. aerogenes* NCTC1006

strain as expected, we do not exclude the possibility of a misleading nomenclature of the collected strain. *(ii) P. aeruginosa* PAO1 primers specifically bound *P. aeruginosa 16s rRNA* gene, but a very fine band was also observed for *P. vulgaris*, suggesting that the primers pairs were able to bind and amplify a region on *P. vulgaris* nucleic acid. All the other pairs of primers showed a species-specific binding exclusive to the expected bacterial DNA. In fact, *16s rRNA* gene primer pairs built for *E. coli, E. faecalis, L. plantarum, S. salivarius*, *P. vulgaris*, *S. aureus*, specifically bound the single bacterial DNA among the tested ones (Figure 3.11). Although primers built against *S. marcescens* and *P. aeruginosa 16s rRNA* genes will require some troubleshooting methods, for instance testing the primer binding using an extended range of annealing temperatures of in order to increase the specificity, or design new primer pairs with a few bases different based on the *in silico* analyses of the species-specific *16s rRNA* genes, our findings displayed that 16s rRNA primer-pairs may represent our an innovative, time and cost-efficient tool for bacterial strain detection.

Primer pairs built against prodigiosin genes and some of the selected housekeeping genes were also tested successfully, binding to the expected species (Appendix III). Cross-reactivity among multiple species was not tested.

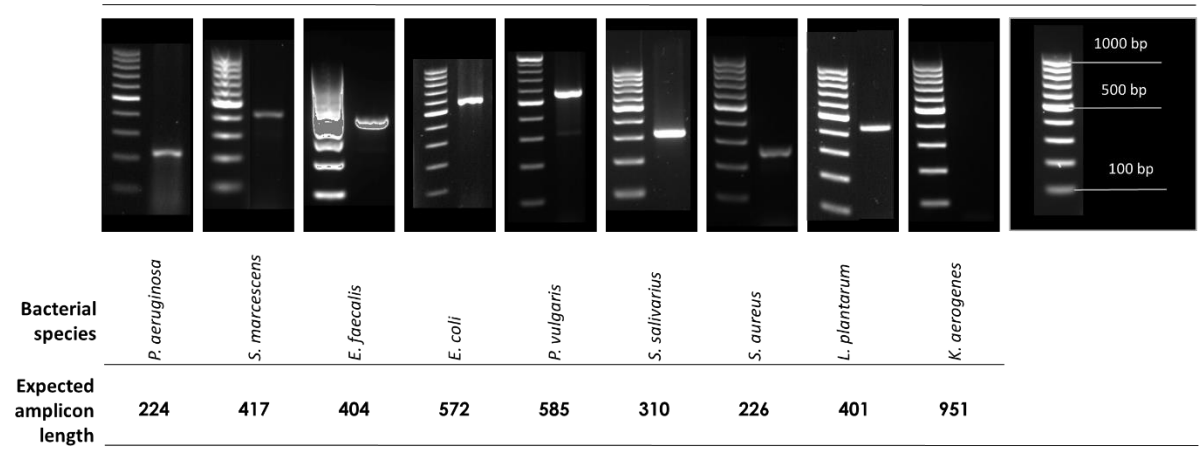

Figure 3.9 : **Species-specific 16s RNA gene amplicon obtained with standard PCR protol as described in the methods.** 100 bp Gene Ruler and DNA Ladder were used.

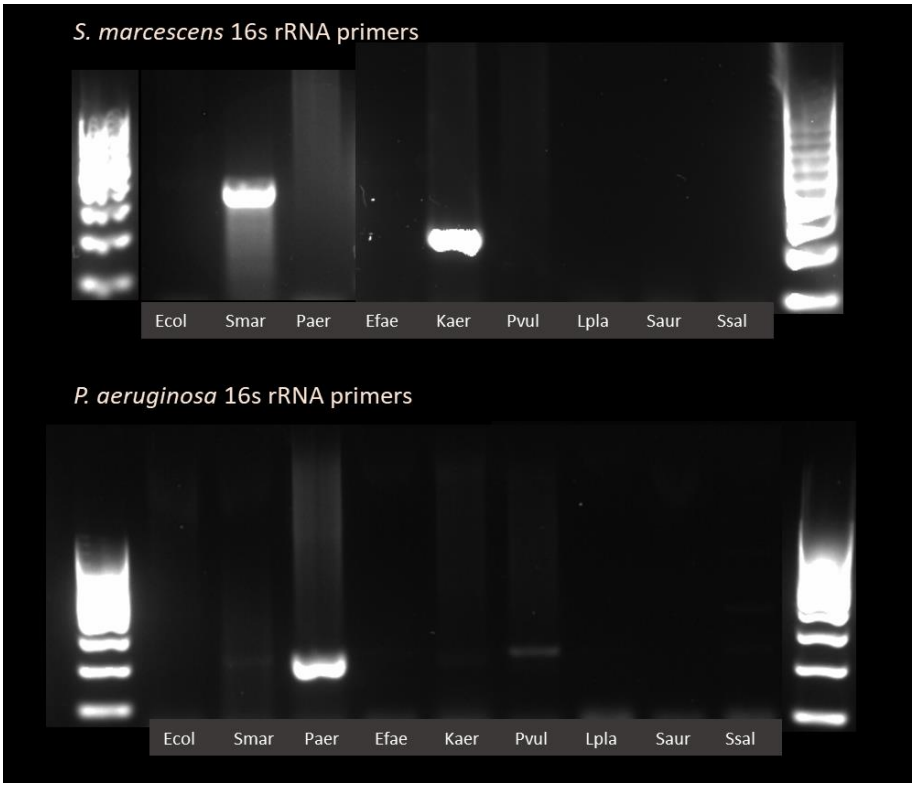

Figure 3.10: ***S. marcescens*** **and** ***P. aeruginosa*** **16s RNA gene primer pairs tested over nine bacterial strains applying standard PCR protocol as described in the methods**. Where P.aer: *P.aeruginosa* PAO1**,** Smar: *S. marcescens* NCTC1377, Efae: *E. faecalis* NCTC775, Ecol: *E. coli* NCTC12241, Pvul: *P. vulgaris* NCTC4175, Ssal: **S.salivarius** NCTC1886, Saur: *S. aureus* NCTC12981 , Lpla: *L. plantarum* NCTC6376 indicates the species-specific extracted DNA. Amplicons expected length and DNA ladder as described in *Figure 3.9*

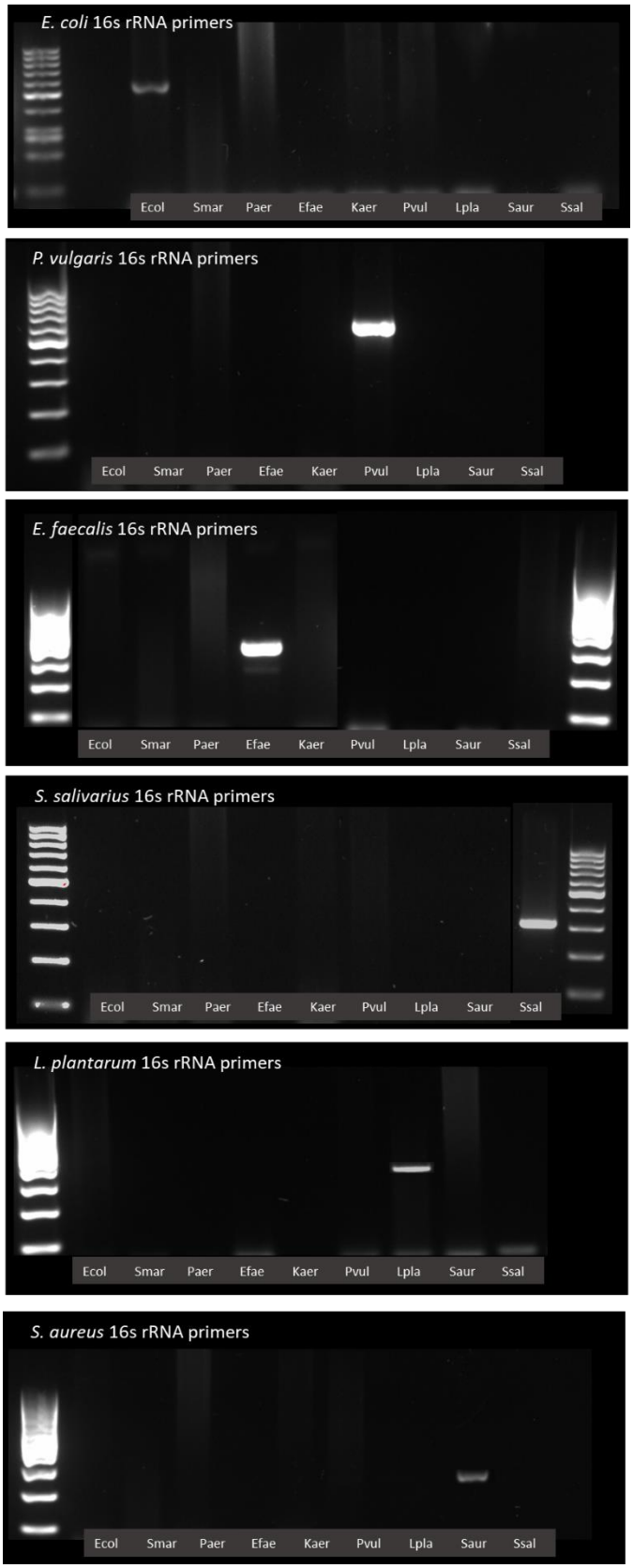

Figure 3.11: **16s RNA gene primer pairs tested over nine bacterial strains applying standard PCR protocol as described in the methods**. (P.aer) *P.aeruginosa PAO1*, **(**Smar) *S. marcescens* NCTC1377, (Efae) *E. faecalis* NCTC775, (Ecol) *E. coli* NCTC12241, (Pvul) *P. vulgaris* NCTC4175, (Ssal) *S. salivarius* NCTC1886, (Saur) *S. aureus* NCTC12981 , (Lpla) *L. plantarum* NCTC6376 indicates the species-specific extracted DNA. Amplicons expected length and DNA ladder as described in *Figure 3.9*

3.6.2 Semi-quantitative analyses of bacterial DNA using conventional PCR

In order to effectively use 16s rRNA primer pairs to quantitatively detect bacterial strains growing in co-cultures, we first did a semi-quantitative analyses of single species DNA serially diluting the DNA products by 10-fold and applying the protocol for conventional qualitative PCR. Results in Figure 3.12 shows that the more diluted the DNA samples were, the less intensely the band was visible, i.e., less amplified product was obtained. The amount of extracted DNA could be estimated based on the number of the cells (10^8 cells/ml) that were initially processed for DNA extraction through freeze-thawing, hence allowing to the approximate determination of the relationship between the band intensity and the actual extracted DNA for each bacterial strain.

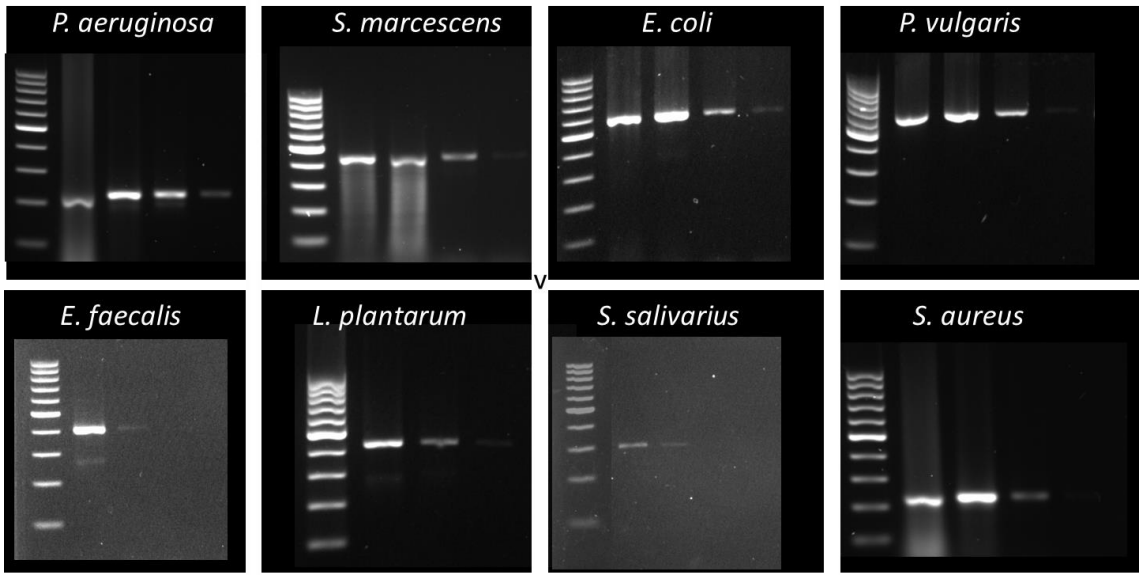

Figure 3.12: **Semi-quantitative PCR results obtained for each species.** Bacterial samples were standardized to a cell density of 10^8 cells/ml prior DNA extraction. For each species, bands on the gel correspond to less diluted (10-fold dilution) to more diluted (4x 10-fold dilutions) samples from left to right. Expected amplicon length and DNA ladder as described in *Figure 3.9*.

The semi-quantitative analyses of bacterial DNA using species-specific 16s rRNA primer pairs seems to be an effective tool for quantitively differentiating the bacterial species in co-culture competition experiments. Figure 3.13 illustrates the semi-quantitative PCR results for *P. aeruginosa* and *S. marcescens* co-culture after 24 and 48 hours in the presence or absence of Zn. The bands on the gel provide evidence that both strains co-exist over-time, independently from the presence of Zn. Nonetheless, those results are in contrast with what we observed from viable colony counts, Figure 3.6C, where we described a significant prevalence of *P. aeruginosa* PAO1 on *S. marcescens* NCTC1377 after 48 hours of growth in the presence of Zn. As *S. marcescens* is known for losing the ability to produce prodigiosin in certain conditions[30], it is conceivable that *P. aeruginosa* PAO1, when in contact with *S. marcescens* NCTC1377 and in the presence of Zn, may induce a de-repression of prodigiosin genes. If this is the case, it is likely that *S. marcescens* NCTC1377 colonies could have been "masked" by *P. aeruginosa* PAO1 which is characterized by large, green, "fried-egg" shapes colonies. The phenomenon and mechanisms need to be further elucidated.

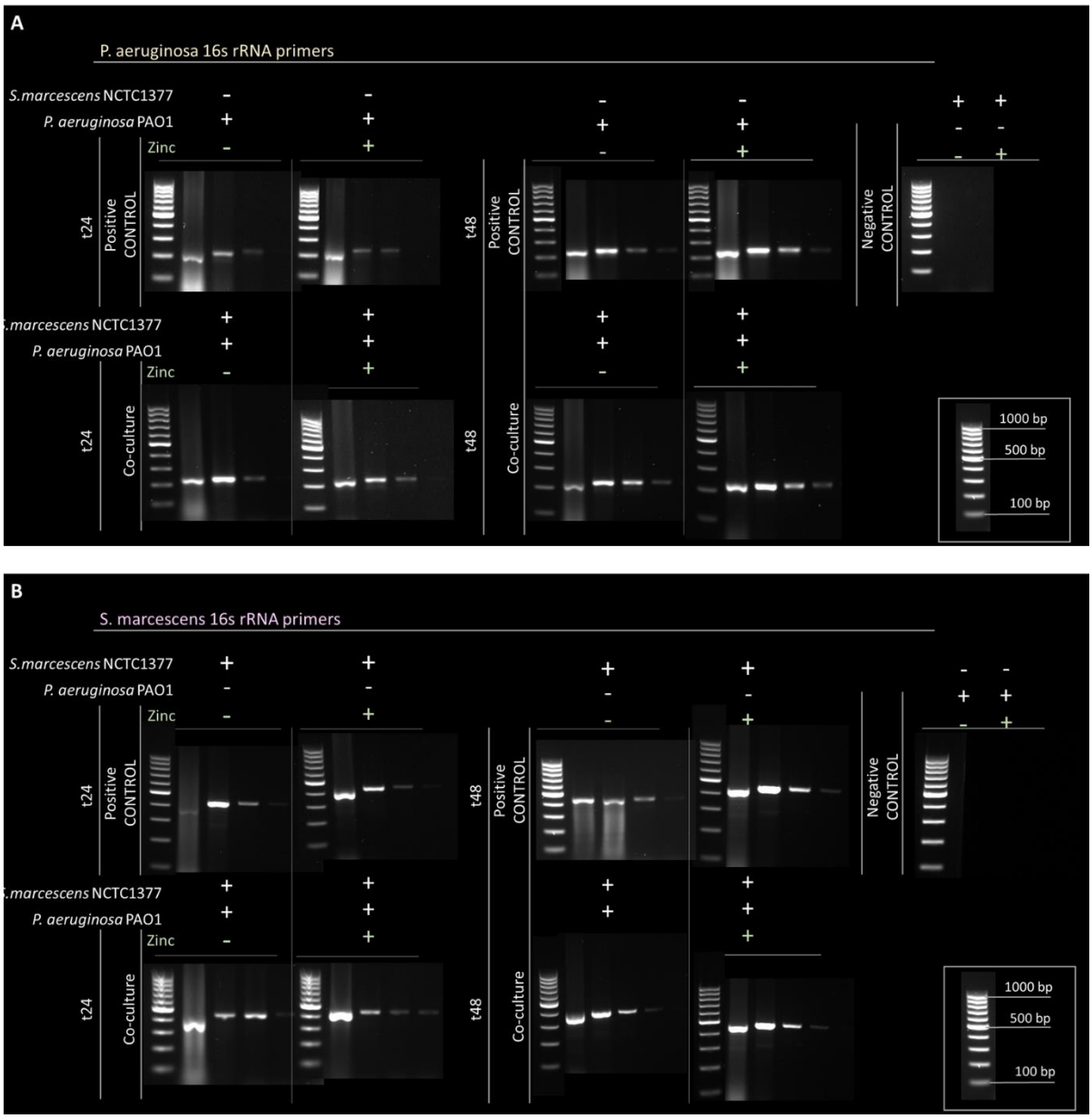

Figure 3.13: **Semi-quantitative PCR results for *P. aeruginosa* and *S. marcescens* co-culture with or without Zn.** Bands on each gel, from left to right, correspond to less diluted (10-fold dilution) to more diluted (4x 10-fold dilutions) DNA templates. 100 bp Gene Ruler and DNA Ladder was used. **A)** Amplicons generated using *P. aeruginosa* 16s rRNA primers; positive control: *P. aeruginosa* as a mono-culture; negative control: *S. marcescens* as a mono-culture. **B)** Amplicons generated using *S. marcescens* 16s rRNA primers. Positive control: *S. marcescens* as a mono-culture; negative control: *P. aeruginosa* as a mono-culture. Expected amplicon length: 224 bp for *P. aeruginosa* 16s rRNA primers, 417 bp for *S. marcescens* 16s rRNA primers.

3.6.3 Quantitative analyses of single bacterial species

The most effective and commonly used for quantitative analyses of nucleic acids is real-time amplification (qPCR). Designed 16s rRNA primer pairs were used to assess their efficacy for future quantification of each bacterial species in co-culture experiments. We plotted the Ct values against the species-specific serially diluted DNA template (Figure 3.14). The non-diluted sample or 10-times diluted were not accurate probably due to the amount of DNA being too high[400]. Most of the primer pairs (*E. coli*, *P. aeruginosa*, *E. faecalis*, *P. vulgaris* and *L. plantarum* 16s rRNA primer pairs) produced signals

even with the control (no DNA template), suggesting the amplification was due to a primer dimer that we did not identify with conventional PCR being less accurate and sensitive.

On the other hand, *S. marcescens*, *S. salivarius* and *S. aureus* 16s rRNA primer pairs produced amplification curves that could be used in further analysis, as the Ct value increased with a decreasing amount of template.

Therefore, the qPCR protocol for the primer pairs which did amplify with no DNA template needs to be adapted and improved, for instance trying with a range of different annealing temperatures, or considering more dilutions for the DNA templates, or again considering the re-design of slightly different primers with an extremely low chance of forming hetero- or homo- dimers.

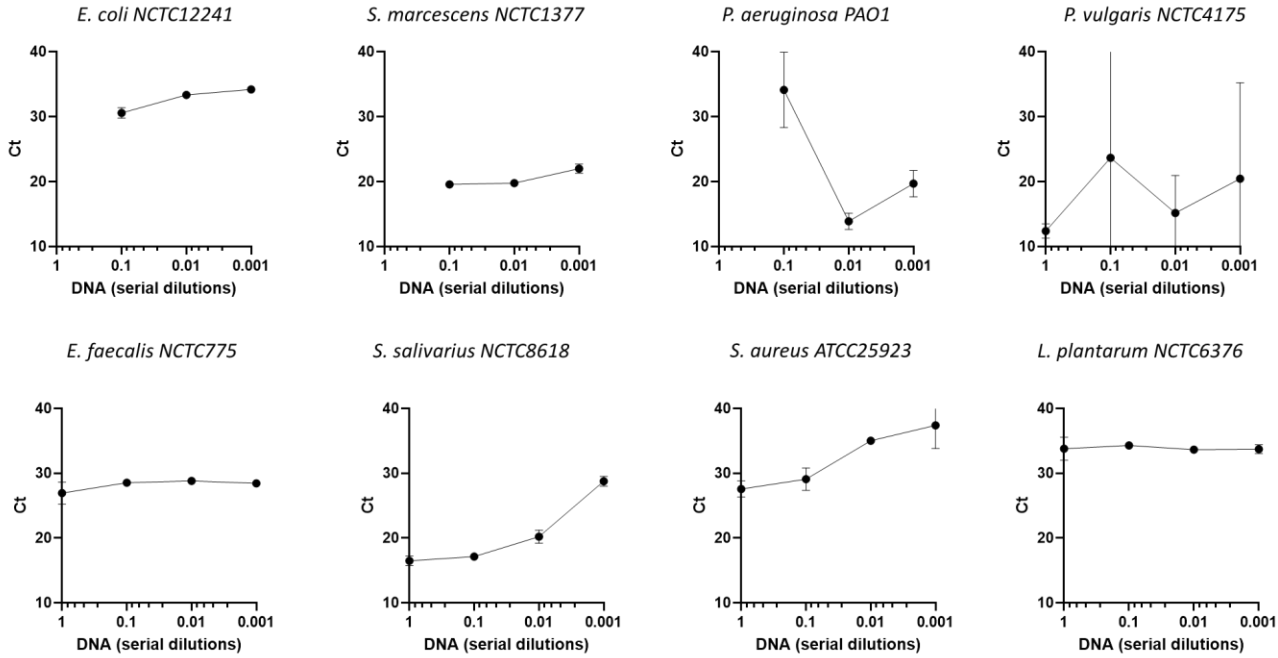

Figure 3.14: ***16s rRNA* genes quantitative amplification plots**. Bacterial samples were standardized to a cell density of 10^8 cells/ml prior DNA extraction. For each species, X axis indicates the dilution factor for the DNA templates, from non-diluted (1) to 3x 10-fold dilution (0.001); Y axis indicates the Ct values. The threshold Ct was automatically set based on the amplification curves.

3.7 Conclusion CHAPTER 3

To study the behaviours of bacterial species in co-culture, we have first determined bacterial fitness growing as single organisms and established the conditions for setting up *in-vitro* co-culture competition experiments, selecting rich growth media that allowed the growth of all bacterial strains (LB and TSB). For *L. plantarum*, a fastidious microorganism, we have developed a novel growth medium (LBEAP1) which contained specific micronutrients and high glucose concentration essential for this bacterial species to growth at a growth rate similar to the other bacterial strains selected for our project. Then, we have determined that 250 µM of Zn was the ideal concentration to use for fulfilling our aims without being toxic for the selected bacterial strains.

To discriminate the bacterial strains when in co-culture, besides the use of selective and differential media, we have designed a subset of primers against *16s rRNA* genes which can allow the rapid and efficient strain-specific detection of the selected bacteria.

Among the pairwise co-cultures, we have found that:

i) *P. aeruginosa* prevailed on *S. aureus* and *S. salivarius* - findings which are also supported by published work. Mechanisms that lead to potential selective advantage of *P. aeruginosa* in our settings need to be determined.
ii) *L. plantarum* can inhibit the growth of *E. coli* and *P. aeruginosa* on solid plates, a cutting-edge finding which may have potential implication in healthcare and food industry.
iii) *P. aeruginosa* led to a potential obliteration or phenotypic changes of *S. marcescens* in the presence of Zn. Again, the phenomena need to be further explored with follow-up experiments.

Ultimately, although no differential prevalence in the co-culture between *E. coli* and *S. marcescens* was found, we have observed the formation of a geometric pattern on solid TSA plates after overnight incubation. The characterization of this pattern is described and discussed in the following chapter.

4 CHAPTER 4

Escherichia coli and *Serratia marcescens* co-culture: The "bull's eye" pattern

To determine if micromolar concentrations of Zn play a role in bacterial population selection and dynamics in *in vitro* co-culture competition experiments, we set pairwise liquid co-culture for a selection of GI bacteria including *S. marcescens* NCTC1377 and *E. coli* NCTC12241. As discussed in Section 3.4.1, this pairwise co-culture, did not lead to any selection of competing bacterial populations over time, as shown in Figure 4.1 and Figure 4.2. We initially measured the CFU resulting from the co-culture (Figure 4.1) which showed that both, *E. coli* and *S. marcescens*, co-existed in liquid medium (LB), with the latter displaying 10-fold more cells after 48 hours of growth independently from the presence or absence of *E. coli*, and with Zn not affecting the bacterial competitive growth. Results from semi-quantitative PCR (Figure 4.2) confirmed the presence of both strains after 24 or 48 hours of growth in liquid co-culture, with or without the micronutrient Zn.

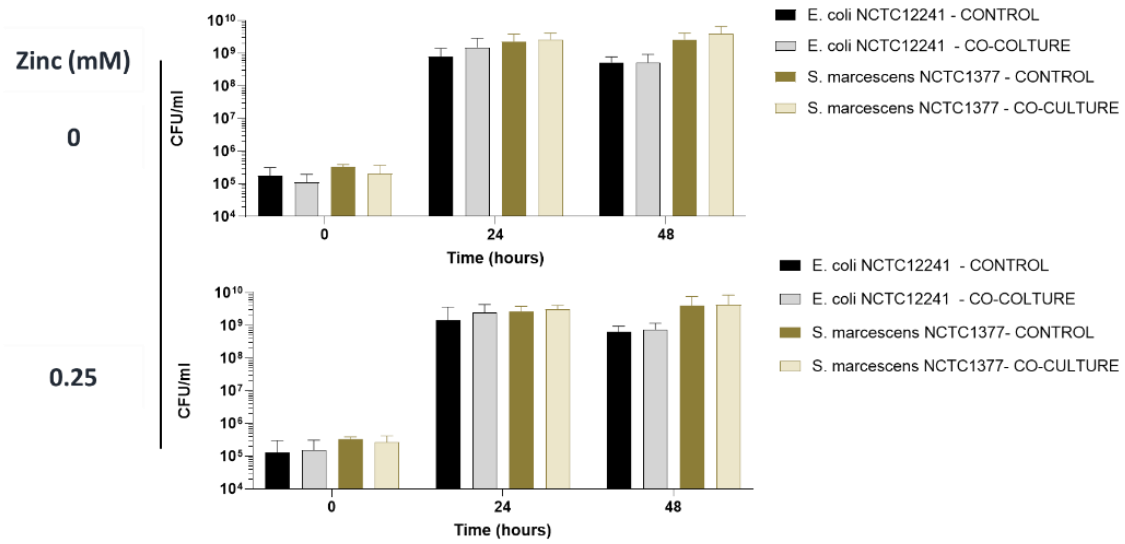

Figure 4.1: **Bacterial liquid co-culture between *E. coli* and *S. marcescens* with or without Zn.** Bacteria from independent exponential growing culture were co-cultured in LB with 0 (top) or 0.25 mM (bottom) ZnCl2 and incubated at 37ºC, 200rpm. Sample for colony counting were collected at the time of inoculation (time 0), after 24 and 48 hours. Results and error bars indicate mean ± SD of three technical replicates using Prism (GraphPad 9.3.1,2021). Graphs show representative data from three independent experiments.

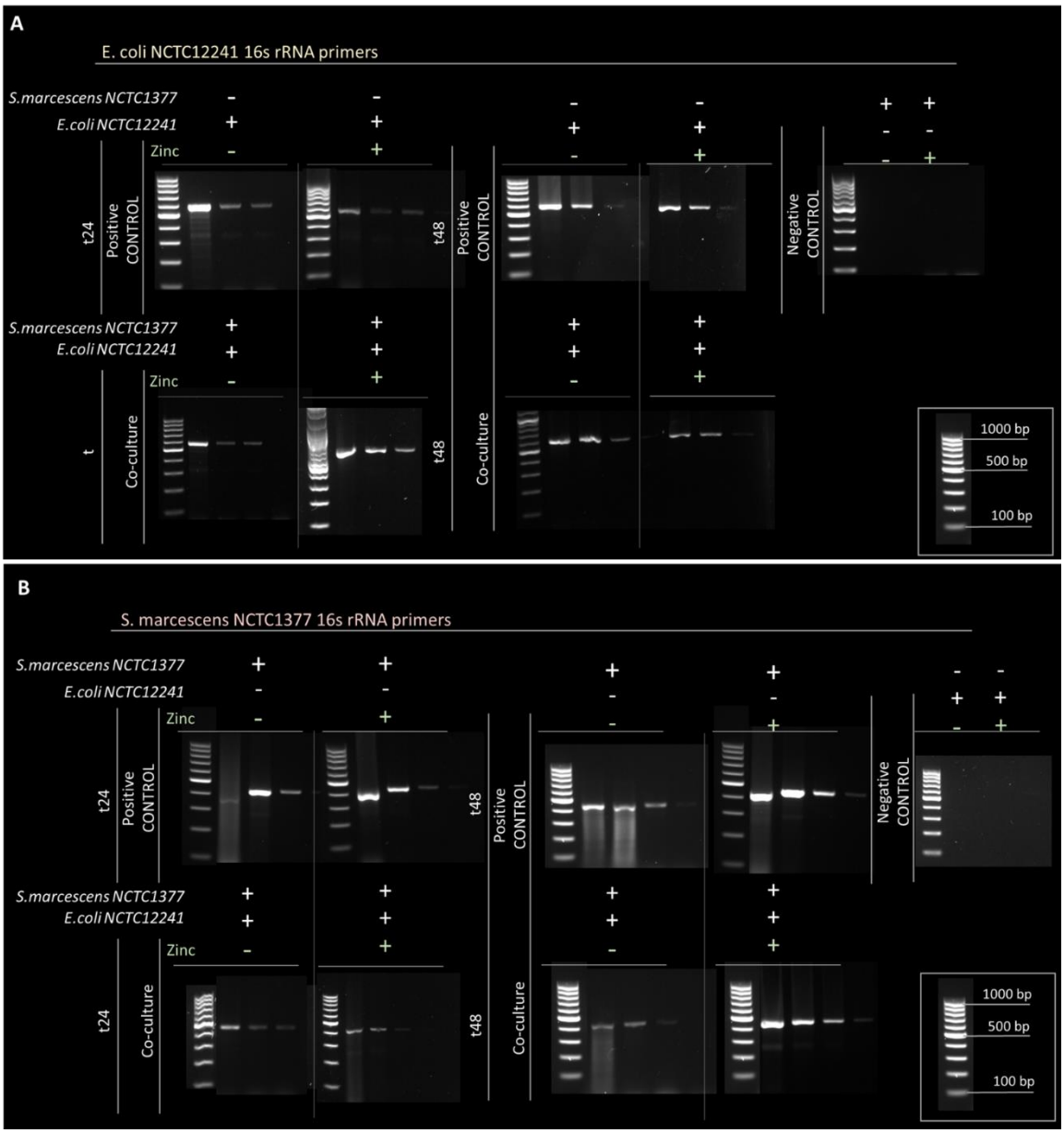

Figure 4.2: **Semi-quantitative PCR results for *S. marcescens* and *E. coli* co-culture with or without Zn.** Bands on each gel, from left to right, correspond to less diluted (10-fold dilution) to more diluted (4x 10-fold dilutions) DNA templates. 100 bp Gene Ruler and DNA Ladder was used. **A)** Amplicons generated using *E. coli* 16s rRNA primers; positive control: *E. coli* as a mono-culture; negative control: *S. marcescens* as a mono-culture. **B)** Amplicons generated using *S. marcescens* 16s rRNA primers. Positive control: *S. marcescens* as a mono-culture; negative control: *E. coli* as a mono-culture. Expected amplicon length: 572 bp *E. coli* 16s rRNA primers, 417 bp for *S. marcescens* 16s rRNA primers.

4.1 The "bull's eye" pattern characterization

Despite no differential prevalence observed between *E. coli* NCTC12241 and *S. marcescens* NTCTC1377 in co-culture, we observed the existence of a striking geometric pattern in some of the colonies resulting from the liquid co-culture. Specifically, when 10 µl drop containing roughly 10^5 to 10^6 cells from a liquid co-culture of *E. coli* NCTC12241 and *S. marcescens* NTCTC1377 was seeded in TSA plates, dried and incubated for 16 hours at 37°C, we could consistently observe a colony characterized by a geometric concentric pattern, with a red outer edge, approximately 1 to 1.5 mm thick, a white middle ring with a thickness of approximately 1.2 to 1.5 mm, and a central red spot with a diameter of 3 to 4.5 mm roughly (Figure 4.3). Due to the white-red concentric pattern, we have named it the "bull's eye" pattern. Of note, we observed that the red pigmentation due to prodigiosin production by *S. marcescens* NCTC1377 was boosted if plates were left at RT, consistent with the fact the maximum pigmentation production occurs between 22 to 27°C[401]; pictures of *S. marcescens* colonies or related co-cultures were taken after incubation at 37°C for 16 hours and further 2 hours at RT, unless otherwise indicated.

.

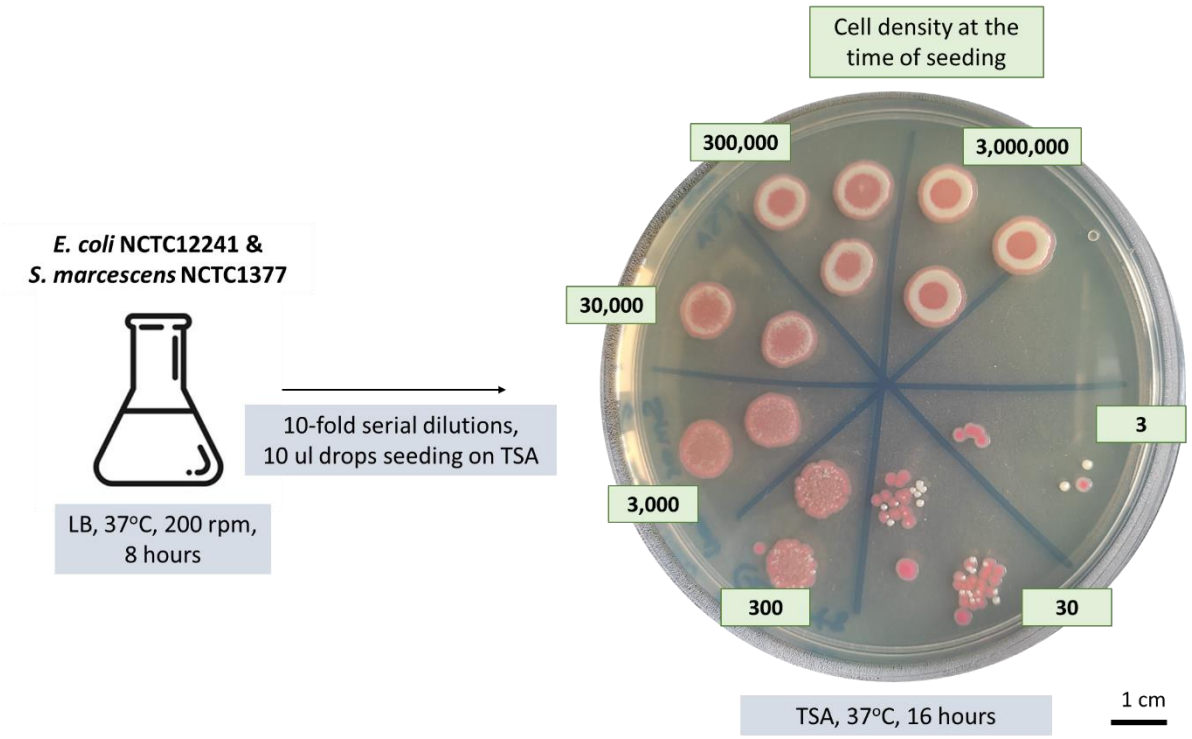

Figure 4.3: **The "bull's eye" pattern** formation: *E. coli* and *S. marcescens* co-culture was grown for 8 hours in LB, 10 µl drops resulted from 10-fold serially diluted samples in PBS from the liquid co-culture were added on a TSA plate, where each sector specifically corresponds to a dilution. The plate was allowed to dry and incubated. After 16 hours at 37°C, we could observe the "bull's eye" pattern from the high cell density-colonies with $3x10^5$ or $3x10^6$ cells at the time of seeding (numbers have been calculated multiplying by 10-fold from the more diluted sector, containing 3 cells per drop)

In order to characterize the "bull's eye" pattern formation and investigate the conditions that led such a geometric pattern to appear, a number of experiments were conducted. Firstly, to verify that the strains involved did not form this pattern when growing as a mono-culture. Secondly, to determine if the pattern changed over time if incubated for longer than 16 hours at 37°C. Thirdly, to define the species identity

(qualitatively and quantitatively) on the “bull’s eye” pattern. The conditions of growth, i.e., nutrients on the solid surface, time of contact between the two strains in liquid, cell density ratio between the two strains, size of the seeding drops, were investigated to figure out possible conditions required for the pattern to form. The “bull’s eye” pattern growth during incubation time was also monitored to describe its formation. The involvement of a different strain and also the presence of a third bacterial species in the co-culture were considered. Eventually, the presence of a signal-mediating the pattern formation was evaluated by testing the “bull’s eye” formation with CM and in the presence of micronutrients.

4.1.1 The “bull’s eye” pattern is maintained over time

Firstly, we showed that *S. marcescens* NCTC1377 or *E. coli* NCTC12241 did not form a pattern when growing alone compared to the co-cultured bacteria and that the pattern did not change over time, with the three areas well-defined even after one week of incubation (Figure 4.4 and Figure 4.5). White rings of an increasing width over time surrounded the “bull’s eye” pattern and the *S. marcescens* NCTC1377 colony, while the *E. coli* NCTC12241 was characterized by the formation of emerging spots at the outer edge.

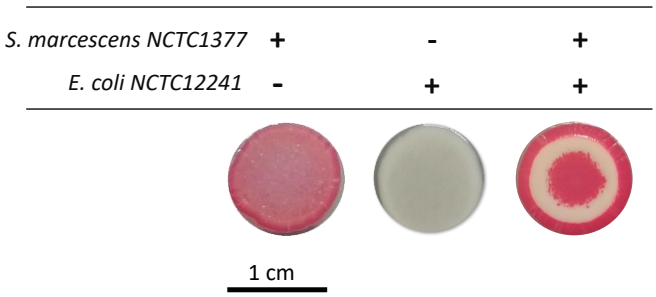

Figure 4.4: **Differential presentation of grown colonies of *S. marcescens* NCTC1377 and *E. coli* NCTC12241**: Colonies grown for 16 hours at 37°C on TSA plate resulted from 10^6 cells/10µl drop inoculation from exponential growing culture in LB at 37°C, 200rpm, of each strain.

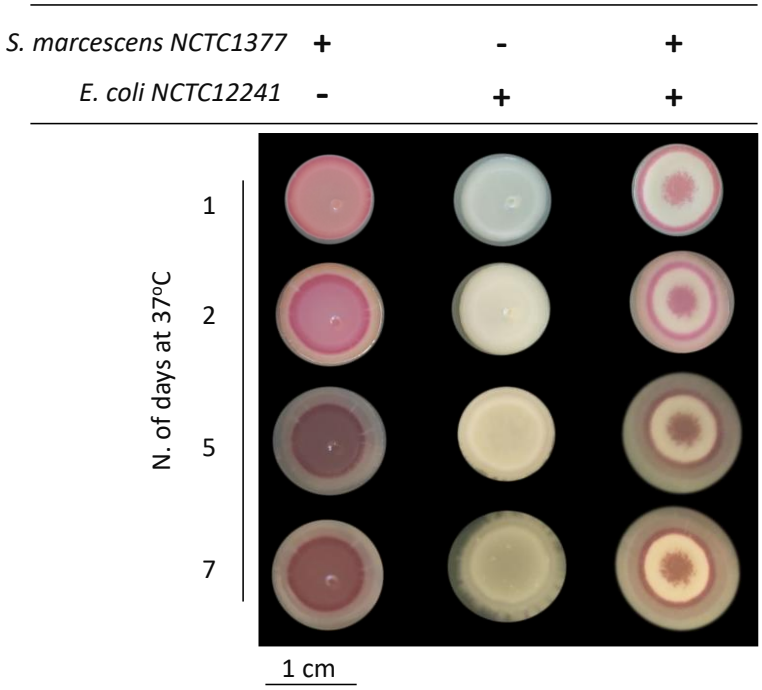

Figure 4.5: **Differential presentation of grown colonies of *S. marcescens* NCTC1377, *E. coli* NCTC12241 and both together over time.** Colonies grown for 7 days at 37oC on TSA plate resulted from 10^6 cells/10µl drop inoculation from exponential growing culture in LB at 37°C, 200rpm, of *E. coli* NCTC12241 and *S. marcescens* NCTC1377

4.1.2 The "bull's eye" pattern is a result of bacterial space distribution

S. marcescens red pigmentation is due to the production of prodigiosin; some *Serratia* strains are known for losing the ability to produce prodigiosin, resulting the white colony appearance. We had therefore considered the possibility that the white area in the pattern may be due to *S. marcescens* NCTC1377 with no prodigiosin production.

In order to investigate this further, we re-streaked samples from the three different areas, i.e., red outer edge, white middle ring and red central spot, to see if the colony characteristics were maintained over time. Results showed that the ratio of red cells:white cells from the outer edge and the central spots were roughly 10:1, vice versa, in the middle ring the ratio was 1:10, and that any single colony re-streaked maintained its characteristics, i.e., colour and morphology, (Figure 4.6, A) suggesting that the red was always *S. marcescens* NCTC1377 and the white was always *E. coli* NCTC12241 (Figure 4.6, B). To further support the consideration above, we extracted DNA from multiple colonies resulting from the re-streaking from the three different areas and amplified with species-specific oligonucleotides built against *S. marcescens* NCTC1377 or *E. coli* NCTC12241 *16s rRNA* genes. Results confirmed that the red colonies were *S. marcescens* and the white ones were *E. coli* (Figure 4.6, C).

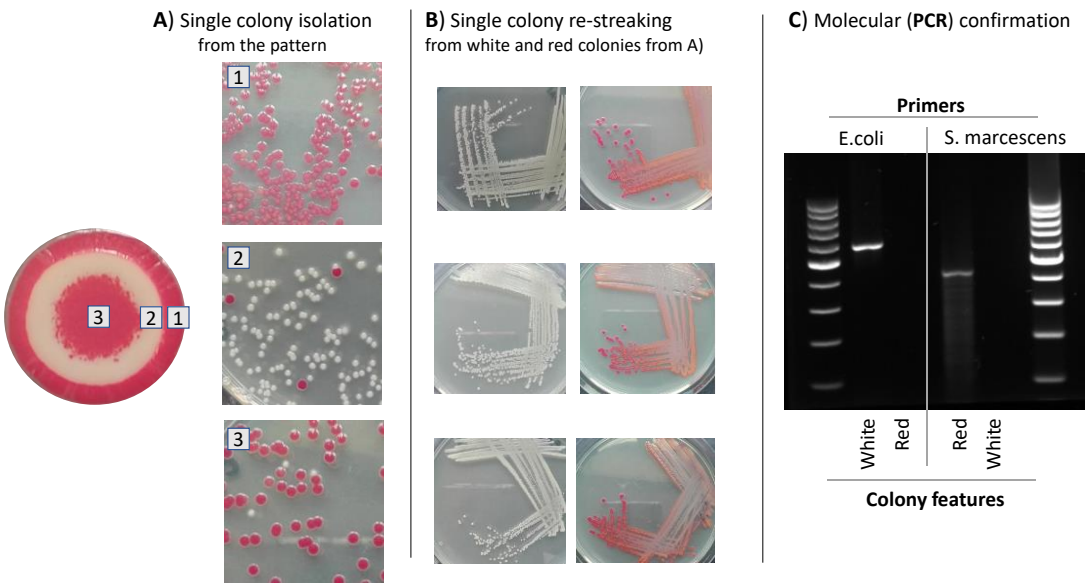

Figure 4.6: **Bacterial species in the "bull's eye" pattern identification**: A) Samples from the "bull's eye" pattern were collected, diluted and plated for single colony isolation. B) A single white colony and a single red colony resulted from each section of the pattern were re-streaked to confirm colony features maintenance. C) Single white colonies and single red colonies were collected and DNA extracted through freeze-boiling protocol; primers built against *16s rRNA* gene of *E. coli* NCTC12241 and *S. marcescens* NCTC1377 were used for DNA amplification (PCR) and molecular identification of the white and red cells.

Also, to quantify the differential distribution of the two species within the "bull's eye" pattern, we collected the bacteria grown on the agar for each sector (i.e., red outer edge, white middle ring, red central spot) separately, resuspended in liquid and quantify through serial dilution and further plating. Results demonstrated that the bacterial species were differentially distributed on the agar surface, with *S. marcescens* NCTC1377 establishing mainly at the outer edge and centre of the colony, while *E. coli* NCTC12241 in the middle ring. The ratio between *E. coli* NCTC12241 and *S. marcescens* NCTC1377 was impressively constant, 10 times more of *S. marcescens* NCTC1377 in the red area, and 10 times less of *Serratia* compared to *E. coli* NCTC12241 in the white area, as shown from the table 4.1.

Table 4.1: **Bacterial species-specific numbers of the "bull's eye" pattern**. A) cell numbers showed in the table resulted from the resuspension of each sector of a "bull's eye" pattern (red edge, white middle ring and red central spot) in 1 ml LB followed by serial dilutions in PBS and samples plating for counting (CFU/ml). B) Same protocol was applied for *S. marcescens* NCTC1377 and *E. coli* NCTC12241 independent growing colonies. Mean (±SD) of three technical replicates is shown.

A **Bull's eye pattern**

	S. marcescens ($x10^7$)	*E. coli* ($x10^7$)	*Total* ($x10^7$)
RED edge	240 (±20.5)	20 (±5.2)	**260**
WHITE middle	12 (±10.7)	150 (±19.8)	**162**
RED centre	110 (±20.8)	7 (±6.8)	**117**
Total ($x10^7$)	335	117	

B **Controls**

	S. marcescens ($x10^7$)	*E. coli* ($x10^7$)
Edge	110 (±16.5)	90 (±11.2)
Middle	220 (±15.7)	95 (±7.5)
Centre	150 (±11.6)	110 (±8.2)
Total ($x10^7$)	480	310

Semi-quantitative analyses also confirmed a prevalence of *E. coli* NCTC12241in the middle ring white area compared to *S. marcescens* NCTC1377 in the outside and centre area of the "bull's eye" pattern (Figure 4.7).

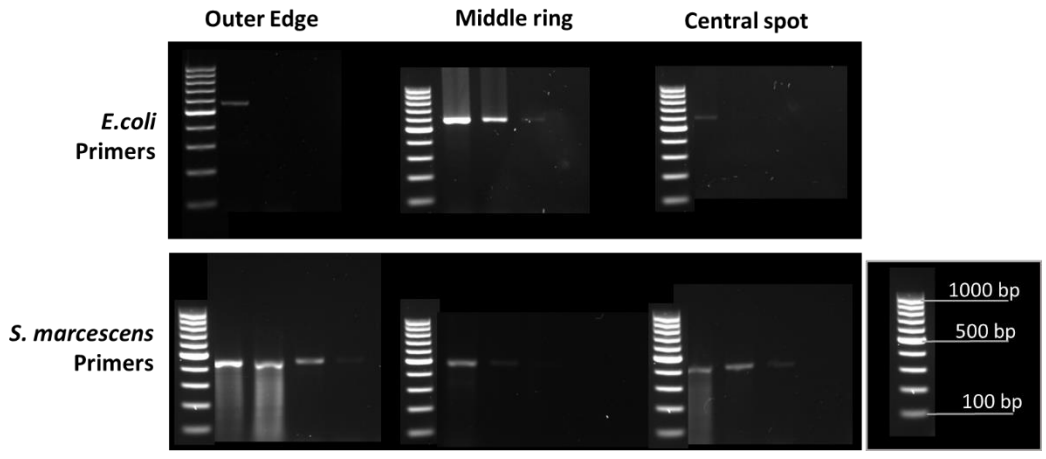

Figure 4.7: **Semi-quantitative PCR results**. Bacterial samples from the outer edge, middle ring or central spot of a grown "bull's eye" pattern was collected, resuspended in liquid media and were standardized to a cell density of 10^8 cells/ml prior DNA extraction. Species specific 16s rRNA primer pairs for each strain were used for semi-quantitative analyses of extracted bacterial DNA, serially diluting of 10-fold the DNA products and applying the protocol for the convention qualitative PCR. Bands on each gel correspond to less diluted (10-fold dilution) to more diluted (4x 10-fold dilutions) samples from left to right.

To observe any possible microscopic morphological changes in bacterial cells, the morphology of bacterial cells from samples from the three areas of the "bull's eye" pattern (outer edge, middle ring,

centre) was studied through Gram-stain coloration followed by microscopical observation. Results showed that most of the bacterial cells from the outer edge or central spot of a "bull's eye" pattern were morphologically very similar to the cells isolated from any sector a *S. marcescens*-colony. On the other hand, most of bacterial cells from the middle ring of a "bull's eye" pattern displayed a longer rod shape, likewise the bacterial cells isolated from any sector a *E. coli*-colony (Figure 4.8). Hence, the microscopic observation of bacterial cells, consistently with what shown above (in Figure 4.6 and Figure 4.7), demonstrated that the outer edge and the central spot of the "bull's eye" pattern were mostly colonies by *S. marcescens*, while the middle ring mainly by *E. coli*.

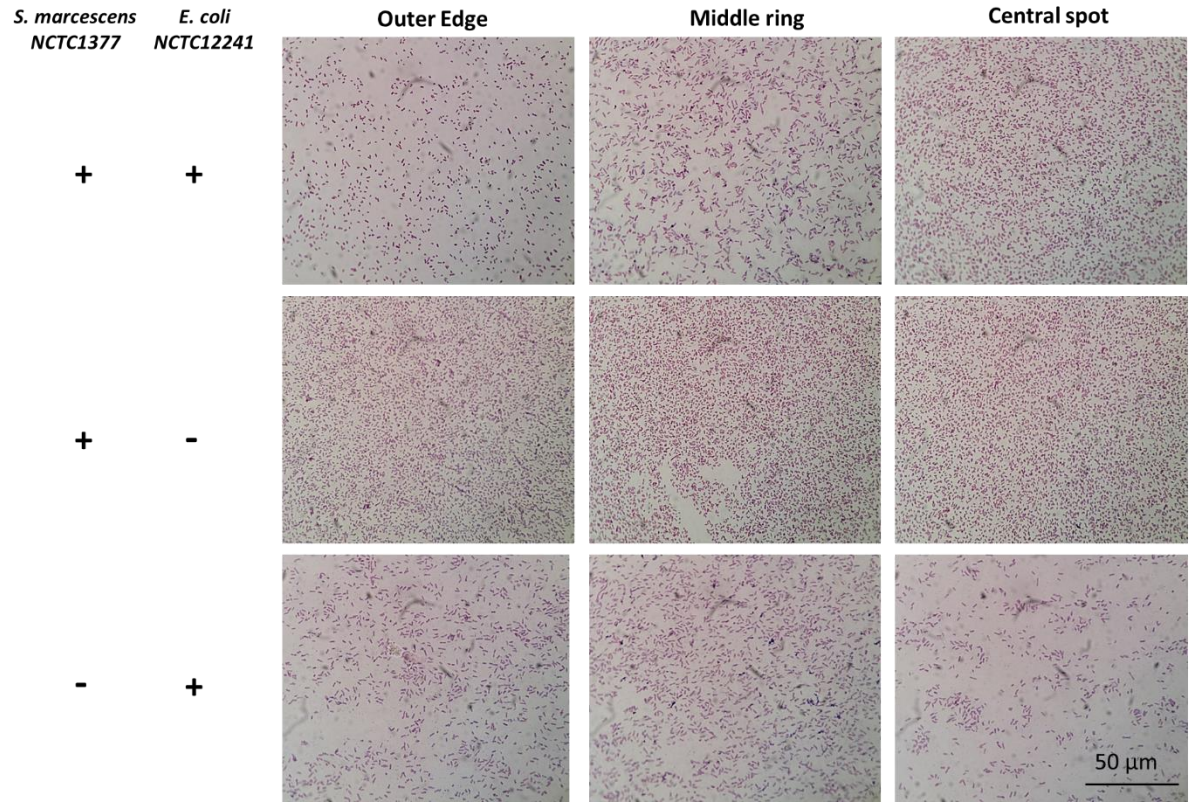

Figure 4.8: **Microscopical observation of bacterial cells the "bull's eye" pattern**. Samples were collected from the three sectors (outer edge, middle ring and central spot) of a "bull's eye" pattern (top row) or colonies grown from respective mono-cultures as controls. Optical microscope: Nikon ECLIPSE E200 Microscope, 40x, 1.000x magnification. Gram-staining colouration.

4.1.3 A time-lapse of the "bull's eye" pattern formation

We showed that a "bull's eye" pattern arose from the growth at 37°C, for 16 hours on TSA, of a 10 µl drop containing 10^6 cells of mixed *E. coli* NCTC12241 and *S. marcescens* NCTC1377. Consequently, we demonstrated that both *E. coli* NCTC12241 and *S. marcescens* NCTC1377 were present in all three sectors, with the density of *S. marcescens* NCTC1377 being higher in the central spot and outer edge and of *E. coli* NCTC12241 in the middle ring, and the difference between the higher and lower density strains in any of the sectors being always 10-fold higher. It was conceivable to question at what stage the pattern starts forming and how *E. coli* NCTC12241 and *S. marcescens* NCTC1377 cells differentially

grow or move toward an area of the solid surface rather than another. To answer those questions, we seeded 10 µl drop with 10^6 of 50:50 *E. coli* NCTC12241 and *S. marcescens* NCTC1377 from exponential growing cultures in TSA, allowed the drop to dry and incubated the plate at 37°C for 24 hours collecting samples from the three area of the colony (outer edge, middle ring, central spot) every 1 to 2 hours until 10 hours and then after 24 hours. The different frequency of *E. coli* NCTC12241 or *S. marcescens* NCTC1377 in the sectors of the colonised solid surface over time was assessed in order to determine the potential differential growth or migration of the two strains over time on the solid surface.

The time-lapse experiment demonstrated that *S. marcescens* NCTC1377 in the middle ring reduces growth rate apparently initiating stationary phase after 5 to 7 hours of growth (Figure 4.9, A), while, in the central spot or the outer edge *S. marcescens* NCTC1377 keep growing at a growth rate equivalent to that in early exponential phase (Figure 4.9, B and Figure 4.9,C). On the other hand, *E. coli* NCTC12241 growth rate was the same across all three sectors during the exponential phase of growth (Figure 4.9, E). *S. marcescens* NCTC1377 had an almost identical growth rate to *E. coli* NCTC12241 for the first four hours. After that, *S. marcescens* NCTC1377 at the outer edge and central spot of the colonised area grew at a faster rate than *E. coli* NCTC12241. These data suggest that the "bull's eye" pattern originated from changes connected to *S. marcescens* NCTC1377 physiology. A migration of a subset of cells of *S. marcescens* NCTC1377 from the middle ring toward the central spot and outer edge after 5 to 7 hours could also be considered. Notably, the cumulative number of *E. coli* NCTC12241 or *S. marcescens* NCTC1377 cells across all three sectors in each timepoints for the observed 10 hours period was identical for both strains (Figure 4.9, F), therefore most likely excluding a cidal effect between the two strains. Considering that *S. marcescens* NCTC1377 at the outer edge and the central spot grew faster than *E. coli* NCTC12241, while the latter had a constant growth rate over the three sectors, it is likely that the "bull's eye" pattern derives from changes connected to *S. marcescens* NCTC1377 physiology.

A model of the bacterial species growing and distributing across the space leading to the "bull's eye" pattern formation over time is shown in Figure 4.10.

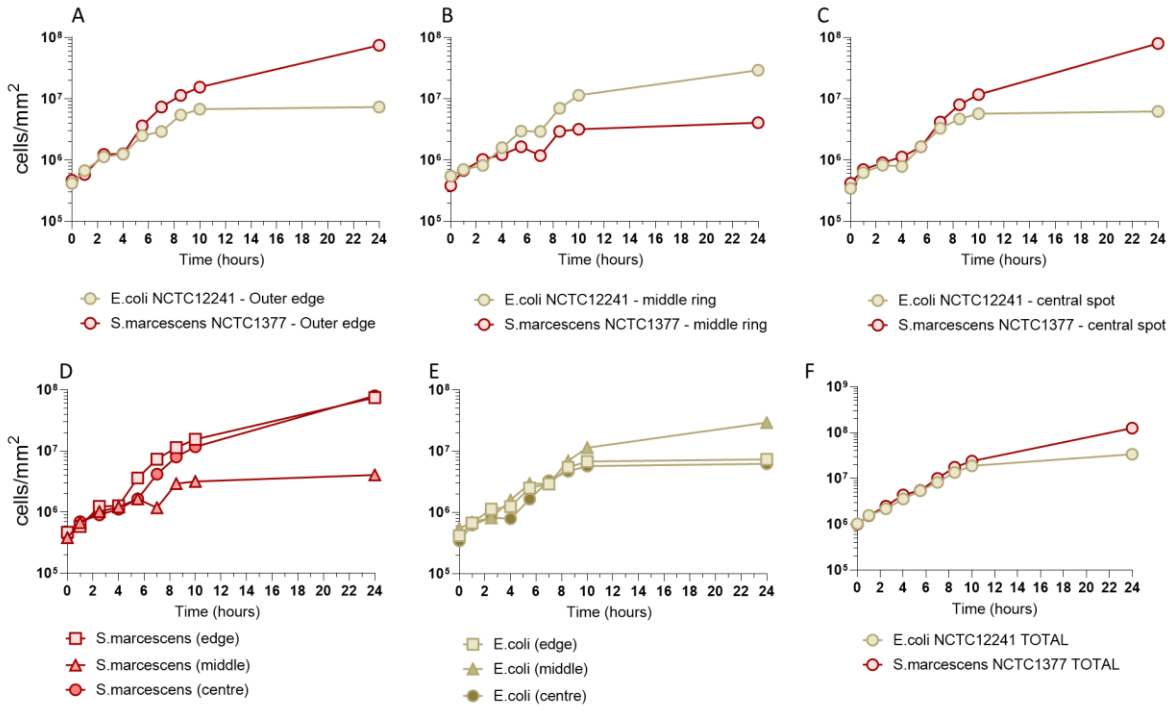

Figure 4.9: **Species-specific space distribution into a "bull's eye" pattern of *S. marcescens* NCTC1377 and *E. coli* NCTC12241 on TSA over time. A)** cells/mm² of *S. marcescens* NCTC1377 in red and of *E. coli* NCTC12241 in cream-white at the edge of the colonies area. **B)** cells/mm² of *S. marcescens* NCTC1377 in red and of *E. coli* NCTC12241 in cream-white at the middle ring of the colonies area. **C)** cells/mm² of *S. marcescens* NCTC1377 in red and of *E. coli* NCTC12241 in yellow/cream-white at the centre of the colonies area. **D)** cells/mm² of *S. marcescens* NCTC1377 from the three sectors. **E)** cells/mm² of *E. coli* NCTC12241 from the three sectors. **F)** cumulative number of *E. coli* NCTC12241 or *S. marcescens* NCTC1377 cells across all three sectors in each timepoints for the observed 10 hours period was identical for both strains.

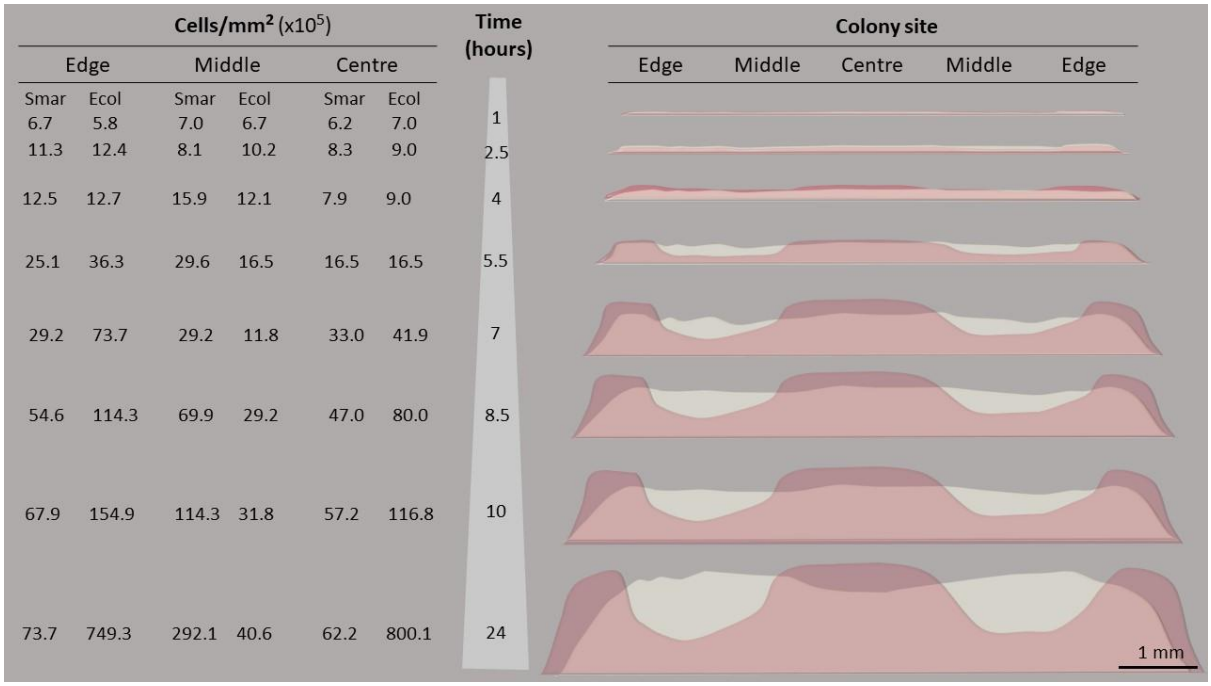

Figure 4.10: **"Bull's eye" pattern model of a developing "bull's eye" pattern**. On the left, numbers (cell/mm²) of *E. coli* NCTC12241 or *S. marcescens* NCTC1377 growing at the edge, middle or centre or the growing colony. Samples were collected over time, reported in within the column "Time(hours)". On the right, a model of *E. coli* NCTC12241 (white) and or *S. marcescens* NCTC1377 (pink) was designed resembling the growing "bull's eye" pattern.

4.1.4 *S. marcescens* NCTC1377 does not form a pattern in the absence of *E. coli* NCTC12241 in the liquid co-culture

A *Serratia* marcescens strain (5965) has been found to form a pattern very similar to the "bull's eye" pattern even when grown on its own but in specific growth conditions (NB agar supplemented with 5% glucose after 5 to 7 days of incubation at 27°C)[244]. To confirm that our strain *S. marcescens* NCTC1377 did not form the "bull's eye" pattern when growing alone, we cultured the bacterial species in multiple solid agar plates and at different temperatures. We demonstrated that *S. marcescens* NCTC1377 did not form the "bull's eye" pattern in the absence of *E. coli* NCTC12241 in any of the different growth media over time (Figure 4.11).

However, different *S. marcescens* NCTC1377 phenotypes appeared based on the growth media. An almost white colony phenotype was developed in a medium with high glucose concentration (glucose-supplemented NBA, TSA, BHIA) over time. Differently, red colonies (with just a thin white rim) appeared in a non-buffered medium lacking glucose regardless of the presence or absence of NaCl (LBA). In CLED, where the sugar substrate is lactose, the colonies were red, most likely due to the poor metabolism of lactose in *S. marcescens.*

Hence, in our conditions, glucose, more than protein or salt concentrations, seemed to downregulate prodigiosin production in *S. marcescens* NCTC1377. In support of this, glucose-mediating *S. marcescens* pigmentation had been reported in the literature for decades[402,403], a process most likely mediated by a the acidification of the media[404], but still not well understood.

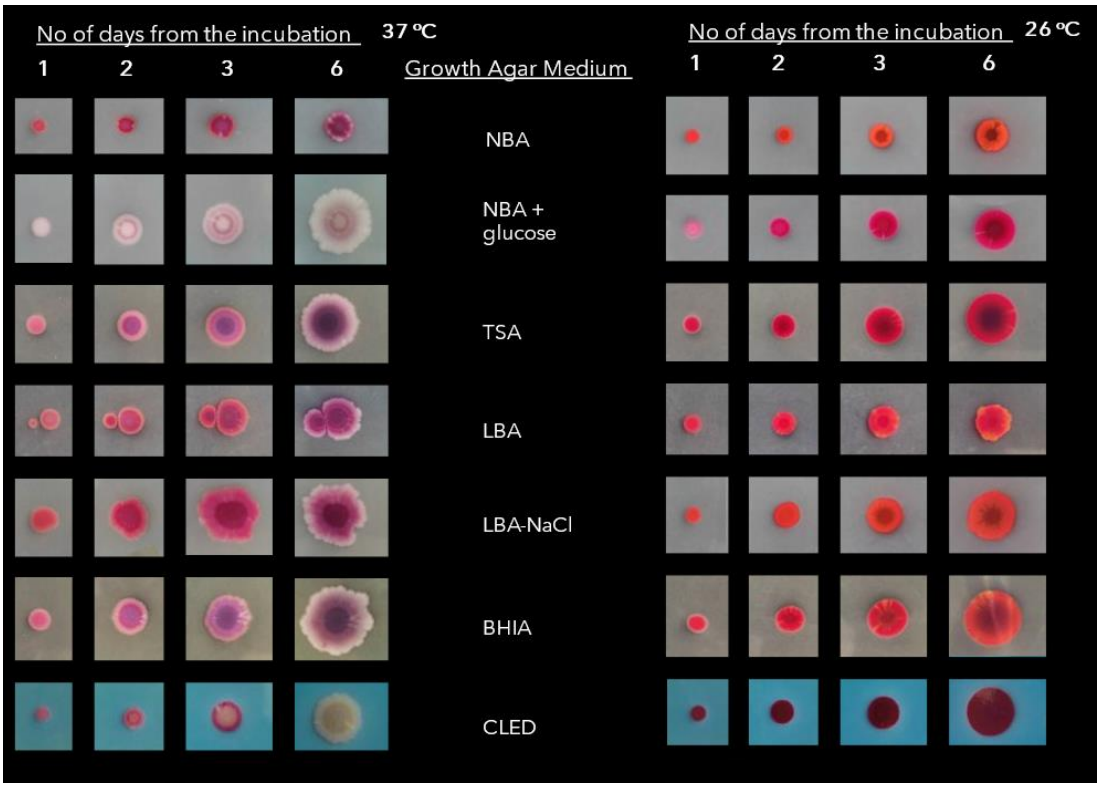

Figure 4.11: ***S. marcescens* NCTC1377 colonies over time in different growth media and at different temperature**. 1 µl drop of 10^5 cells *S. marcescens* in different media incubated at 37ºC or at 26ºC for 6 days.

4.1.5 Glucose may play a role in the "bull's eye" pattern formation

The "bull's eye" pattern was initially observed on TSA, a growth medium containing glucose, proteins, NaCl and K_2HPO_4 as a buffer. The less rich LBA did not support the formation of the "bull's eye" pattern and to test which of the components may be responsible for this, LBA medium was supplemented with glucose, NaCl or K_2HPO_4 or a combination of them. We could show that when LB was supplemented with glucose alone or glucose and buffer, a "bull's eye" similar pattern appeared, suggesting that glucose was required for the pattern to form. This suggestion was supported by the formation of white-red rings in BHIA, a medium also rich in glucose. In contrast, such a geometric pattern was not observed in NBA, even when glucose was supplemented, most likely associated with a different protein composition, an aspect that has not been further investigated. Interestingly, we did not observe any "bull's eye" pattern on CLED, but the co-culture was instead characterized by a substantial repression of prodigiosin expression, with a homogenous yellow colony and some red spots at the edge of the colony. This may be due to the differential sugar composition or source and the ability of *S. marcescens* or *E. coli* to metabolize lactose, aspects not further investigated. Of note is that CLED is rich in L-cystine, the oxidized derivative of Cys, an intermediary compound in the biochemical pathway leading to the synthesis of AHL derivatives used for QS signalling in Gram-negative bacteria; hence, there was scope to consider the effect of Cys as a nutrient or a signal, likely to mediate the cell-to-cell (in this case *S. marcescens* NCTC1377-*E. coli* NCTC12241) communication.

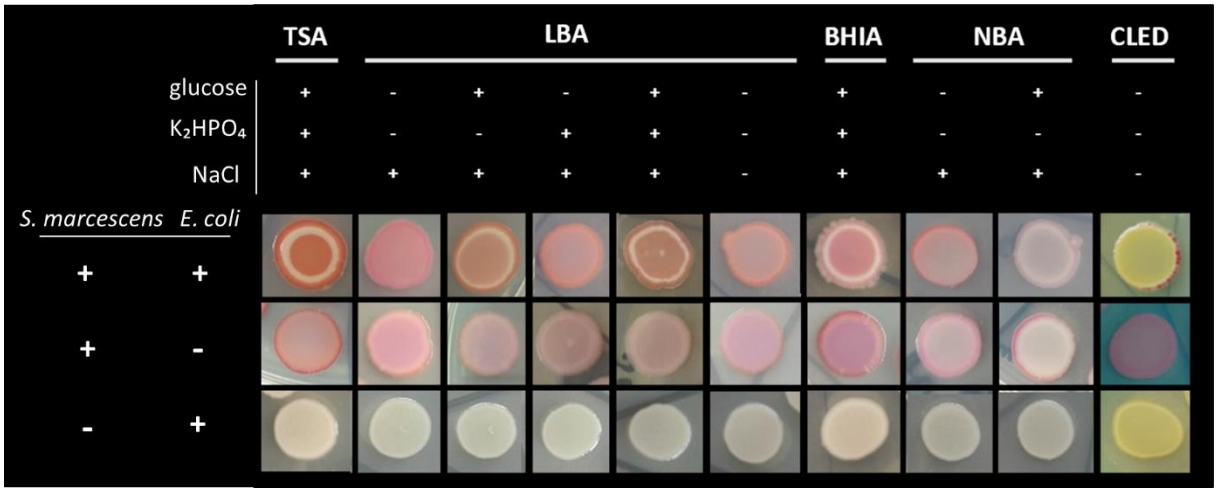

Figure 4.12: **Colony patterning of *E. coli* NCTC12241 and *S. marcescens* NCTC1377 co-culture and respective control in different growth media.** 10^6 cells in a 10 µl drop from co-culture of *S. marcescens* NCTC1377 & *E. coli* NCTC12241 and respective controls on different growth media, incubated for 16 hours at 37°C. Other media components besides glucose, K_2HPO_4 or NaCl, were not indicated here as superfluous for the aim of this experiment.

4.1.6 The ratio of *S. marcescens* to *E. coli* cell numbers is critical to "bull's eye" pattern formation

We initially observed the appearance of the "bull's eye" pattern when a 10µl drop of *E. coli* NCTC12241 and *S. marcescens* NCTC1377 liquid co-culture with a cell density of 10^5 – 10^6 was plated on TSA and incubated at 37°C for hours. To study whether the contact-in-liquid between the two bacterial strains before plating was essential to enable the pattern formation, the same amount of independent growing exponential cultures of *E. coli* NCTC12241 and *S. marcescens* NCTC1377 were mixed and immediately seeded at the desired concentration. Results showed that the contact-in-liquid was not required for leading the bacteria to form the "bull's eye" pattern (data not shown as pictures not available).

We then questioned whether cell density of each bacterial species may play a role in the pattern formation. The explore that, we seeded 10 µl drops of liquid co-cultures in TSA plates containing an increasing range of *E. coli* NCTC12241 or *S. marcescens* NCTC1377. Results showed that equal seeding densities (at concentrations 1:1 ratio *E. coli* : *S. marcescens*) of approximately 10^4 to 10^6 cells generated an increasingly defined "bull's eye" pattern (Figure 4.13). Moreover, we observed a further alteration of the pattern with cell density higher than 10^6, with a white rim enclosing a red circle when we had 10^7 cells each.

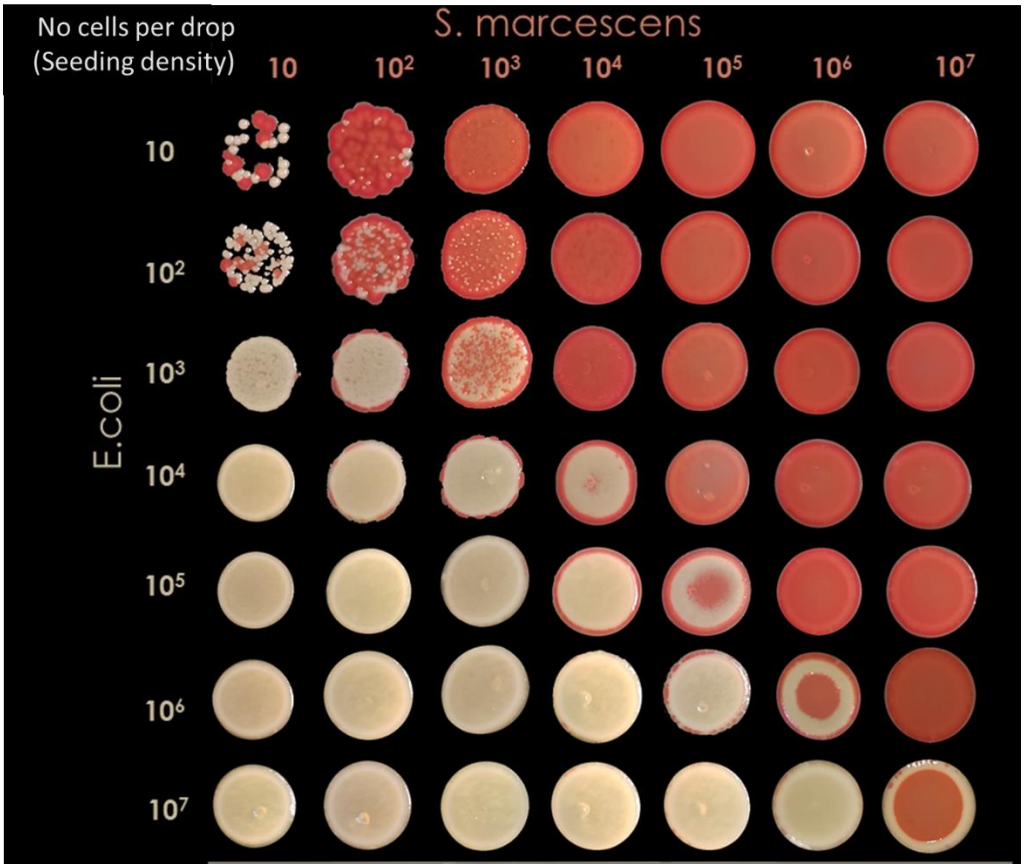

Figure 4.13: **Colony patterning of *E. coli* NCTC12241 and *S. marcescens* NCTC1377 mixed and plated at different ratios**. We mixed a range of number of bacterial cells – from 10 to 10^7 - for each species and immediately seeded 10 µl drops on TSA plates. Incubation for 16 hours at 37°C. Images show representative data from two independent experiments.

4.1.7 *E. coli* NCTC12241 influences prodigiosin production in *S. marcescens* NCTC1377

Results showed in Figure 4.13 also suggested that the presence of *E. coli* NCTC12241 in the co-culture leads *S. marcescens* to a reduced prodigiosin production. Specifically, we observed a seemingly homogeneous and obviously prevalent distribution of *S. marcescens* in the colony at 10:1 ratios or above of *S. marcescens* : *E. coli* and, vice versa, there was a seemingly homogeneous and obviously prevalent distribution of *E. coli* in the colony at 1:10 ratios or below of *S. marcescens* : *E. coli*, with an apparent downregulation of prodigiosin expression.

To investigate this further, we grew *S. marcescens* NCTC1377 colonies in the vicinity of an *E. coli* NCTC12241 smear on solid agar plates, with a variable distance between the two strains, in order to see whether the prodigiosin production was connected to the vicinity of *E. coli*. Results demonstrated a downregulation of prodigiosin expression mediated by *E. coli* NCTC12241 presence, as shown the by less intense colour of *S. marcescens* colony located in proximity of the *E. coli* smear compared to the colony grown a few cm further from the *E. coli* (Figure 4.14, A).

Ultimately, prodigiosin production was observed in liquid (LB) cultures. In support of what is displayed on solid plates, we observed a lack of prodigiosin production in the liquid co-culture of *S. marcescens* NCTC1377 and *E. coli* NCTC12241 compared to the respective mono-cultures (controls) (Figure 4.14, B). Of note, the downregulation of prodigiosin displayed in LB, a growth medium lacking in glucose,

suggested that the *E. coli* NCTC12241-mediated downregulation of prodigiosin may be glucose-independent.

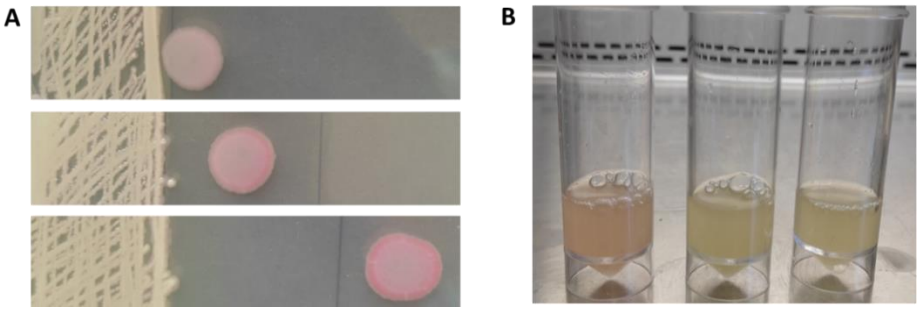

Figure 4.14: ***E. coli* NCTC12241 effect on the production of prodigiosin in *S. marcescens* NCTC1377**. A) *S. marcescens* colonies with seeding densities of 10^5 independently grown cultures in the vicinity of *E. coli* NCTC12241 matrices, incubated in TSA 37ºC for 16 hours. B) From left to right: liquid cultures grown for 15 hours at 37ºC, 200rpm of *S. marcescens* NCTC1377, *E. coli* NCTC12241 and both strains mixed.

4.1.8 The "bull's eye" pattern is unique to *S. marcescens* NCTC1377 and *E. coli* NCTC12241 co-culture

As part of the *in vitro* co-culture competition experiments (Section 3.4.1) *S. marcescens* NCTC1377 was grown in co-culture with a set of bacterial strains, none of which led to a formation a "bull's eye" or similar pattern. To further investigate whether the formation of such a pattern was species (*E. coli*) – specific, we put *S. marcescens* NCTC1377 in contact with *E. coli* NCTC10418 under the same conditions that led *S. marcescens* to form the "bull's eye" pattern when co-cultured with *E. coli* NCTC12241. Strikingly, the contact between *S. marcescens* NCTC1377 with *E. coli* NCTC10418 did not display any "bull's eye" pattern, but rather a homogenous red colony surrounded by a very thin white rim when the ratio *E. coli* NCTC10418:*S. marcescens* NCTC1377 was 1:1, with the rim getting thicker with a ratio 10:1. The described results pointed out that the a "bull's eye" pattern formation was strain-specific, probably as a result of exclusive signal released by *E. coli* NCTC12241 and sensed by *S. marcescens* NCTC1377 when in contact on the plate (Figure 4.15). Moreover, when the ratio *E. coli* NCTC10418:*S. marcescens* NCTC1377 was 10:1 or 100:1, no downregulation of prodigiosin was observed, in contrast to what we described in Figure 4.17, where 10 to 100-fold more of *E. coli* led to the appearance of a non-pigmented colony, hence suggesting that *E. coli* NCTC10418 did not affect prodigiosin production on solid plates.

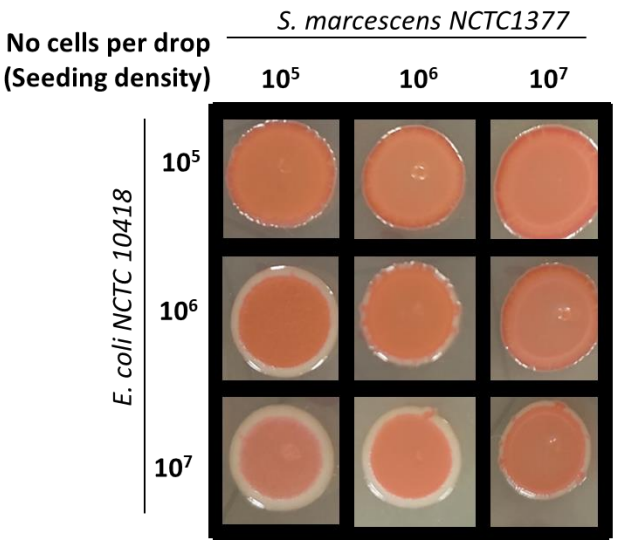

Figure 4.15: **Colony patterning of *E. coli* NCTC10418 and *S. marcescens* NCTC1377 mixed and plated at different ratios**. We have mixed a range of number of bacterial cells – from 10^5 to 10^7 - for each species and immediately seeded 10 µl drops on TSA plates. Incubation for 16 hours at 37ºC. Images show representative data from two independent experiments.

To further investigate the prodigiosin production in *S. marcescens* NCTC1377 when in contact with *E. coli* NCTC10418 rather than *E. coli* NCTC12241, we observed colours of the liquid (LB) cultures of each *E. coli* strain mixed with *S. marcescens* NCTC1377 and respective controls. Results confirmed that when *S. marcescens* NCTC1377 was in co-culture with *E. coli* NCTC12241, it lost the red colour that characterizes the strain growing on its own. On the contrary, when *S. marcescens* NCTC1377 was growing with *E. coli* NCTC10418, the co-culture appeared as red as the *S. marcescens* NCTC1377 growing alone (Figure 4.16), again suggesting that *E. coli* NCTC10418 did not induce a downregulation of prodigiosin production in *S. marcescens* NCTC1377.

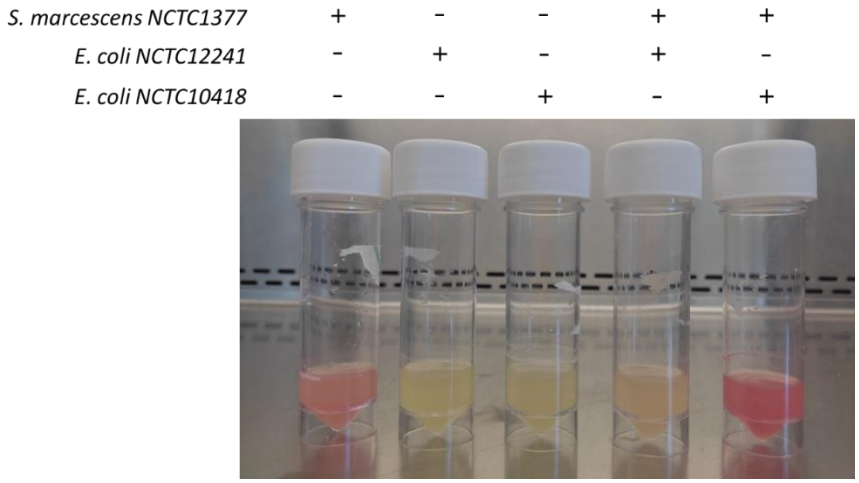

Figure 4.16: ***E. coli* strains-mediating the production of prodigiosin in *S. marcescens* NCTC1377**. Liquid cultures (LB) grown for 24 hours at 37ºC, 200rpm, of *S. marcescens* NCTC1377, *E. coli* NCTC12241, *E. coli* NCTC10418 and respective co-cultures.

4.1.9 The presence of a third strain in co-culture with *E. coli* NCTC12241 and *S. marcescens* NCTC1377 do not disturb the pattern formation

To determine whether the presence of a third strain in the mix would have disrupted the formation of the "bull's eye" pattern, we added to *E. coli* NCTC12241 and *S. marcescens* NCTC1377 co-culture, at conditions known to form the pattern, a Gram-positive, *E. faecalis NCTC775* , or a Gram-negative *E. coli* NCTC10418, at a ratio 1:1:1. Results showed that the presence of none of them, *E. faecalis* or *E. coli* NCTC10418, in contact with *E. coli* NCTC12241 and *S. marcescens* NCTC1377, changed the ability of the latter to distribute in the space, forming the same pattern as they did when only *E. coli* NCTC12241 and *S. marcescens* NCTC1377 were in the mix (Figure 4.17).

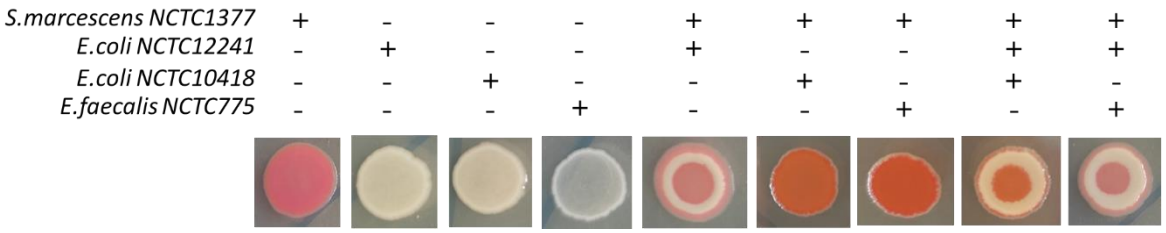

Figure 4.17: **Colony patterning of *S. marcescens* NCTC1377, *E. coli* NCTC12241, *E. coli* NCTC10418, E. faecalis NCTC775 and respective co-culture.** A 10 µl drop containing 10^6 bacterial cells of *E. coli* NCTC12241 or *S. marcescens* NCTC1377 or E. faecalis NCTC775 exponential growing cultures (LB) at 37ºC were plated on TSA plates. For the pairwise co-cultures, a 10 µl drop containing 10^6 bacterial cells of *E. coli* NCTC12241 and *S. marcescens* NCTC1377 or *S. marcescens* NCTC1377 and E. faecalis NCTC775 (at a ratio 1:1), were mixed and immediately plated on TSA. Same was applied for all three strains (*S. marcescens* NCTC1377 and *S. marcescens* NCTC1377 and *E. faecalis* NCTC775, ratio 1:1:1). Plates were incubated at 37ºC for 16 hours.

4.2 The "bull's eye"-mediating signal

4.2.1 The removal of the conditioned medium still leads the "bull's eye" pattern formation

We have shown that "bull's eye" pattern only forms when *S. marcescens* NCTC1377 was co-cultured with *E. coli* NCTC12241. Hence, it was conceivable that an extracellular signal mediating the formation of the pattern may be released by this specific strain, or even that *S. marcescens* NCTC1377 itself produced the signal required for the pattern to form only when in contact with *E. coli* NCTC12241. Any of those potential signals may be released in the CM (or supernatant). Hence, to investigate whether any molecules produced by *E. coli* NCTC12241 or *S. marcescens* NCTC1377 itself facilitated the switch that led to the "bull's eye" pattern formation, we firstly seeded the co-culture after depletion of CM and washing the pellet in buffer, removing all soluble potential factors secreted into the media during the time of co-culture in liquid. The results showed that the "bull's eye" pattern was formed independently from the CM removal, suggesting that the contact between the cells on the plate, rather than the CM, was essential to lead such a pattern (Figure 4.18). Of note, the drop on the right in Figure 4.18 had different shape which was a result due to plating rather than a different pattern appearance.

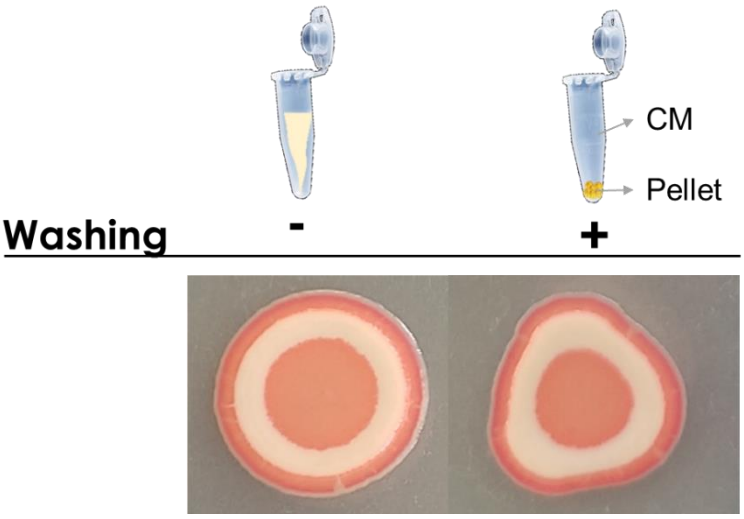

Figure 4.18: **Colony patterning of *S. marcescens* NCTC1377 and *E. coli* NCTC1224 at ratio 1:1 with or without washing.** 10^6 cells in a 10 µl drop from co-culture of *S. marcescens* & *E. coli* plated on TSA with (+) or without (-) washing, incubation at 37°C for 16 hours. Washing consisted in centrifugation of the liquid culture at 13.000rpm for 1 minute; CM disposal, resuspension of cells (pellet) in LB.

To further exclude any potential signals released in the CM produced by *E. coli* NCTC12241 or *S. marcescens* NCTC1377, alone or in co-culture, were involved in the formation of the "bull's eye" pattern, we re-suspended CM collected from growing *E. coli* NCTC12241 or *S. marcescens* NCTC1377 or co-cultured species at multiple timepoints, from 8 to 24 hours from the inoculation. These different CM were then mixed with *S. marcescens* NCTC1377 pellets and seeded on TSA plates at density known to form the pattern. Results showed that *S. marcescens* NCTC1377 cells re-suspended in any of the CM, was not able to form the "bull's eye" pattern, but instead appeared as a typical *S. marcescens* red colony, suggesting that the signal leading the space distribution was not in the CM and that the contact with *E. coli* NCTC12241 cells was essential for the pattern to form (Figure 4.19).

Ultimately, we considered the possibility that a signal may be released only when both strains were on the agar plate, in conditions known to form the "bull's eye" pattern. To test that, bacterial cells from grown "bull's eye" patterns were collected, resuspended in liquid medium, centrifuged and the resultant CM was mixed with . *S. marcescens* NCTC1377 pellet prior plating on TSA. The experiment showed that *S. marcescens* NCTC1377 cells with the collected CM did not lead to the "bull's eye" pattern formation (picture not shown as photograph not taken), but rather to a typical *S. marcescens NCTC1377* colony.

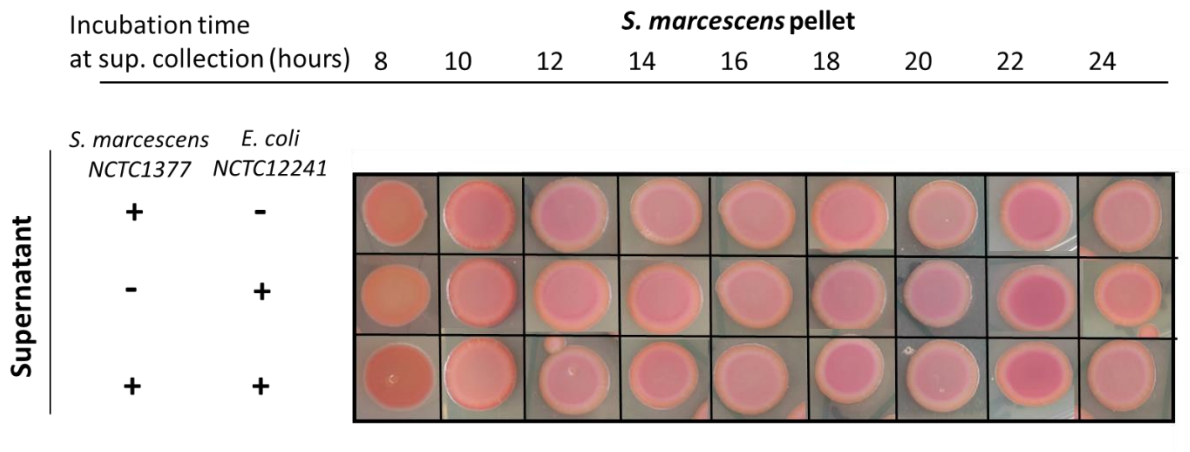

Figure 4.19: ***S. marcescens* NCTC1377 cells in contact with CM isolated from liquid cultures of *S. marcescens* NCTC1377, *E. coli* NCTC12241 or both mixed.** re-suspended bacterial CM collected from growing *E. coli* NCTC12241 or *S. marcescens* NCTC1377 or both at multiple timepoints from 8 to 24 hours from the inoculation and mixed with 10^6 cells of *S. marcescens* and seeded on TSA, incubation 37°C for 16 hours.

4.2.2 Micromolar concentration of methionine dissipates the "bull's eye" pattern

Čepl and co-workers have shown the ability of a *S. marcescens* strain 5965 to form a "bull's eye" pattern on Nutrient Broth medium supplemented with 27 mM glucose after 7 days incubation at 26°C [244]. The authors proposed growth-death rate, nutrient concentrations, metabolic waste, and signal mediated processes as parameters to determine the formation of the pattern. They went onto showing that pH changes potentially due to the differential and sequential use of glucose and AAs during growth influenced pattern formation. Ultimately, the mechanism, its components and their interplay leading to such phenomenon are unknown. The strain used in my study, *S. marcescens* NCTC1377, did not form the "bull's eye" pattern when grown by itself in any of the solid growth media assayed, (Figure 4.4). However, the fact that the presence of *E. coli* NCTC12241 in co-culture with *S. marcescens* NCTC1377 on TSA at 37°C resulted on the formation of such geometric pattern suggested (i) that *S. marcescens* NCTC1377 was likely to have the genetic make-up for the pattern to form and, (ii) that a mediator -in this case provided by *E. coli* NCTC12241 - enabled the activation of this molecular machinery. The mediator may be a nutrient, a waste product, or an intra- and inter-species extracellular signal.

Even though CM from liquid or solid cultures of *E. coli* NCTC12241, *S. marcescens* NCTC1377 or both in co-culture (Figure 4.19) were unable to lead *S. marcescens* NCTC1377 to forming the "bull's eye" pattern, the possibility of an extracellular signal mediating the process cannot be excluded. The observation shown above (Figure 4.12) that *S. marcescens* NCTC1377 growing on a Cysteine-rich medium (CLED) did not form the pattern compared to its growth on TSA in defined conditions may be due to the differential sugar and/or protein composition or source as discussed above. It was also possible that the pattern may be there but prodigiosin expression was repressed. Alternatively, we wanted to test whether Cys played a role as a nutrient or a signal. Interestingly, Cys, alongside with Met, can work as either signals or precursors of signalling molecules in QS in bacteria. Specifically, Met is intermediary compound in the biochemical pathway leading to the synthesis of AHL and A-I2

derivatives used for QS signalling in Gram-negative bacteria. It seemed therefore reasonable to explore the potential role of Cys and Met in the “bull’s eye” pattern formation.

First, we wanted to test whether addition of one, Cys or Met, or both of them, on TSA plates may alter the “bull’s eye” pattern formation, at conditions normally known to lead its appearance. Selected concentration of Cys was based on its concentration on CLED agar medium (2 mM), while for Met we used 50 μM, a concentration that, based on the literature, would not affect the bacterial growth but may play a role at a molecular level[405,406].

Results showed that the supplementation of TSA plates with 2 mM Cys did not alter growth or the absence of a pattern in single cultures of *S. marcescens* NCTC1377 (Figure 4.20) and similarly it did not affect growth of *E. coli* strains. A similar observation was made when supplementated with Met or the combination of both AAs. Colony growth of the co-culture on TSA in the presence of Cys still showed the “bull’s eye” pattern suggesting that Cys, at that concentration and in that medium, was not influencing the process. The same results were obtained when Met at 50 μM, instead of Cys, was used as a supplement in the medium, hence excluding a role for Met in those conditions. Surprisingly, the joint addition of Met and Cys led to a dissipation of the “bull’s eye” pattern. The 50 μM of concentration of Met was 100-fold lower that the concentration of Cys (2 mM). In fact, the Met concentration importantly correspond to a concentration lower that those expected for a nutrient. Consequently, it seemed unlikely that Met was playing a role as a nutrient or functioning as an antioxidant, but rather it may act as a signalling molecule.

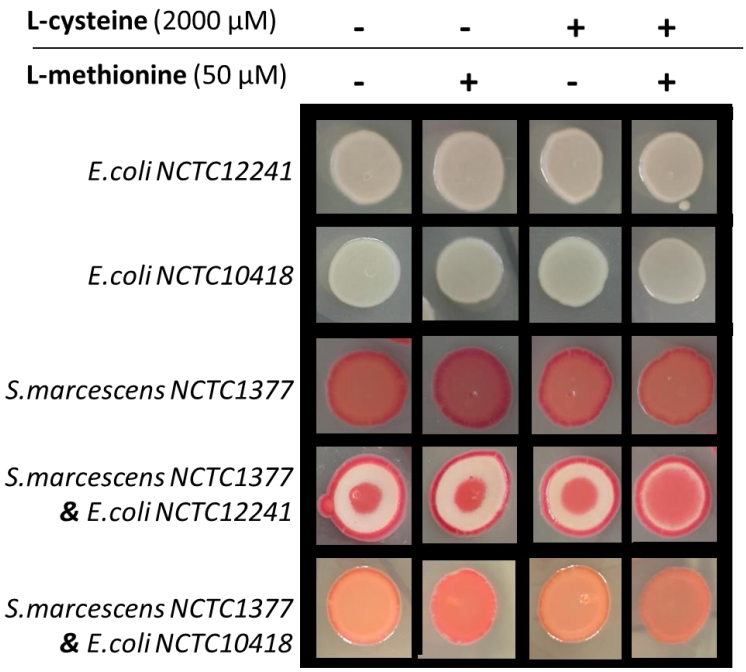

Figure 4.20: **Colony patterning of *S. marcescens* NCTC1377 in single and mixed cultures in response to AAs at micronutrient concentrations.** A volume of 10 µl from LB cultures containing 10^6 cells was deposited on TSA, allowed to dry and grown for 16 hours at 37ºC. *S. marcescens* and *E. coli* LB cultures were independently grown and mixed 50:50 prior to inoculation on the plates.

4.2.3 Structural differences in strain-specific MetR protein in *E. coli* strains

Considering that the presence of a micromolar concentrations of Met, an intermediary compound in the biosynthesis of QS-molecules in Gram-negative bacteria, led to a change in the pattern formation of *S. marcescens* NCTC1377 in co-culture with and *E. coli* NCTC12241, but not when in co-culture with *E. coli* NCTC10418, I analysed some of the key players in the interrelated methyl-cycle and QS pathways at a genetic and translational level: MetR and MetE. MetR is the main regulator of Met synthesis: when the gene *metR* gene is transcribed, MetR binds to the upstream region of *metE*, promoting the transcription of MetE, a Met synthase B_{12}-independent that catalyses the final step in the biosynthesis of Met[211].

We have identified, extracted, and translated the genes *metR* and *metE* from both genomes *E. coli* NCTC12241, *E. coli* NCTC10418. BLAST-based analyses of each translated sequences and the phylogenetic analyses within *Escherichia coli* species showed that both, *metR* and *metE* were well conserved proteins among *Escherichia coli* strains.

A further analysis of the upstream regions of *metR* and *metE* in *E. coli* were 100% identical between the two strains. Not surprisingly, phylogenetic analyses of the 117 bp length sequence revealed that the region was well-conserved among all *Escherichia coli* species within BLAST nucleotide database. A graphical representation of *metR* and *metE* genes and the intercalating region is shown in Figure 4.21. The *metR* box, or binding site, for Gram-negative bacteria is a motif containing four symmetrical bases interrupted by four variable bases, (5' TGAA----TTCA 3')[210]. The described motif was identified in both our *E. coli* strains, NCTC12241 and *E. coli* 10418 in Geneious Prime® 2022.1.1. Of note, I found

that the motif 5' TGAA----TTCA 3' was widely spread on both *E. coli* genomes suggesting a pleiotropic role of *metR*.

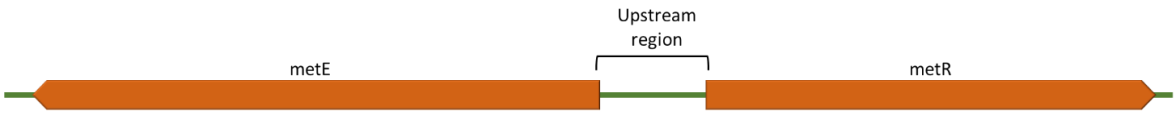

Figure 4.21: ***MetE* and *metR* genes in *E. coli***. Graphical representation of MetE and MetR genes and the intercalating region upstream of both of them in *Escherichia coli* adapted from *E. coli* ATCC25922 in Geneious Prime® 2022.1.1

Even if well conserved among *E. coli* species, we did not exclude the possibility of minor differences in the AA sequences of MetR or MetE between *E. coli* NCTC12241 and *E. coli* NCTC10418. To investigate this, the AA sequence pairwise alignments for each protein were performed in Geneious Prime® 2022.1. Alignment resulting from MetR isolated from *E. coli* NCTC12241 and *E. coli* NCTC10418, displayed a pairwise identity between the two *E. coli* of 99.37% - where only two different AAs, a Serine (Ser) in *E. coli* NCTC12241 in position 110 replaced by an Asparagine (Asn) in *E. coli* NCTC10418, and an Isoleucine (Ile) in *E. coli* NCTC12241, position 227, replaced by a Valine (Val) in *E. coli* NCTC10418 (Table 4.2). Ser and Asn are both AAs with polar uncharged side chains, while Ile and Val have both hydrophobic side chains. Thus, both replacements may be considered conservative changes which, in principle, were not expected to cause any difference in the structure of MetR.

The same analyses for MetE was conducted and revealed differences in 4 AAs between the two *E. coli* strains. For MetE, two of the AA differences represented conservative changes, i.e., Ile to Val and Lysine (Lys) to Arginine (Arg). On the other hand, Alanine (Ala), of neutral charge was substituted by a polar AA, Threonine (Thr), which contains a hydroxyl group able to form hydrogen bonds with polar substrates. Also, in position 38, a Lys, positively charged, in *E. coli* NCTC12241 was substituted by an Asn, uncharged. Those two differences may be implied in a potential differential 3D structure of the protein.

Table 4.2: **Amino acids differences between *E. coli* NCTC12241 and *E. coli* NCTC10418 in MetR and MetE.** Protein alignment was conducted in Geneious Prime® 2022.1.1. In bold, conserved amino acidic changes

Position	*E. coli* 12241	*E. coli* 10418
MetR – 317 AAs - homodimer		
110	Serine	Asparagine
277	Isoleucine	Valine
MetE – 753 AAs		
38	Alanine	Threonine
156	Lysine	Asparagine
165	Isoleucine	Valine
466	Lysine	Arginine

3D structure of the proteins may tell us whether these changes can impact the structure of the proteins and therefore the regulatory fitness. To visualize and compare the 3D structures of MetR and MetE in both *E. coli* strains, the protein structure predictor AlphaFold was used. MetR is a homodimer protein with each dimer containing 317 amino acids and a molecular weight of roughly 35.6; each dimer has *a leucin zipper* motif between AAs 19 and 40 (four leucine residues spaced seven amino acids apart in a helical region of the protein) close to the amino-terminal end of the sequence, highlighted within a red box in the Figure 4.22. Most likely, the leucin zipper motif would facilitate the dimerization of the dimers or the interaction with adjacent DNA regions. In fact, the DNA-binding site in MetR is located just in the proximity of the zipper motifs, as shown in the Figure 4.22. The 3D protein structures of MetR in *E. coli* NCTC12241 and *E. coli* NCCT10418 displayed a minor difference (only 1 nm) in the pocket size of the proteins, where homocysteine or MetJ may bind, modulating the activity of MetR[211,212]. It is very unlikely that such a minor structural difference in MetR proteins of *E. coli* NCTC12241 and *E. coli* NCTC10418 may result in changes in Met sensing and Met-mediated signalling molecules differential production.

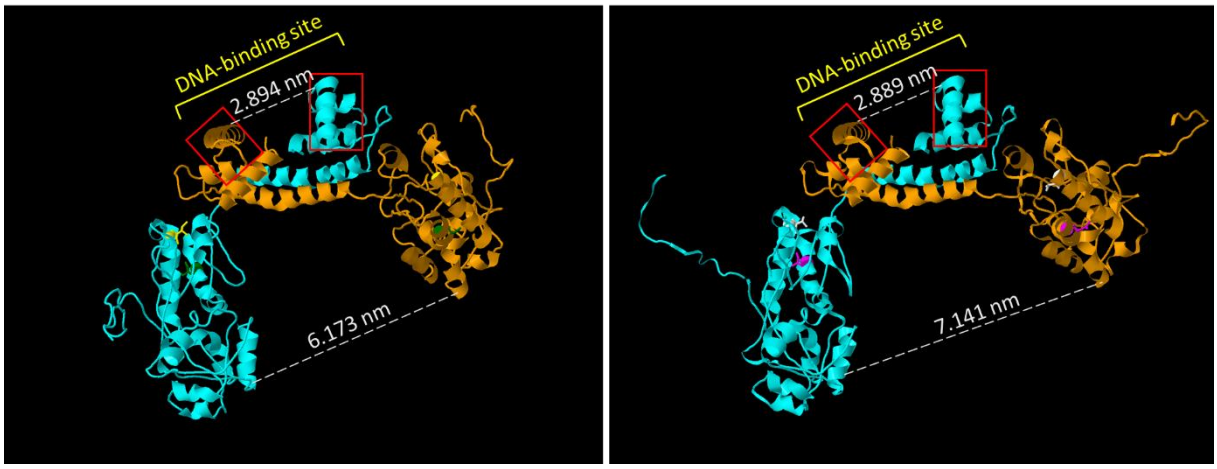

Figure 4.22: **Predicted 3D structure of MetR in *E. coli* NCTC12241 (left) and *E. coli* NCTC10418 (right).** The coloured chains in cyan and orange indicate the 2 homodimers. AAs that differ between MetR isolated from *E. coli* 12241, on the right, and from *E. coli* 10418 on the left, are highlighted in different colours, specifically: green for serine, yellow for Isoleucine, white for asparagine and magenta for valine. In red, leucine-zipper motifs

Despite some AA changed, the structure of MetE for both *E. coli* was almost identical, suggesting that those AA differences were not actually affecting the folding of the of the proteins. Data showed in Appendix IV.

A proteome-broad analyses of *E. coli* NCTC12241 and *E. coli* NCTC10418 (restricted to the AA sequences) have been conducted to compare the two strains on a large scale. We found that, among all 4830 of the translated AA sequences of *E. coli* NCTC10418, almost 20% were identical (100% identity) to proteins in *E. coli* NCTC12241, more than 50% displayed an identity between 90 and 99.99%, and a substantial amount (11.2%) were not identified in the *E. coli* NCTC12241 translated sequence (Figure 4.23). Although the two bacterial strains are phylogentically very close, sharing 88% identity in the genome (alignment conducted in Geneious Prime, Appendix V), the analyses of translated sequences relevaed critical differences for a large amount of proteins. In particular, it is worth considering the AA sequences from *E. coli* NCTC10418 that did not produce any match in *E. coli*

NCTC12241 to evaluate whether any of these may be involved in metabolic or physiological pathway connected to the phenomenological differences that we have identified between the two *E. coli* strains, when in co-culture with *S. marcescens* NCTC1377.

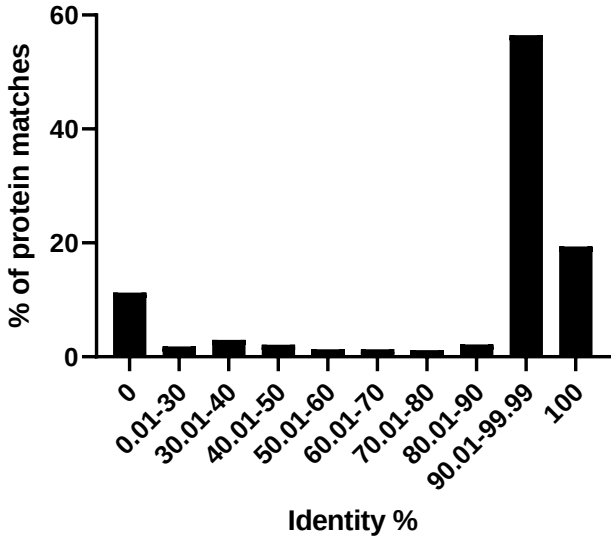

Figure 4.23: **Percentage of translated proteins from *E. coli* NCTC10418 that matches with translated sequenses of *E. coli* NCTC12241**. The comparison was conducted in Protein BLAST (NCBI). Search set consisted of Non-redundant protein sequences as a database only within the organism *E. coli* ATCC25922/NCTC12241. General Algorithm parameters were the following: Max target sequence (100), Expected threshold (0.05), Word size (6), Max matches in a query range (1). Results included: Name of the sequence (Query), Accession codes (or sequence ID) of the matched Subjects, identity (%), Query Coverage(%), Length, Gap, Query start and end, Subject start and end, E-value, score bites. The full translations list was imported and analyses in Geneious Prime®2021.1.1 and Microsoft Excel. Y axis indicates the percentage of translated sequences from *E. coli* NCTC10418 that match with translated sequences of *E. coli* NCTC12241 with a certain identity (x axis)

4.3 The "bull's eye" pattern simulation: mathematical model

A mathematical model able to explain and simulate the differential bacterial distribution of *E. coli* and *S. marcescens* on TSA plates leading to the appearance of a "bull's eye" pattern, was performed in collaboration with Čepl Jaroslav[iv], Scholtz Vladimir[v] and Jirina Scholtzova[vi]

For the simulation, two parameters were considered: (i) replication coefficient for each bacterial population (*E. coli*, white and *S. marcescens*, red) and (ii) diffusion coefficient, again, for each bacterial population. The model is a result of approx. one thousand of iterations (i.e. life cycles). Analytical steps were used to streamline the process.

The model revealed that the white cells preferentially grew in height, while the red grew more in width (diffused). One would assume that the white cells would determine the pattern, as the white is confined to a certain location while the red continue to grow in width. The reason why the red is excluded in the white middle ring may be due to the overgrowth of white on the top of the red.

[iv] University of Live Sciences, Prague, Czech Republic
[v] University of Chemistry and Technology, Prague, Czech Republic
[vi] Czech Technical University, Prague, Czech Republic

The growth also depends on the diffusion of nutrients and signalling substances. The signal under consideration is a product of multiple signals (metabolites, waste products, nutrients etc), combining to create a single "signal" for bacteria to change their behaviour as a reaction. At present, the signal acts as a threshold for *E. coli* replication; they stops their growth if, at the particular virtual cell in the dish, the signal overgrowth some threshold value. In summary**,** the pattern is a result of (i) differential growth, (ii)sensitivity to the signal.

The distribution of *E. coli* and *S. marcescens* is a function of the differential occupancy in space by these strains as they replicate, one growing more in height and one more in width and diffused (proliferated), and the presence of a signal that favours the growth of one in a sector and the other to continue beyond.

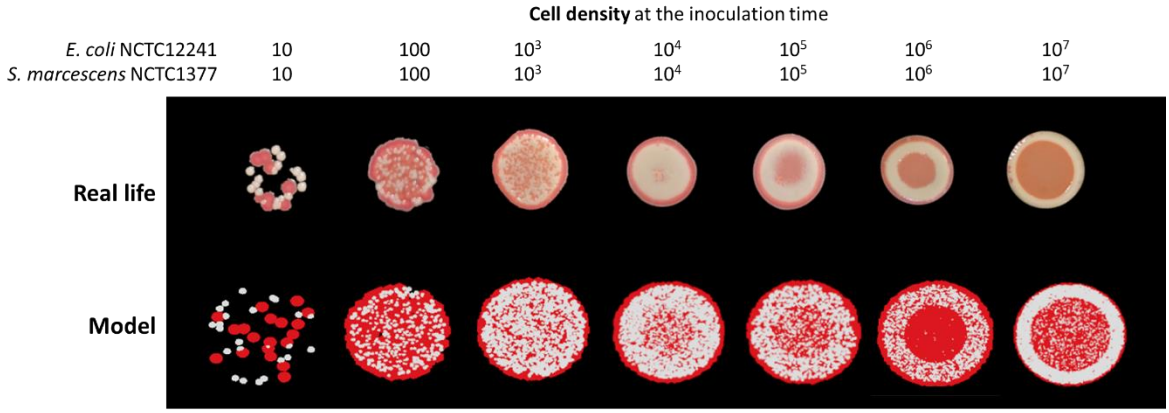

Figure 4.24 **The simulation of the colony's growth.** Picture of the real colonies (top row grown for 16 hours at 37°C, and the simulation of the colonies (bottom row). White cells are *E. coli* and red cells represent *S. marcescens*. Cell density of each bacterial strains at the time of inoculation are indicated.

4.4 Conclusion CHAPTER 4

In this chapter we have conducted a dissection of the "bull's eye" pattern that we had initially observed when 10 µl drop containing roughly 10^5 to 10^6 cells from a liquid co-culture of *E. coli* NCTC12241 and *S. marcescens* NTCTC1377 was seeded in TSA plates, dried and incubated for 16 hours at 37°C. Our experiments revealed that the pattern was a result of bacterial space distribution that happened between 5 to 7 hours from the inoculation and incubation at 37°C on the TSA plates, where both *E. coli* NCTC12241 and *S. marcescens* NCTC1377 were present in all three sectors, and cell density of each species was critical to determine the "bull's eye". We have found that the growth media also influenced the patter formation, with glucose being an essential component for the phenomenon to happen. Also, the "bull's eye" pattern seemed to be strain specific, as it did not appear when *S. marcescens* NTCTC1377 was in co-culture with strains different from *E. coli* NCTC12241. We hypothesised that a potential extracellular signal may enable *S. marcescens* NTCTC1377 to form the pattern. However, results showed that that cell-to-cell contact between the two cultured strains was required, as CM isolated from different conditions was not leading *S. marcescens* NTCTC1377 to form the "bull's eye" pattern in the absence of *E. coli* cells. We have also tested whether Cys and Met, AAs that can work as precursors of signalling molecules in QS in bacteria, can affect the pattern and found that the presence

of both AAs together led to a dissipation of the central red sector in the colony pattern, suggesting that QS may be involved in the mechanisms leading to the “bull’s eye” formation.

A mathematical simulation of the phenomenon, built by collaborators from the University of Prague, displayed that the “bull’s eye” pattern formation can be attributed to the differential space distribution of *E. coli* and *S. marcescens* as a function of their replication and the influence of nutrients and/or signalling substances - not determined yet.

Once defined the conditions that led the bull’s eye” pattern to form, we aimed to gain an insight into phenotypic changes in *E. coli* and *S. marcescens* in conditions leading to the specific pattern. Results of the subset of experiments conducted to explore potential shifts in virulence or antimicrobial resistance are described in the following chapter.

5 CHAPTER 5

Characterization of the virulence of the "bull's eye" pattern

The phenotypic characteristics of bacterial colonies in growth medium, in our specific case *S. marcescens* NCTC1377 and *E. coli* NCTC12241 co-culture forming a "bull's eye" pattern on TSA, at 37^{o}C, with a seeding cell density of 10^5 to 10^6 at a 1:1 ratio, may be correlated to genome-wide changes in gene expression profile for each strain. Further investigations in this can be eventually harnessed towards the understanding of bacterial virulence and pathogenesis.

5.1 *S. marcescens* from the "bull's eye" pattern is more resistant to levofloxacin

Antibiotic resistance is an increasing global public health threat, leading to deaths, prolonged illness and hospitalization, hence dramatically contributing to national and worldwide economic burden. Notably, *Serratia sp*. is among the major AMR pathogens in the WHO Global Priority Pathogens List [25]. It is well known that antibiotic resistance of microorganisms can be acquired by mutation or horizontal transfer of resistance genes. Furthermore, findings have revealed that environmental factors can also lead to a different phenotypic (or physiological) resistance to a number of antibiotics [118,123].

The phenotypic manifestation we encountered with *S. marcescens* NCTC1377 and *E. coli* NCTC12241 co-culture may be accompanied by a change in antibiotic susceptibility in one or both strains. To study that, we tested the susceptibility for a few antibiotics widely used in the clinics and available in our setting, i.e., LFX, ampicillin and vancomycin, to *S. marcescens* NCTC1377 and *E. coli* NCTC12241 growing as a "bull's eye" pattern.

First, we tested whether the bacteria from the different sectors of the pattern were more or less resistant to LFX, by inoculating bacteria grown on agar plates for 16 hours in a liquid culture containing LFX and measuring their CFU. The results show that *S. marcescens* NCTC1377 isolated from different sectors of the pattern had a diverse tolerance to LFX compared to *S. marcescens* growing on its own (control). Specifically, *S. marcescens* NCTC1377 from the outer edge and central red spot of the "bull's eye" pattern, were 2 to 3 log more resistant in comparison to *S. marcescens* NCTC1377 in the middle white ring of the pattern (P-values respectively 0.0212 and 0.0228) and of the control (P-values respectively 0.0211 and 0.0214) (Figure 5.1). At 0.5 µg/ml LFX, *S. marcescens* from the outer ring and centre of the pattern survived almost as well as *S. marcescens* from the middle or control with 0.2 µg/ml LFX. Consistently, at 0.6 µg/ml LFX, *S. marcescens* from the outer ring and centre, displayed a 10-fold more resistance than the control and approx. 50 to 80-fold more resistance than the cells isolated from the middle ring. Interestingly, at 0.8 µg/ml LFX, while no cells from the control or middle of the pattern were detected, a few hundred *S. marcescens* cells from the outer ring and centre survived the antibiotic treatment. The antibiotic susceptibility for *E. coli* NCTC12241 did not vary among samples collected from the "bull's eye" pattern of the control.

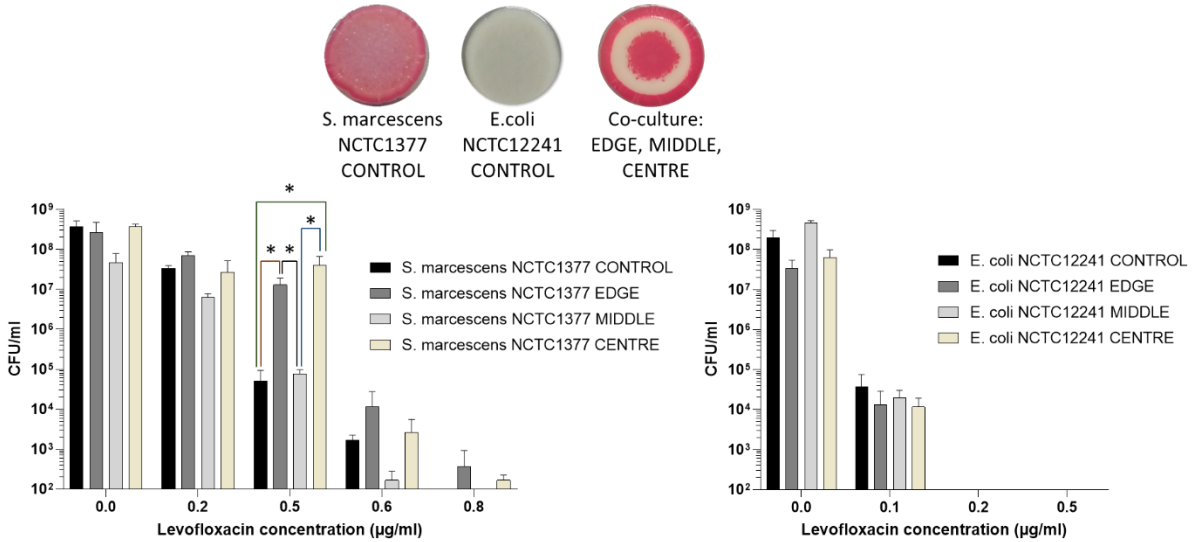

Figure 5.1: **Levofloxacin susceptibility in bacterial samples collected from *S. marcescens* NCTC1377 (control), *E. coli* NCTC12241 (control) and from the sectors of the pattern (Edge, Middle, Centre).** Samples were in contact with LFX for 16 hours at 37°C, 200 rpm. Cell viability was assessed measuring CFU (Miles Misra method). X axis indicates the LFX concentration (µg/ml), Y axis indicates CFU/ml. Results and error bars indicate mean ± SD of three technical replicates. Data analysis was performed with unpaired t-test (GraphPad 9.3.1,2021). Asterisks indicate significant values (P-value < 0.05). Graphs show representative data from two independent experiments

Considering that *S. marcescens* NCTC1377 from the outer edge and central spot of a "bull's eye" pattern showed an increased resistance to LFX compared to the bacterial cells in the middle ring of the pattern, we cannot exclude the possibility that this difference is associated purely with the location of the bacterial cells on the colonized area, independently from the presence of *E. coli* NCTC12241 and/or the formation of the "bull's eye" pattern. To exclude that, we collected samples from three sectors (outer, middle, centre) in a *S. marcescens* NCTC1377 colony (control) and tested for antibiotic resistance. Results revealed that the sensitivity to LFX did not change among the collected samples (Figure 5.2), hence supporting the hypothesis that the increased resistance to the antibiotic is connected to the presence of *E. coli* NCTC12241 in the colony and/or the formation of the "bull's eye" pattern.

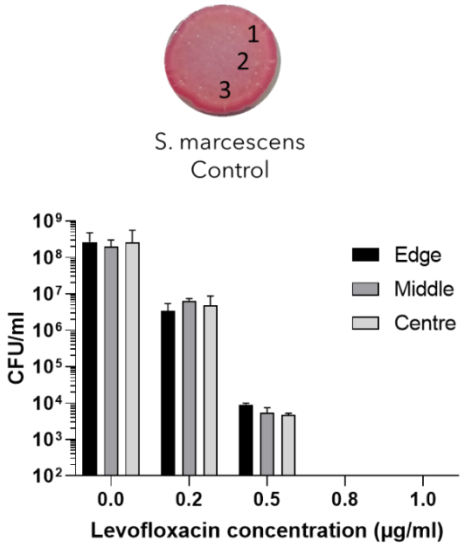

Figure 5.2: **Levofloxacin susceptibility in bacterial samples collected from *S. marcescens* NCTC1377 from the sectors of the colony patch (Edge, Middle, Centre).** Samples were in contact with LFX o/n at 37°C, 200 rpm. Cells viability was assessed measuring CFU (Miles Misra method). X axis indicates the LFX concentration (µg/ml), Y axis indicates CFU/ml. Results and error bars indicate mean ± SD of three technical replicates (GraphPad 9.3.1,2021).

The observed increased antibiotic resistance may have resulted from a genetic change, specifically from a mutation in genes encoding for the antibiotic resistance. Or the phenomenon seen is due to a phenotypic or physiological resistance, such non-inherited characteristics which are only facilitated by specific processes or conditions, for instance, in this case, the formation of the formation of the "bull's eye" pattern. To investigate if the resistance carried by *S. marcescens* NCTC1377 in outer edge or central spot of the "bull's eye" pattern was an inherited, genetic feature or a non-inherited phenotypic change, we isolated *S. marcescens* NCTC1377 samples from the "bull's eye" pattern, grew them for 16 hours at 37°C on TSA plates, and then tested the LFX susceptibility for all those samples. If the previous observed resistance was a genetic resistance, we would have expected it to be maintained. However, results show that *S. marcescens* NCTC1377 samples deriving from any of the sectors of the pattern did not show an increased resistance to LFX compared to the control, meaning that the increased resistance is likely to be a physiological or phenotypic non-inherited change, which only occurred in the presence of *E. coli* NCTC12241 and/or the formation of the "bull's eye" pattern (Figure 5.4).

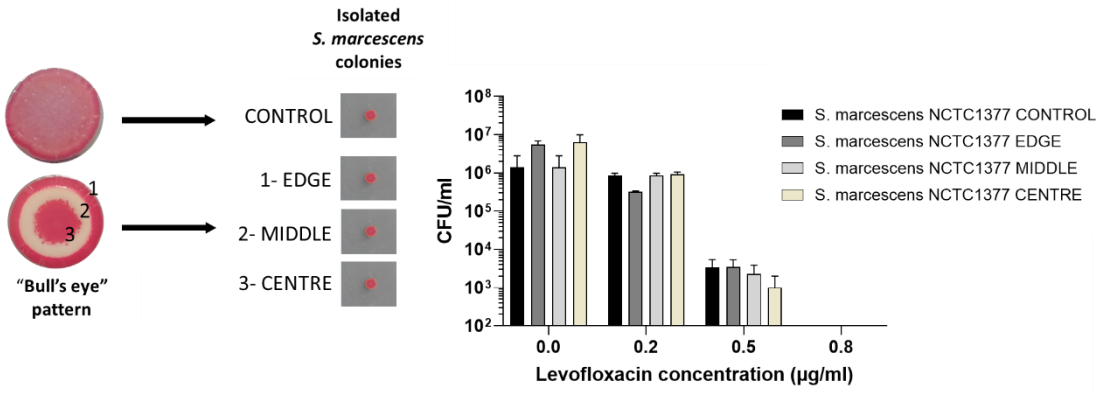

Figure 5.3: **Levofloxacin susceptibility in *S. marcescens* NCTC1377 samples isolated and re-sub-cultured from the sectors of a "bull's eye" pattern (Edge, Middle, Centre).** Samples were in contact with LFX o/n at 37oC, 200 rpm. Cell viability was assessed measuring CFU (Miles Misra method). X axis indicates the LFX concentration (µg/ml), Y axis indicates CFU/ml. Results and error bars indicate mean ± SD of three technical replicates. Data analysis was performed with 2-way ANOVA (GraphPad 9.3.1,2021), P value 0.05. Data were not statistically significant.

We demonstrated that "bull's eye" pattern was strain specific – at least among our tested strains – occurring only when *S. marcescens* NCTC1377 was in contact with *E. coli* NCTC12241. To investigate whether also the observed increased LFX resistance was exclusive to the presence of *E. coli* NCTC12241 and not of other strain such as *E. coli* NCTC10418, we tested the antibiotic resistance for samples in a colony resulting from *S. marcescens* NCTC1377 in contact with *E. coli* NCTC10418.

As this specific strain did not lead to the "bull's eye" pattern, it was unsurprising that *S. marcescens* NCTC1377 in the presence of *E. coli* NCTC10418 was not more resistant to LFX than the control, therefore suggesting that the presence of this specific *E. coli* NCTC12241 strain and/or the formation of the "bull's eye" pattern was required for the phenotypic resistance to happen (Figure 5.5).

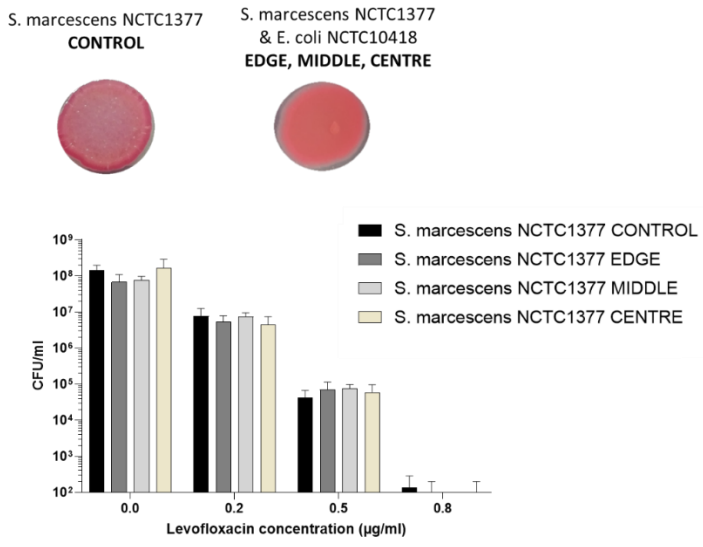

Figure 5.4: **Levofloxacin susceptibility in bacterial samples collected from *S. marcescens* NCTC1377 (control) colony, and from sectors of a colony resulted from *E. coli* NCTC10418 and *S. marcescens* NCTC1377 co-culture.** Samples were in contact with LFX o/n at 37°C, 200 rpm. Cell viability was assessed measuring CFU (Miles Misra method). X axis indicates the LFX concentration (µg/ml), Y axis indicates CFU/ml. Results and error bars indicate mean ± SD of three technical replicates (GraphPad 9.3.1,2021).

Ultimately, to determine whether the increased LFX resistance in *S. marcescens* NCTC1377 was merely due to the contact with *E. coli* NCTC12241, rather than the formation of the pattern on TSA, we tested the antibiotic sensitivity for *E. coli* NCTC12241 and *S. marcescens* NCTC1377 growing in liquid co-culture. Results showed that *S. marcescens* NCTC1377 from the liquid co-coculture with *E. coli* NCTC12241, did not develop any increased resistance compared to the control, hence suggesting that the "bull's eye" pattern was required for the increased LFX resistance in *S. marcescens* NCTC1377 (Figure 5.5).

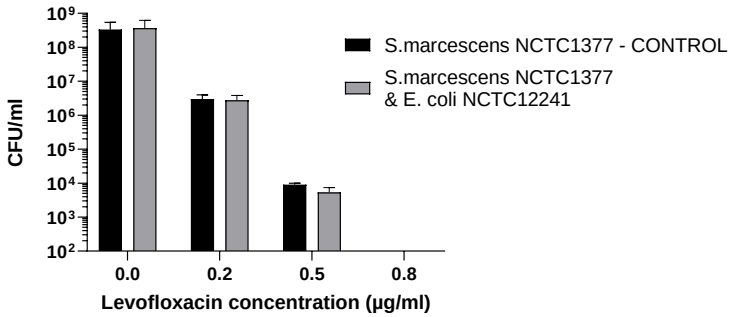

Figure 5.5: **Levofloxacin susceptibility in *S. marcescens* NCTC1377 growing in liquid LB at 37°C, 200rpm, by its own (control) or with *E. coli* NCTC12241**. Samples were in contact with LFX o/n at 37°C, 200 rpm. Cell viability was assessed measuring CFU (Miles Misra method). X axis indicates the LFX concentration (µg/ml), Y axis indicates CFU/ml. Results and error bars indicate mean ± SD of three technical replicates (GraphPad 9.3.1,2021).

5.1.1 Other antibiotics: ampicillin and vancomycin

To further explore whether phenotypic changes connected to antibiotic sensitivity and resistance were not exclusive to LFX, ampicillin and vancomycin were also tested on the "bull's eye" pattern and controls. Although *S. marcescens*, and likewise *E. coli*,[407]is known for being naturally resistant to ampicillin and other beta-lactams, as a carrier of the *ampC* gene which encode for hydrolytic proteins (beta-lactamases) which inactivate the antibiotics[116], we did not exclude the possibility of a phenotypic or genetic changes in the "bull's eye" pattern which may have rendered the bacteria sensitive to ampicillin. Similarly, vancomycin is known to be ineffective towards Gram-negative strains as it is impermeable to the external lipid membrane that characterize Gram-negative bacteria[408]. Hence, we wanted to test whether the co-culture conditions would have led to a change in vancomycin sensitivity in *S. marcescens* and/or *E. coli* most likely mediated by a change in the membrane composition.

Results did not show any difference in resistance between *S. marcescens* NCTC1377 or *E. coli* NCTC12241 growing on their own (control) and bacteria from the "bull's eye" pattern (Figure 5.6). Specifically, both were not sensitive to highest tested concentrations, 100 and 50 µg/ml of ampicillin and vancomycin respectively.

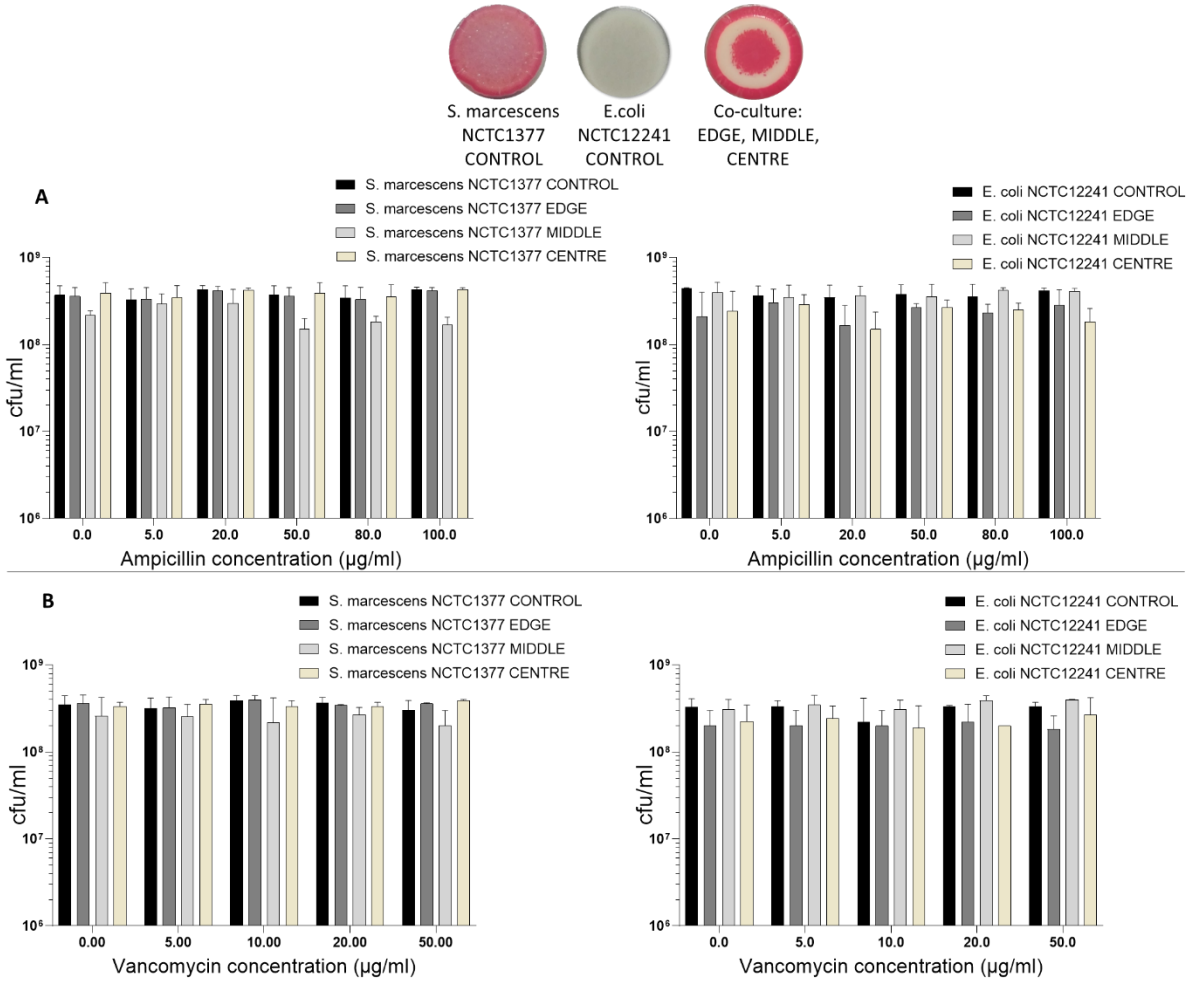

Figure 5.6: **Ampicillin and vancomycin susceptibility in bacterial samples collected from *S. marcescens* NCTC1377 (control), *E. coli* NCTC12241 (control) and from the sectors of the pattern (Edge, Middle, Centre).** Samples were in contact with ampicillin (A) or vancomycin (B) for 16 hours at 37°C, 200 rpm. Cell viability was assessed measuring CFU (Miles Misra method). X axis indicates the antibiotic concentration (µg/ml), Y axis indicates CFU/ml. Results and error bars indicate mean ± SD of three technical replicates. Data analysis was performed with unpaired t-test (GraphPad 9.3.1,2021). No significant values (P-value < 0.05). Experiments were conducted in collaboration with Ignacio Gabriel Picco, a visiting medical student from the University of Buenos Aires.

5.1.2 Antibiotic resistance may be oxidative stress-mediated

There is evidence that *qnr* expression leads to fluoroquinolone resistance competing for the antibiotics binding sites[144,145]. Also, *qnr* genes are located upstream of the LexA binding site, a well conserved sequence among Gram-negative bacteria[150–153] and they are regulated through the SOS response in a LexA/RecA-dependent manner[136]. To test whether DNA damages, and subsequent activation of RecA, LexA autocleavage and *qnr* expression[143,146,147] can increase LFX resistance in *S. marcescens* NCTC1377, we have exposed the bacterial culture to H_2O_2, at a not toxic concentration, but at a concentration that may lead to DNA damage-oxidated stress mediated.

We first identified a concentration and exposure time to H_2O_2 for *S. marcescens* not affecting the bacterial growth in liquid at 37°C, 200 rpm. We demonstrated that exposure of *S. marcescens* NCTC1377 to a concentration of 0.3 mM H_2O_2 for 90 minutes did not affect the bacterial growth (Figure 5.7), whereas higher concentrations decreased the measured OD_{600}, especially above 1 mM. In fact,

the growth curves of *S. marcescens* with no H_2O_2 and with 0.3 mM H_2O_2 were almost identical for the first 90 minutes of growth, while it slightly decreased at after 120 minutes. *S. marcescens* growth seemed to not be affected by 0.6 mM H_2O_2 for the first 75 minutes, however, a noticeably slower growth was observed from 90 minutes. Similarly, the bacteria displayed a much slower growth with 1 mM H_2O_2 compared to control (no H_2O_2). A concentration of 3 mM H_2O_2, instead, seemed to have a bacteriostatic effect on the bacterial growth after 45 minutes of exposure.

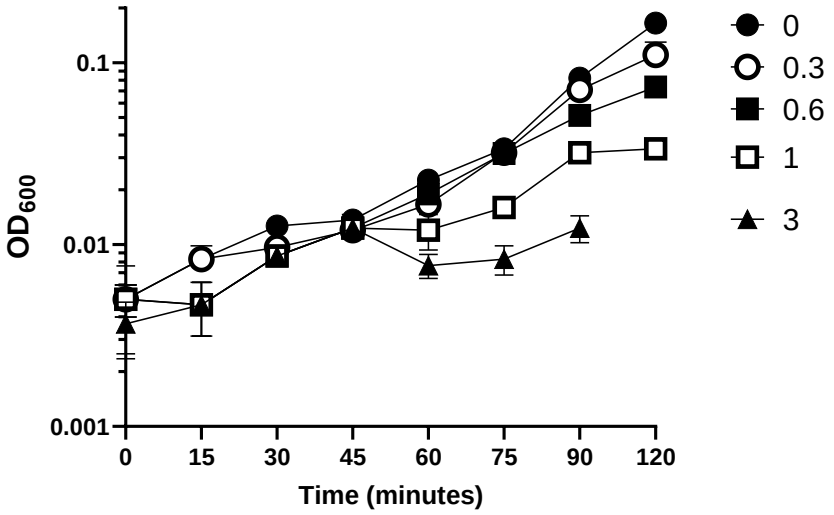

Figure 5.7: **Exponential culture of *S. marcescens* NCTC1377 exposed to increasing concentration of H_2O_2 over time.** X axis indicates the time of exposure with H_2O_2, Y axis indicates OD_{600} measured for the liquid culture. Results and error bars indicate mean ± SD of three technical replicates (GraphPad 9.3.1,2021).

Given those considerations, we exposed *S. marcescens* NCTC1377 to 0.3 mM H_2O_2 for 90 minutes prior the contact with LFX. Results indicated that the exposure of *S. marcescens* NCTC1377 to 0.3 mM H_2O_2 induced a 10-fold increased resistance to 0.5 µg/ml LFX (P-value 0.0212) (Figure 5.8). It is possible that the increased antibiotic resistance in *S. marcescens* may be mediated by DNA damage – and consequent RecA/LexA and *qnr* activation – induced by the exposure to H_2O_2. While our results clearly showed that H_2O_2 influences the sensitivity of *S. marcescens* to LFX, we do not know whether the antibiotic resistance observed for *S. marcescens* in the "bull's eye" pattern is elicited by *E. coli* ROS production. Further experiments need to be conducted to have a mechanistic understanding of the observe phenomena and confirm whether *E. coli* can induce LFX resistance in *S. marcescens* producing ROS.

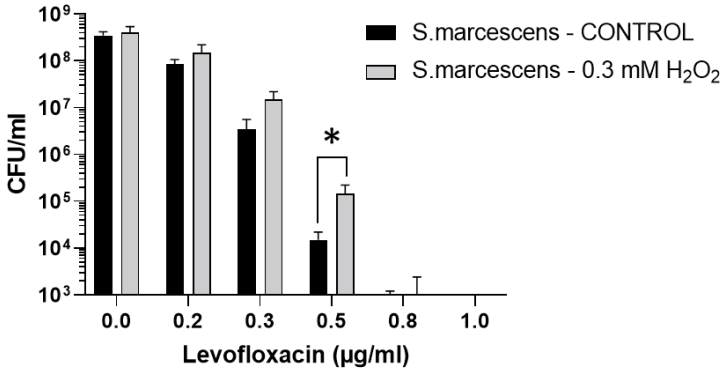

Figure 5.8: **Exponential growing culture of *S. marcescens* exposed for 90 minutes to 0.3 mM H_2O_2 and then to increasing concentrations of LFX (0 to 1µg).** Cells viability was assessed measuring CFU (Miles Misra method). X axis indicates the LFX concentration (µg/ml), Y axis indicates CFU/ml. Results and error bars indicate mean ± SD of three technical replicates. Data analysis was performed with unpaired t-test (GraphPad 9.3.1,2021). Asterisks indicate significant values (P value < 0.05). Graphs show representative data from two independent experiments.

5.1.3 Oxidative stress not leading *S. marcescens* to form the "bull's eye" pattern

If *E. coli* NCTC12441-mediating oxidative stress in *S. marcescens* NCTC1377 may be the cause for an increased antibiotic resistance and for leading *S. marcescens* NCTC1377 to form the "bull's eye" pattern, it is conceivable that the exposure to H_2O_2 may also lead *S. marcescens* NCTC1377 to form such a pattern. To study that, we have first exposed *S. marcescens* NCTC1377 to 0.3 mM H_2O_2 for 90 minutes, a concentration and exposure time seen to not be toxic for the bacteria (Figure 5.7), and subsequently plated *S. marcescens* NCTC1377 on TSA. Also, an exponentially growing culture of *S. marcescens* NCTC1377 was plated on TSA supplemented with 0.3 mM H_2O_2.

Results showed that, in both conditions, *S. marcescens* NCTC1377 did not form a "bull's eye" pattern, but rather a typical homogeneous red colony pattern in both conditions tested (data not shown as photographs of these specific experiment's results not available). Those data reinforced the hypothesis that *E. coli* NCTC12441 was required on the agar plate for *S. marcescens* NCTC1377 to form the "bull's eye" pattern and for other phenotypic changes to happen, such as the increased LFX resistance.

5.2 Swimming motility of *S. marcescens* NCTC1377 is inhibited in co-culture with *E. coli* NCTC 12241

Bacterial motility contributes to pathogenesis by facilitating bacteria-host interactions, biofilm formation, adherence and invasion[409]. Moreover, migration may come into play when we consider the possibility that a subset of cells of *S. marcescens* NCTC1377 from the middle ring may move toward the central spot and outer edge. Therefore, we aimed to test both swarming and swimming motility in *S. marcescens* NCTC1377 when in contact with *E. coli* NCTC12241 to investigate whether the motility of the strains may change when growing as mono- or co-cultures. The *E. coli* strain which did not seem to play a role in the pattern formation and antibiotic resistance change, NCTC10418, was also assessed for motility, again alone or in co-culture. Swarming and swimming motility were assessed by inoculating 2µl drops of exponentially growing of *S. marcescens* and both *E. coli* strains, mono- and respective

pairwise co-cultures, in soft agar plates, specifically 0.3 % agar for swimming and 0.7 % agar for swarming.

Results showed that swarming motility was limited for all the tested strains, in mono- or co-cultures- on TSA swarm plates (0.7% agar, Figure 5.9), with diameters ranging from 1.2 (± 0.11) to 1.4 (± 0.12) cm in each colony, while once would have expected the swarmer bacteria colonizing an area of approx. 5 to 8 cm large on a conventional Petri dish[410] . Likewise, *E. coli* NCTC12241 did not show any motility on swim plates (0.3% agar), with a colony of approx. 1.4 cm in diameter (Figure 5.9). In contrast, in swim plates, *E. coli* NCTC10418 and *S. marcescens* NCTC1377 mono-cultures, displayed a remarkable ability to swim, with colonies reaching diameters of approximately 4.3 and 4.6 cm respectively. Crucially, *S. marcescens* NCTC1377 ability to swim in monoculture was significantly increased (P-value 0.0025, unpaired t-test) with colony diameter of 4.9 cm (± 0.43), compared to its swimming ability in the presence of *E. coli* NCTC12241, colony diameter of 1.8 cm (± 0.55). No difference was observed between *S. marcescens* NCTC1377 or *E. coli* NCTC10418 and the co-culture *S. marcescens* NCTC1377 and *E. coli* NCTC10418 (Figure 5.9), the latter with a colony diameter of 5.0 cm (± 0.55).

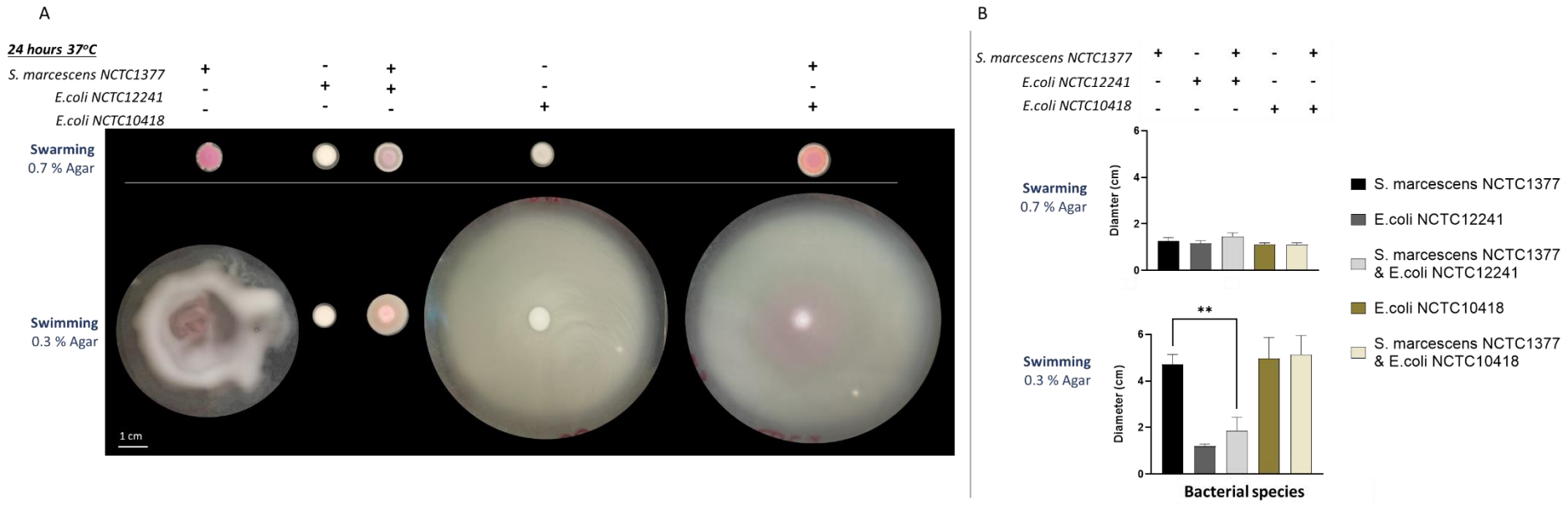

Figure 5.9: **Bacterial cultures (*S. marcescens* NCTC1377, *E. coli* NCTC12241, *E. coli* NCTC10418 mono- and respective co-cultures) grown on swim and swarm plates.** A) On top row, cultures grown on 0.7% agar to assess swarming, at bottom row cultures grown on 0.3% agar to assess swimming. Images show representative data from three independent experiments. B) quantification of the shown colonies in diameter (Y axis) of each grown colony on swarm (top graph) and swim (bottom graph) plates mono- or co-culture (N=3). Bacterial species are indicated above the graph and in the legend. Asterisks indicate significant values; unpaired t-test (P-value<0.05) applied, error bars correspond to Standard Error of measurement (SEM).

It is known that optimum temperature for prodigiosin production in *Serratia* is 22 to 27°C[401]. Consistently, we observed that our *S. marcescens* NCTC1377 increased its red pigmentation when left at room temperature (data not shown as pictures not available). It was reasonable that red-white patterns on soft agar plates with *S. marcescens* NCTC1377 and *E. coli* strains may have appeared. Hence, to enhance prodigiosin production on plates and observe putative patterns on swarms and swim plates, colonies resulting from *S. marcescens* NCTC1377 in co-culture with *E. coli* NCTC12241 or NCTC10418, were left at room temperature for further 8 hours. Resulting colonies were characterized by concentric white-pink-red rings, which were different to the "bull's eye" pattern and also differed among the growth conditions (agar %) (Figure 5.10). Importantly, no "bull's eye" pattern was observed in the co-culture between *E. coli* NCTC12241 and *S. marcescens* NCTC1377, suggesting that variation in agar concentration on the solid surface influenced the pattern formation, and strongly supporting the fact that motility is involved in the process.

Next to quantitively and qualitative assess the bacterial species grown on the different coloured sectors on swim and swarm co-culture plates, we collected samples of approx. 1 mm^2 from each sector, resuspended in PBS(1x), serially diluted, plated on TSA plates, and incubated for 16 hours at 37°C. Once grown, CFU were determined (Figure 5.10). Results revealed that *S. marcescens* NCTC1377 mostly grew in the outer sectors of the colonised area when growing in co-culture with *E. coli* NCTC12241, which was unable to swim or swarm, as shown in Figure 5.9. On the contrary, when in contact with *E. coli* NCTC10418, *S. marcescens* NCTC1377 mainly occupied the central part of the area, most probably due to the ability to swim of *E. coli* NCTC10418 compared to the strain NCTC12241. Additional to these changes in pattern formation, we observed that *S. marcescens* NCTC1377 also partially lost their pigmentation. Noticeably at the outer edge of the 0.7% agar-colony, and at both the outer edge and central spot of the 0.3% agar-colony, pigmentation was decreased, pointing again towards the negative modulation of prodigiosin production in the presence of *E. coli* NCTC12241. Differently, this lack of pigmentation was not observed when *S. marcescens* NCTC1377 is in contact with *E. coli* NCTC10418 in both swarm and swim plates (Figure 5.10). A summary of the described observations is reported in Table 5.1.

When looking at the distribution of the two different *E. coli* strains used, it was clear that the non-motile *E. coli* NCTC12241 grew pre-dominantly in the central spot on the colonised agar, in both swim and swarm plates (Figure 5.10). On the other hand, *E. coli* NCTC10418 colonises the outer rings of the observed areas, also in both swim and swarm plates, indicating the role of bacterial motility in pattern formation (Figure 5.10 and Table 5.1).

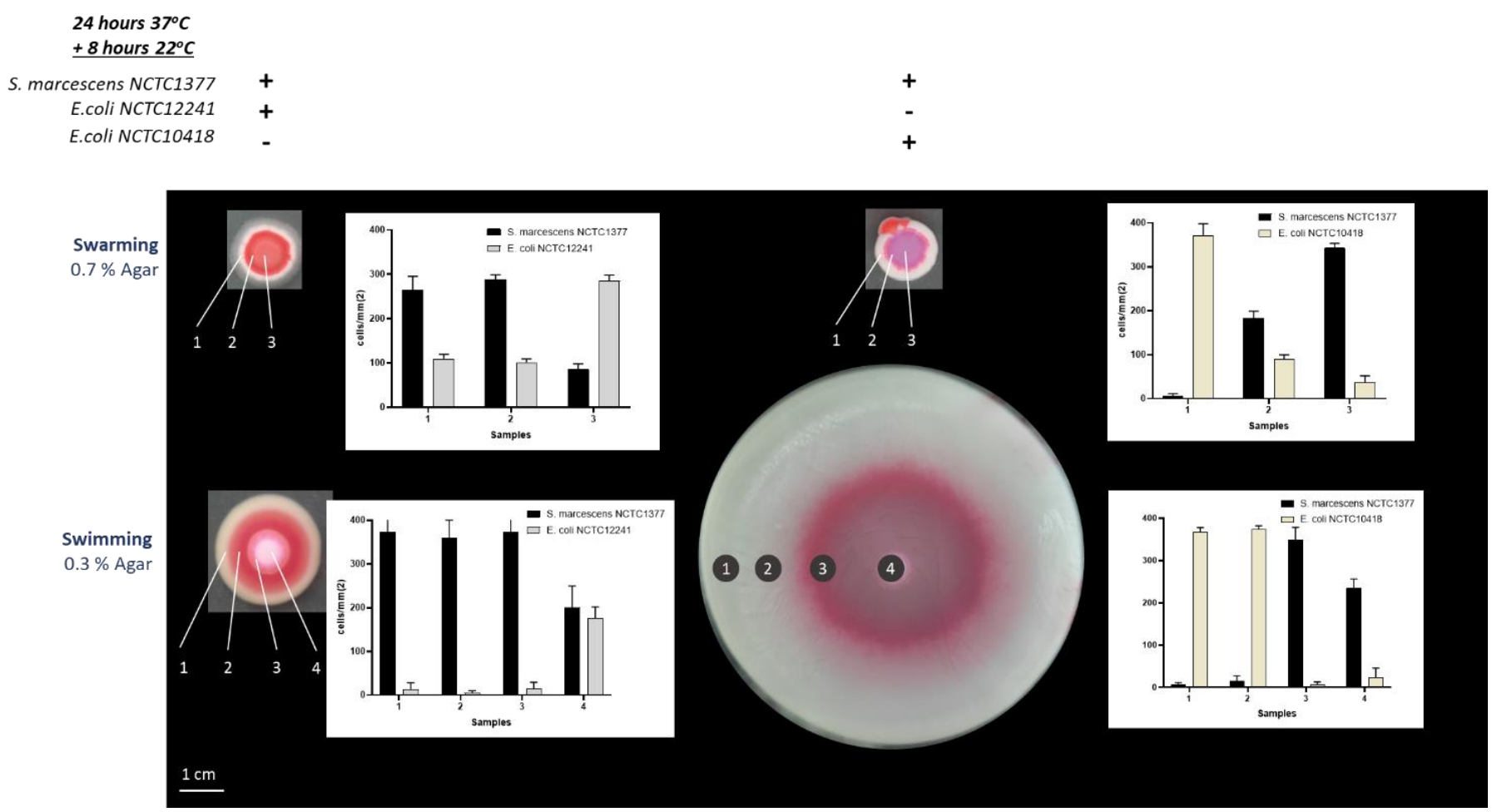

Figure 5.10: **Bacterial cells grown on soft agar plates for 24 hours at 37°C and left at room temperature for further 8 hours to enhance pigmentation**. 0.7 %, top row, and 0.3%, bottom row. Samples (1 to 4) were characterized for bacterial species identification. Images represent examples of three independent experiments and graphs indicate the number of cells/mm² (Y axis) for each sample collected (x axis) on swarm (top graphs) from swim (bottom graphs) plates of co-cultures, error bars indicate SD calculated from three repeated measurements. Bacterial species are indicated above the graph and in the legend.

Table 5.1: **Comparison of *S. marcescens* NCTC1377 behaviours (i) travel distance (ii)prodigiosin expression** between *S. marcescens* NCTC1377 growing alone on swarm (0.7%) and swim (0.3%) plates and *S. marcescens* NCTC1377 in co-culture with the *E. coli* strains

		S. marcescens *travel* distance		Prodigiosin expression			
				Centre spot		***Outer edge***	
	Co-culture partner	E.coli NCTC12241	E.coli NCTC10418	E.coli NCTC12241	E.coli NCTC10418	E.coli NCTC12241	E.coli NCTC10418
Condition	**Swarming** 0.7 % Agar	=	=	=	=	↓	-
	Swimming 0.3 % Agar	↓	=	↓	=	↓	-

Where:
= no change compared to *S. marcescens* NCTC1377 alone
↓ decrease compared to *S. marcescens* NCTC1377 alone
- not applicable

5.3 *S. marcescens* reduces the ability of *E. coli* NCTC10418 to grow as a biofilm

Multi-species bacterial biofilms represent almost 80% of microbial infections, often causing nosocomial infections[411]. Bacterial communication and coordination are essential for biofilm establishment and bacterial survival. Considering signal-mediating space distribution as a “bull’s eye” pattern between *S. marcescens* NCTC1377 and *E. coli* NCTC12241 and other phenotypic changes observed, it is also reasonable to expect a change in biofilm formation when the strains were growing in co-culture rather than by mono-culture.

To study that, bacterial biofilms of the strains alone (*S. marcescens* NCTC1377, *E. coli* NCTC 12241, *E. coli* NCTC10418) and the respective co-cultures were tested in our well-established biofilm formation assay in a 96-well plate (Allott et al, unpublished). After 24 hours of incubation, *S. marcescens* NCTC1377 biofilm in LB or LB supplemented with glucose displayed a concentric pattern mainly colonizing the outer edge-side of the wells (Figure 5.11). *E. coli* NCTC12241 formed instead a poor biofilm with scattered colonized area in the wells, in both LB or LB with glucose. Surprisingly, on the contrary, *E. coli* NCTC10418 formed a thick biofilm distributed all over the wells in LB. Surprisingly when grown in LB with glucose, *E. coli* NCTC10418 only colonised the plate in a sparse fashion. It seemed that the presence of glucose importantly diminished the bacterial biofilm capacity, with a few scattered ‘dots’ in the wells (Figure 5.11). However, the number of cells resulting from the biofilm-viability assay did not show any significant difference between the biofilm formed in LB and LB supplemented with glucose (Figure 5.12).

Biofilms of the co-culture *S. marcescens* NCTC1377and *E. coli* NCTC12241, seemed to slightly reduce the typical *S. marcescens* concentric pattern, while bacterial numbers in the biofilm mass did not vary (Figure 5.11, Figure 5.12)

In the co-culture between *S. marcescens* NCTC1377and *E. coli* NCTC10418, the ability of the latter to form a biofilm in LB was significantly reduced (unpaired t-test, P-value 0.002). No difference were observed when the biofilm was growing in LB with glucose (Figure 5.12).

We also cultured the two *E. coli* strains as a biofilm: results showed that the *E. coli* NCTC10418 biofilm mass may be slightly reduced in LB when growing with *E. coli* NCTC12241.

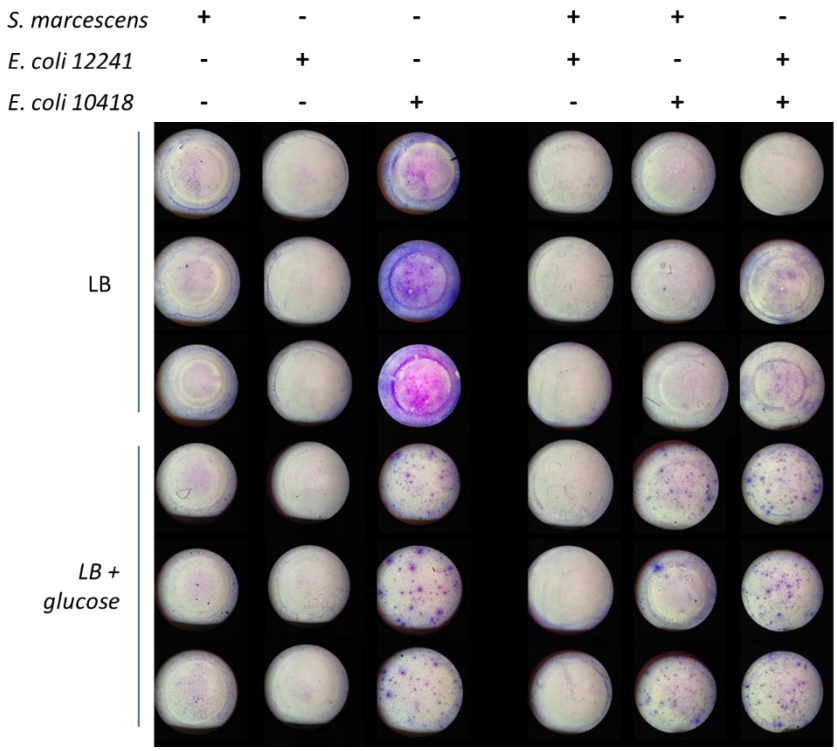

Figure 5.11: **Multi-species biofilm in 96-well plate.** S. marcescens NCTC1377, *E. coli* NCTC12241, *E. coli* NCTC10418 and respective cocultures were grown in a 96-well plate with LB or LB supplemented with glucose (0.5%), at 37°C for 24 hours in static condition and controlled humidity. For staining CV 0.1% was used. Each sphere represents a well of the 96-well plate observed at the microscope (40x).

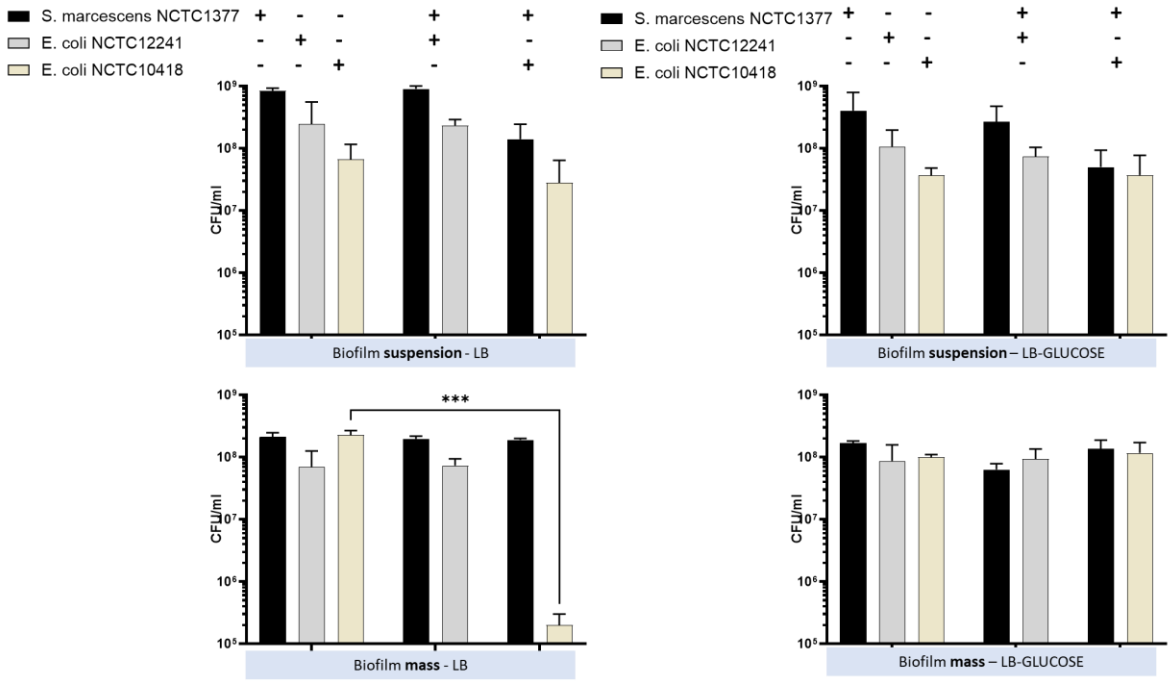

Figure 5.12: **Assessment of biofilm viability**. On top, cells grown in suspension on both condition, LB or LB supplemented with glucose. At bottom, cells grown as a biofilm resulting from scratching the bottom of the 96-well plate. In each graph, first three columns represent the control (each species growing on its own), the other paired columns indicate the co-cultures. Results and error bars indicate mean ± SD of three technical replicates. Asterisks indicate significant values; unpaired t-test (P-value<0.05) applied (GraphPad 9.3.1,2021).

5.4 Proteolytic and haemolytic activity

5.4.1 Proteolytic activity of *S. marcescens* NCTC1377 is inhibited in co-culture with *E. coli* NCTC12241

Given the crucial role proteolysis in establishing infections, we tested the protease activity of *S. marcescens* NCTC1377, *E. coli* NCTC12241, *E. coli* NCTC10418 and the respective co-cultures, by inoculating 10 µl drops of the exponential growing cultures on TSA supplemented with skim-milk (2.5%) and incubating at 37°C for 16 hours.

Results showed that *S. marcescens* NCTC1377 had a remarkable proteolytic activity, displayed by the presence of thick transparent halo surrounding its colony, while both *E. coli* strains displayed a por proteolytic activity (Figure 5.13). Surprisingly, the proteolytic activity of *S. marcescens* NCTC1377 was inhibited in liquid co-culture with *E. coli* NCTC12241, as displayed by the almost complete absence of halo surrounding the grown colony of *S. marcescens* NCTC1377 and *E. coli* NCTC12241 co-culture (Figure 5.13). In contrast, when in co-culture with *E. coli* NCTC10418, *S. marcescens* NCTC1377 still formed a surrounding transparent halo indicating proteolytic activity (Figure 5.13). The quantification of the proteolytic activity was achieved by measuring the number of image pixels per mm of transparent (proteolytic) area and expressing this as a ratio with the number of image pixels in the growth colony. Results indicated a significant (unpaired t-test, P-value 0.0175) reduction of the proteolytic area in the co-culture *S. marcescens* – *E. coli* NCTC12241 compared to *S. marcescens* alone (Figure 5.14)

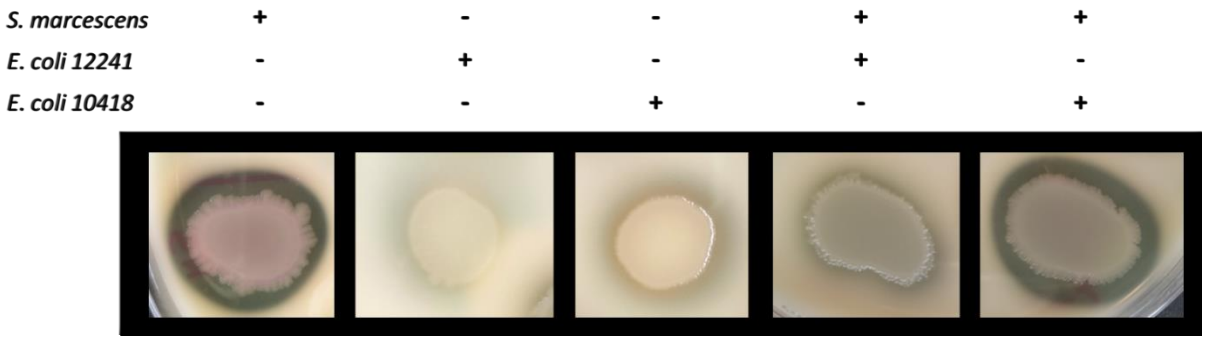

Figure 5.13: **Proteolytic activity of liquid mono- or co-culture tested on TSA enriched with skim milk (2.5%).** 10 µl drops of the exponential growing cultures of *S. marcescens* and both *E. coli* strains and respective pairwise co-cultures were inoculated on the plates and incubated at 37°C for 16 hours.

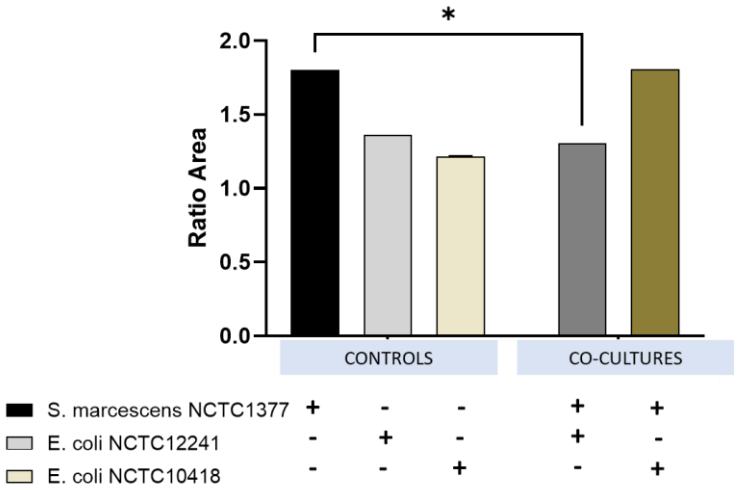

Figure 5.14: **Proteolytic activity of liquid mono- or co-culture quantified by measuring the "transparent" halo.** Fiji-ImageJ[412] were used for images quantification (pixels/mm). The ratio indicates the area defined by the proteolytic-halo and the grown-colony (Y axis). Bacteral sample composition (X axis) is indicated below the graph. Results and error bars indicate mean ± SD of three technical replicates. Asterisks indicate significant values; unpaired t-test (P-value<0.05) applied (GraphPad 9.3.1,2021). Each column was compared with the black column (*S. marcescens* NCTC1377), and when no significance was observed was not indicated in the graph for simplicity.

Proteolytic activity was also tested for samples collected from a from a "bull's eye" pattern. Results showed a significant (unpaired t-test P-value 0.0358) inhibition of proteolytic activity between the middle ring of the "bull's eye" pattern compared to the middle area of *S. marcescens* growing on its own (control). In contrast, we did not observed differences in the proteolytic activity between samples collected from the outer or the centre of the "bull's eye" pattern and controls (Figure 5.15). In the middle ring the "bull's eye" pattern we expected to have 10-fold less of *S. marcescens* NCTC1377 compared to *E. coli* NCTC12241, as previously described in Section 4.1.2. It is conceivable that this difference between *S. marcescens* NCTC1377 and *E. coli* NCTC12241 in favour of the latter in the middle ring, may be enough to reduce the proteolytic activity of *S. marcescens* NCTC1377 on the "bull's eye pattern".

One of the most abundant AA in skim milk is Met[413,414], whose effect on the "bull's eye" pattern has been addressed in Section 4.2.2. Of note, no difference was observed whether the skim milk powder was added on TSA or LBA, including the lack of pattern on both the media, supporting our hypothesis

that in the presence of Met, for instance in skim milk agar plates, the “bull’s eye” pattern may be disturbed.

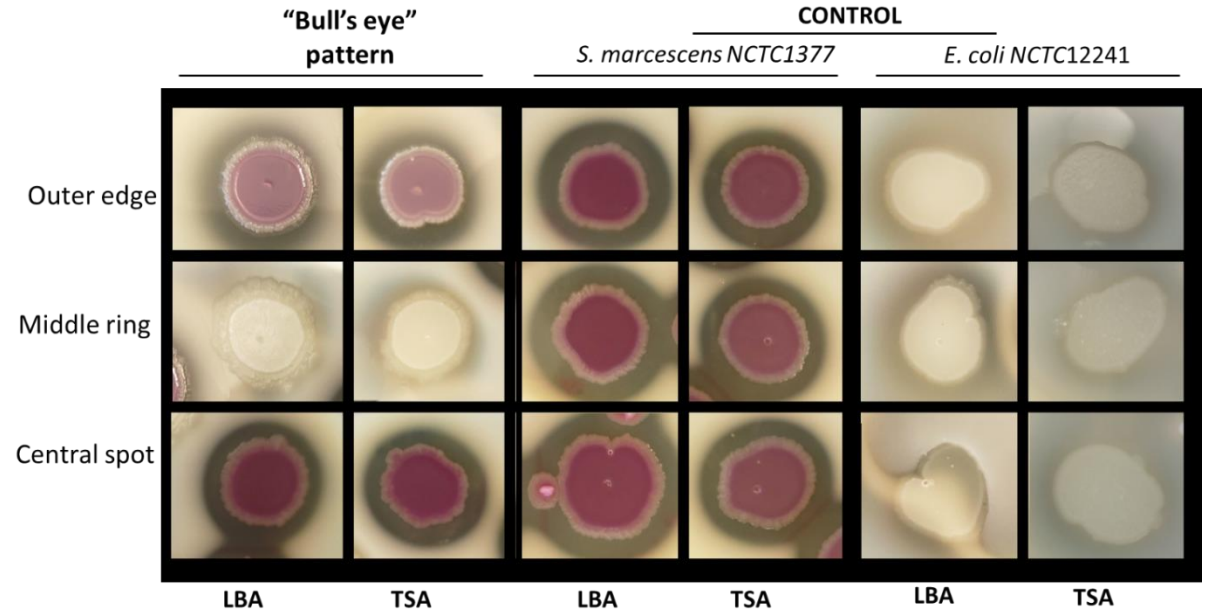

Figure 5.15: **Proteolytic activity of samples collected from each sector of a “bull’s eye” pattern and controls.** Samples from the outer edge, the middle ring or the central spot of a “bull’s eye” pattern were collected, resuspended in liquid medium and inoculated in 10 µl drops in LBA or TSA supplemented with skim-milk (2.5%). For the control, three samples, respectively from the outer, middle or centre were collected from growth colonies of *S. marcescens* NCTC1377 or *E. coli* NCTC12241 (mono-cultures), resuspended and inoculated on the skim-milk plates.

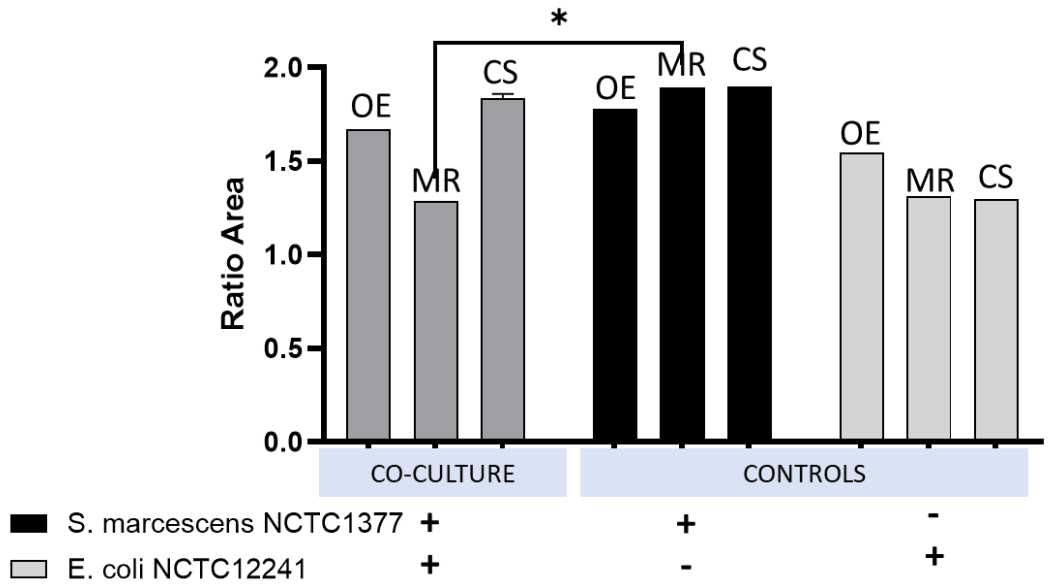

Figure 5.16: **Proteolytic activity of samples collcted from a “bull’s eye” pattern (co-culture) or controls, estimated by measuring the “trasparent” halo.** Fiji-ImageJ[412] were used for images quantification (pixels/mm). The ratio indicates the area defined by the proteolytic-halo and the growth-colony. Where OE: Outer Edge, MR: Middle Ring, CS: Central Spot. Bacteral samples (X axis) are indicated below the graph. Results and error bars indicate mean ± SD of three technical replicates. Asterisks indicate significant values; unpaired t-test (P-value<0.05) applied (GraphPad 9.3.1,2021).

5.4.2 Haemolytic activity of *S. marcescens* or *E. coli* NCTC12241 does not change between mono- or co-cultures

Next to the proteolytic activity we also wanted to test the haemolytic activity of *S. marcescens* NCTC1377, *E. coli* NCTC12241 and *E. coli* NCTC10418 and their respective co-cultures. Haemolysis is a critical in clinical strain determination, but also crucial to determine the pathogenicity of bacteria. We used TSA supplemented with sheep blood at both 37°C and 26°C to test the haemolytic activity of indicated strains.

S. marcescens NCTC1377 haemolytic activity at 26°C was characterized by the formation of a clearly defined transparent rim, typical of beta-haemolysis. Samples from the outer edge and the central spot of a "bull's eye" pattern gave the same results as the control, confirming that *S. marcescens* NCTC1377 was prevalent in those sectors of the pattern. In contrast, samples taken from the middle ring, where *E. coli* NCTC12241 prevailed compared to *S. marcescens* NCTC1377, did not show this transparent ring, but, instead, resembled the diffused halo observed in *E. coli* NCTC12241 alone, typical of alpha-haemolysin (Figure 5.17, 26°C).

At 37°C, bacterial samples grown on blood agar plates from both controls and "bull's eye" pattern, were different from what observed at 26°C. *S. marcescens* NCTC1377 colonies. They were encircled by diffused halo of 1.5 cm roughly, which was approx. 10 times bigger than the halo observed at 26°C; *E. coli* NCTC12241 colonies were also surrounded by a diffuse halo which tended to occupy the whole plate. Haemolytic activity for samples collected from the "bull's eye" pattern showed the same results as the *S. marcescens* NCTC1377 control. However, from the samples collected from the outer edge and centre of the pattern, i.e., the areas dominated by *S. marcescens* NCTC1377, a remarkable unique morphopattern was observed, characterized by a fluted edge (Figure 5.17, 37°C).

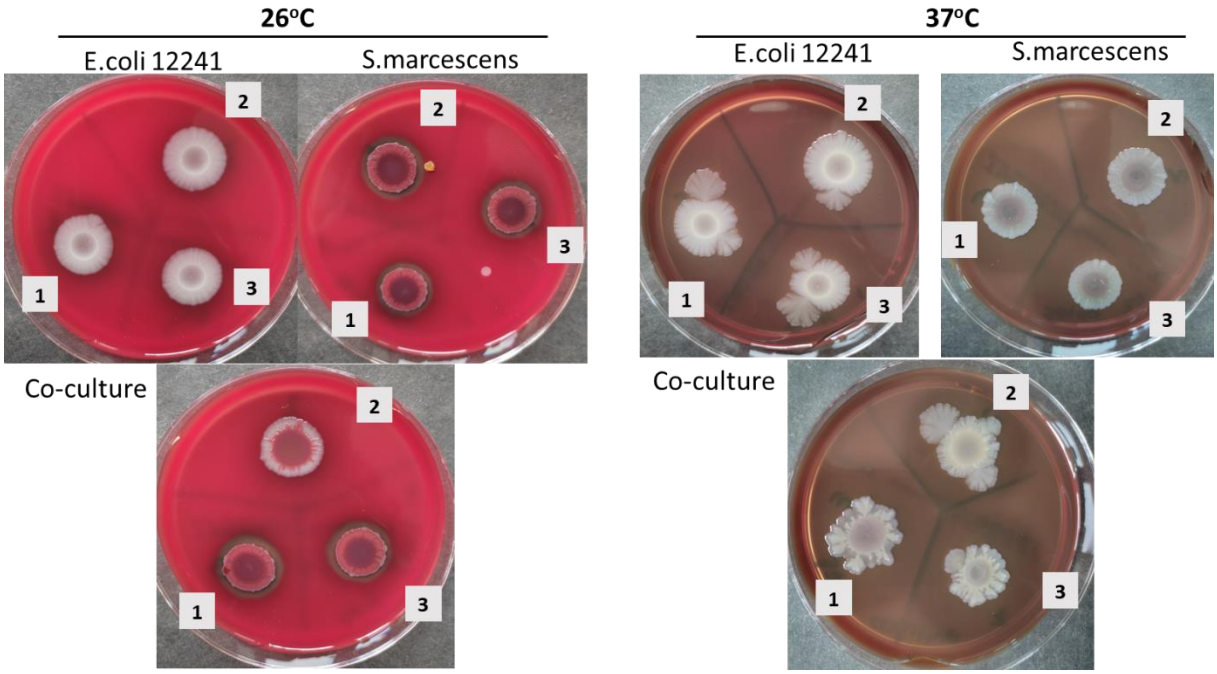

Figure 5.17: **Hemolytic activity of samples collected from each sector of a "bull's eye" pattern and controls**. Samples were incubated with a seeding density: 10^7cells/10µl on TSA-blood agar and kept 4 days at 37°C or 26°C. Outer edge (1), Middle ring (2), Central spot (3).

The proteolytic activity of bacteria growing from liquid cultures was also tested: at 26°C *S. marcescens* NCTC1377 as mono-culture and both co-culture colonies were fenced by a well-defined transparent rim, suggesting that the presence of other strains in the liquid co-culture with *S. marcescens* NCTC1377, did not affect the haemolytic activity *of S. marcescens* NCTC1377. At 37°C, similar results to what was observed from samples collected from the colonies/pattern were seen. In fact, diffused halos for both *S. marcescens* NCTC1377, *E. coli* NCTC12241, *E. coli* NCTC10418 alone (controls) and for the co-cultured bacteria appeared. Moreover, the previous described fluted-edge pattern was likewise observed for the *S. marcescens* NCTC1377 and *E. coli* NCTC12241 coculture. Due to the lack of prodigiosin development at 37°C on *S. marcescens* NCTC1377 together the "bull's eye" pattern could not be observed for the bacteria growing on blood agar plates. However, it is unclear whether the "bull's eye" pattern still formed; further experiments, including the spatial distribution of the two bacteria need to be undertaken to address these questions.

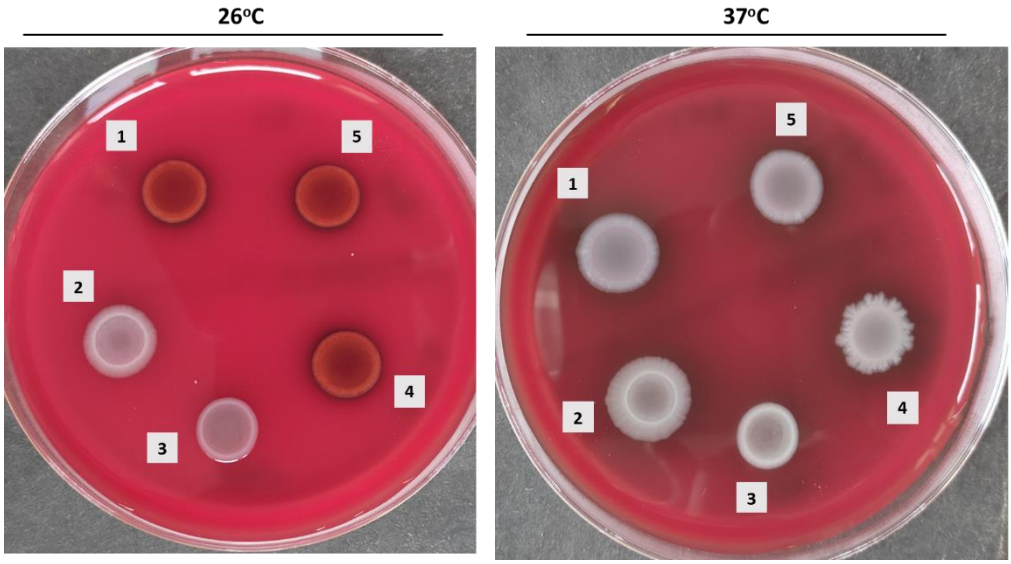

Figure 5.18: **Hemolytic activity of liquid mono- or co-culture at different temperature.** Samples were incubated with a seeding density: 10^7cells/10 µl on TSA-blood agar and kept 2 days at 37°C or 26°C. *S. marcescens*(1), *E.coli* 12241 (2), *E.coli* 10418 (3), Co-colture *S. marcescens-E. coli* 12241 (4), Co-colture *S. marcescens-E .coli* 10418 (5).

5.5 Infection assay: the role of the "bull's eye" at the host-pathogen interaction level

S. marcescens NCTC1377 displayed changes in virulence (i.e., antibiotic resistance (Section 5.1), motility (Section 5.2) and proteolytic activity (Section 5.2)) when growing in co-culture with *E. coli* NCTC12241. To test whether any virulence changes may also occur on tissue culture cells, we set up a co-culture between the bacterial cells grown in a "bull's eye" pattern (and appropriate controls) and mammalian epithelial cells (MDCK).

Previous experiments conducted by colleague Matthew Allott (MA) demonstrated that an MOI of 1 was enough for *S. marcescens* NCTC1377 to infect and survive in co-culture with MDCK (data not shown as conducted by MA), therefore this infection rate was selected for this experiment.

Results demonstrated that *S. marcescens* NCTC1377 collected from the outer edge of the "bull's eye" pattern and put in contact with MDCK with an MOI of 1 for 30 minutes, adhered significantly less (P-value 0.0211) than to *S. marcescens* NCTC1377 growing on its own. This reduction in adherence for *S. marcescens* NCTC1377 was accompanied by an increase in adherence for *E. coli* NCTC12241 collected from outer edge of a "bull's eye" pattern compared to the control (Figure 5.19).

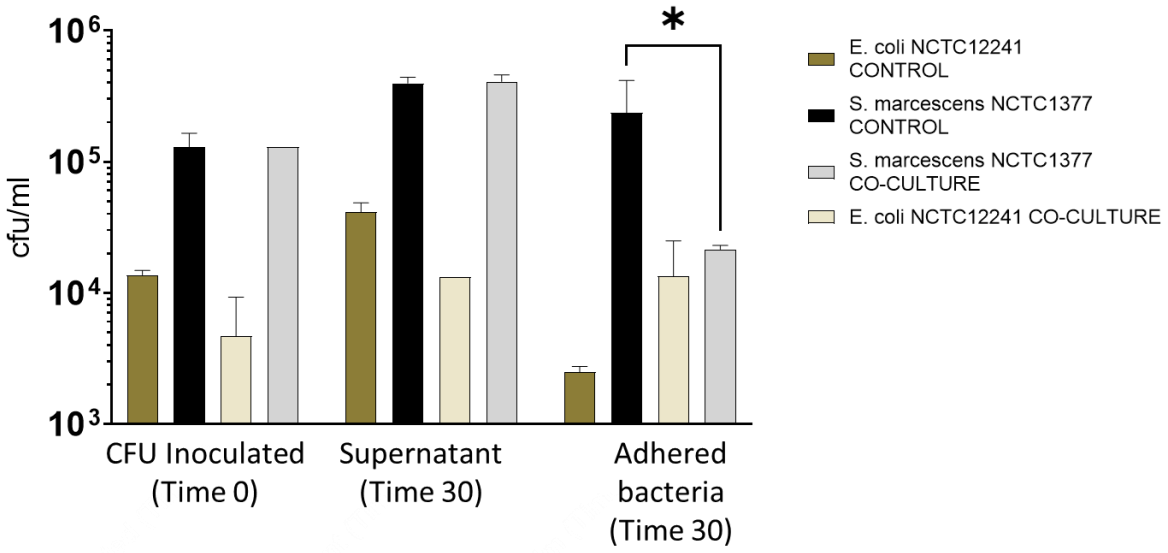

Figure 5.19: **MDCK infection assay:** Bacterial cells of *S. marcescens* NCTC1377 (black), *E. coli* NCTC12241 (brown) and outer edge of a "bull's eye" pattern (grey for *S. marcescens* and yellow for *E. coli* cells) were inoculated with an MOI of 1 for *S. marcescens* NCTC1377 and the co-culture, and an MOI of 0.1 for *E. coli* NCTC12241)- as a 1:10 ratio between *E. coli* NCTC12241: *S. marcescens* NCTC1377 is expected from the outer edge of the pattern – on the top of MDCK *(CFU Inoculated (Time 0)*. After 30 minutes, CFU/ml were determined for the supernatant (*Supernatant (Time 30))* and adhered bacteria (*Adhered bacteria (Time 30))*. Results and error bars indicate mean ± SD of three technical replicates. Asterisks indicate significant values; 2-way ANOVA (P-value<0.05) applied (GraphPad 9.3.1,2021). Graph shows representative data from two independent experiments.

To test whether bacterial cells were internalized by MDCK, gentamicin was added to each MDCK-bacteria-containing wells in order to kill bacterial cells in suspension or in the biofilm. Gentamicin cannot penetrate mammalian cells[415] and hence bacterial cells internalized by MDCK, were not affected. Results showed a significant (P-value 0.0079) reduction of *S. marcescens* NCTC1377 cells from the outer edge of the pattern compared to the control, meaning that the former were not internalized readily as the control cells, suggesting virulence modulation mediated by *E. coli* NCTC12241.

Interestingly *E. coli* in co-culture was slightly increased when compared to their mono-culture, so there might also be an effect on *E. coli*'s pathogenicity in the co-culture. However, these initial findings need to be verified with bigger sample numbers and slightly adjusted assay set up, as measurements were at the detection limit.

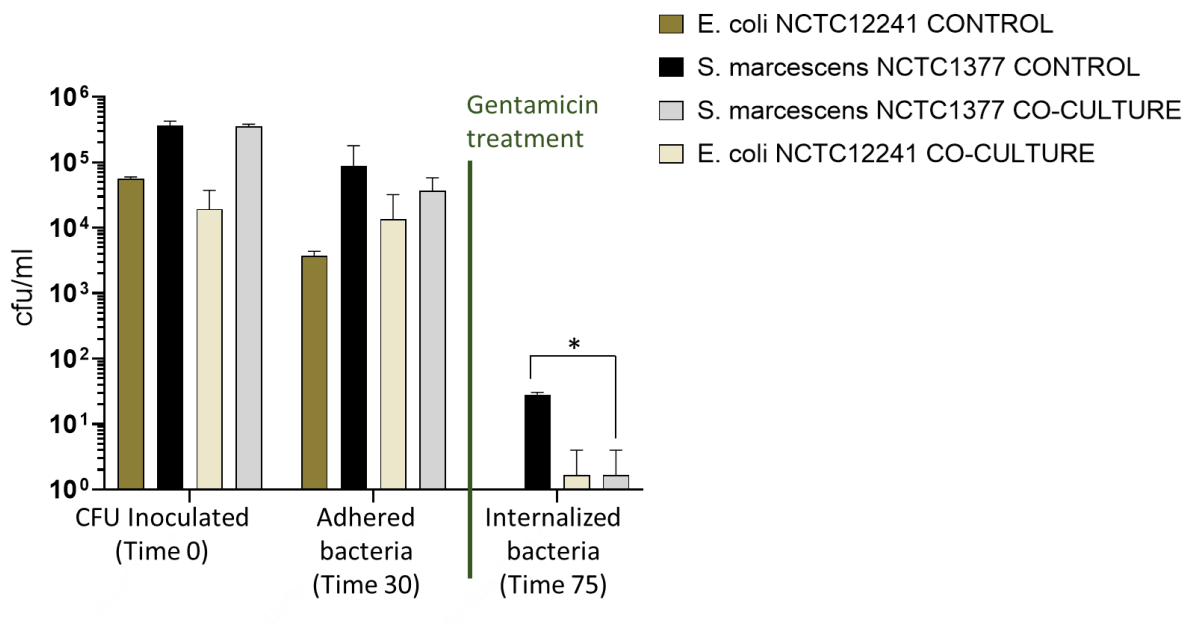

Figure 5.20: **MDCK infection assay and gentamicin protection**: Bacterial cells of *S. marcescens* NCTC1377 (black), *E. coli* NCTC12241 (brown) and outer edge of a "bull's eye" pattern (grey for *S. marcescens* and yellow for *E. coli* cells) were inoculated with an MOI of 1 for *S. marcescens* NCTC1377 and the co-culture, and an MOI of 0.1 for *E. coli* NCTC12241)- as a 1:10 ratio between *E. coli* NCTC12241: *S. marcescens* NCTC1377 is expected from the outer edge of the pattern – on the top of MDCK (*CFU Inoculated (Time 0*)). After 30 minutes, CFU/ml were determined for adhered bacteria (*Adhered bacteria (Time 30)*). At the same time, gentamicin was added in further MDCK-bacteria-containing wells. After further 45 minutes, CFU/ml were determined for internalized bacteria (*Internalized bacteria* (Time 75)). Results and error bars indicate mean ± SD of three technical replicates. Unpaired t-test (P-value<0.05) applied (GraphPad 9.3.1,2021).

5.6 Conclusion CHAPTER 5

The "bull's eye" structure resulted from the co-culture between *S. marcescens* NCTC1377 and *E. coli* NCTC12241 displayed to be accompanied by changes in bacterial functions. We have demonstrated that there was an increase in LFX resistance in *S. marcescens* from specific sectors of the pattern and showed that the increased resistance was a phenotypic change. Phenotypic LFX resistance in *S. marcescens* and other Gram-negative bacteria may be associated with the expression of *qnr* genes activated in response to SOS system, the latter triggered by DNA damages. The exposure to H_2O_2 also led our *S. marcescens* to an increase in LFX resistance, suggesting that a DNA damage induced by oxidative stress may also led to *qnr* expression and LFX resistance. One could speculate that *E. coli* can trigger oxidative stress - or other DNA damage-mediators - in *S. marcescens*, therefore increasing the antibiotic resistance. Further investigation needs to be done to gain a mechanistic understanding of the phenotypic change that accompanied the "bull's eye" pattern. Other changes in virulence that suggested the existence of genome-wide shifts in the co-culture were: i) a significant reduction in swimming motility and ii) proteolysis in *S. marcescens.* Those changes were consistent with the reduced ability of *S. marcescens* to adhere to mammalian cells.

The discovery of this novel pattern connected to LFX resistance and virulence is critical to underpin cutting-edge research aimed to study effective interventions to treat infectious diseases and tackle antibiotic resistance.

6 DISCUSSION

If the human body is a machine the microbiota is an essential part of its engine. In fact, the human microbiota is essential for the detoxification of harmful chemicals, the generation of metabolic precursors from nutrients and non-metabolized components, the fitness-based competitions to fend off pathogens and similarly the production of antimicrobial components, and priming of the immune system for immediate action before infectious agents. Consequently, microbiota imbalances will impair physiological functions (dysbiosis).

Tremendous advances have been made in understanding the composition of the microbiota in health and disease. The human microbiota consists of trillions of bacteria of tenths of thousands of species and the accompanying panoply of diverse metabolites, metabolic activities and regulatory signals. Studies of mixed bacterial populations in natural environments has been a staple characteristic of research since the onset of microbiology from the sea to the human body. In the same manner that during the 70s there was a boom in studies of bacterial ecology in aquatic and soil niches, for the past twenty years there had been an unparallel growth in the knowledge of the human and animal microbiota. However, due to the complexity of these ecosystems, most of that knowledge, even if seminal, had addressed a descriptive listing of their members with a few advances on metabolites and other components of the microbiome and to a less extent some studies on the interplay between those bacterial species and their chemical mediators.

A fundamental gap of knowledge driving the research questions that underpin this PhD thesis is the need for further mechanistic understanding of the interplay between species *in vitro* level to inform our research question: how bacteria in the microbiota may compete among themselves, interplay with the host and distribute the space to fend off pathogens and influencing human and animal physiology.

To address our researched questions, we have studied in vitro bacterial interactions among different bacterial strains known to be part of the human gut microbiota and, some of them, potential pathogens. Specifically, we aimed to elucidate bacterial population dynamics, competition and selection in response to i) an essential micronutrient for both, human and bacterial cells, Zn, which exert regulatory role for a range of genes within human and bacterial species; and ii) a potential underrated pathogen, *Serratia marcescens*.

6.1 Human microbiota *in vitro* co-culture competition experiments

6.1.1 Mono-culture growth in rich media

To study the complex ecosystem that inhabits the human intestine, we selected Gram-negative and Gram-positive bacterial species which grow aerobically and anaerobically in rich growth media, conditions akin to gastrointestinal physiology.

Our preliminary studies on the growth characteristics of each of the strains as a mono-culture were designed to determine the feasibility of concomitant growth of two different strains in bacterial co-culture. These studies revealed that all of the bacterial strains tested grew at 37^{o}C in rich media (LB and TSB) with agitation. Growth rates were similar among the Gram-negative and among the Gram-

positive, with the latter growing more slowly (Section 3.1). *K. aerogenes* in LB *and L. plantarum* in TSB were exceptions, they grew much slower than comparable Gram-negative and Gram-positive bacteria, respectively. Growth dynamic differences of each of the species in mono-culture need to be considered as part of the competition when grown as co-cultures. However, it is possible that the dynamics in co-culture may vary from those in mono-culture as a by-product of synergistic or antagonistic processes, whether metabolic, antimicrobial or others[335].

The development a modified LB medium (LBEAP1), rich in glucose and minerals (manganese and magnesium) allowed the fastidious microorganism *L. plantarum* to grow at a speed approx. like the rest of the strains (Figure 3.3). Also, the modified growth medium LBEAP1 represents a novel cost- and time-efficient growth media for multiple bacterial species without being selective (rather than, for instance, selective medium MRS conventional used for growing lactobacilli[373]) hence ideal for the study of *in vitro* co-cultures. The differential fitness between strains in LBEAP1 will need to be considered in co-culture experiments. Importantly, *L. plantarum* is a lactic-acid bacterium of relevance in food industry as a probiotic with potential beneficial effects in gut physiology[416]. Our developed medium, LBEAP1 – may be considered as a potential effective growth medium to be used for industrial applications too.

An important microbiological tool is to estimate the CFU from the OD of a growing culture. This was very much possible for most strains, as the colony viability curves were consistent with those of turbidity, especially when grown in LB (Figure 3.2). However, bacterial growth showed some discrepancy between the two methods for two of the Gram-positive cocci, *E. faecalis* NCTC377 and *S. salivarius* NCTC8618 when growing in TSB (Figure 3.1), with an initial lag phase by OD_{600} that was not reflected by the apparent exponential growth seen by CFU. One may consider that this discrepancy between viability and OD_{600} in these species could derive for instance, from a decreased cell size of daughter cells during the early stages of growth that will keep similar OD_{600} values while the total number of cells in the population is actually increasing. Alternatively, it is possible that in the time between measurement of OD_{600} and plating of the sample for the determination of CFU, there may be further rounds of cells division within those populations. It may be of value to consider this behavioural difference in the growth dynamics of these species when studying their properties in co-culture with other species[417]. TSB and LB have different composition, with TSB considered richer. TSB contains glucose and twice the amount of proteins than LB; of note, the protein source is also slightly different. While both of them have tryptone (pancreatic digest of casein), TSB has also soybean digest. Another difference are the salts, with LB containing twice the amount of NaCl but lacks the K_2HPO_4 present in TSB, that may also offer buffering potential. A critical difference, may be the exclusive presence of yeast extract in LB. Therefore, it is likely that those difference in nutrient composition may have led to the slight differences observed for bacterial growing in LB or TSB, and in particular the enhanced similarity in growth dynamics across all the species in LB. Our observations ultimately also suggest that there may be a variability in the presentation of the phenomena discovered in this PhD thesis as a function of the growth conditions of single and mixed populations of bacteria. The relevance of such consideration is not restricted to an *in vitro* setting but is in fact of paramount physiological importance as it may be a key contributor to the switch between health and disease given the variability of our microbiota ecosystem across individuals.

Similarly, it may play a role in food spoilage, the colonization of natural environments, the transmission of microorganism with pathogenic potential and the expression of virulence factors. The determination of rich growth media which allowed all bacterial strains to grow at similar growth dynamics represented a critical step to inform the selection of the species likely to lead to productive co-culture competition experiments, with the growth medium being possibly influential but not a limiting or selecting factor.

6.1.2 Zn toxicity is nutrient-dependent

The micronutrient Zn is an essential mineral for all forms of life including bacteria, playing structural, functional and signalling roles. At micromolar concentrations, Zn modulates the expression of genes involved in mineral transport, ribosomal proteins, metabolism and even bacterial virulence and pathogenesis. Moreover, the physiological intestinal concentration of Zn after a meal has been estimated to be around 100 µM[290], a concentration not toxic to bacteria, but most likely active at a cellular and molecular level. Despite its crucial role in bacterial virulence and the unavoidable interplay between Zn and bacteria in the human microbiota, how this micronutrient may affect the bacterial population dynamics within niches in the microbiota, is still unclear. In the light of these considerations, we selected Zn, to explore as a potential switch, able to shift bacterial population selection and dynamics.

Yet, Zn is toxic above a certain amount. Zn toxicity to bacteria vary among species and growth conditions with MIC ranging from 1 mM to 4 mM for *E. coli* [418–421] growing in rich medium. In contrast, other bacteria such as *Lactobacillus* spp., *Bifidobacterium* spp., *Streptococcus* spp., were found to tolerate quite well Zn, surviving at concentrations higher than 4 mM[422,423]. In our experimental study, we found that bacterial strains from our collection, including *Streptococcus* and *Lactobacillus* species, were not affected by 4 mM $ZnCl_2$ when growing in rich medium (TSB) (Figure 3.5). Critically, bacterial growth was instead impacted when grown in nutrient poorer, but still not minimal media - LB even at much lower concentrations (Figure 3.4). In fact, we showed that 4 mM was toxic for *E. coli*, *K. aerogenes*, *S. aureus*, *S. salivarius* and *L. plantarum*, and bacteriostatic for *S. marcescens* and *P. vulgaris*. Furthermore, 2.5 mM had a bacteriostatic effect for *K. aerogenes, S. aureus*, *S. salivarius* and *L. plantarum*. While 1 mM of Zn did not affect the growth of any of the Gram-negative bacteria, the Gram-positive *S. salivarius* and *L. plantarum* grew much slower than the rest, suggesting a higher tolerance to Zn in Gram-negative bacteria rather than in Gram-positive species, with the exception of *E. faecalis* which was not affected by any of the tested concentrations of Zn in LB. Isolated *E. faecalis* strains from piglets also exhibited a very high tolerance to Zn and copper[424].This high tolerance to Zn in *E. faecalis*, may be connected to the fact that Zn is required for both survival and virulence in this bacterial species[425], and, indeed, Zn homeostasis is critically regulated by the adcACB and adcAII system.

It has been shown that Zn can impact glucose metabolism in bacteria[426]. Thus, one may consider that the presence of Zn may facilitate glucose uptake and metabolism in bacteria, supporting their growth rather than acting as a toxicant. It is also plausible that some other micronutrients (minerals or vitamins) in TSB may interact and bind Zn preventing its toxic effect, both areas that could have been considered. However, as for this project we were interested in micronutrient concentrations of Zn likely to exert

regulatory functions of bacterial cells, further experiments to elucidate the high tolerance to Zn in TSB for most of the bacterial strains.

For our system, we selected a micronutrient concentration of 250 µM, 4- to 12-fold below toxic, but high enough to play a role in gene expression, as it was shown that 250 µM of Zn disturbed the QS-system, motility and biofilm formation in *S. typhimurium*[335,396].

Furthermore at lower centration, 200 µM, Zn altered the expression of numerous genes involved in motility, biofilm formation, stress response and metal homeostasis in *E. coli*[397]. Thus, those findings supported our choice of working with 250 µM of Zn as a potential switch in bacterial population selection and dynamics, however conclusive evidence still remains to be confirmed by undertaking for instance gene expression profiling experiments or verification of the regulation of specific genes.

6.1.3 *P. aeruginosa* takes over some Gram-positive cocci bacteria

To study the bacterial population dynamics in a limited number of species, we used models of two bacterial strains growing on conventional growth media, in the absence or presence of a potential switch, Zn. We showed that the bacterial pathogen *P. aeruginosa* PAO1 was taking over the Gram-positive *S. aureus* NCTC12981 or *S. salivarius* NCTC8618, based on colony counts (Figure 3.6 A,B). *P. aeruginosa* and *S. aureus* are major pathogens for respiratory and wound infections[427], and they are commonly found to grow together in biofilm. The interaction between *P. aeruginosa* and other opportunistic pathogens such as *Agrobacterium tumefaciens*[347], *S. aureus*[348,350,351,353] and *Candida albicans*[428], was studied in co-culture experiments. When co-cultured with *S. aureus*, *P. aeruginosa* was found to disturb the electron transport chain, to compete for micronutrients and to produce antimicrobial substances which limited the establishment of *S. aureus*[350]. Moreover, Filkins *et al.* had showed that the presence of *P. aeruginosa* lead *S. aureus* to switch its' metabolism from aerobic respiration to fermentation[350]. Also, glucose is the carbon preferred source for *S. aureus* during infection[429]. In the light of these considerations, it is reasonable that the possible aerobic-to-anaerobic shift and nutrient competition may lead *P. aeruginosa* to take over *S. aureus* in our co-culture. To test this hypothesis, oxygen measurements together with metabolic activity determination, using for instance seahorse techniques could be undertaken.

We showed that *S. salivarius* NCTC8618 was also obliterated by *P. aeruginosa* PAO1 when growing in co-culture (Figure 3.6). Interestingly, Scott et all had showed that *P. aeruginosa* limited *Streptococcus* sp. growth through nutrients competition[354]. Also, when growing in mono-cultures, *S. salivarius* grew more slowly than *P. aeruginosa* in both growth medium, LB or TSB. Therefore, it is reasonable to assume that when in co-culture, *S. salivarius* is outcompeted by *P. aeruginosa* due to better ability of the latter to use available nutrients. Another possibility to consider is the cidal effect mediated by bacteriophages, obligate parasites (virus) of bacteria which can shape bacterial communities through changing their abundance, diversity, and virulence and providing a competitive advantage to different species. Bacteriophages are the least explored component of the human microbiota, even if they are the most abundant biological entity in the world and generally highly bacterial species specific, thus enabling targeted bacterial killing or manipulation. In fact, bacteriophages had been proven to control

selection of bacterial populations in nature[430], evidenced as offering competitive advantages to selected human commensal bacterial species[431], and considered as a viable alternative to the critical health threat problem of antimicrobial resistance AMR[432]. In various countries bacteriophages have been used for therapy, or proposed as therapeutic tools to control bacterial pathogens in humans and animals in developing countries[433–435]. In the light of this, it is worth considering *P. aeruginosa*-released bacteriophages as mediator of this species-dependent advantage controlling bacterial population selection and dynamics. Before exploring these hypotheses further, our findings would need to be first confirmed with molecular tools, which we started to develop as described in Section 3.6.2, and mechanisms that specifically lead to a potential bacterial selection in favour of *P. aeruginosa* needs to be elucidated.

6.1.4 The probiotic *L. plantarum* seems to prevail on potential pathogens

L. plantarum is a probiotic strain, known for providing health benefits to the gut health, competing for niches and nutrients with potential pathogens and producing antimicrobial and anti-inflammatory substances[436,437].

Considered the lower growth rate of *L. plantarum* compared to other Gram-negative, such as *E. coli* or *P. aeruginosa*, one would expect those ones to prevail when in co-culture with *L. plantarum.* Surprisingly, we found that, in LBEAP1 co-cultures, *L. plantarum* was significantly prevailing on *E. coli* or *P. aeruginosa* (Figure 3.7). Colony morphology of the cells on the agar plates were also observed at the microscope to confirm their identity, i.e., *L. plantarum* cells. In support of this, lactobacilli had been found to limit the establishment of pathogens through adhesion by fimbriae and release of antimicrobial compounds[438]. However, with the Gram-staining of the liquid co-cultures (both, *L. plantarum* with on *E. coli* or *P. aeruginosa)* we observed the presence of both, Gram-negative and Gram-positive cells, suggesting that both strains co-existed in the liquid co-culture (LBEAP1), in contrast we displayed on plates. Even if unlikely, it is possible that the observed cells at the microscope were not necessary an indication of alive cells in liquid co-culture, meaning that *E. coli* or *P. aeruginosa* cells were present but dead– live/dead staining needs to be done to confirm this hypothesis. Instead, it is most likely that the growth inhibition of *P. aeruginosa* or *E. coli* mediated by *L. plantarum* may happen only on solid surface, when the probiotic strain is able to get established and grow competing for niches and nutrients to the detriment of the opportunistic pathogens, *E. coli* or *P. aeruginosa*.

Lactobacillus spp. seem to be effective in controlling food spoilage due to their antimicrobial activity against pathogenic bacteria common as foodborne pathogens, such as *E. coli* and *Listeria monocytogenes*[439], thanks to their ability to produce bacteriocin and lowering pH[440]. In support of this, a recent study showed that *Lactobacillus casei* supernatant, rich in lactic acid and bacteriocins, inhibited growth of pathogenic *E. coli*[441]. In addition, and anti-adhesion properties on epithelial cells against pathogens have been also demonstrated[442,443]. At present, it seems reasonable to use probiotic strains, such as *L. plantarum*, in the field of food industry and public hygiene for control and prevention of infections. To confirm the findings in our setting and have a comprehensive understanding of the phenomena, further molecular (quantitative and qualitative) analyses need to be done, for instance one could use forward and/or reverse genetics to create mutants, testing those in the established co-culture assays to determine the genes involved in this process.

6.1.5 The micronutrient zinc plays a role in bacterial population selection

Serratia marcescens is a Gram-negative enterobacterium, widespread in the environment and also present in the human gut microbiota. Although outbreaks of *S. marcescens* have been reported frequently in hospitals in UK and many other countries in the last two decades[40], the study of this opportunistic pathogens infecting humans, rather than insect of plants, is at its infancy. Moreover, in 2017, *S. marcescens* was listed by the WHO among antibiotic-resistant "priority pathogens"[25], representing a crucial health threat. Given the need to understand the bacterial population dynamic and selection in response to an underrated opportunistic pathogen, *S. marcescens,* and the resulting impact on the host, we have included this strain among the selected bacteria for the study of pairwise *in vitro* co-culture competition experiments.

Our initial experiments using CFU determination of non-selective media showed that, based on viable counts of colonies, Zn mediated population selection in *P. aeruginosa* PAO1 and *S. marcescens* NCTC1377 co-culture with a competitive advantage to *P. aeruginosa* over *S. marcescens*, probably driven by gene expression changes (Figure 3.6 C). This was supported by the findings of Li *et al.* who showed that in co-culture, *P. aeruginosa* mediated the upregulation of Zn transporter gene expression in *S. sanguinis*, favouring the latter growth[355]. Zn exposure significantly promoted the expression and secretion of factors involved in QS, motility, biosurfactants and toxins. Hence, we propose that the presence of the mineral may harness the commensal-to-pathogen transition of *P. aeruginosa*[342,] explaining the dominance of *P. aeruginosa.* However, with molecular analyses (semi-quantitative PCR) we had subsequently observed that both strains (*P. aeruginosa* PAO1 and *S. marcescens* NCTC1377) co-existed after 24 and 48 hours with or without Zn, in contrast with what we observed from the colony counts. As the methods used are highly likely to be an accurate representation of the vitality of the cells at the time of co-culture, compared to the CFU determination, i.e., a more indirect measurement of the surviving cells after 24 hours of co-culture, we looked into possible explanations for these discrepancies. It had been demonstrated that some Serratia strains can lose the ability to produce prodigiosin in certain conditions, such as high temperature or low pH[30], producing cells appear then white or translucent[444]. Also, spontaneous colour mutants arising after a few generations were characterized by a growth advantage compared to red cells of *S. marcescens*[51,75]. In the light of this, it is possible that in the presence of *P. aeruginosa* PAO1, Zn enhances the expression of a non-pigmented phenotype in *S. marcescens* NCTC1377, and *S. marcescens* colonies were counted as *P. aeruginosa,* which naturally would lead to an over-representation in numbers of *P. aeruginosa.* To our knowledge there is not a single selective media that would distinguish white *S. marcescens* from *P. aeruginosa,* so alternative molecular technologies like 16s sequencing should be applied to verify the preliminary results of our study.

While some evidence exists on *P. aeruginosa* and *S. aureus* or *Streptococcus spp.*[348,350,351,353]*,* as already described, *P. aeruginosa* and *S. marcescens* co-culture seems to represent a novel insight, setting the stage towards promising findings in the imminent future. Genome-wide studies will also need to be conducted to complement and further elaborate the selective establishment of one bacterial strain rather than another.

6.2 The "bull's eye" pattern : a novel discovery

Despite no differential prevalence was observed for the co-culture between *E. coli* NCTC12241 and *S. marcescens* NCTC1377, we have encountered a remarkable observation on TSA plates: the appearance of a geometric pattern. Further analysis of this revealed that this pattern occurred only in certain conditions, in specific when 10 µl drops with 10^5 - 10^6 cells from the liquid co-culture were placed on TSA plates and grown at 37°C for 16 hours. The observed consistent colony-pattern was characterized by a geometric concentric shape, with a red outer edge, approximately 1 to 1.5 mm thick, a white middle ring with a thickness of approximately 1.2 to 1.5 cm, and a central red spot with a diameter of 3 to 4.5 mm, thus we named it the "bull's eye" pattern (Figure 4.3). One may consider that the pattern results from a differential bacterial space distribution, where red is always *S. marcescens* and white is always *E. coli*. However, Čepl and co-authors[244] using a different strain of *S. marcescens* (CNCTC 5965), had reported the presence of a similar pattern developed by this strain when growing on its own on glucose-supplemented NBA plates at 27°C. Hence, we tested whether *S. marcescens* NCTC1377 would have been able to lead the formation of this pattern in the absence of *E. coli* NCTC12241.

Using elastic light scattering patterns, circular structures have been identified for a variety of bacteria species, including *E. coli*. However, the technique encodes the micro- and macro-structural morphology of the colony onto an interrogating wavefront[445]. They have been developed to identify bacterial species quickly, when growing on agar plates, but as far as we are aware our study is the first to see and examine macroscopic centric pattern formation visible by the naked eye due to co-culture conditions.

6.2.1 *Serratia marcescens* NCTC1377 alone does not form a "bull's eye" pattern

We studied the colony development of *S. marcescens* NCTC1377 using a variety of different media (TSA, LBA, LBA depleted from NaCl, BHIA, CLED, NBA, NBA supplemented with glucose), and observed red-to-white colony phenotypes in *S. marcescens* NCTC1377 growing in media with high glucose concentration (NBA with glucose, BHIA, TSA) (Figure 4.11). Initially we hypothesized that the appearance of white pigmentation was due to the high glucose content. This observation was also underpinned by red colonies (with just a thin white). If this hypothesis was correct, we would have expected to obtain white colonies on solid media having lactose as a sugar substrate (CLED), which would ultimately result in glucose availability upon degradation. However, the observation that those colonies in CLED agar were actually red would be in agreement with the poor metabolism of lactose, characteristic of *S. marcescens*[446]. We have hypothesized that during the first two days of growth, the bacterial cells on CLED may use the protein sources as the main energy source; only after a number of days, lactose degradation may slowly release the mono-saccharides glucose and galactose, and the bacterial cells may start using glucose as an energy source and the loss of prodigiosin becomes more evident.

Whether this glucose-mediated regulation occurs directly by glucose, or indirectly through downstream metabolites resulting from its degradation, or leading to changes in signalling pathways, remains to be determined. It has been known since 1946 that glucose can reduce prodigiosin production[403,447].

However, evidence had shown that the reduction of prodigiosin is mediated by the acidification of the growth medium[404,448], but genes involved in the process leading to this reduced expression mediated by the pH change were not identified as yet. Although a fall in pH has been implicated in the mechanism underpinning prodigiosin downregulation[244,449], our results did not support this theory. In fact, a variation in the pH, sufficient to reduce prodigiosin expression in such a short time on a growth medium containing buffer (TSA), is unlikely to happen. Moreover, if we assume that a pH change in the presence of glucose triggered the formation of the "bull's eye", we would also have observed the formation of the pattern in *S. marcescens* NCTC1377 alone on TSA at 37°C, which we did not. However, this theory could be further explored by the use of pH sensitive additives like phenol red in the agar plates to estimate any pH change in the growing colonies.

Similarly, protein concentration did not seem to influence the production of the pigment. In summary, in our conditions, glucose seemed to downregulate prodigiosin production, compared to potential differences in pH changes, NaCl, or protein concentration.

6.2.2 *E. coli* NCTC12241 is required to lead *S. marcescens* NCTC1377 to form the "bull's eye" pattern

We demonstrated that both *E. coli* NCTC12241 and *S. marcescens* NCTC1377 were present in all three sectors of the "bull's eye" pattern, the red outer edge, the white middle ring and the red central spot (Figure 4.6). The density of *S. marcescens* NCTC1377 was higher in the central spot and the outer edge, and of *E. coli* NCTC12241 in the middle ring. The difference between the higher and lower density strains in any of the sectors was always 10-fold higher (Table 4.1). Moreover, we displayed that the differential distribution of space of both strains within the pattern was initiated after between 5 to 7 hours of growth in these conditions (Section 4.1.3). Čepl and co-authors, when describing the similar pattern developed by *S. marcescens* CNCTC 5965, referred to pH as the factor leading to such space distribution[244]. It would be reasonable to conceive that a pH variation may be responsible for the bull's eye pattern revealed by our *S. marcescens* strain (NCTC1377). It was shown that there was a drop in the pH in liquid TSB from 7 to 5.6 within 3 hours of growth of *E. coli* [450]. Subsequently, the pH regularly increased to a value of 8.5 after 3 days[450]. This initial pH variation could be attributed to the preferential use of glucose as a favoured substrate for energy production and metabolic precursor generation to support growth. Ng and co-authors had demonstrated a lack of fluctuation of pH values of *E. coli* growing in LB, which does not contain glucose[450]. These considerations would be consistent with our observation that in media lacking glucose, including LB, NB or CLED, *S. marcescens* NCTC1377 did not form a "bull's eye" pattern in the presence of *E. coli* NCTC12241. In contrast, the co-culture of those two species in growth media containing glucose (TSA, BHIA and glucose supplemented-LBA) supported the formation of the pattern.

6.2.2.1 pH and glucose as potential mediators of the "bull's eye" pattern

Despite the similarity in the colony characteristics between *S. marcescens* CNCTC5965 and *S. marcescens* NCTC1377, both manifestations could be a product of different processes or variations of the same process including different stimuli to trigger the pattern. A critical difference between both processes was that while *S. marcescens* CNCTC5965 was able the form the pattern on its own in

certain growth conditions albeit with a significant variability (personal communication Jaroslav Čepl and our own experiments with their strain *S. marcescens* CNCTC5965 and growth media), our strain *S. marcescens* NCCT1377 was able to generate the pattern robustly and reproducibly yet it required the presence of *E. coli* NCTC12241. The consideration of pH as the leading factor for the "bull's eye" pattern formation in our strain, *S. marcescens* NCTC1377, needed to be re-considered in the light of a few observations. My experiments revealed equivalent growth rates for *E. coli* NCTC12241 and *S. marcescens* NCTC1377 in liquid cultures (TSB and LB), as shown in Section 3.1. It therefore seems likely that *E. coli* NCTC12241 and *S. marcescens* NCTC1377 have a very similar usage of glucose and thus we would reasonably expect similar pH changes of the medium over time. Consequently, if pH was the trigger for the "bull's eye" pattern generation, *S. marcescens* NCTC1377 should form the pattern growing on TSA plates on its own, as this strain would likely be using glucose at a rate not necessarily different from that of the co-culture, but that is not the case. Moreover, the formation of the "bull's eye" pattern did not happen when *S. marcescens* NCTC1377 was concomitantly growing with a different *E. coli* strain (NCTC10418) that has an identical growth rate to the *E. coli* responsible for leading the pattern formation, strain NCTC12241. Therefore, this supports the notion that glucose usage from the point of view of pH changes of the medium seems an unlikely reason for the appearance of the pattern with *S. marcescens* NCTC1377. In fact, it is possible that although the pattern formed by *S. marcescens* CNCTC5965 coincides with pH changes, it could be a by-product of other processes concomitantly occurring. In any case, it could be possible, even if unlikely, that the co-culture of *E. coli* NCTC12241 and *S. marcescens* NCTC1377 strains may result in different growth rates for any of these strains compared to their growth in monoculture. Therefore, the growth rate of both strains when in co-culture need to be tested to exclude a metabolic competition effect. pH changes over time on TSA supporting the growth of *S. marcescens* NCTC1377, *E. coli* NCTC12241 and *E. coli* NCTC10418 as mono- and co-cultures remains to be measured. Related to pH, it may also be of value to determine prodigiosin expression during that period as it had been shown that glucose metabolism-mediated pH decrease resulted in the reduction of prodigiosin production[449]. The latter would enable to study a putative link between pattern formation which in our system occurs after 5 to 7 hours of growth on TSA and the expression of prodigiosin biosynthetic gene or the production of prodigiosin itself. Prodigiosin was not only the indicator revealing a differential space distribution in the co-culture of *S. marcescens* NCTC1377 and *E. coli* NCTC12241, but we demonstrated that it was not expressed in the middle ring of the colony despite a high density of *S. marcescens* NCTC1377 in that section as well as the absence of a decrease in apparent prodigiosin presence in liquid co-culture of those two strains. At that stage of growth, the TSB would be expected to have an alkaline pH that according to Čepl *et al.* would lead to the expression of prodigiosin and the presence of the pattern.

Another observation that warrants reflection is that Čepl and co-authors connected the formation of the outer rim in a colony of *S. marcescens* CNCTC5965 to the alkalinization of pH occurring after 5 to 7 days of growth on glucose-supplemented NBA at 27°C[244]. Paradoxically, we demonstrated that the differential distribution of *S. marcescens* NCTC1377 in the co-culture colony with *E. coli* NCTC12241 occurs mainly after 5 to 7 hours on TSA at 37°C. Moreover, at that stage of growth one would expect acidic conditions in the growth medium[450]. Hence, the "bull's eye" pattern on both *S. marcescens* strains,

and perhaps others that we have not assessed yet, may be a strain-dependent phenomenon, possibly responding to different inducers, such as generic metabolites or dedicated signal molecules, which need to be considered. For instance, even if volatile ammonia as put forward by Čepl and co-authors as the agent possibly underpinning the alkalinization of pH resulting from protein deamination at late stages of growth by *S. marcescens* CNCTC5965, ammonia was also connected to QS-mediated specific signalling processes[451].

The "bull's eye" pattern could be explained by a situation of *S. marcescens* NCTC1377 presence and of *E. coli* NCTC12241 absence in the central spot and the outer edge of the colony on TSA revealed by apparent prodigiosin presence at both sites. Conversely, the absence of prodigiosin in the middle ring could be understood by the presence of *E. coli* NCTC12241 and absence of *S. marcescens* NCTC1377. Unexpectedly, my experiments with overnight co-culture colonies revealed that actually both *E. coli* NCTC12241 and *S. marcescens* NCTC1377 were present in all three sectors (Figure 4.9). Even if the density of *S. marcescens* NCTC1377 was higher in the central spot and outer edge and that of *E. coli* NCTC12241 in the middle ring, the difference between the higher and lower density strains in any of the sectors was just 10-fold higher (Table 4.1).

6.2.2.2 Physiology as a reason to the "bull's eye" pattern formation

The decrease in number of *S. marcescens* NCTC1377 cells in the middle ring of the co-culture colony could be a result of two different and not mutually exclusive processes. Based on the result of my time-lapse experiments (Section 4.1.3), first the growth rate of *S. marcescens* NCTC1377 in the middle ring seemed to slow down, seemingly initiating a stationary phase after 5 to 7 hours of growth on TSA. In contrast those in the central spot and in the outer edge kept growing at a growth rate equivalent to that in early exponential phase. Alternatively, or concomitantly one can propose a cidal effect of *S. marcescens* NCTC1377 on *E. coli* NCTC12241 in the centre and outer edge, and reciprocally a cidal effect of *E. coli* NCTC12241 on *S. marcescens* NCTC1377 in the middle ring. However, this is unlikely because (i) the total cumulative number of *E. coli* NCTC12241 or *S. marcescens* NCTC1377 cells across all three sectors in each timepoint for the observed 10 hours period was identical for both strains, (ii) *E. coli* NCTC12241 growth rate is the same across all three sectors during the exponential phase of growth. *S. marcescens* NCTC1377 displayed an almost identical growth rate to *E. coli* NCTC12241 for the first 4 hours. It is reasonable to speculate that the "bull's eye" pattern derives from changes connected to *S. marcescens* NCTC1377 physiology as *S. marcescens* at the outer edge and centre of the colonised area grew at a faster rate than *E. coli* NCTC12241. A differential space distribution due to nutrient consumption, accessibility and/or waste production needs to be determined. However, it seems unlikely that they use nutrients or produce waste differently when they have a virtually identical growth rate in liquid, additional to being identical *E. coli* strains, fitness-wise as far as we have determined (NCTC12241 and NCTC10418) lead to a different behaviour in *S. marcescens* NCTC1377.

One may consider the existence of oscillatory dynamics in the colony expansion determined by the interplay between cell growth and nutrient availability. Period oscillations in biofilm expansion as a function of nutrient availability was studied in *B. subtilis*[452]. The authors showed that glutamate (nitrogen

source) was regulating the population space distribution of bacterial cells in a co-dependence state, where the cells colonizing the interior of the biofilm were responsible for ammonia production, while the cells at the outside exploited the produced ammonia, most likely to avoid a rapid diffusion of the metabolite if they would had produced it[452]. Of note, they had shown that when the colony was small, this metabolic oscillation did not happen, as nutrients (in this specific case glutamate) were equally diffused in the colonized area; in contrast, when the biofilm grew, and glutamate was needed for both biomass production and ammonia synthesis, oscillations were generated in order to distribute the nutrient availability between the interior and peripheral population designing the optimal survival strategy[453].

B. subtilis colony patterning had been studying since early 90s. Golding *et al.* studied the sectors forming in growing bacterial colonies on minimal media, including diffusion, food consumption and cell growth rate, as features affecting the branching patterns[240]. They described, through mathematical modelling, branched patterns of *Paenibacillus dendritiformis* and *B. subtilis* growing with low levels of nutrients in solid agar (1.75-2% agar)[240]*. B. subtilis* cells were, in fact, known to produce cells with different morphological features based on nutrient availability, agar concentration and population density[241]*.* However, considered variables, such as nutrients and waste diffusion, cell growth and death, were not sufficient to completely explain the phenomena. The authors pointed out the need to understand additional driving forces for such patterns to form, for instance chemotaxis signalling[240]*.* Similarly*, P. aeruginosa* colonies formed thin branches in a nutrient-poor environment[454]. The authors suggested that colonies with branches represent an adaptation of bacteria growing in adverse conditions (such as a nutrient-poor environment) and resulted from cell-to-cell communication and coordination. Again, three soil bacteria, *Azotobacter vinelandii*, *Bacillus licheniformis* and *Paenibacillus curdlanolyticus,* have been used as a model for studying the interspecies interaction among soil microorganisms. The researchers found that the spatial structure was associated with the competition and interaction within the bacterial community[242], and that disturbing the QS-signalling molecules could alter the bacterial biogeography. More recently, Martinez-Rabert *et al.* proposed a model of three populations, and studied inter-species interactions[181], such as competition, predation, and mutualism, as potential factors affecting the biogeography of bacterial communities. However, they have also demonstrated that the environment, including the availability of nutrients, pH, temperature and humidity, were critical driving forces for the spatial distribution of bacteria[181]*.*

The cited studies evidenced that the spatial organization of bacterial cells is dictated by a complex process which involves communication, coordination, and regulation between the cells in response to environmental factors, such as nutrient availability. Thus, it is reasonable that “bull’s eye” pattern may result from a crosstalk between *S. marcescens* NCTC1377 and *E. coli* NCTC12241 mediated by potential signals released by one strain or another when in contact and influenced by the presence of nutrients on the solid surface.

6.2.2.3 Motility may play a role in the "bull's eye" pattern formation

Although it is possible to conceive that *E. coli* NCTC12241 in the middle ring leads to growth inhibition or decrease competitiveness of *S. marcescens* NCTC1377 in that sector, a motility-mediated space distribution can also be considered. Indeed, it cannot be ignored that after 5 to 7 hours of growth there was a migration of a subset of cells of *S. marcescens* NCTC1377 in the middle ring toward the centre and the outer edge after 5 to 7 hours. Xiong *et al.* reported the formation a flower-like colony pattern derived from the co-culture of *E. coli* and *Acinetobacter baylyi (A. baylyi)*, the latter much more motile compared to *E. coli* strain used in the study when grown as a mono-culture. Surprisingly, the authors found that the co-culture of both strains led to both species growing and spreading rapidly on LB medium, forming structures absent when the strains were growing by themselves, in the same conditions as the co-culture[455]. According to their model, the flower-like pattern resulted from a combination of motility of *A. baylyi*, "hitchhiking" of non-motile *E. coli* with the motile *A. baylyi* , and strong friction from the non-motile strain that adhered to the agar surface[455]. In swarming conditions, *P. mirabilis* colonies were characterized by a pattern composed of several concentric rings, visible by the contrast between high-cell-density zones and less-dense translucent zones, where nutrient availability or waste accumulation were not determinative factors for the concentric pattern to form[456,457]. The differentiation into swarmer cells required specific environmental conditions in *P. mirabilis* , such as surface contact, sufficient cell density and cell-to-cell signalling[100]. It is conceivable that *E. coli* NCTC12241 produces some signals in certain conditions (e.g., certain cell density or presence of glucose) which may lead to a motile behaviour displacing *S. marcescens* from the middle ring of the "bull's eye" pattern colony, a hypothesis supported by the *E. coli* - *S. marcescens* interplay shown in the motility experiments described in Section 5.2. In fact, we observed a robust decreased in swimming motility in *S. marcescens* NCTC1377 when growing in co-culture with the *E. coli* responsible for the pattern, NCTC12241, but not with *E. coli* NCTC10418 (described later).

6.2.2.4 Potential signal-mediating the "bull's eye" pattern formation

A downregulation of prodigiosin in *S. marcescens* was also limited to the presence of *E. coli* NCTC12241, in both liquid and solid growth media, but not mediated by the presence of *E. coli* NCTC10418 (Figure 4.14 and Figure 4.16), further supporting the existence of a strain-specific signal able to change *S. marcescens* phenotypic characteristics. Moreover, our data demonstrated that *S. marcescens* NCTC1377 and *E. coli* NCTC12241 co-culture plated at conditions that lead to the "bull's eye" pattern on TSA, on CLED agar led to a homogenous yellowish colony, due to a lack of prodigiosin (Figure 4.12). CLED is rich in L-cystine, the oxidized derivative of Cys, an intermediary compound, together with Met, in the biochemical pathway leading to the synthesis of AHL and AI-2 derivatives used for QS signalling in Gram-negative bacteria[389,458,459]. As AHLs regulates bacterial communication and coordination, for instance affecting biofilm formation and swimming motility[460]**,** it seems at hand that Met metabolism may trigger the expression of genes involved in bacterial motility, biofilm formation, antibiotic production and resistance, affecting bacterial establishment and survival. Also that, in our case, the addition of Met and Cys together may influence the crosstalk between the two species, *E. coli*

NCTC12241 and *S. marcescens* NCTC1377, leading to a different pattern, possibly based on nutrients availability or signal-dependent shift. In fact, our results showed that a discrete amount of Cys and a micromolar amount of Met led to a pattern characterized by a larger red central spot compared to the "bull's eye" pattern observed on TSA or TSA supplemented with Met or Cys alone (Figure 4.20). A similar pattern was observed in LB supplemented with glucose (Figure 4.12). In contrast, in LB alone, a conventional growth media rich in Met (5.9 mM) and poor in Cys (0.4 mM)[461], we did not observe the "bull's eye" or similar patterns. It is conceivable that, in LB, Met can be used as a precursor for protein synthesis or as a substrate for energy in the lack glucose. However, this would have been compensated by the use of high glucose LB. As there was no effect of this media this theory does likely not apply Moreover, LB, unlike TSB, contains a discrete amount of yeast extract, rich in vitamin B_{12}; hence, it is likely that MetH, B_{12}-dependent, is more active that MetE resulting in an endogenous production of Met. The putative Met deficiency condition in TSA may lead to MetR activation supposedly for Met production, but eventually also resulting in the modulation of other targets, as demonstrated by its pleiotropic role in *S. marcescens* by Pan *et al.*[84].

Based on this assumption, it is possible that *E. coli* NCTC12241 senses the low concentration of Met, and the consequent low production of SAM is insufficient to regulate MetJ (repressor) but enough to synthesis AI-2, signals senses by *S. marcescens* NCTC1377, affecting the crosstalk between the strains space distribution. The AAs succinate and aspartate were also involved in *E. coli* and *S. typhimurium* space distribution on agar plates. Tyson *et al.* reported high-density aggregates arranged in geometrical patterns in *E. coli* or *S. typhimurium* colonies[239]. The pattern was influenced by the bacterial secretion of succinate and aspartate, the latter functioning as a chemo-attractant, hence as a signal rather than a nutrient[239]. Specifically, S. *typhimurium* formed concentric rings resulting from low-density and high-density rings of bacteria in semi-solid medium; at stationary phase, spotted rings replaced the continuous rings. In *E. coli*, the initial swarm ring of cells in semi-solid agar diffused, with bacterial cell density constantly increasing; some non-motile bacterial aggregates appeared as bright spots, defining a pattern characterized by concentric rings with non-motile bacteria-radial-spots[239].

To further investigate the role of Met in the pattern formations we could test the prodigosin formation on agar plates with increasing concentration of Met, hypothesising that the colonies may led to a uniform totally red colony. Also further elucidating Met's role, the determination of colony patterning for our strains in Met-deficient media, i.e., minimal media with AAs supplementations, could also be tested – however it is unlikely that the "bull's eye" would form in minimal media as we have previously shown that a rich medium is a requirement for the pattern to occur.

Considering that the addition of Met or Cys or both did not alter the homogenous colony pattern observed for *S. marcescens* NCTC1377 and *E. coli* NCTC10418, we questioned whether, although both *E. coli* share almost identical genetic sequences (88% identity, determined though pairwise alignment on Geneious Primer®2021.1) there may be differences in the translated sequences, or the 3D structures of MetR and MetE. To visualize and compare the 3D structures of MetR and MetE in both *E. coli* strains, the protein structure predictor AlphaFold was used. The latest version of AlphaFold is a novel machine learning approach that combines physical and biological knowledge about protein

structure; the software finds homologous sequences to the input, then extracts and incorporates information using neural network architectures, and finally predicts the 3D structures incorporating the known evolutionary, physical and geometric constraints of protein structure[395,462]. Our results revealed a minor change in the pocket size which characterizes MetR structure, most likely a pocket for accommodating MetJ which modulates MetR activity (Figure 4.21). Whether this apparent change in the pocket size of MetR from *E. coli* NCTC12241 and MetR from *E. coli* NCTC10418 may be one of the reasons for the phenotypic differences observed in *S. marcescens* NCTC1377, is not conclusive, but, given the minor difference in the pocket size of only 1 nm, is very unlikely. However, we can use this rational to undertake some point directed mutagenesis and conduct structure function studies, using our efficient experimental system. Other point mutations leading to different AA translation between *E. coli* NCTC12241 and *E. coli* NCTC10418 sequences could be further investigated to better describe the phenomenon. Additionally, we can use this approach to investigate further potential proteins which may be in involved in the bacterial interplay and influence the "bull's eye" pattern formation.

Zinc is also required for the catalytic activity of both Met synthase enzymes[463]. It is reasonable to test whether the addition of Zn can further support the Met-mediating phenotypic variation in *S. marcescens* NCTC1377. Even though we have seen that the addition of 250 µM of $ZnCl_2$ on TSA plate did not lead to any substantial variation of the "bull's eye" pattern (data not shown as pictures not available), we cannot exclude the possibility of Zn affecting inter cellular communication between *S. marcescens* and *E. coli*.

6.2.2.5 A mathematical simulation of the "bull's eye" pattern

Our collaborators Čepl Jaroslav[7], Scholtz Vladimir[8] and Jirina Scholtzova[9] have developed a mathematical model of the colony patterning between *E. coli* NCTC12241 and *S. marcescens* NCTC1377 mixed at increasing cell density with a constant ratio 1:1, from 10 to 10^7 cells each for understanding the behaviours of the bacteria in response to environmental factors (nutrients and potential signals) and related changes in fitness of the bacterial cells during growth (Section 4.3). The model showed that the "bull's eye" pattern formation can be attributed to the differential space distribution of *E. coli* and *S. marcescens* as a function of their replication which is influenced by nutrient availability and signalling substances. Thus, the pattern results from a differential growth, with the white cells (*E. coli*) preferentially growing in height, while the red (*S. marcescens*) grew in width, and sensitivity to the signal. However, the simulation represents a simplification of colony growth in real life, and has several limitations. For instance, the diffusion of signal was replaced by an analytic function to streamline the process; also, the simulation needed to be interrupted after several iterations otherwise the outer red edge would have grown infinitely. The formula will need to be optimized introducing, for instance, functions that consider the stationary and death phases to limit the infinite expansion of the colony. Moreover, the signal considered was an absolute by-product of multiple signals, all factored in the same "signal" (metabolites, waste products, nutrients etc); more variables that consider the nature

[7] University of Live Sciences, Prague, Czech Republic
[8] University of Chemistry and Technology, Prague, Czech Republic
[9] Czech Technical University, Prague, Czech Republic

or structure and usage of different signals will need to be considered to validate the actual model or to obtain a more accurate one.

Mathematical models simulating the real processes leading to spatial distribution have been described for several bacterial species. For instance, they have been used for showing *E. coli* colonies growing with a constant rate depending on nutrient and oxygen[238], or for explaining that cell growth, cell death and nutrient consumption[240] , or even cell density[241], were factors affecting branching pattern in *S. subtilis*. Mathematical models may predict real-life colony patterns and help us to understand fundamental aspects that govern the dynamics of microbial life, and eventually harnessed to predict and control bacterial growth or to develop new treatment to combat bacterial infections. Overall, our presented model fits the morphology of the colonies, setting the stage for the design of more complex and advanced simulations.

6.2.3 The "bull's eye" pattern and its structure-function relationship

The macroscopic manifestations of bacterial cells on solid surfaces result, as described, from environmental factors, such as nutrients and signalling substances, but seem also to be coupled to genome-wide changes, some of which may crucially impact bacterial virulence and pathogenesis. For instance, in *P. mirabilis*, swarmer cells, characterized by concentric colony-pattern[456,457], were found to increase the expression of some genes involved in virulence, such as urease, haemolysis and protease genes compare to non-motile cells[100]. *Listeria monocytogenes* colonies had displayed concentric opaque and translucent rings on solid agar in response to light exposure[464]. Importantly, bacterial cells in the opaque rings were more resistant to oxidative stress as demonstrated by the higher survival rate when exposed to H_2O_2 . In our study, we found phenotypic changes in *S. marcescens* NCTC1377 when in contact with *E. coli* NCTC12241, which are (i) the reduction in prodigiosin production, observed in liquid and solid growth media, (ii) inhibition of swimming motility and (iii) a decrease in proteolytic activity. Moreover, other phenotypic and virulent changes associated with *S. marcescens* NCTC1377, i.e., an increase in antibiotic resistance (Section 5.1) and changes in epithelial cells infection ability (Section 5.5), were displayed for this strain when it was co-cultured on solid agar (TSA) with *E. coli* NCTC12241 in condition leading to the formation of a "bull's eye" pattern.

6.2.3.1 *E. coli* NCTC12241 reduces *S. marcescens* NCTC1377 motility and proteolytic activity

Bacteria benefit from proteolysis for degrading protein and using AAs as a source of energy. While *S. marcescens* NCTC1377 in mono-culture displayed a remarkable proteolysis on growth media rich in protein (skim-milk agar), when in contact with *E. coli* NCTC12241 in liquid co-culture proteolytic ability of *S. marcescens* NCTC1377 was significantly reduced (Section 5.2). Samples from the middle ring of "bull's eye" pattern - where we have 10-fold less *S. marcescens* NCTC1377 compared to *E. coli* NCTC12241 - showed a significant inhibition of proteolytic activity compared to samples collected from the outer edge or central spot of the pattern or *S. marcescens* NCTC1377 grown on its own, suggesting the cell density and the ratio *E. col i*: *S. marcescens* were crucial for affecting proteolysis in *S. marcescens*.

The main protease in *Serratia* sp. is the metalloprotease serralysin, encoded by *prtS* gene[465]. Coulthurst and co-authors demonstrated that the protease production in Serratia spp. was regulated by QS-system, together with other virulent processes[74]. They had postulated that the SmaI/SmaR (QS) system in *Serratia* sp. may regulate the expression of a pleiotropic factor (not identified) which in turn would modulate prodigiosin expression, protease production, swarming motility and biofilm formation. Importantly, the whole cascade mechanisms seemed to depend on cell density. Later, it was demonstrated that that global regulator 3',5'-cyclic AMP (cAMP) and its partner cyclic-AMP receptor protein (CRP) can regulate many processes in *Serratia* sp. , including PrtS expression[465], flagella production required for motility, and prodigiosin production[79]. Similarly, EepR response regulator was found to positively modulate the production protease PrtS and prodigiosin in Serratia[80]. EepR was found to be in turn regulated by HexS, the latter involved in virulence and motility in the plant pathogen *Erwinia carotovora*[108]. These findings support the possibility that in our system, an inter-species cellular communication mediated by potential signals occurred between *S. marcescens* NCTC1377 and *E. coli* NCTC12241, impacting metabolic functions and virulence.

Of note, the addition of skimmed milk powder to TSA or LBA resulted in the absence of a "bull's eye" pattern on both the media, supporting our hypothesis that (i) the nutrient content of the solid surface is crucial for the pattern to form, and (ii) in the presence of a higher concentration of Met (as occurring in skim milk), the "bull's eye" pattern is not formed. As explained, Met has been shown to play a role as either signals or precursors of signalling molecules in QS mechanisms[389]. The fact that in high concentration of Met in the growth media (e.g., TSA supplemented with Met or skimmed milk medium) we have observed pattern different from the "bull's eye" manifested on TSA, may indicate that above a certain threshold Met concentrations can influence the crosstalk between the two bacterial species, leading to a different pattern.

As described in Table 1.4 multiple genes known to regulate prodigiosin production, simultaneously affect the bacterial virulence, including motility and proteolytic activity. For instance, the negative regulator of prodigiosin PigX reduces swarming, most likely repressing the genes involved in surfactant production[65,66]. In general, non-motile bacteria display less virulence, mainly associated with reduced invasion and colonization of the host[98]. For instance, the differentiation into swarmer cells in *Proteus mirabilis* was correlated with the expression of some virulence genes encoding urease, haemolysis and proteases[100]. Similarly, *P. aeruginosa* swarmer cells exhibited an increase expression of proteolysis, iron transportation and type III secretion system genes, compared to non-motile mutants. Our results showed that, in the presence of *E. coli* NCTC12241, but not of the *E. coli* NCTC1418, *S. marcescens* NCTC1377 displayed (i) reduced swimming motility (ii) inhibited proteolysis (iii) reduced prodigiosin production. Although the reduced motility and proteolysis suggest a reduction in virulence for *S. marcescens* NCTC1377, this is not necessarily true for prodigiosin. In fact, white mutants of *Serratia* seemed to display a growth advantage[51,76] compared to pigmented ones. Alternatively, a decrease in prodigiosin production had been associated with increased virulence in both *Serratia* sp. ATCC39006 and *S. marcescens* NCTC1377[68,444]. Likewise, our finding that *S. marcescens* NCTC1377 in "bull's eye"

pattern exhibited an increased antibiotic resistance, discussed in the following section, does not support the hypothesis of a decreased virulence in *S. marcescens* NCTC1377.

6.2.3.2 *S. marcescens* NCTC1377 in the "bull's eye" pattern has an increased resistance to the antibiotic levofloxacin

Serratia spp. are among pathogens reported by WHO in the list of global priority pathogens with critical AR[25]. Besides its intrinsic resistance to beta-lactamases as a carrier of the *ampC* genes[116], *S. marcescens* isolates displayed resistance to other classes of antibiotics, for instance fluoroquinolones. The latter interfere with the binding site of DNA gyrase or topoisomerase IV, involved in bacterial DNA topology, consequently interrupting the DNA synthesis[130,132,133]. DNA damage caused by the exposure to the antibiotics lead to the activation of the SOS response system, regulated by LexA and RecA proteins [136]. LexA, when active, binds to the promoter region of the SOS system, inhibiting its activation. In the presence of DNA damage, *recA* gene is expressed with consequent RecA protein translation, and LexA is repressed, hence promoting SOS response pathways and activation of DNA repair machinery. Fluoroquinolone resistance has been associated with different mechanisms: (i) mutations in genes encoding for DNA gyrase or topoisomerase IV; (ii) an increased expression of MRD efflux pumps; and (iii) *qnr* -mediated resistance, peptides known to confer fluoroquinolone resistance in bacteria binding to DNA gyrase and topoisomerase IV, are expressed and hence masking the binding site from the DNA[144,145]. Genes encoding for *qnr* were initially identified in bacterial plasmids[143,146,147]. Subsequent studies have demonstrated the existence of *qnr* genes on bacterial chromosome as well[148]. A *qnr* sequence has also been identified in *S. marcescens*, sharing 80% AAs sequence identity with the *qnr* sequence in *E. coli* plasmid[149]. *Qnr* expression is regulated through the SOS response in a LexA/RecA-dependent manner. In fact, *qnr* genes are located upstream of the LexA binding site, a well conserved sequence among enterobacteria[150–153], including our strain *Serratia marcescens* NCTC1377. Moreover, the LexA binding site is not limited to regions flanking *qnr* genes, but spread over the genome: in *E. coli* more than 30 genes had been found to be regulated by LexA[154], suggesting a pleiotropic role for this regulator. Therefore, one would expect that the exposure to the antibiotic may first lead to RecA activation, then consequent inactivation of LexA, and finally the expression of the *qnr* gene located upstream of the LexA binding site. Encoded Qnr proteins may then induce LFX resistance interacting with antibiotic targets.

The increased resistance to LFX displayed in *S. marcescens* NCTC1377 cells from the outer ring and central spot of the "bull's eye" pattern is unlikely to be associated with genetic mutations, as we have showed that the resistance is not retained from one generation to another (Section 5.1). Instead, it is most likely a physiological resistance that only occurs when *S. marcescens* NCTC1377 is in contact with *E. coli* NCTC12241 in conditions that allow the "bull's eye" pattern to form. In our *S. marcescens* strain NCTC1377 we have identified the CTGTATAAATAAACAG sequence, identical to the LexA box identified by Briales at al. in *S. marcescens* Db11, upstream of the *qnr* family pentapeptide repeat protein gene[144]. It is feasible that in conditions leading to the "bull's eye" pattern formation, *S. marcescens* NCTC1377 cells acquire an increased resistance to LFX due to *qnr* expression regulated through the SOS response in a LexA/RecA-dependent manner.

6.2.3.3 Into the mechanistic understanding of the increased levofloxacin resistance in *S. marcescens*: some hypothesis

What triggers the DNA damage and consequently increases *qnr* expression in these circumstances? We postulated that reactive oxygen species, generated by the exposure to sublethal concentrations of H_2O_2, can induce a stress response which may lead to *qnr* expression in *S. marcescens*. Hence, we exposed *S. marcescens* NCTC1377 cells to non-toxic concentrations of H_2O_2 and tested the resistance of the treated cells to LFX. Our results clearly showed that when *S. marcescens* was exposed to H_2O_2 prior the antibiotic, it exhibited an increase in resistance to LFX compared to the control (not exposed to H_2O_2) (Figure 5.8). It is speculative to hypothesise that *E. coli*-mediating ROS production may also elicit the observed resistance to LFX in *S. marcescens* in conditions leading to the "bull's eye" pattern formation. However, as there is no evidence that *E. coli* induces oxidative stress in mixed bacterial cultures, our hypothesis remains speculative and tenuous. ROS production needs to be measured. Another hypothesis (also highly speculative) could be that *S. marcescens* produces ROS endogenously during aerobic respiration[466] and the co-culture with *E. coli* may render *S. marcescens* less able to deal with ROS, resulting in in an up-regulation of the SOS response and subsequent *qnr* gene expression.

Also, it is possible that *E. coli* may induce a metabolic modulation in *S. marcescens* which in turn lead to an increase resistance to LFX. In support of this, the close relationship between bacterial metabolism and antibiotic efficacy has been extensively investigated in the last few decades, as summarised in the review of Stokes *et al.*[467]. Although it is clear that antibiotic exposure affects the bacterial metabolic state, it is also true that their metabolic state influences bacterial efficacy[467]. For instance, it is known that bacterial cells in stationary phase or embedded in biofilm can be more resistant to antibiotics. The intracellular ATP level has been associated with antibiotic tolerance in *E. coli* and *S. aureus*, specifically, it has been demonstrated that a drop in the ATP level can lead to an increase in ciprofloxacin tolerance[468], most likely due to the accumulation of insoluble endogenous proteins in stationary phase[469]. Also, rates of bacterial cellular respiration have been found to impact bactericidal efficacy in *E. coli.* Lobritz *et al.* have demonstrated that the inhibition of cellular respiration increased norfloxacin resistance, while acceleration of basal respiration potentiated the antibiotic effect[470]**.** In biofilm conditions, some bacterial cells are characterized by reduced metabolic activity[471], dormant variants or *persister* cells, which are more resistant to drugs in *E. coli* [173] or *P. aeruginosa*[174]. It has been showed that, while a metabolically active subpopulation in *P. aeruginosa* biofilm was able to develop increased tolerance to colistin, the same subpopulation was more sensitive to fluoroquinolones. On the other hand, fluoroquinolones treatment was not effective against the subpopulation with low metabolic activity[472]**.**

Other stressors which can increase stress conditions in *S. marcescens*, such as a nitric oxide generator, can be also tested to evaluate that the increased antibiotic resistance in the presence of *E. coli* NCTC12241 is mediated via the activation of the SOS response and downstream pathways. Importantly, ROS concentrations will need to be measure in bacterial populations prior to and during co-culture and thus pattern formation to confirm that ROS may be the specific agents leading to the increased resistance.

Phenotypic or physiological resistance mechanisms are poorly described compared to genetic mechanisms. It had been demonstrated that bacteria growing as a biofilm rather than as planktonic cells carry increased resistance to antibiotics[162–165]. In *E. coli*, the exposure to a low concentration of ciprofloxacin can induce the differentiation into cells which are more resistant to the antibiotic itself, through the activation of the SOS response[173]. The expression and activation of recA had been also associated with other bacterial behaviours, such as motility. In *E. coli* and *S. enterica*[177–179], the lack of recA led to a reduction in swimming and swarming ability. Motile cells of *P. aeruginosa, E. coli, S. marcescens* and *B. subtilis* displayed an increased resistance to fluoroquinolones and beta-lactams[94,101]. In *S. aureus*, antibiotic resistance had been associated with expression of haemolysin genes[473]. Therefore, it seems that an association between phenotypic changes, for instance alteration in motility, and antibiotic resistance in bacteria of clinical significance is emerging. The observed increased resistance to LFX in *S. marcescens* NCTC1377 from the "bull's eye" pattern, may represent an example of a phenotypic change that alludes to a genome-associated shift, induced by the presence of signal produced exclusively in conditions that led the pattern to form and that can affect multiple features (physiological and virulent) in *S. marcescens*.

Ampicillin and vancomycin are other two antibiotics regularly used to treat common bacterial infections of clinical significance. Ampicillin is a beta-lactam which acts by interfering with the peptidoglycan synthesis and binding to penicillin-binding proteins. We know that *S. marcescens* and other Gram-negative bacteria are naturally resistant to ampicillin and other beta-lactam antibiotics as carrier of the *ampC* genes, which encodes for a beta-lactamase, able to hydrolyse and inactivate the antibiotics[116]. In contrast, vancomycin is typically ineffective against Gram-negative bacteria due to its inability to penetrate the outer lipid membrane that characterizes Gram-negative species. It has been known since the 1970s that the outer membrane of Gram-negative bacteria is subject to change in composition in response to the composition of the growth medium and growth temperature[474,475]. Recently, it had been demonstrated that *E. coli* growing at low temperature became susceptible to vancomycin, an effect mediated by a change in the lipid composition of the outer membrane[476]. Given the observed phenotypic changes in *S. marcescens* in co-culture condition, it was reasonable to consider (i) a possible change at a genetic or transcriptomic level which may render *S. marcescens* susceptible to ampicillin, and/or (ii) possible alterations in the bacterial outer membrane composition which could affect vancomycin effectivity. However, our results showed that *S. marcescens* or *E. coli* from the "bull's eye" pattern was as equally resistant to ampicillin or vancomycin as the bacterial strains growing in monoculture, suggesting the co-culture and resulting pattern did not induce phenotypic or genetic changes connected to ampicillin or vancomycin effectivity (Figure 5.6).

In the light of our finding about the increased resistance to LFX in the conditions which led to the formation of the "bull's eye" pattern, it would be appropriate to test further antibiotics to provide supporting evidence that the resistance could be *qnr*-mediated, including other fluoroquinolones and other antibiotics commonly used to treat Gram-negative and specifically *Serratia* spp. infections (e.g., kanamycin, gentamicin, or chloramphenicol[477].

6.2.3.4 Co-culture of mammalian cells and bacteria for investigating host-pathogen interactions

Virulence factors in bacteria are essential for them to invade the host, cause the disease and evade the host immune defences. Considered the phenotypic changes we have observed in *S. marcescens* in the "bull's eye" pattern colony compared to *S. marcescens* growing on its own (i.e. increased LFX resistance, decreased motility and proteolysis), it was conceivable to test the ability of this strain to infect mammalian cells when in co-culture with *E. coli* in condition leading to the pattern formation. We have found a remarkable difference between *S. marcescens* NCTC1377 from the "bull's eye" pattern and *S. marcescens* growing in monoculture. Results demonstrated that *S. marcescens* NCTC1377 from the outer edge of the "bull's eye" pattern adhered much less to mammalian cells (MDCK), compared to *S. marcescens* NCTC1377 growing in monoculture (Section 5.5, Figure 5.19). It is reasonable to propose that the inhibition of motility (swimming) in *S. marcescens* when in co-culture with *E. coli* NCTC12241 may be connected with the reduced capacity to adhere to the mammalian cells. In fact Josenhans *et al.* also demonstrated that non-motile mutants of *S. typhimurium, S. enteridis, P. aeruginosa* and other Gram-negative display a reduced ability to invade and colonize the host[98]. In pathogenic *E. coli*, a reduction in motility and decreased adhesion to epithelial cells was related to a reduction in AI-2 molecules, hence showing the crucial role of QS-signalling in the modulation of bacterial virulence[214]. Considering that *E. coli* NCTC12241 formed a very poor biofilm on plastic surfaces compared to *S. marcescens* NCTC1377 (Figure 5.11), one would expect *E. coli* to not adhere much on MDCK. However, our results displayed that *E. coli* cells collected from the outer edge of the "bull's eye" pattern were able to adhere more than the control (*E. coli* growing alone), suggesting that phenotypic changes were also affecting *E. coli,* even if other differences in any of the previously tested behaviours were observed. *Serratia*'s proteolytic activity is crucial for the bacteria to invade human tissues[104–106]. *S. marcescens* protease, serralysin, has been demonstrated to facilitate invasion into mammalian cells and to cause keratitis in murine models [478]. Thus, given the observed reduction in proteolytic activity of *S. marcescens* when in contact with *E. coli* NCTC12241, it is conceivable that this may limit the ability of *S. marcescens* to infect human cells.

Although phagocytosis in epithelial cells is typically lower than phagocytosis exerted by macrophages and neutrophils, yet the cells can utilise this mechanisms to internalise and kill bacteria[479,480]. Usually, bacterial cells are transported intracellularly after internalisation to the lysosome, where bacterial killing takes place. However, internalization may also represent a strategy for bacterial cells to safely persist and replicate within the mammalian cells[481,482]. In fact, internalized bacterial cells, if not killed, undergo adaptive changes in order to survive; for instance, *S. aureus* invading bronchial epithelial cells and internalized, have been found to differentiate into two sub-populations, a replicating and a dormant one, with the latter exhibiting increased virulence[481]. In support of this, it had been demonstrated that bacteria internalized by epithelial cells constitute an intracellular population more resistant to antibiotic compared to not internalized-cells, indicating that the internalized bacteria may be a reservoir of a more virulent bacterial population[483].

In the light of this, in our study we treated the MDCK-bacteria co-culture with gentamicin in order to kill bacterial cells that were not internalized by the mammalian cells and consequently evaluated the survival rate of potential internalized bacterial cells. Results showed only a few of the *S. marcescens* NCTC1377 cells from the outer edge survived after gentamicin treatment, much less than *S. marcescens* NCTC1377 control (monoculture), (Figure 5.20), hence suggesting that the bacteria from the co-culture were not internalized readily as the control cells.

Considered the reduced ability to adhere and to be internalized by the mammalian cells, one would speculate a reduction in bacterial virulence in *S. marcescens* NCTC1377 from the "bull's eye" pattern compared to *S. marcescens* alone, consistent with the reduced motility or proteolysis previously observed. To further assist this hypothesis, the ability to get killed need to also to be tested. It would also be interesting to know which internalisation pathways are utilised by the bacteria and whether they are different, depending on the culture method, working with specific endocytosis / phagocytosis inhibitors as well as life microscopy would elucidate the molecular mechanism of adherence, internalisation and killing.

Nonetheless, regardless of the virulence and pathogenic outcomes, i.e., one being more or less virulent, the critical aspect is that we demonstrated the existence of a morphogenetic variation, macroscopically manifested as the appearance of a pattern, which may also be accompanied by changes in gene expression in two bacterial strains, *E. coli* NCTC1221 and *S. marcescens* NCTC1377, as suggested by changes in antibiotic resistance and other virulence in one or the other strains; molecular and genetics aspects will need to be investigated.

6.3 Conclusion

6.3.1 Summary of our main findings and future implications

The dynamics of microbial communities relies on multi-species interaction, communication and coordination in response to the surrounding environment. Using models of mixed bacterial species on agar plates, we have addressed fundamental questions regarding the selection, dynamics and spatial competition of bacteria, which may have, in turn, implications for the health of the host. The identification of species-specific 16s rRNA primer-pairs for a number of bacterial species of clinical significance may represent an innovative, time and cost-efficient tool for bacterial strain detection in microbial communities. We have obtained evidence from *in vitro* co-culture competition experiments that the micronutrient Zn, at micromolar concentrations, led to a differential physiological or competitive advantage to *P. aeruginosa* over *S. marcescens*, setting the stage towards promising advances regarding the regulatory role of Zn on bacterial physiology and virulence. Also, the probiotic *Lactobacillus plantarum* inhibited the growth potential pathogens, *E. coli* and *P. aeruginosa* on agar plates, preliminary findings need to be confirmed with molecular analysis. We have discovered that *S. marcescens* and *E. coli* differentially distribute the space as function of cell density, nutrients and a potential signal which seems to strain-specific, a novel phenomenon in microbial ecology. The resulting bacterial pattern may accompany genome-wide changes in genes involved in physiological and virulent factors in *S. marcescens*, hence representing the foundation for understanding bacterial species

interaction and identifying structure/function relationships in bacterial pathogens. The most critical value is the discovery and characterization of an innovative phenomenon connected to antimicrobial resistance, a global human threat and a strategic priority within international health systems and governments.

6.3.2 Limitations of the study and future work

While the research study described above provides valuable insights into the dynamics of a bacterial community, it also has some limitations that should be considered:

1. Simplified model: the co-culture experiments involved a limited number of bacterial species and do not account for the diversity and complexity of the human gut microbiota; the interactions observed may not accurately represent the dynamics in a bacterial community of trillions of species. We will consider to incorporate a broader range of commensal and pathogen bacteria and to investigate how these interactions relate to the development of diseases and the efficacy of interventions, such as antibiotic treatments or probiotics supplementation. In addition, other factors besides the micronutrient Zn may play equally or more significant roles in bacterial dynamics. The use of advanced bioinformatics and omics approaches (metagenomics, transcriptomics, proteomics) will be considered to gain a deeper understanding of microbial communities, their functional potential, and their responses to external factors.
2. Lack of comprehensive mechanistic insights into the observed phenomena: we acknowledge that the reasons behind the differential distribution patterns and their impact on health are not fully clarified. Further experiments employing molecular biology and genetic techniques will need to be conducted to elucidate the underlying mechanisms responsible for the observed microbial interactions, such as the potential cidal effect of *P. aeruginosa* on *S. marcescens* or the mechanistic understanding of the "bull's eye" pattern.
3. *In vitro* setting: the study primarily relies on *in vitro* co-culture experiments, which may not fully replicate the complex environment of the human gut; findings from those experiments may not directly translate to real-life interactions within the human body.
4. Applicability to animal/human models: while the study explores *in vitro* microbial interactions and their potential implications, it lacks evidence of the applicability of the findings to animals and human models. Gut microbiota can differ significantly between species, and what works in one *in vitro* model may not apply directly to other *in vivo* models. Conducting *in vivo* experiments using animal models to investigate how the observed microbial interactions and patterns translate to a more complex living system will help to bridge the gap between *in vitro* observations and real-life gut microbiota dynamics. We aim to explore the potential clinical applications of the findings, such as developing targeted interventions for infectious diseases and antibiotic resistance in clinical settings.

Addressing these limitations and conducting further research can enhance the study's scientific validity, applicability to human health, and potential contributions to our understanding of the gut microbiota's role in health and disease.

References

1. Martinson, J. N. V. & Walk, S. T. *Escherichia coli* residency in the gut of healthy human adults. *EcoSal Plus* **9**, 10.1128/ecosalplus.ESP-0003–2020 (2020).
2. Rossi, E. *et al.* "It's a gut feeling" – *Escherichia coli* biofilm formation in the gastrointestinal tract environment. *Critical Reviews in Microbiology* **44**, 1–30 (2018).
3. Hancock, V., Dahl, M. & Klemm, P. Probiotic *Escherichia coli* strain Nissle 1917 outcompetes intestinal pathogens during biofilm formation. *J Med Microbiol* **59**, 392–399 (2010).
4. *E. coli* (*Escherichia coli*) | *E. coli* | CDC. https://www.cdc.gov/ecoli/index.html (2021).
5. Abrantes, M. C., Lopes, M. de F. & Kok, J. Impact of manganese, copper and zinc ions on the transcriptome of the nosocomial pathogen *Enterococcus* faecalis V583. *PLoS One* **6**, e26519 (2011).
6. Kaur, C. P., Vadivelu, J. & Chandramathi, S. Impact of *Klebsiella pneumoniae* in lower gastrointestinal tract diseases. *J Dig Dis* **19**, 262–271 (2018).
7. *Enterococci: From Commensals to Leading Causes of Drug Resistant Infection*. (Massachusetts Eye and Ear Infirmary, 2014).
8. Beganovic, M. *et al.* A Review of Combination Antimicrobial Therapy for *Enterococcus faecalis* Bloodstream Infections and Infective Endocarditis. *Clinical Infectious Diseases* **67**, 303–309 (2018).
9. Couvigny, B. *et al.* Commensal *Streptococcus salivarius* Modulates PPARγ Transcriptional Activity in Human Intestinal Epithelial Cells. *PLoS One* **10**, e0125371 (2015).
10. Mujagic, Z. *et al.* The effects of *Lactobacillus plantarum* on small intestinal barrier function and mucosal gene transcription; a randomized double-blind placebo controlled trial. *Sci Rep* **7**, 40128 (2017).
11. Global Health Estimates: Life expectancy and leading causes of death and disability. https://www.who.int/data/gho/data/themes/mortality-and-global-health-estimates.
12. Bunn, S. UK Trends in Infectious Disease. (2017).
13. Davies, S. Annual Report of the Chief Medical Officer Volume Two, 2011 Infections and the rise of antimicrobial resistance. 154 (2011).
14. Global health estimates: Leading causes of death. https://www.who.int/data/gho/data/themes/mortality-and-global-health-estimates/ghe-leading-causes-of-death.
15. Gray, A. & Sharara, F. Global and regional sepsis and infectious syndrome mortality in 2019: a systematic analysis. *The Lancet Global Health* **10**, S2 (2022).
16. Arefian, H. *et al.* Estimating extra length of stay due to healthcare-associated infections before and after implementation of a hospital-wide infection control program. *PLOS ONE* **14**, e0217159 (2019).
17. Troeger, C. *et al.* Estimates of the global, regional, and national morbidity, mortality, and aetiologies of lower respiratory infections in 195 countries, 1990–2016: a systematic analysis for the Global Burden of Disease Study 2016. *The Lancet Infectious Diseases* **18**, 1191–1210 (2018).
18. Giusti, M. & Cerutti, E. Antibiotic stewardship programs and the internist's role. *Ital. J. Med.* **10**, 329–338 (2016).
19. Surveillance of antimicrobial resistance in Europe 2017. *European Centre for Disease Prevention and Control* https://www.ecdc.europa.eu/en/publications-data/surveillance-antimicrobial-resistance-europe-2017 (2018).
20. Ranghar, S., Sirohi, P., Verma, P. & Agarwal, V. Nanoparticle-based drug delivery systems: promising approaches against infections. *Brazilian Archives of Biology and Technology* **57**, 209–222 (2014).
21. Vissichelli, N. C. & Stevens, M. P. Antibiotics in the Pipeline for Treatment of Infections due to Gram-Negative Organisms. *Curr Treat Options Infect Dis* **11**, 115–144 (2019).

22. Cassini, A. *et al.* Attributable deaths and disability-adjusted life-years caused by infections with antibiotic-resistant bacteria in the EU and the European Economic Area in 2015: a population-level modelling analysis. *The Lancet Infectious Diseases* **19**, 56–66 (2019).
23. Zhen, X., Lundborg, C. S., Sun, X., Hu, X. & Dong, H. Economic burden of antibiotic resistance in ESKAPE organisms: a systematic review. *Antimicrob Resist Infect Control* **8**, 137 (2019).
24. AMR Review Paper - Tackling a crisis for the health and wealth of nations_1.pdf.
25. Asokan, G. V., Ramadhan, T., Ahmed, E. & Sanad, H. WHO Global Priority Pathogens List: A Bibliometric Analysis of Medline-PubMed for Knowledge Mobilization to Infection Prevention and Control Practices in Bahrain. *Oman Med J* **34**, 184–193 (2019).
26. Suay-García, B. & Pérez-Gracia, M. T. Present and Future of Carbapenem-resistant Enterobacteriaceae (CRE) Infections. *Antibiotics (Basel)* **8**, 122 (2019).
27. Roca, I. *et al.* The global threat of antimicrobial resistance: science for intervention. *New Microbes and New Infections* **6**, 22–29 (2015).
28. Grimont, P. A. D. & Grimont, F. The Genus *Serratia*. *Annual Review of Microbiology* **32**, 221–248 (1978).
29. Williams, D. J. *et al.* The genus *Serratia* revisited by genomics. *Nat Commun* **13**, 5195 (2022).
30. Williamson, N. R., Fineran, P. C., Leeper, F. J. & Salmond, G. P. C. The biosynthesis and regulation of bacterial prodiginines. *Nat Rev Microbiol* **4**, 887–899 (2006).
31. Yu, V. L. *Serratia marcescens*: historical perspective and clinical review. *N Engl J Med* **300**, 887–893 (1979).
32. Hasan, M. F., Islam, M. A. & Sikdar, B. First report of *Serratia marcescens* associated with black rot of Citrus sinensis fruit , and evaluation of its biological control measures in Bangladesh. *F1000Res* **9**, 1371 (2022).
33. Kozlova, E. V. *et al.* Microbial interactions in the mosquito gut determine *Serratia* colonization and blood-feeding propensity. *ISME J* **15**, 93–108 (2021).
34. Khayat, M. T. *et al.* Diminishing the Pathogenesis of the Food-Borne Pathogen *Serratia marcescens* by Low Doses of Sodium Citrate. *Biology (Basel)* **12**, 504 (2023).
35. Estimating the burden of foodborne diseases. https://www.who.int/activities/estimating-the-burden-of-foodborne-diseases.
36. Nutrition, C. for F. S. and A. Foodborne Pathogens. *FDA* https://www.fda.gov/food/outbreaks-foodborne-illness/foodborne-pathogens (2023).
37. CDC. Foodborne Illnesses and Germs. *Centers for Disease Control and Prevention* https://www.cdc.gov/foodsafety/foodborne-germs.html (2022).
38. Ochieng, J. B. *et al. Serratia marcescens* is injurious to intestinal epithelial cells. *Gut Microbes* **5**, 729–736 (2014).
39. Mahlen, S. D. *Serratia* Infections: from Military Experiments to Current Practice. *Clin Microbiol Rev* **24**, 755–791 (2011).
40. Bullock, D. W. *et al.* Outbreaks of hospital infection in southwest England caused by gentamicin-resistant *Serratia marcescens*. *J Hosp Infect* **3**, 263–273 (1982).
41. Yu, W. L., Lin, C. W. & Wang, D. Y. *Serratia marcescens* bacteremia: clinical features and antimicrobial susceptibilities of the isolates. *J Microbiol Immunol Infect* **31**, 171–179 (1998).
42. Haddy, R. I. *et al.* Nosocomial infection in the community hospital: severe infection due to *Serratia* species. *J Fam Pract* **42**, 273–277 (1996).
43. Kim, S. B. *et al.* Risk Factors for Mortality in Patients with *Serratia marcescens* Bacteremia. *Yonsei Med J* **56**, 348–354 (2015).
44. Luzzaro, F. *et al.* Repeated epidemics caused by extended-spectrum beta-lactamase-producing *Serratia marcescens* strains. *Eur J Clin Microbiol Infect Dis* **17**, 629–636 (1998).
45. Yu, V. L. *Serratia marcescens*: historical perspective and clinical review. *N Engl J Med* **300**, 887–893 (1979).

46. Sandner-Miranda, L., Vinuesa, P., Cravioto, A. & Morales-Espinosa, R. The Genomic Basis of Intrinsic and Acquired Antibiotic Resistance in the Genus *Serratia*. *Frontiers in Microbiology* **9**, (2018).
47. Song, E., Mejías, A. & Antonara, S. 145 - *Serratia* Species. in *Principles and Practice of Pediatric Infectious Diseases (Fifth Edition)* (eds. Long, S. S., Prober, C. G. & Fischer, M.) 835-837.e1 (Elsevier, 2018). doi:10.1016/B978-0-323-40181-4.00145-6.
48. Moradigaravand, D., Boinett, C. J., Martin, V., Peacock, S. J. & Parkhill, J. Recent independent emergence of multiple multidrug-resistant *Serratia marcescens* clones within the United Kingdom and Ireland. *Genome Res* **26**, 1101–1109 (2016).
49. Arivizhivendhan, K. V. *et al.* Antioxidant and antimicrobial activity of bioactive prodigiosin produces from *Serratia marcescens* using agricultural waste as a substrate. *J Food Sci Technol* **55**, 2661–2670 (2018).
50. Fineran, P. C., Slater, H., Everson, L., Hughes, K. & Salmond, G. P. C. Biosynthesis of tripyrrole and β-lactam secondary metabolites in *Serratia*: integration of quorum sensing with multiple new regulatory components in the control of prodigiosin and carbapenem antibiotic production. *Molecular Microbiology* **56**, 1495–1517 (2005).
51. Xiang, T. *et al.* Transcriptomic Analysis Reveals Competitive Growth Advantage of Non-pigmented *Serratia marcescens* Mutants. *Front Microbiol* **12**, 793202 (2021).
52. Danevčič, T., Borić Vezjak, M., Zorec, M. & Stopar, D. Prodigiosin - A Multifaceted *Escherichia coli* Antimicrobial Agent. *PLoS One* **11**, e0162412 (2016).
53. Kimyon, Ö. *et al. Serratia* Secondary Metabolite Prodigiosin Inhibits *Pseudomonas aeruginosa* Biofilm Development by Producing Reactive Oxygen Species that Damage Biological Molecules. *Front. Microbiol.* **7**, (2016).
54. Yip, C.-H., Mahalingam, S., Wan, K.-L. & Nathan, S. Prodigiosin inhibits bacterial growth and virulence factors as a potential physiological response to interspecies competition. *PLoS One* **16**, e0253445 (2021).
55. Herráez, R., Mur, A., Merlos, A., Viñas, M. & Vinuesa, T. Using prodigiosin against some gram-positive and gram-negative bacteria and Trypanosoma cruzi. *J Venom Anim Toxins Incl Trop Dis* **25**, e20190001 (2019).
56. Kurz, C. L. *et al.* Virulence factors of the human opportunistic pathogen *Serratia marcescens* identified by in vivo screening. *The EMBO Journal* **22**, 1451–1460 (2003).
57. Liu, Y. *et al.* Prodigiosin Inhibits Proliferation, Migration, and Invasion of Nasopharyngeal Cancer Cells. *CPB* **48**, 1556–1562 (2018).
58. Montaner, B. *et al.* Prodigiosin from the supernatant of *Serratia marcescens* induces apoptosis in haematopoietic cancer cell lines. *British Journal of Pharmacology* **131**, 585–593 (2000).
59. Ji, S. *et al.* Prodigiosin induces apoptosis and inhibits autophagy via the extracellular signal-regulated kinase pathway in K562 cells. *Toxicology in Vitro* **60**, 107–115 (2019).
60. Hu, D. X., Withall, D. M., Challis, G. L. & Thomson, R. J. Structure, Chemical Synthesis, and Biosynthesis of Prodiginine Natural Products. *Chem Rev* **116**, 7818–7853 (2016).
61. Jia, X. *et al.* Identification of Essential Genes Associated With Prodigiosin Production in *Serratia marcescens* FZSF02. *Front Microbiol* **12**, 705853 (2021).
62. Pan, X. *et al.* LysR-Type Transcriptional Regulator MetR Controls Prodigiosin Production, Methionine Biosynthesis, Cell Motility, H2O2 Tolerance, Heat Tolerance, and Exopolysaccharide Synthesis in *Serratia marcescens*. *Appl Environ Microbiol* **86**, e02241-19 (2020).
63. Gristwood, T., McNeil, M. B., Clulow, J. S., Salmond, G. P. C. & Fineran, P. C. PigS and PigP Regulate Prodigiosin Biosynthesis in *Serratia* via Differential Control of Divergent Operons, Which Include Predicted Transporters of Sulfur-Containing Molecules. *J Bacteriol* **193**, 1076–1085 (2011).

64. Shanks, R. M. Q. *et al.* A *Serratia marcescens* PigP Homolog Controls Prodigiosin Biosynthesis, Swarming Motility and Hemolysis and Is Regulated by cAMP-CRP and HexS. *PLOS ONE* **8**, e57634 (2013).
65. Fineran, P. C., Williamson, N. R., Lilley, K. S. & Salmond, G. P. C. Virulence and Prodigiosin Antibiotic Biosynthesis in *Serratia* Are Regulated Pleiotropically by the GGDEF/EAL Domain Protein, PigX. *Journal of Bacteriology* (2007) doi:10.1128/JB.00671-07.
66. Williamson, N. R., Fineran, P. C., Ogawa, W., Woodley, L. R. & Salmond, G. P. C. Integrated regulation involving quorum sensing, a two-component system, a GGDEF/EAL domain protein and a post-transcriptional regulator controls swarming and RhlA-dependent surfactant biosynthesis in *Serratia*. *Environ Microbiol* **10**, 1202–1217 (2008).
67. Thomson, N. R., Crow, M. A., McGowan, S. J., Cox, A. & Salmond, G. P. C. Biosynthesis of carbapenem antibiotic and prodigiosin pigment in *Serratia* is under quorum sensing control. *Molecular Microbiology* **36**, 539–556 (2000).
68. Coulthurst, S. J., Kurz, C. L. & Salmond, G. P. C. luxS mutants of *Serratia* defective in autoinducer-2-dependent 'quorum sensing' show strain-dependent impacts on virulence and production of carbapenem and prodigiosin. *Microbiology* **150**, 1901–1910 (2004).
69. Williamson, N. R., Simonsen, H. T., Harris, A. K. P., Leeper, F. J. & Salmond, G. P. C. Disruption of the copper efflux pump (CopA) of *Serratia marcescens* ATCC 274 pleiotropically affects copper sensitivity and production of the tripyrrole secondary metabolite, prodigiosin. *J Ind Microbiol Biotechnol* **33**, 151–158 (2006).
70. Gristwood, T., Fineran, P. C., Everson, L., Williamson, N. R. & Salmond, G. P. The PhoBR two-component system regulates antibiotic biosynthesis in *Serratia* in response to phosphate. *BMC Microbiology* **9**, 112 (2009).
71. Williams, R. P., Gott, C. L., Qadri, S. M. H. & Scott, R. H. Influence of Temperature of Incubation and Type of Growth Medium on Pigmentation in *Serratia marcescens*. *J Bacteriol* **106**, 438–443 (1971).
72. Petersen, L. M., LaCourse, K., Schöner, T. A., Bode, H. & Tisa, L. S. Inactivation of the Major Hemolysin Gene Influences Expression of the Nonribosomal Peptide Synthetase Gene swrA in the Insect Pathogen *Serratia* sp. Strain SCBI. *Journal of Bacteriology* **199**, e00333-17 (2017).
73. Poole, K. & Braun, V. Influence of growth temperature and lipopolysaccharide on hemolytic activity of *Serratia marcescens*. *J Bacteriol* **170**, 5146–5152 (1988).
74. Coulthurst, S. J., Williamson, N. R., Harris, A. K. P., Spring, D. R. & Salmond, G. P. C. Metabolic and regulatory engineering of *Serratia marcescens*: mimicking phage-mediated horizontal acquisition of antibiotic biosynthesis and quorum-sensing capacities. *Microbiology (Reading)* **152**, 1899–1911 (2006).
75. Finkel, S. E. Long-term survival during stationary phase: evolution and the GASP phenotype. *Nat Rev Microbiol* **4**, 113–120 (2006).
76. Qin, H. *et al.* RpoS is a pleiotropic regulator of motility, biofilm formation, exoenzymes, siderophore and prodigiosin production, and trade-off during prolonged stationary phase in *Serratia marcescens*. *PLOS ONE* **15**, e0232549 (2020).
77. Carbonell, G. V. *et al.* Clinical relevance and virulence factors of pigmented *Serratia marcescens*. *FEMS Immunology & Medical Microbiology* **28**, 143–149 (2000).
78. Haddix, P. L. & Shanks, R. M. Q. Prodigiosin pigment of *Serratia marcescens* is associated with increased biomass production. *Arch Microbiol* **200**, 989–999 (2018).
79. Stella, N. A. & Shanks, R. M. Q. Cyclic-AMP inhibition of fimbriae and prodigiosin production by *Serratia marcescens* is strain-dependent. *Arch Microbiol* **196**, 323–330 (2014).
80. Shanks, R. M. Q. *et al.* Suppressor analysis of *eepR* mutant defects reveals coordinate regulation of secondary metabolites and serralysin biosynthesis by EepR and HexS. *Microbiology (Reading)* **163**, 280–288 (2017).

81. Quintero-Yanes, A., Lee, C. M., Monson, R. & Salmond, G. The FloR master regulator controls flotation, virulence and antibiotic production in *Serratia* sp. ATCC 39006. *Environmental Microbiology* **22**, 2921–2938 (2020).
82. Sun, D. *et al.* Fnr Negatively Regulates Prodigiosin Synthesis in *Serratia* sp. ATCC 39006 During Aerobic Fermentation. *Frontiers in Microbiology* **12**, (2021).
83. Stella, N. A. *et al.* An IgaA/UmoB Family Protein from *Serratia marcescens* Regulates Motility, Capsular Polysaccharide Biosynthesis, and Secondary Metabolite Production. *Applied and Environmental Microbiology* **84**, e02575-17 (2018).
84. Pan, X. *et al.* LysR-Type Transcriptional Regulator MetR Controls Prodigiosin Production, Methionine Biosynthesis, Cell Motility, H2O2 Tolerance, Heat Tolerance, and Exopolysaccharide Synthesis in *Serratia marcescens*. *Applied and Environmental Microbiology* **86**, e02241-19 (2020).
85. Lee, C. M., Monson, R. E., Adams, R. M. & Salmond, G. P. C. The LacI–Family Transcription Factor, RbsR, Is a Pleiotropic Regulator of Motility, Virulence, Siderophore and Antibiotic Production, Gas Vesicle Morphogenesis and Flotation in *Serratia*. *Frontiers in Microbiology* **8**, (2017).
86. Horng, Y.-T., Chang, K.-C., Liu, Y.-N., Lai, H.-C. & Soo, P.-C. The RssB/RssA two-component system regulates biosynthesis of the tripyrrole antibiotic, prodigiosin, in *Serratia marcescens*. *Int J Med Microbiol* **300**, 304–312 (2010).
87. Horng, Y.-T. *et al.* The LuxR family protein SpnR functions as a negative regulator of N-acylhomoserine lactone-dependent quorum sensing in *Serratia marcescens*. *Mol Microbiol* **45**, 1655–1671 (2002).
88. Sun, E. *et al.* Broad-Spectrum Adaptive Antibiotic Resistance Associated with *Pseudomonas aeruginosa* Mucin-Dependent Surfing Motility. *Antimicrob Agents Chemother* **62**, e00848-18 (2018).
89. Alberti, L. & Harshey, R. M. Differentiation of *Serratia marcescens* 274 into swimmer and swarmer cells. *J Bacteriol* **172**, 4322–4328 (1990).
90. Kearns, D. B. A field guide to bacterial swarming motility. *Nat Rev Microbiol* **8**, 634–644 (2010).
91. Palma, V., Gutiérrez, M. S., Vargas, O., Parthasarathy, R. & Navarrete, P. Methods to Evaluate Bacterial Motility and Its Role in Bacterial–Host Interactions. *Microorganisms* **10**, 563 (2022).
92. Partridge, J. D. & Harshey, R. M. Investigating Flagella-Driven Motility in *Escherichia coli* by Applying Three Established Techniques in a Series. *JoVE* 61364 (2020) doi:10.3791/61364.
93. Daniels, R., Vanderleyden, J. & Michiels, J. Quorum sensing and swarming migration in bacteria. *FEMS Microbiology Reviews* **28**, 261–289 (2004).
94. Lai, S., Tremblay, J. & Déziel, E. Swarming motility: a multicellular behaviour conferring antimicrobial resistance. *Environ Microbiol* **11**, 126–136 (2009).
95. Izquierdo, L. *et al.* The inner-core lipopolysaccharide biosynthetic waaE gene: function and genetic distribution among some Enterobacteriaceae. *Microbiology (Reading)* **148**, 3485–3496 (2002).
96. Matsuyama, T., Bhasin, A. & Harshey, R. M. Mutational analysis of flagellum-independent surface spreading of *Serratia marcescens* 274 on a low-agar medium. *J Bacteriol* **177**, 987–991 (1995).
97. Dudin, O., Geiselmann, J., Ogasawara, H., Ishihama, A. & Lacour, S. Repression of Flagellar Genes in Exponential Phase by CsgD and CpxR, Two Crucial Modulators of *Escherichia coli* Biofilm Formation. *J Bacteriol* **196**, 707–715 (2014).
98. Josenhans, C. & Suerbaum, S. The role of motility as a virulence factor in bacteria. *International Journal of Medical Microbiology* **291**, 605–614 (2002).
99. Kao, C. Y. *et al.* The complex interplay among bacterial motility and virulence factors in different *Escherichia coli* infections. *Eur J Clin Microbiol Infect Dis* **33**, 2157–2162 (2014).
100. Rather, P. N. Swarmer cell differentiation in *Proteus mirabilis*. *Environ Microbiol* **7**, 1065–1073 (2005).

101. Overhage, J., Bains, M., Brazas, M. D. & Hancock, R. E. W. Swarming of *Pseudomonas aeruginosa* Is a Complex Adaptation Leading to Increased Production of Virulence Factors and Antibiotic Resistance. *J Bacteriol* **190**, 2671–2679 (2008).
102. Figaj, D., Ambroziak, P., Przepiora, T. & Skorko-Glonek, J. The Role of Proteases in the Virulence of Plant Pathogenic Bacteria. *Int J Mol Sci* **20**, 672 (2019).
103. Petersen, L. M. & Tisa, L. S. Molecular Characterization of Protease Activity in *Serratia* sp. Strain SCBI and Its Importance in Cytotoxicity and Virulence. *J Bacteriol* **196**, 3923–3936 (2014).
104. Kamata, R., Matsumoto, K., Okamura, R., Yamamoto, T. & Maeda, H. The *Serratia*l 56K protease as a major pathogenic factor in *Serratia*l keratitis. Clinical and experimental study. *Ophthalmology* **92**, 1452–1459 (1985).
105. Marty, K. B., Williams, C. L., Guynn, L. J., Benedik, M. J. & Blanke, S. R. Characterization of a cytotoxic factor in culture filtrates of *Serratia marcescens*. *Infect Immun* **70**, 1121–1128 (2002).
106. Matsumoto, K., Maeda, H., Takata, K., Kamata, R. & Okamura, R. Purification and characterization of four proteases from a clinical isolate of *Serratia marcescens* kums 3958. *J Bacteriol* **157**, 225–232 (1984).
107. Bruna, R. E., Molino, M. V., Lazzaro, M., Mariscotti, J. F. & García Véscovi, E. CpxR-Dependent Thermoregulation of *Serratia marcescens* PrtA Metalloprotease Expression and Its Contribution to Bacterial Biofilm Formation. *J Bacteriol* **200**, e00006-18 (2018).
108. Harris, S. J., Shih, Y. L., Bentley, S. D. & Salmond, G. P. The hexA gene of Erwinia carotovora encodes a LysR homologue and regulates motility and the expression of multiple virulence determinants. *Mol Microbiol* **28**, 705–717 (1998).
109. Goluszko, P. & Nowacki, M. R. Extracellular haemolytic activity of *Serratia marcescens*. *FEMS Microbiol Lett* **52**, 207–211 (1989).
110. Schönherr, R., Tsolis, R., Focareta, T. & Braun, V. Amino acid replacements in the *Serratia marcescens* haemolysin ShlA define sites involved in activation and secretion. *Mol Microbiol* **9**, 1229–1237 (1993).
111. Shimuta, K. *et al.* The hemolytic and cytolytic activities of *Serratia marcescens* phospholipase A (PhlA) depend on lysophospholipid production by PhlA. *BMC Microbiology* **9**, 261 (2009).
112. Lin, C.-S. *et al.* RssAB-FlhDC-ShlBA as a Major Pathogenesis Pathway in *Serratia marcescens*. *Infect Immun* **78**, 4870–4881 (2010).
113. Ash, R. J., Mauck, B. & Morgan, M. Antibiotic Resistance of Gram-Negative Bacteria in Rivers, United States. *Emerg Infect Dis* **8**, 713–716 (2002).
114. Ball, A. P., McGhie, D. & Geddes, A. M. *Serratia marcescens* in a general hospital. *Q J Med* **46**, 63–71 (1977).
115. Evans, M. E., Feola, D. J. & Rapp, R. P. Polymyxin B sulfate and colistin: old antibiotics for emerging multiresistant gram-negative bacteria. *Ann Pharmacother* **33**, 960–967 (1999).
116. Jacoby, G. A. AmpC beta-lactamases. *Clin Microbiol Rev* **22**, 161–182, Table of Contents (2009).
117. Weber, L., Jansen, M., Krüttgen, A., Buhl, E. M. & Horz, H.-P. Tackling Intrinsic Antibiotic Resistance in *Serratia marcescens* with a Combination of Ampicillin/Sulbactam and Phage SALSA. *Antibiotics* **9**, 371 (2020).
118. Hughes, D. & Andersson, D. I. Environmental and genetic modulation of the phenotypic expression of antibiotic resistance. *FEMS Microbiology Reviews* **41**, 374–391 (2017).
119. Shirshikova, T. V. *et al.* The ABC-Type Efflux Pump MacAB Is Involved in Protection of *Serratia marcescens* against Aminoglycoside Antibiotics, Polymyxins, and Oxidative Stress. *mSphere* **6**, e00033-21 (2021).
120. Begic, S. & Worobec, E. A. The role of the *Serratia marcescens* SdeAB multidrug efflux pump and TolC homologue in fluoroquinolone resistance studied via gene-knockout mutagenesis. *Microbiology (Reading)* **154**, 454–461 (2008).
121. Haifei Yang. Mechanisms of antimicrobial resistance in *Serratia marcescens*. *Afr. J. Microbiol. Res.* **6**, (2012).

122. Sandner-Miranda, L., Vinuesa, P., Cravioto, A. & Morales-Espinosa, R. The Genomic Basis of Intrinsic and Acquired Antibiotic Resistance in the Genus *Serratia*. *Front Microbiol* **9**, 828 (2018).
123. Corona, F. & Martinez, J. L. Phenotypic Resistance to Antibiotics. *Antibiotics (Basel)* **2**, 237–255 (2013).
124. Hasan, C. M., Dutta, D. & Nguyen, A. N. T. Revisiting Antibiotic Resistance: Mechanistic Foundations to Evolutionary Outlook. *Antibiotics (Basel)* **11**, 40 (2021).
125. Begic, S. & Worobec, E. A. Fluoroquinolone resistance of *Serratia marcescens*: sucrose, salicylate, temperature, and pH induction of phenotypic resistance. *Can. J. Microbiol.* **53**, 1239–1245 (2007).
126. Tavares-Carreon, F., De Anda-Mora, K., Rojas-Barrera, I. C. & Andrade, A. *Serratia marcescens* antibiotic resistance mechanisms of an opportunistic pathogen: a literature review. *PeerJ* **11**, e14399 (2023).
127. Ray, C., Shenoy, A. T., Orihuela, C. J. & González-Juarbe, N. Killing of *Serratia marcescens* biofilms with chloramphenicol. *Ann Clin Microbiol Antimicrob* **16**, 19 (2017).
128. Cisse, H. *et al.* Treatment of bone and joint infections caused by Enterobacter cloacae with a fluoroquinolone–cotrimoxazole combination. *International Journal of Antimicrobial Agents* **54**, 245–248 (2019).
129. Lo, C.-L. *et al.* Fluoroquinolone therapy for bloodstream infections caused by extended-spectrum beta-lactamase-producing *Escherichia coli* and *Klebsiella pneumoniae*. *Journal of Microbiology, Immunology and Infection* **50**, 355–361 (2017).
130. Correia, S., Poeta, P., Hébraud, M., Capelo, J. L. & Igrejas, G. Mechanisms of quinolone action and resistance: where do we stand? *J Med Microbiol* **66**, 551–559 (2017).
131. Bush, N. G., Diez-Santos, I., Abbott, L. R. & Maxwell, A. Quinolones: Mechanism, Lethality and Their Contributions to Antibiotic Resistance. *Molecules* **25**, 5662 (2020).
132. Aldred, K. J., Kerns, R. J. & Osheroff, N. Mechanism of Quinolone Action and Resistance. *Biochemistry* **53**, 1565–1574 (2014).
133. Blondeau, J. M. Fluoroquinolones: mechanism of action, classification, and development of resistance. *Survey of Ophthalmology* **49**, S73–S78 (2004).
134. Helgesen, E., Sætre, F. & Skarstad, K. Topoisomerase IV tracks behind the replication fork and the SeqA complex during DNA replication in *Escherichia coli*. *Sci Rep* **11**, 474 (2021).
135. Wang, X., Zhao, X., Malik, M. & Drlica, K. Contribution of reactive oxygen species to pathways of quinolone-mediated bacterial cell death. *J Antimicrob Chemother* **65**, 520–524 (2010).
136. Friedberg, E. C. *et al.* DNA repair: From molecular mechanism to human disease. *DNA Repair* **5**, 986–996 (2006).
137. Qin, T.-T. *et al.* SOS response and its regulation on the fluoroquinolone resistance. *Ann Transl Med* **3**, 358 (2015).
138. Kumar, A. & Worobec, E. A. Fluoroquinolone resistance of *Serratia marcescens*: involvement of a proton gradient-dependent efflux pump. *Journal of Antimicrobial Chemotherapy* **50**, 593–596 (2002).
139. Poole, K. Efflux pumps as antimicrobial resistance mechanisms. *Annals of Medicine* (2009) doi:10.1080/07853890701195262.
140. Strahilevitz, J., Jacoby, G. A., Hooper, D. C. & Robicsek, A. Plasmid-mediated quinolone resistance: a multifaceted threat. *Clin Microbiol Rev* **22**, 664–689 (2009).
141. Robicsek, A. *et al.* Fluoroquinolone-modifying enzyme: a new adaptation of a common aminoglycoside acetyltransferase. *Nat Med* **12**, 83–88 (2006).
142. Sun, H. I. *et al.* A novel family (QnrAS) of plasmid-mediated quinolone resistance determinant. *Int J Antimicrob Agents* **36**, 578–579 (2010).
143. Yamane, K. *et al.* New Plasmid-Mediated Fluoroquinolone Efflux Pump, QepA, Found in an *Escherichia coli* Clinical Isolate. *Antimicrob Agents Chemother* **51**, 3354–3360 (2007).

144. Briales, A. *et al.* Exposure to diverse antimicrobials induces the expression of *qnrB1*, *qnrD* and *smaqnr* genes by SOS-dependent regulation. *Journal of Antimicrobial Chemotherapy* **67**, 2854–2859 (2012).
145. Yang, H.-F., Cheng, J., Hu, L.-F., Ye, Y. & Li, J.-B. Identification of a *Serratia marcescens* Clinical Isolate with Multiple Quinolone Resistance Mechanisms from China. *Antimicrob Agents Chemother* **56**, 5426–5427 (2012).
146. Jacoby, G. A. *et al.* qnrB, Another Plasmid-Mediated Gene for Quinolone Resistance. *Antimicrob Agents Chemother* **50**, 1178–1182 (2006).
147. Martínez-Martínez, L., Pascual, A. & Jacoby, G. A. Quinolone resistance from a transferable plasmid. *Lancet* **351**, 797–799 (1998).
148. Salah, F. D. *et al.* Distribution of quinolone resistance gene (*qnr*) in ESBL-producing *Escherichia coli* and Klebsiella spp. in Lomé, Togo. *Antimicrobial Resistance & Infection Control* **8**, 104 (2019).
149. Velasco, C. *et al. Smaqnr*, a new chromosome-encoded quinolone resistance determinant in *Serratia marcescens*. *Journal of Antimicrobial Chemotherapy* **65**, 239–242 (2010).
150. Baharoglu, Z. & Mazel, D. SOS, the formidable strategy of bacteria against aggressions. *FEMS Microbiology Reviews* **38**, 1126–1145 (2014).
151. Da Re, S. *et al.* The SOS response promotes *qnrB* quinolone-resistance determinant expression. *EMBO Rep* **10**, 929–933 (2009).
152. Erill, I., Campoy, S. & Barbé, J. Aeons of distress: an evolutionary perspective on the bacterial SOS response. *FEMS Microbiology Reviews* **31**, 637–656 (2007).
153. Wang, M., Jacoby, G. A., Mills, D. M. & Hooper, D. C. SOS Regulation of *qnrB* Expression. *Antimicrob Agents Chemother* **53**, 821–823 (2009).
154. Fernández de Henestrosa, A. R. *et al.* Identification of additional genes belonging to the LexA regulon in *Escherichia coli*. *Molecular Microbiology* **35**, 1560–1572 (2000).
155. Schroder, W., Goerke, C. & Wolz, C. Opposing effects of aminocoumarins and fluoroquinolones on the SOS response and adaptability in *Staphylococcus aureus*. *Journal of Antimicrobial Chemotherapy* **68**, 529–538 (2013).
156. Yamaguchi, Y., Tomoyasu, T., Takaya, A., Morioka, M. & Yamamoto, T. Effects of disruption of heat shock genes on susceptibility of *Escherichia coli* to fluoroquinolones. *BMC Microbiology* **3**, 16 (2003).
157. Donlan, R. M. Biofilms: microbial life on surfaces. *Emerging Infect. Dis.* **8**, 881–890 (2002).
158. Pohlon, E., Marxsen, J. & Küsel, K. Pioneering bacterial and algal communities and potential extracellular enzyme activities of stream biofilms. *FEMS Microbiol Ecol* **71**, 364–373 (2010).
159. Flemming, H.-C., Neu, T. R. & Wozniak, D. J. The EPS Matrix: The "House of Biofilm Cells". *J Bacteriol* **189**, 7945–7947 (2007).
160. Flemming, H.-C. & Wingender, J. The biofilm matrix. *Nat. Rev. Microbiol.* **8**, 623–633 (2010).
161. Fong, J. N. C. & Yildiz, F. H. Biofilm Matrix Proteins. *Microbiol Spectr* **3**, (2015).
162. Donlan, R. M. Role of biofilms in antimicrobial resistance. *ASAIO J.* **46**, S47-52 (2000).
163. Mah, T. F. & O'Toole, G. A. Mechanisms of biofilm resistance to antimicrobial agents. *Trends Microbiol.* **9**, 34–39 (2001).
164. Rasmussen, T. B. & Givskov, M. Quorum sensing inhibitors: a bargain of effects. *Microbiology (Reading, Engl.)* **152**, 895–904 (2006).
165. Stewart, P. S. Antimicrobial Tolerance in Biofilms. *Microbiol Spectr* **3**, (2015).
166. Davies, D. Understanding biofilm resistance to antibacterial agents. *Nature Reviews Drug Discovery* **2**, 114–122 (2003).
167. Jamal, M. *et al.* Bacterial biofilm and associated infections. *Journal of the Chinese Medical Association* **81**, 7–11 (2018).
168. Joo, H.-S. & Otto, M. Molecular basis of in-vivo biofilm formation by bacterial pathogens. *Chem Biol* **19**, 1503–1513 (2012).

169. Billings, N. *et al.* The Extracellular Matrix Component Psl Provides Fast-Acting Antibiotic Defense in *Pseudomonas aeruginosa* Biofilms. *PLOS Pathogens* **9**, e1003526 (2013).
170. Colvin, K. M. *et al.* The Pel Polysaccharide Can Serve a Structural and Protective Role in the Biofilm Matrix of *Pseudomonas aeruginosa*. *PLOS Pathogens* **7**, e1001264 (2011).
171. Bae, J., Oh, E. & Jeon, B. Enhanced Transmission of Antibiotic Resistance in Campylobacter jejuni Biofilms by Natural Transformation. *Antimicrobial Agents and Chemotherapy* **58**, 7573–7575 (2014).
172. Hoffman, L. R. *et al.* Aminoglycoside antibiotics induce bacterial biofilm formation. *Nature* **436**, 1171–1175 (2005).
173. Dörr, T., Lewis, K. & Vulić, M. SOS Response Induces Persistence to Fluoroquinolones in *Escherichia coli*. *PLOS Genetics* **5**, e1000760 (2009).
174. Pan, J., Bahar, A. A., Syed, H. & Ren, D. Reverting Antibiotic Tolerance of *Pseudomonas aeruginosa* PAO1 Persister Cells by (Z)-4-bromo-5-(bromomethylene)-3-methylfuran-2(5H)-one. *PLoS One* **7**, e45778 (2012).
175. Wood, T. K., Knabel, S. J. & Kwan, B. W. Bacterial Persister Cell Formation and Dormancy. *Appl Environ Microbiol* **79**, 7116–7121 (2013).
176. Drenkard, E. & Ausubel, F. M. *Pseudomonas* biofilm formation and antibiotic resistance are linked to phenotypic variation. *Nature* **416**, 740–743 (2002).
177. Mayola, A. *et al.* RecA Protein Plays a Role in the Chemotactic Response and Chemoreceptor Clustering of *Salmonella enterica*. *PLOS ONE* **9**, e105578 (2014).
178. Gómez-Gómez, J.-M., Manfredi, C., Alonso, J.-C. & Blázquez, J. A novel role for RecA under non-stress: promotion of swarming motility in *Escherichia coli* K-12. *BMC Biol* **5**, 14 (2007).
179. Frutos-Grilo, E., Marsal, M., Irazoki, O., Barbé, J. & Campoy, S. The Interaction of RecA With Both CheA and CheW Is Required for Chemotaxis. *Frontiers in Microbiology* **11**, (2020).
180. Lyons, N. A. & Kolter, R. On The Evolution of Bacterial Multicellularity. *Curr Opin Microbiol* **24**, 21–28 (2015).
181. Martinez-Rabert, E., Amstel, C. van, Smith, C., Sloan, W. T. & Gonzalez-Cabaleiro, R. Environmental and ecological controls of the spatial distribution of microbial populations in aggregates. *PLOS Computational Biology* **18**, e1010807 (2022).
182. Rutherford, S. T. & Bassler, B. L. Bacterial Quorum Sensing: Its Role in Virulence and Possibilities for Its Control. *Cold Spring Harb Perspect Med* **2**, a012427 (2012).
183. Falà, A. K., Álvarez-Ordóñez, A., Filloux, A., Gahan, C. G. M. & Cotter, P. D. Quorum sensing in human gut and food microbiomes: Significance and potential for therapeutic targeting. *Frontiers in Microbiology* **13**, (2022).
184. Davey, M. E. & O'toole, G. A. Microbial biofilms: from ecology to molecular genetics. *Microbiol Mol Biol Rev* **64**, 847–867 (2000).
185. Lequette, Y. & Greenberg, E. P. Timing and localization of rhamnolipid synthesis gene expression in *Pseudomonas aeruginosa* biofilms. *J Bacteriol* **187**, 37–44 (2005).
186. Banin, E., Vasil, M. L. & Greenberg, E. P. Iron and *Pseudomonas aeruginosa* biofilm formation. *Proc Natl Acad Sci U S A* **102**, 11076–11081 (2005).
187. Diggle, S. P. *et al.* The galactophilic lectin, LecA, contributes to biofilm development in *Pseudomonas aeruginosa*. *Environ Microbiol* **8**, 1095–1104 (2006).
188. Zhao, X., Yu, Z. & Ding, T. Quorum-Sensing Regulation of Antimicrobial Resistance in Bacteria. *Microorganisms* **8**, 425 (2020).
189. Nealson, K. H., Platt, T. & Hastings, J. W. Cellular Control of the Synthesis and Activity of the Bacterial Luminescent System1. *J Bacteriol* **104**, 313–322 (1970).
190. Pereira, C. S., Thompson, J. A. & Xavier, K. B. AI-2-mediated signalling in bacteria. *FEMS Microbiology Reviews* **37**, 156–181 (2013).
191. Miller, M. B. & Bassler, B. L. Quorum Sensing in Bacteria. *Annual Review of Microbiology* **55**, 165–199 (2001).

192. Monnet, V. & Gardan, R. Quorum-sensing regulators in Gram-positive bacteria: 'cherchez le peptide '. *Molecular Microbiology* **97**, 181–184 (2015).
193. Bejerano-Sagie, M. & Xavier, K. B. The role of small RNAs in quorum sensing. *Current Opinion in Microbiology* **10**, 189–198 (2007).
194. Hengge, R. *et al.* Recent Advances and Current Trends in Nucleotide Second Messenger Signaling in Bacteria. *J Mol Biol* **431**, 908–927 (2019).
195. Jenal, U., Reinders, A. & Lori, C. Cyclic di-GMP: second messenger extraordinaire. *Nat Rev Microbiol* **15**, 271–284 (2017).
196. Willett, J. L. E., Ruhe, Z. C., Goulding, C. W., Low, D. A. & Hayes, C. S. Contact-Dependent Growth Inhibition (CDI) and CdiB/CdiA Two-Partner Secretion Proteins. *J Mol Biol* **427**, 3754–3765 (2015).
197. Anderson, M. S., Garcia, E. C. & Cotter, P. A. Kind discrimination and competitive exclusion mediated by contact-dependent growth inhibition systems shape biofilm community structure. *PLoS Pathog* **10**, e1004076 (2014).
198. Guilhabert, M. R. & Kirkpatrick, B. C. Identification of Xylella fastidiosa antivirulence genes: hemagglutinin adhesins contribute a biofilm maturation to X. fastidios and colonization and attenuate virulence. *Mol Plant Microbe Interact* **18**, 856–868 (2005).
199. Neil, R. B. & Apicella, M. A. Role of HrpA in biofilm formation of Neisseria meningitidis and regulation of the hrpBAS transcripts. *Infect Immun* **77**, 2285–2293 (2009).
200. Ruhe, Z. C. *et al.* CdiA promotes receptor-independent intercellular adhesion. *Mol Microbiol* **98**, 175–192 (2015).
201. Winzer, K., Hardie, K. R. & Williams, P. LuxS and Autoinducer-2: Their Contribution to Quorum Sensing and Metabolism in Bacteria. in *Advances in Applied Microbiology* vol. 53 291–396 (Academic Press, 2003).
202. Hondorp, E. R. & Matthews, R. G. Methionine. *EcoSal Plus* **2**, (2006).
203. Vendeville, A., Winzer, K., Heurlier, K., Tang, C. M. & Hardie, K. R. Making 'sense' of metabolism: autoinducer-2, LUXS and pathogenic bacteria. *Nat Rev Microbiol* **3**, 383–396 (2005).
204. Shin, D., Frane, N. D., Brecht, R. M., Keeler, J. & Nagarajan, R. A Comparative Analysis of Acyl-Homoserine Lactone Synthase Assays. *ChemBioChem* **16**, 2651–2659 (2015).
205. Grundy, F. J. & Henkin, T. M. The S box regulon: a new global transcription termination control system for methionine and cysteine biosynthesis genes in gram-positive bacteria. *Mol Microbiol* **30**, 737–749 (1998).
206. Liu, M., Prakash, C., Nauta, A., Siezen, R. J. & Francke, C. Computational Analysis of Cysteine and Methionine Metabolism and Its Regulation in Dairy Starter and Related Bacteria. *Journal of Bacteriology* **194**, 3522–3533 (2012).
207. Rodionov, D. A., Vitreschak, A. G., Mironov, A. A. & Gelfand, M. S. Comparative genomics of the methionine metabolism in Gram-positive bacteria: a variety of regulatory systems. *Nucleic Acids Res* **32**, 3340–3353 (2004).
208. Ferla, M. P. & Patrick, W. M. Bacterial methionine biosynthesis. *Microbiology* **160**, 1571–1584 (2014).
209. Deobald, D., Hanna, R., Shahryari, S., Layer, G. & Adrian, L. Identification and characterization of a bacterial core methionine synthase. *Sci Rep* **10**, 2100 (2020).
210. Old, I. G., Phillips, S. E. V., Stockley, P. G. & Saint Girons, I. Regulation of methionine biosynthesis in the enterobacteriaceae. *Progress in Biophysics and Molecular Biology* **56**, 145–185 (1991).
211. Maxon, M. E., Wigboldus, J., Brot, N. & Weissbach, H. Structure-function studies on *Escherichia coli* MetR protein, a putative prokaryotic leucine zipper protein. *Proc Natl Acad Sci U S A* **87**, 7076–7079 (1990).
212. Sperandio, B. *et al.* Control of Methionine Synthesis and Uptake by MetR and Homocysteine in Streptococcus mutans. *J Bacteriol* **189**, 7032–7044 (2007).

213. Niu, C. *et al.* LuxS influences *Escherichia coli* biofilm formation through autoinducer-2-dependent and autoinducer-2-independent modalities. *FEMS Microbiology Ecology* **83**, 778–791 (2013).
214. Sperandio, V., Li, C. C. & Kaper, J. B. Quorum-sensing *Escherichia coli* regulator A: a regulator of the LysR family involved in the regulation of the locus of enterocyte effacement pathogenicity island in enterohemorrhagic *E. coli*. *Infect Immun* **70**, 3085–3093 (2002).
215. Sircili, M. P., Walters, M., Trabulsi, L. R. & Sperandio, V. Modulation of Enteropathogenic *Escherichia coli* Virulence by Quorum Sensing. *Infect Immun* **72**, 2329–2337 (2004).
216. Cole, S. P., Harwood, J., Lee, R., She, R. & Guiney, D. G. Characterization of monospecies biofilm formation by *Helicobacter pylori*. *J Bacteriol* **186**, 3124–3132 (2004).
217. Wen, Z. T. & Burne, R. A. LuxS-mediated signaling in *Streptococcus mutans* is involved in regulation of acid and oxidative stress tolerance and biofilm formation. *J Bacteriol* **186**, 2682–2691 (2004).
218. Burgess, N. A. *et al.* LuxS-dependent quorum sensing in *Porphyromonas gingivalis* modulates protease and haemagglutinin activities but is not essential for virulence. *Microbiology* **148**, 763–772 (2002).
219. Lyon, W. R., Madden, J. C., Levin, J. C., Stein, J. L. & Caparon, M. G. Mutation of luxS affects growth and virulence factor expression in *Streptococcus pyogenes*. *Molecular Microbiology* **42**, 145–157 (2001).
220. Kim, S. Y. *et al.* Regulation of Vibrio vulnificus virulence by the LuxS quorum-sensing system. *Molecular Microbiology* **48**, 1647–1664 (2003).
221. Van Houdt, R., Givskov, M. & Michiels, C. W. Quorum sensing in *Serratia*. *FEMS Microbiology Reviews* **31**, 407–424 (2007).
222. Kohn, K. P., Underwood, S. M. & Cooper, M. M. Connecting Structure–Property and Structure–Function Relationships across the Disciplines of Chemistry and Biology: Exploring Student Perceptions. *LSE* **17**, ar33 (2018).
223. Ultee, E., Ramijan, K., Dame, R. T., Briegel, A. & Claessen, D. Stress-induced adaptive morphogenesis in bacteria. *Adv Microb Physiol* **74**, 97–141 (2019).
224. Horvath, D. J. *et al.* Morphological plasticity promotes resistance to phagocyte killing of uropathogenic *Escherichia coli*. *Microbes Infect* **13**, 426–437 (2011).
225. Andersen, L. P. & Rasmussen, L. *Helicobacter pylori*-coccoid forms and biofilm formation. *FEMS Immunology & Medical Microbiology* **56**, 112–115 (2009).
226. Ikeda, N. & Karlyshev, A. V. Putative mechanisms and biological role of coccoid form formation in *Campylobacter jejuni*. *Eur J Microbiol Immunol (Bp)* **2**, 41–49 (2012).
227. Jiang, C., Caccamo, P. D. & Brun, Y. V. Mechanisms of bacterial morphogenesis: Evolutionary cell biology approaches provide new insights. *Bioessays* **37**, 413–425 (2015).
228. Nadell, C. D., Drescher, K. & Foster, K. R. Spatial structure, cooperation and competition in biofilms. *Nat Rev Microbiol* **14**, 589–600 (2016).
229. Ibberson, C. B., Barraza, J. P., Holmes, A. L., Cao, P. & Whiteley, M. Precise spatial structure impacts antimicrobial susceptibility of S. aureus in polymicrobial wound infections. *Proceedings of the National Academy of Sciences* **119**, e2212340119 (2022).
230. Dechesne, A. *et al.* A novel method for characterizing the microscale 3D spatial distribution of bacteria in soil. *Soil Biology and Biochemistry* **35**, 1537–1546 (2003).
231. Nunan, N., Wu, K., Young, I. M., Crawford, J. W. & Ritz, K. Spatial distribution of bacterial communities and their relationships with the micro-architecture of soil. *FEMS Microbiology Ecology* **44**, 203–215 (2003).
232. Young, I. M. & Crawford, J. W. Interactions and Self-Organization in the Soil-Microbe Complex. *Science* **304**, 1634–1637 (2004).
233. Donaldson, G. P., Lee, S. M. & Mazmanian, S. K. Gut biogeography of the bacterial microbiota. *Nat Rev Microbiol* **14**, 20–32 (2016).

234. Kim, D. *et al.* Spatial mapping of polymicrobial communities reveals a precise biogeography associated with human dental caries. *Proceedings of the National Academy of Sciences* **117**, 12375–12386 (2020).
235. Alber, M. S., Kiskowski, M. A., Glazier, J. A. & Jiang, Y. On Cellular Automaton Approaches to Modeling Biological Cells. in *Mathematical Systems Theory in Biology, Communications, Computation, and Finance* (eds. Rosenthal, J. & Gilliam, D. S.) 1–39 (Springer, 2003). doi:10.1007/978-0-387-21696-6_1.
236. Bandini, S., Mauri, G. & Serra, R. Cellular automata: From a theoretical parallel computational model to its application to complex systems. *Parallel Computing* **27**, 539–553 (2001).
237. Xiao, X., Wang, P. & Chou, K.-C. Cellular automata and its applications in protein bioinformatics. *Curr Protein Pept Sci* **12**, 508–519 (2011).
238. Pirt, S. J. A Kinetic Study of the Mode of Growth of Surface Colonies of Bacteria and Fungi. *Microbiology* **47**, 181–197 (1967).
239. Tyson, R., Lubkin, S. R. & Murray, J. D. A minimal mechanism for bacterial pattern formation. *Proc Biol Sci* **266**, 299–304 (1999).
240. Golding, I., Cohen, I. & Ben-Jacob, E. Studies of sector formation in expanding bacterial colonies. *EPL* **48**, 587 (1999).
241. Matsushita, M. *et al.* Interface growth and pattern formation in bacterial colonies. *Physica A: Statistical Mechanics and its Applications* **249**, 517–524 (1998).
242. Kim, H. J., Boedicker, J. Q., Choi, J. W. & Ismagilov, R. F. Defined spatial structure stabilizes a synthetic multispecies bacterial community. *Proceedings of the National Academy of Sciences* **105**, 18188–18193 (2008).
243. Čepl, J., Scholtz, V. & Scholtzová, J. The fitness change and the diversity maintenance in the growing mixed colony of two *Serratia* rubidaea clones. *Arch Microbiol* **198**, 301–306 (2016).
244. Čepl, J., Scholtz, V. & Scholtzová, J. Modeling of concentric pattern of *Serratia marcescens* colony. *Arch Microbiol* **201**, 87–92 (2019).
245. Čepl, J. J., Pátková, I., Blahůšková, A., Cvrčková, F. & Markoš, A. Patterning of mutually interacting bacterial bodies: close contacts and airborne signals. *BMC Microbiology* **10**, 139 (2010).
246. Pátková, I. *et al.* Developmental plasticity of bacterial colonies and consortia in germ-free and gnotobiotic settings. *BMC Microbiology* **12**, 178 (2012).
247. Rieger, T., Neubauer, Z., Blahůšková, A., Cvrčková, F. & Markoš, A. Bacterial body plans. *Commun Integr Biol* **1**, 78–87 (2008).
248. Hillman, E. T., Lu, H., Yao, T. & Nakatsu, C. H. Microbial Ecology along the Gastrointestinal Tract. *Microbes Environ* **32**, 300–313 (2017).
249. Thursby, E. & Juge, N. Introduction to the human gut microbiota. *Biochem J* **474**, 1823–1836 (2017).
250. Almeida, A. *et al.* A new genomic blueprint of the human gut microbiota. *Nature* **568**, 499–504 (2019).
251. Sender, R., Fuchs, S. & Milo, R. Revised Estimates for the Number of Human and Bacteria Cells in the Body. *PLOS Biology* **14**, e1002533 (2016).
252. Maynard, C. L., Elson, C. O., Hatton, R. D. & Weaver, C. T. Reciprocal interactions of the intestinal microbiota and immune system. *Nature* **489**, 231–241 (2012).
253. Helander, H. F. & Fändriks, L. Surface area of the digestive tract - revisited. *Scand. J. Gastroenterol.* **49**, 681–689 (2014).
254. Hevia, A., Delgado, S., Sánchez, B. & Margolles, A. Molecular Players Involved in the Interaction Between Beneficial Bacteria and the Immune System. *Front Microbiol* **6**, 1285 (2015).
255. Hooper, L. V., Littman, D. R. & Macpherson, A. J. Interactions between the microbiota and the immune system. *Science* **336**, 1268–1273 (2012).
256. Brestoff, J. R. & Artis, D. Commensal bacteria at the interface of host metabolism and the immune system. *Nat. Immunol.* **14**, 676–684 (2013).

257. Primec, M., Mičetić-Turk, D. & Langerholc, T. Analysis of short-chain fatty acids in human feces: A scoping review. *Analytical Biochemistry* **526**, 9–21 (2017).
258. de Aguiar Vallim, T. Q., Tarling, E. J. & Edwards, P. A. Pleiotropic Roles of Bile Acids in Metabolism. *Cell Metab* **17**, 657–669 (2013).
259. Nieuwdorp, M., Gilijamse, P. W., Pai, N. & Kaplan, L. M. Role of the microbiome in energy regulation and metabolism. *Gastroenterology* **146**, 1525–1533 (2014).
260. Dey, P. Gut microbiota in phytopharmacology: A comprehensive overview of concepts, reciprocal interactions, biotransformations and mode of actions. *Pharmacological Research* **147**, 104367 (2019).
261. Qin, J. *et al.* A human gut microbial gene catalogue established by metagenomic sequencing. *Nature* **464**, 59–65 (2010).
262. Lozupone, C. A., Stombaugh, J. I., Gordon, J. I., Jansson, J. K. & Knight, R. Diversity, stability and resilience of the human gut microbiota. *Nature* **489**, 220–230 (2012).
263. Wu, G. D. *et al.* Linking long-term dietary patterns with gut microbial enterotypes. *Science* **334**, 105–108 (2011).
264. Lakshminarayanan, B., Stanton, C., O'Toole, P. W. & Ross, R. P. Compositional dynamics of the human intestinal microbiota with aging: Implications for health. *J Nutr Health Aging* **18**, 773–786 (2014).
265. Saffouri, G. B. *et al.* Small intestinal microbial dysbiosis underlies symptoms associated with functional gastrointestinal disorders. *Nat Commun* **10**, (2019).
266. Li, B., Selmi, C., Tang, R., Gershwin, M. E. & Ma, X. The microbiome and autoimmunity: a paradigm from the gut–liver axis. *Cell Mol Immunol* **15**, 595–609 (2018).
267. Scher, J. U. *et al.* Expansion of intestinal *Prevotella copri* correlates with enhanced susceptibility to arthritis. *Elife* **2**, e01202 (2013).
268. Kostic, A. D. *et al. Fusobacterium nucleatum* potentiates intestinal tumorigenesis and modulates the tumor-immune microenvironment. *Cell Host Microbe* **14**, 207–215 (2013).
269. Wang, Z. *et al.* Gut flora metabolism of phosphatidylcholine promotes cardiovascular disease. *Nature* **472**, 57–63 (2011).
270. Borre, Y. E., Moloney, R. D., Clarke, G., Dinan, T. G. & Cryan, J. F. The Impact of Microbiota on Brain and Behavior: Mechanisms & Therapeutic Potential. in *Microbial Endocrinology: The Microbiota-Gut-Brain Axis in Health and Disease* (eds. Lyte, M. & Cryan, J. F.) 373–403 (Springer, 2014). doi:10.1007/978-1-4939-0897-4_17.
271. Collins, S. M., Surette, M. & Bercik, P. The interplay between the intestinal microbiota and the brain. *Nat. Rev. Microbiol.* **10**, 735–742 (2012).
272. Larsen, P. E. & Dai, Y. Metabolome of human gut microbiome is predictive of host dysbiosis. *Gigascience* **4**, 42 (2015).
273. Sarangi, A. N., Goel, A. & Aggarwal, R. Methods for Studying Gut Microbiota: A Primer for Physicians. *Journal of Clinical and Experimental Hepatology* **9**, 62–73 (2019).
274. Salazar, N., Valdés-Varela, L., González, S., Gueimonde, M. & de Los Reyes-Gavilán, C. G. Nutrition and the gut microbiome in the elderly. *Gut Microbes* **8**, 82–97 (2017).
275. Caporaso, J. G. *et al.* Moving pictures of the human microbiome. *Genome Biology* **12**, R50 (2011).
276. Costello, E. K. *et al.* Bacterial community variation in human body habitats across space and time. *Science* **326**, 1694–1697 (2009).
277. Yang, B., Wang, Y. & Qian, P.-Y. Sensitivity and correlation of hypervariable regions in 16S rRNA genes in phylogenetic analysis. *BMC Bioinformatics* **17**, (2016).
278. MetaHIT Consortium *et al.* A human gut microbial gene catalogue established by metagenomic sequencing. *Nature* **464**, 59–65 (2010).
279. The Human Microbiome Project Consortium. Structure, function and diversity of the healthy human microbiome. *Nature* **486**, 207–214 (2012).

280. Martínez, N., Hidalgo-Cantabrana, C., Delgado, S., Margolles, A. & Sánchez, B. Filling the gap between collection, transport and storage of the human gut microbiota. *Sci Rep* **9**, 8327 (2019).
281. Mowat, A. M. & Agace, W. W. Regional specialization within the intestinal immune system. *Nat Rev Immunol* **14**, 667–685 (2014).
282. Jalili-Firoozinezhad, S. *et al.* A complex human gut microbiome cultured in an anaerobic intestine-on-a-chip. *Nat Biomed Eng* **3**, 520–531 (2019).
283. McGrath, C. J. *et al.* Development of a novel human intestinal model to elucidate the effect of anaerobic commensals on *Escherichia coli* infection. *Dis Model Mech* dmm.049365 (2022) doi:10.1242/dmm.049365.
284. Valles-Colomer, M. *et al.* The person-to-person transmission landscape of the gut and oral microbiomes. *Nature* 1–11 (2023) doi:10.1038/s41586-022-05620-1.
285. Chitturi, R., Baddam, V. R., Prasad, L., Prashanth, L. & Kattapagari, K. A review on role of essential trace elements in health and disease. *J NTR Univ Health Sci* **4**, 75 (2015).
286. Kau, A. L., Ahern, P. P., Griffin, N. W., Goodman, A. L. & Gordon, J. I. Human nutrition, the gut microbiome and the immune system. *Nature* **474**, 327–336 (2011).
287. Lu, J., Stewart, A. J., Sadler, P. J., Pinheiro, T. J. T. & Blindauer, C. A. Albumin as a zinc carrier: properties of its high-affinity zinc-binding site. *Biochm. Soc. Trans.* **36**, 1317–1321 (2008).
288. *Vitamin and mineral requirements in human nutrition*. (2004).
289. Krebs, N. F. Overview of zinc absorption and excretion in the human gastrointestinal tract. *J. Nutr.* **130**, 1374S–7S (2000).
290. Maares, M. & Haase, H. A Guide to Human Zinc Absorption: General Overview and Recent Advances of In Vitro Intestinal Models. *Nutrients* **12**, (2020).
291. Lech, T. & Sadlik, J. K. Zinc in postmortem body tissues and fluids. *Biol Trace Elem Res* **142**, 11–17 (2011).
292. Cousins, R. J. *et al.* Regulation of Zinc Metabolism and Genomic Outcomes. *J Nutr* **133**, 1521S-1526S (2003).
293. Maret, W. Zinc Biochemistry: From a Single Zinc Enzyme to a Key Element of Life12. *Adv Nutr* **4**, 82–91 (2013).
294. Ibs, K.-H. & Rink, L. Zinc-altered immune function. *J. Nutr.* **133**, 1452S–6S (2003).
295. Lowe, N. M. *et al.* EURRECA—Estimating Zinc Requirements for Deriving Dietary Reference Values. *Critical Reviews in Food Science and Nutrition* **53**, 1110–1123 (2013).
296. Choi, S. & Bird, A. J. Zinc'ing sensibly: controlling zinc homeostasis at the transcriptional level. *Metallomics : integrated biometal science* **6**, 1198–1215 (2014).
297. Marreiro, D. D. N. *et al.* Zinc and Oxidative Stress: Current Mechanisms. *Antioxidants* **6**, 24 (2017).
298. Yu, K.-N. *et al.* Zinc oxide nanoparticle induced autophagic cell death and mitochondrial damage via reactive oxygen species generation. *Toxicology in Vitro* **27**, 1187–1195 (2013).
299. Lee, S. R. Critical Role of Zinc as Either an Antioxidant or a Prooxidant in Cellular Systems. *Oxid Med Cell Longev* **2018**, 9156285 (2018).
300. Ivanov, A. V., Bartosch, B. & Isaguliants, M. G. Oxidative Stress in Infection and Consequent Disease. *Oxid Med Cell Longev* **2017**, 3496043 (2017).
301. Gammoh, N. Z. & Rink, L. Zinc in Infection and Inflammation. *Nutrients* **9**, 624 (2017).
302. Cassandri, M. *et al.* Zinc-finger proteins in health and disease. *Cell Death Discov.* **3**, 1–12 (2017).
303. Mikhaylina, A., Ksibe, A. Z., Scanlan, D. J. & Blindauer, C. A. Bacterial zinc uptake regulator proteins and their regulons. *Biochem. Soc. Trans.* **46**, 983–1001 (2018).
304. Haas, C. E. *et al.* A subset of the diverse COG0523 family of putative metal chaperones is linked to zinc homeostasis in all kingdoms of life. *BMC Genomics* **10**, 470 (2009).
305. Sankaran, B. *et al.* Zinc-Independent Folate Biosynthesis: Genetic, Biochemical, and Structural Investigations Reveal New Metal Dependence for GTP Cyclohydrolase IB. *Journal of Bacteriology* **191**, 6936–6949 (2009).

306. Reed, S. *et al.* Alterations in the Gut (*Gallus gallus*) Microbiota Following the Consumption of Zinc Biofortified Wheat (*Triticum aestivum*)-Based Diet. *J. Agric. Food Chem.* **66**, 6291–6299 (2018).
307. Reed, S. *et al.* Chronic Zinc Deficiency Alters Chick Gut Microbiota Composition and Function. *Nutrients* **7**, 9768–9784 (2015).
308. Broom, L. J., Miller, H. M., Kerr, K. G. & Knapp, J. S. Effects of zinc oxide and *Enterococcus faecium* SF68 dietary supplementation on the performance, intestinal microbiota and immune status of weaned piglets. *Research in Veterinary Science* **80**, 45–54 (2006).
309. Ou, D. *et al.* Dietary supplementation with zinc oxide decreases expression of the stem cell factor in the small intestine of weanling pigs. *J. Nutr. Biochem.* **18**, 820–826 (2007).
310. Pieper, R., Vahjen, W., Neumann, K., Van Kessel, A. G. & Zentek, J. Dose-dependent effects of dietary zinc oxide on bacterial communities and metabolic profiles in the ileum of weaned pigs. *J Anim Physiol Anim Nutr (Berl)* **96**, 825–833 (2012).
311. Bolick, D. T. *et al.* Zinc deficiency alters host response and pathogen virulence in a mouse model of enteroaggregative *Escherichia coli*-induced diarrhea. *Gut Microbes* **5**, 618–627 (2014).
312. Zackular, J. P. *et al.* Dietary zinc alters the microbiota and decreases resistance to *Clostridium difficile* infection. *Nature Medicine* **22**, 1330–1334 (2016).
313. Souffriau, J. *et al.* Zinc inhibits lethal inflammatory shock by preventing microbe-induced interferon signature in intestinal epithelium. *EMBO Mol Med* **12**, (2020).
314. Q.S. Medeiros, P. H. *et al.* A murine model of diarrhea, growth impairment and metabolic disturbances with *Shigella flexneri* infection and the role of zinc deficiency. *Gut Microbes* **10**, 615–630 (2019).
315. Roura, E. *et al.* Critical review evaluating the pig as a model for human nutritional physiology. *Nutrition Research Reviews* **29**, 60–90 (2016).
316. Yu, T. *et al.* Dietary High Zinc Oxide Modulates the Microbiome of Ileum and Colon in Weaned Piglets. *Front Microbiol* **8**, 825 (2017).
317. Starke, I. C., Pieper, R., Neumann, K., Zentek, J. & Vahjen, W. The impact of high dietary zinc oxide on the development of the intestinal microbiota in weaned piglets. *FEMS Microbiol Ecol* **87**, 416–427 (2014).
318. Sazawal, S. *et al.* Efficacy of high zinc biofortified wheat in improvement of micronutrient status, and prevention of morbidity among preschool children and women - a double masked, randomized, controlled trial. *Nutrition Journal* **17**, 86 (2018).
319. Yazar, A. S., Güven, Ş. & Dinleyici, E. Ç. Effects of zinc or synbiotic on the duration of diarrhea in children with acute infectious diarrhea. *Turk J Gastroenterol* **27**, 537–540 (2016).
320. Galetti, V. *et al.* Efficacy of highly bioavailable zinc from fortified water: a randomized controlled trial in rural Beninese children. *Am. J. Clin. Nutr.* **102**, 1238–1248 (2015).
321. Sturniolo, G. C., Di Leo, V., Ferronato, A., D'Odorico, A. & D'Incà, R. Zinc Supplementation Tightens "Leaky Gut" in Crohn's Disease. *Inflamm Bowel Dis* **7**, 94–98 (2001).
322. Finamore, A., Massimi, M., Conti Devirgiliis, L. & Mengheri, E. Zinc deficiency induces membrane barrier damage and increases neutrophil transmigration in Caco-2 cells. *J. Nutr.* **138**, 1664–1670 (2008).
323. Miyoshi, Y., Tanabe, S. & Suzuki, T. Cellular zinc is required for intestinal epithelial barrier maintenance via the regulation of claudin-3 and occludin expression. *American Journal of Physiology-Gastrointestinal and Liver Physiology* **311**, G105–G116 (2016).
324. Lee, L. J., Barrett, J. A. & Poole, R. K. Genome-Wide Transcriptional Response of Chemostat-Cultured *Escherichia coli* to Zinc. *Journal of Bacteriology* **187**, 1124–1134 (2005).
325. Yamamoto, K. & Ishihama, A. Transcriptional Response of *Escherichia coli* to External Zinc. *Journal of Bacteriology* **187**, 6333–6340 (2005).
326. Xue, Y., Osborn, J., Panchal, A. & Mellies, J. L. The RpoE Stress Response Pathway Mediates Reduction of the Virulence of Enteropathogenic *Escherichia coli* by Zinc. *Appl Environ Microbiol* **81**, 3766–3774 (2015).

327. Coelho Abrantes, M., Lopes, M. de F. & Kok, J. Impact of Manganese, Copper and Zinc Ions on the Transcriptome of the Nosocomial Pathogen *Enterococcus* faecalis V583. *PLoS ONE* **6**, e26519 (2011).
328. Eckelt, E., Jarek, M., Frömke, C., Meens, J. & Goethe, R. Identification of a lineage specific zinc responsive genomic island in Mycobacterium avium ssp. paratuberculosis. *BMC Genomics* **15**, 1076 (2014).
329. Velasco, E. *et al.* A new role for Zinc limitation in bacterial pathogenicity: modulation of α-hemolysin from uropathogenic *Escherichia coli*. *Sci Rep* **8**, 1–11 (2018).
330. Corbin, B. D. *et al.* Metal Chelation and Inhibition of Bacterial Growth in Tissue Abscesses. *Science* **319**, 962–965 (2008).
331. Kloosterman, T. G., Witwicki, R. M., van der Kooi-Pol, M. M., Bijlsma, J. J. E. & Kuipers, O. P. Opposite Effects of Mn2+ and Zn2+ on PsaR-Mediated Expression of the Virulence Genes *pcpA*, *prtA*, and *psaBCA* of *Streptococcus pneumoniae*. *Journal of Bacteriology* **190**, 5382–5393 (2008).
332. Manzoor, I., Shafeeq, S., Afzal, M. & Kuipers, O. P. The Regulation of the AdcR Regulon in *Streptococcus pneumoniae* Depends Both on Zn2+- and Ni2+-Availability. *Front Cell Infect Microbiol* **5**, (2015).
333. Holley, C. L. *et al.* DksA and (p)ppGpp Have Unique and Overlapping Contributions to *Haemophilus ducreyi* Pathogenesis in Humans. *Infect Immun* **83**, 3281–3292 (2015).
334. Yun, J. *et al.* Role of the DksA-Like Protein in the Pathogenesis and Diverse Metabolic Activity of *Campylobacter jejuni*. *Journal of Bacteriology* **190**, 4512–4520 (2008).
335. Ammendola, S. *et al.* High-Affinity Zn2+ Uptake System ZnuABC Is Required for Bacterial Zinc Homeostasis in Intracellular Environments and Contributes to the Virulence of *Salmonella enterica*. *Infection and Immunity* **75**, 5867–5876 (2007).
336. Ammendola, S. *et al.* Zinc is required to ensure the expression of flagella and the ability to form biofilms in *Salmonella enterica* sv *Typhimurium*. *Metallomics* **8**, 1131–1140 (2016).
337. Nielubowicz, G. R., Smith, S. N. & Mobley, H. L. T. Zinc Uptake Contributes to Motility and Provides a Competitive Advantage to *Proteus mirabilis* during Experimental Urinary Tract Infection. *Infection and Immunity* **78**, 2823–2833 (2010).
338. Lim, J. *et al.* YkgM and ZinT proteins are required for maintaining intracellular zinc concentration and producing curli in enterohemorrhagic *Escherichia coli* (EHEC) O157:H7 under zinc deficient conditions. *International Journal of Food Microbiology* **149**, 159–170 (2011).
339. Conrady, D. G. *et al.* A zinc-dependent adhesion module is responsible for intercellular adhesion in staphylococcal biofilms. *Proceedings of the National Academy of Sciences* **105**, 19456–19461 (2008).
340. Geoghegan, J. A. *et al.* Role of Surface Protein SasG in Biofilm Formation by *Staphylococcus aureus*. *Journal of Bacteriology* **192**, 5663–5673 (2010).
341. Pederick, V. G. *et al.* ZnuA and zinc homeostasis in *Pseudomonas aeruginosa*. *Sci Rep* **5**, 13139 (2015).
342. Wu, T. *et al.* Zinc Exposure Promotes Commensal-to-Pathogen Transition in *Pseudomonas aeruginosa* Leading to Mucosal Inflammation and Illness in Mice. *International Journal of Molecular Sciences* **22**, 13321 (2021).
343. Hancock, V., Dahl, M. & Klemm, P. Abolition of Biofilm Formation in Urinary Tract *Escherichia coli* and Klebsiella Isolates by Metal Interference through Competition for Fur. *Appl. Environ. Microbiol.* **76**, 3836–3841 (2010).
344. Bolick, D. T. *et al.* Critical Role of Zinc in a New Murine Model of Enterotoxigenic *Escherichia coli* Diarrhea. *Infect Immun* **86**, (2018).
345. Crane, J. K., Broome, J. E., Reddinger, R. M. & Werth, B. B. Zinc protects against shiga-toxigenic *Escherichia coli* by acting on host tissues as well as on bacteria. *BMC Microbiol* **14**, 145 (2014).

346. Li, K., Gifford, A. H., Hampton, T. H. & O'Toole, G. A. Availability of Zinc Impacts Interactions between *Streptococcus sanguinis* and *Pseudomonas aeruginosa* in Coculture. *J Bacteriol* **202**, (2020).
347. An, D., Danhorn, T., Fuqua, C. & Parsek, M. R. Quorum sensing and motility mediate interactions between *Pseudomonas aeruginosa* and *Agrobacterium tumefaciens* in biofilm cocultures. *PNAS* **103**, 3828–3833 (2006).
348. Cendra, M. del M., Blanco-Cabra, N., Pedraz, L. & Torrents, E. Optimal environmental and culture conditions allow the in vitro coexistence of *Pseudomonas aeruginosa* and *Staphylococcus aureus* in stable biofilms. *Sci Rep* **9**, 16284 (2019).
349. Cendra, M. del M. & Torrents, E. *Pseudomonas aeruginosa* biofilms and their partners in crime. *Biotechnology Advances* **49**, 107734 (2021).
350. Filkins, L. M. *et al.* Coculture of *Staphylococcus aureus* with *Pseudomonas aeruginosa* Drives S. aureus towards Fermentative Metabolism and Reduced Viability in a Cystic Fibrosis Model. *J Bacteriol* **197**, 2252–2264 (2015).
351. Yang, L. *et al.* Pattern differentiation in co-culture biofilms formed by *Staphylococcus aureus* and *Pseudomonas aeruginosa*. *FEMS Immunol Med Microbiol* **62**, 339–347 (2011).
352. Gounani, Z., Şen Karaman, D., Venu, A. P., Cheng, F. & Rosenholm, J. M. Coculture of P. aeruginosa and S. aureus on cell derived matrix - An in vitro model of biofilms in infected wounds. *J Microbiol Methods* **175**, 105994 (2020).
353. Tognon, M., Köhler, T., Luscher, A. & van Delden, C. Transcriptional profiling of *Pseudomonas aeruginosa* and *Staphylococcus aureus* during in vitro co-culture. *BMC Genomics* **20**, 30 (2019).
354. Scott, J. E. *et al. Pseudomonas aeruginosa* Can Inhibit Growth of Streptococcal Species via Siderophore Production. *J Bacteriol* **201**, e00014-19 (2019).
355. Li, K., Gifford, A. H., Hampton, T. H. & O'Toole, G. A. Availability of Zinc Impacts Interactions between *Streptococcus sanguinis* and *Pseudomonas aeruginosa* in Coculture. *Journal of Bacteriology* **202**, (2020).
356. Kim, H. W., Kim, J. K., Park, I. & Lee, S. J. Establishing in vitro and in vivo Co-culture Models of *Staphylococcus epidermidis* and *Enterococcus faecalis* to Evaluate the Effect of Topical Fluoroquinolone on Ocular Microbes. *Front Med (Lausanne)* **8**, 670199 (2021).
357. Cucaita, A., Piochon, M. & Villemur, R. Co-culturing *Hyphomicrobium nitrativorans* strain NL23 and *Methylophaga nitratireducenticrescens* strain JAM1 allows sustainable denitrifying activities under marine conditions. *PeerJ* **9**, e12424 (2021).
358. Mansky, J. *et al.* The Influence of Genes on the 'Killer Plasmid' of *Dinoroseobacter shibae* on Its Symbiosis With the *Dinoflagellate Prorocentrum* minimum. *Front Microbiol* **12**, 804767 (2021).
359. Reina, J. C., Pérez, P. & Llamas, I. Quorum Quenching Strains Isolated from the Microbiota of Sea Anemones and Holothurians Attenuate *Vibriocorallilyticus* Virulence Factors and Reduce Mortality in Artemiasalina. *Microorganisms* **10**, 631 (2022).
360. Hamilton, A. L., Kamm, M. A., Ng, S. C. & Morrison, M. *Proteus* spp. as Putative Gastrointestinal Pathogens. *Clin Microbiol Rev* **31**, e00085-17 (2018).
361. Raineri, E. J. M. *et al. Staphylococcus aureus* populations from the gut and the blood are not distinguished by virulence traits—a critical role of host barrier integrity. *Microbiome* **10**, 239 (2022).
362. Oxoid - Dedicated to Microbiology. http://www.oxoid.com/UK/blue/index.asp?c=UK&lang=EN.
363. Naylor, P. G. D. The Effect of Electrolytes or Carbohydrates in a Sodium Chloride Deficient Medium on the Formation of Discrete Colonies of *Proteus* and the Influence of these Substances on Growth in Liquid Culture. *Journal of Applied Bacteriology* **27**, 422–431 (1964).
364. Jung, B. & Hoilat, G. J. MacConkey Medium. in *StatPearls* (StatPearls Publishing, 2023).
365. Mannitol Salt Agar | Principle | Preparation | Interpretation. https://microbiologie-clinique.com/Mannitol-Salt-Agar.html.

366. Jones, B. v., Sun, F. & Marchesi, J. r. Using skimmed milk agar to functionally screen a gut metagenomic library for proteases may lead to false positives. *Letters in Applied Microbiology* **45**, 418–420 (2007).
367. Tryptone Soy Broth. *https://www.neogen.com* https://www.neogen.com/en-gb/categories/microbiology/tryptone-soy-broth/?utm_medium=SocialShare.
368. Sezonov, G., Joseleau-Petit, D. & D'Ari, R. *Escherichia coli* Physiology in Luria-Bertani Broth. *J Bacteriol* **189**, 8746–8749 (2007).
369. Brain Heart Infusion Agar (Dehydrated). https://www.thermofisher.com/order/catalog/product/CM1136B.
370. Nutrient Broth (Dehydrated). https://www.thermofisher.com/order/catalog/product/CM0001B.
371. Tankeshwar, A. CLED Agar: Composition, Uses, Colony Characteristics • Microbe Online. *Microbe Online* https://microbeonline.com/cled-agar-composition-uses-typical-colony-characteristics/ (2015).
372. Blood Agar Base No. 2 with Sheep Blood. https://www.thermofisher.com/order/catalog/product/PB0115A.
373. de man, rogosa and sharpe (MRS) agar. in *Progress in Industrial Microbiology* (eds. Corry, J. E. L., Curtis, G. D. W. & Baird, R. M.) vol. 37 511–513 (Elsevier, 2003).
374. Determination of Bacterial CFU Using 'Miles And Misra Technique'. https://www.biotechnologyforums.com/thread-2028.html.
375. The Madin Darby Canine Kidney (MDCK) Epithelial Cell Monolayer as a Model Cellular Transport Barrier | SpringerLink. https://link.springer.com/article/10.1023/A:1015807904558.
376. Woese, C. R. & Fox, G. E. Phylogenetic structure of the prokaryotic domain: the primary kingdoms. *Proc Natl Acad Sci U S A* **74**, 5088–5090 (1977).
377. Silva. https://www.arb-silva.de/.
378. NCIMB | Microbiology | Analytical Services | Biomaterial Storage. https://www.ncimb.com/.
379. GenScript Pcr Primer Design. https://www.genscript.com/tools/pcr-primers-designer.
380. OligoAnalyzer Tool - primer analysis | IDT. https://eu.idtdna.com/pages/tools/oligoanalyzer?returnurl=%2Fcalc%2Fanalyzer.
381. Oligo Analyzer For Tm Calculation & Primer Analysis. https://www.sigmaaldrich.com/GB/en/technical-documents/technical-article/genomics/pcr/oligo-analyzer-for-tm-calculation-primer-analysis.
382. MAN0012027_TaqDNAPolymerase_recombinant_5_UuL_500U_UG.pdf.
383. Jia, X. *et al.* Identification of Essential Genes Associated With Prodigiosin Production in *Serratia marcescens* FZSF02. *Frontiers in Microbiology* **12**, 2101 (2021).
384. Besler, K. R. & Little, E. L. Diversity of *Serratia marcescens* Strains Associated with Cucurbit Yellow Vine Disease in Georgia. *Plant Dis* **101**, 129–136 (2017).
385. Duary, R. K., Batish, V. K. & Grover, S. Expression of the atpD gene in probiotic *Lactobacillus plantarum* strains under in vitro acidic conditions using RT-qPCR. *Res Microbiol* **161**, 399–405 (2010).
386. Sakuraoka, R., Suzuki, T. & Morohoshi, T. Distribution and Genetic Diversity of Genes Involved in Quorum Sensing and Prodigiosin Biosynthesis in the Complete Genome Sequences of *Serratia marcescens*. *Genome Biology and Evolution* **11**, 931–936 (2019).
387. Zhang, Y., Wang, H., Li, Y., Hou, Y. & Hao, C. Drug susceptibility and molecular epidemiology of *Escherichia coli* in bloodstream infections in Shanxi, China. *PeerJ* **9**, e12371 (2021).
388. Čepl, J., Scholtz, V. & Scholtzová, J. Modeling of concentric pattern of *Serratia marcescens* colony. *Arch Microbiol* **201**, 87–92 (2019).
389. Aswad, D. & Koshland, D. E. Role of methionine in bacterial chemotaxis. *J Bacteriol* **118**, 640–645 (1974).

390. ROMANOWSKI, E. G. *et al.* Thermoregulation of Prodigiosin Biosynthesis by *Serratia marcescens* is Controlled at the Transcriptional Level and Requires HexS. *Pol J Microbiol* **68**, 43–50 (2019).
391. Sun, Y. *et al.* Improved Prodigiosin Production by Relieving CpxR Temperature-Sensitive Inhibition. *Front. Bioeng. Biotechnol.* **8**, (2020).
392. Mun, J. J., Tam, C., Evans, D. J. & Fleiszig, S. M. J. Modulation of epithelial immunity by mucosal fluid. *Sci Rep* **1**, 8 (2011).
393. ATCC: The Global Bioresource Center. https://www.atcc.org/.
394. BLAST: Basic Local Alignment Search Tool. https://blast.ncbi.nlm.nih.gov/Blast.cgi.
395. Jumper, J. *et al.* Highly accurate protein structure prediction with AlphaFold. *Nature* **596**, 583–589 (2021).
396. Ammendola, S. *et al.* Zinc is required to ensure the expression of flagella and the ability to form biofilms in *Salmonella enterica* sv *Typhimurium*. *Metallomics* **8**, 1131–1140 (2016).
397. Lee, L. J., Barrett, J. A. & Poole, R. K. Genome-wide transcriptional response of chemostat-cultured *Escherichia coli* to zinc. *J Bacteriol* **187**, 1124–1134 (2005).
398. Lane, D. J. *et al.* Rapid determination of 16S ribosomal RNA sequences for phylogenetic analyses. *Proc Natl Acad Sci U S A* **82**, 6955–6959 (1985).
399. Tamaki, H. *et al.* Analysis of 16S rRNA Amplicon Sequencing Options on the Roche/454 Next-Generation Titanium Sequencing Platform. *PLOS ONE* **6**, e25263 (2011).
400. RT-PCR / RT-qPCR Troubleshooting. https://www.sigmaaldrich.com/GB/en/technical-documents/technical-article/genomics/pcr/troubleshooting.
401. Gallardo, K., Candia, J. E., Remonsellez, F., Escudero, L. V. & Demergasso, C. S. The Ecological Coherence of Temperature and Salinity Tolerance Interaction and Pigmentation in a Non-marine Vibrio Isolated from Salar de Atacama. *Frontiers in Microbiology* **7**, (2016).
402. Bunting, M. I., Robinow, C. F. & Bunting, H. Factors Affecting The Elaboration Of Pigment And Polysaccharide By *Serratia Marcescens*. *J Bacteriol* **58**, 114–115 (1949).
403. Clements-Jewery, S. The reversal of glucose repressed prodigiosin production in *Serratia marcescens* by the cyclic 3'5'-adenosine monophosphate inhibitor theophylline. *Experientia* **32**, 421–422 (1976).
404. Solé, M., Rius, N. & Lorén, J. G. Rapid extracellular acidification induced by glucose metabolism in non-proliferating cells of *Serratia marcescens*. *Int Microbiol* **3**, 39–43 (2000).
405. Jochim, A. *et al.* Methionine Limitation Impairs Pathogen Expansion and Biofilm Formation Capacity. *Appl Environ Microbiol* **85**, e00177-19 (2019).
406. Luo, S. & Levine, R. L. Methionine in proteins defends against oxidative stress. *FASEB J* **23**, 464–472 (2009).
407. Peter-Getzlaff, S. *et al.* Detection of AmpC Beta-Lactamase in *Escherichia coli*: Comparison of Three Phenotypic Confirmation Assays and Genetic Analysis ▿ . *J Clin Microbiol* **49**, 2924–2932 (2011).
408. Antonoplis, A., Zang, X., Wegner, T., Wender, P. A. & Cegelski, L. A Vancomycin-Arginine Conjugate Inhibits Growth of Carbapenem-resistant *E. coli* and Targets Cell-Wall Synthesis. *ACS Chem Biol* **14**, 2065–2070 (2019).
409. Duan, Q., Zhou, M., Zhu, L. & Zhu, G. Flagella and bacterial pathogenicity. *Journal of Basic Microbiology* **53**, 1–8 (2013).
410. Jose, R. & Singh, V. Swarming in Bacteria: A Tale of Plasticity in Motility Behavior. *J Indian Inst Sci* **100**, 515–524 (2020).
411. Jamal, M. *et al.* Bacterial biofilm and associated infections. *J Chin Med Assoc* **81**, 7–11 (2018).
412. Schindelin, J. *et al.* Fiji: an open-source platform for biological-image analysis. *Nat Methods* **9**, 676–682 (2012).
413. Landi, N., Ragucci, S. & Di Maro, A. Amino Acid Composition of Milk from Cow, Sheep and Goat Raised in Ailano and Valle Agricola, Two Localities of 'Alto Casertano' (Campania Region). *Foods* **10**, 2431 (2021).

414. Teichert, J. *et al.* Milk fermentation affects amino acid and fatty acid profile of mare milk from Polish Coldblood mares. *International Dairy Journal* **121**, 105137 (2021).
415. Sharma, A. & Puhar, A. Gentamicin Protection Assay to Determine the Number of Intracellular Bacteria during Infection of Human TC7 Intestinal Epithelial Cells by *Shigella flexneri*. *Bio Protoc* **9**, e3292 (2019).
416. Seddik, H. A. *et al. Lactobacillus plantarum* and Its Probiotic and Food Potentialities. *Probiotics & Antimicro. Prot.* **9**, 111–122 (2017).
417. Pletnev, P., Osterman, I., Sergiev, P., Bogdanov, A. & Dontsova, O. Survival guide: *Escherichia coli* in the stationary phase. *Acta Naturae* **7**, 22–33 (2015).
418. Aarestrup, F. M., Cavaco, L. & Hasman, H. Decreased susceptibility to zinc chloride is associated with methicillin resistant *Staphylococcus aureus* CC398 in Danish swine. *VET MICROBIOL* **142**, 455–457 (2010).
419. Ghazisaeedi, F. *et al.* Phenotypic zinc resistance does not correlate with antimicrobial multi-resistance in fecal *E. coli* isolates of piglets. *Gut Pathogens* **12**, 4 (2020).
420. Johanns, V. C. *et al.* Effects of a Four-Week High-Dosage Zinc Oxide Supplemented Diet on Commensal *Escherichia coli* of Weaned Pigs. *Front. Microbiol.* **10**, (2019).
421. Yamamoto, K. & Ishihama, A. Transcriptional Response of *Escherichia coli* to External Zinc. *Journal of Bacteriology* **187**, 6333–6340 (2005).
422. Leonardi, A. *et al.* Zinc Uptake by Lactic Acid Bacteria. *ISRN Biotechnology* vol. 2013 e312917 https://www.hindawi.com/journals/isrn/2013/312917/ (2013).
423. Ong, C. Y., Walker, M. J. & McEwan, A. G. Zinc disrupts central carbon metabolism and capsule biosynthesis in *Streptococcus pyogenes*. *Sci Rep* **5**, (2015).
424. Mazaheri Nezhad Fard, R., Heuzenroeder, M. W. & Barton, M. D. Antimicrobial and heavy metal resistance in commensal enterococci isolated from pigs. *Veterinary Microbiology* **148**, 276–282 (2011).
425. Lam, L. N., Brunson, D. N., Molina, J. J., Flores-Mireles, A. L. & Lemos, J. A. The AdcACB/AdcAII system is essential for zinc homeostasis and an important contributor of *Enterococcus faecalis* virulence. *Virulence* **13**, 592–608.
426. Ong, C. Y., Walker, M. J. & McEwan, A. G. Zinc disrupts central carbon metabolism and capsule biosynthesis in *Streptococcus pyogenes*. *Sci Rep* **5**, 10799 (2015).
427. Fazli, M. *et al.* Nonrandom Distribution of *Pseudomonas aeruginosa* and *Staphylococcus aureus* in Chronic Wounds. *Journal of Clinical Microbiology* **47**, 4084–4089 (2009).
428. Doing, G., Koeppen, K., Occipinti, P., Harty, C. E. & Hogan, D. A. Conditional antagonism in co-cultures of *Pseudomonas aeruginosa* and *Candida albicans:* An intersection of ethanol and phosphate signaling distilled from dual-seq transcriptomics. *PLOS Genetics* **16**, e1008783 (2020).
429. Vitko, N. P., Grosser, M. R., Khatri, D., Lance, T. R. & Richardson, A. R. Expanded Glucose Import Capability Affords *Staphylococcus aureus* Optimized Glycolytic Flux during Infection. *mBio* **7**, e00296-16 (2016).
430. Naureen, Z. *et al.* Bacteriophages presence in nature and their role in the natural selection of bacterial populations. *Acta Biomed* **91**, e2020024 (2020).
431. Duerkop, B. A., Clements, C. V., Rollins, D., Rodrigues, J. L. M. & Hooper, L. V. A composite bacteriophage alters colonization by an intestinal commensal bacterium. *Proc Natl Acad Sci U S A* **109**, 17621–17626 (2012).
432. Brives, C. & Pourraz, J. Phage therapy as a potential solution in the fight against AMR: obstacles and possible futures. *Palgrave Commun* **6**, 1–11 (2020).
433. Khalid, A., Lin, R. C. Y. & Iredell, J. R. A Phage Therapy Guide for Clinicians and Basic Scientists: Background and Highlighting Applications for Developing Countries. *Frontiers in Microbiology* **11**, 3417 (2021).

434. Makumi, A., Mhone, A. L., Odaba, J., Guantai, L. & Svitek, N. Phages for Africa: The Potential Benefit and Challenges of Phage Therapy for the Livestock Sector in Sub-Saharan Africa. *Antibiotics (Basel)* **10**, 1085 (2021).
435. Nagel, T. E. *et al.* The Developing World Urgently Needs Phages to Combat Pathogenic Bacteria. *Frontiers in Microbiology* **7**, 882 (2016).
436. Hill, C. *et al.* The International Scientific Association for Probiotics and Prebiotics consensus statement on the scope and appropriate use of the term probiotic. *Nat Rev Gastroenterol Hepatol* **11**, 506–514 (2014).
437. Kotzampassi, K. & Giamarellos-Bourboulis, E. J. Probiotics for infectious diseases: more drugs, less dietary supplementation. *Int J Antimicrob Agents* **40**, 288–296 (2012).
438. Li, X., Wang, Q., Hu, X. & Liu, W. Current Status of Probiotics as Supplements in the Prevention and Treatment of Infectious Diseases. *Frontiers in Cellular and Infection Microbiology* **12**, (2022).
439. Mokoena, M. P., Omatola, C. A. & Olaniran, A. O. Applications of Lactic Acid Bacteria and Their Bacteriocins against Food Spoilage Microorganisms and Foodborne Pathogens. *Molecules* **26**, (2021).
440. Gao, Z. *et al.* Inhibitory Effect of Lactic Acid Bacteria on Foodborne Pathogens: A Review. *J Food Prot* **82**, 441–453 (2019).
441. Rocha-Ramírez, L. M., Hernández-Chiñas, U., Moreno-Guerrero, S. S., Ramírez-Pacheco, A. & Eslava, C. A. In Vitro Effect of the Cell-Free Supernatant of the *Lactobacillus casei* Strain IMAU60214 against the Different Pathogenic Properties of Diarrheagenic *Escherichia coli*. *Microorganisms* **11**, 1324 (2023).
442. Osset, J., Bartolomé, R. M., García, E. & Andreu, A. Assessment of the capacity of Lactobacillus to inhibit the growth of uropathogens and block their adhesion to vaginal epithelial cells. *J Infect Dis* **183**, 485–491 (2001).
443. Lee, J.-E., Lee, N.-K. & Paik, H.-D. Antimicrobial and anti-biofilm effects of probiotic *Lactobacillus plantarum* KU200656 isolated from kimchi. *Food Sci Biotechnol* **30**, 97–106 (2020).
444. Lee, C. M., Monson, R. E., Adams, R. M. & Salmond, G. P. C. The LacI–Family Transcription Factor, RbsR, Is a Pleiotropic Regulator of Motility, Virulence, Siderophore and Antibiotic Production, Gas Vesicle Morphogenesis and Flotation in *Serratia*. *Frontiers in Microbiology* **8**, (2017).
445. Robinson, J. P. *et al.* Using Scattering to Identify Bacterial Pathogens. *Optics & Photonics News* **22**, 20 (2011).
446. Front Matter. in *Mandell, Douglas, and Bennett's Principles and Practice of Infectious Diseases (Eighth Edition)* (eds. Bennett, J. E., Dolin, R. & Blaser, M. J.) i–ii (W.B. Saunders, 2015). doi:10.1016/B978-1-4557-4801-3.00325-8.
447. Bunting, M. I., Robinow, C. F. & Bunting, H. Factors Affecting The Elaboration Of Pigment And Polysaccharide By *Serratia Marcescens*. *J Bacteriol* **58**, 114–115 (1949).
448. Solé, M., Francia, A., Rius, N. & Lorén, J. g. The role of pH in the 'glucose effect' on prodigiosin production by non-proliferating cells of *Serratia marcescens*. *Letters in Applied Microbiology* **25**, 81–84 (1997).
449. Fender, J. E. *et al. Serratia marcescens* Quinoprotein Glucose Dehydrogenase Activity Mediates Medium Acidification and Inhibition of Prodigiosin Production by Glucose. *Appl Environ Microbiol* **78**, 6225–6235 (2012).
450. Ng, W. High Cell Density Cultivation of *Escherichia coli* DH5α in Shake Flasks with a New Formulated Medium. *BTBP* **2**, 01–11 (2021).
451. Zhang, Q., Fan, N.-S., Fu, J.-J., Huang, B.-C. & Jin, R.-C. Role and application of quorum sensing in anaerobic ammonium oxidation (anammox) process: A review. *Critical Reviews in Environmental Science and Technology* **51**, 626–648 (2021).

452. Liu, J. *et al.* Metabolic co-dependence gives rise to collective oscillations within biofilms. *Nature* **523**, 550–554 (2015).
453. Bocci, F., Suzuki, Y., Lu, M. & Onuchic, J. N. Role of metabolic spatiotemporal dynamics in regulating biofilm colony expansion. *Proc Natl Acad Sci U S A* **115**, 4288–4293 (2018).
454. Luo, N., Wang, S., Lu, J., Ouyang, X. & You, L. Collective colony growth is optimized by branching pattern formation in *Pseudomonas aeruginosa*. *Mol Syst Biol* **17**, e10089 (2021).
455. Xiong, L. *et al.* Flower-like patterns in multi-species bacterial colonies. *eLife* **9**, e48885 (2020).
456. Matsuyama, T. *et al.* Dynamic aspects of the structured cell population in a swarming colony of *Proteus mirabilis*. *J Bacteriol* **182**, 385–393 (2000).
457. Rauprich, O. *et al.* Periodic phenomena in *Proteus mirabilis* swarm colony development. *J Bacteriol* **178**, 6525–6538 (1996).
458. Kang, Y. *et al.* Unraveling the role of quorum sensing-dependent metabolic homeostasis of the activated methyl cycle in a cooperative population of *Burkholderia glumae*. *Sci Rep* **9**, 11038 (2019).
459. Bin, P. *et al.* Perspective: Methionine Restriction–Induced Longevity—A Possible Role for Inhibiting the Synthesis of Bacterial Quorum Sensing Molecules. *Advances in Nutrition* **11**, 773 (2020).
460. Zhu, Y. L., Hou, H. M., Zhang, G. L., Wang, Y. F. & Hao, H. S. AHLs Regulate Biofilm Formation and Swimming Motility of Hafnia alvei H4. *Front Microbiol* **10**, 1330 (2019).
461. Sezonov, G., Joseleau-Petit, D. & D'Ari, R. *Escherichia coli* Physiology in Luria-Bertani Broth. *Journal of Bacteriology* **189**, 8746–8749 (2007).
462. Rubiera, C. O. AlphaFold 2 is here: what's behind the structure prediction miracle | Oxford Protein Informatics Group. https://www.blopig.com/blog/2021/07/alphafold-2-is-here-whats-behind-the-structure-prediction-miracle/ (2021).
463. Peariso, K., Goulding, C. W., Huang, S., Matthews, R. G. & Penner-Hahn, J. E. Characterization of the Zinc Binding Site in Methionine Synthase Enzymes of *Escherichia coli*: The Role of Zinc in the Methylation of Homocysteine. *J. Am. Chem. Soc.* **120**, 8410–8416 (1998).
464. Tiensuu, T., Andersson, C., Rydén, P. & Johansson, J. Cycles of light and dark co-ordinate reversible colony differentiation in Listeria monocytogenes. *Mol Microbiol* **87**, 909–924 (2013).
465. Shanks, R. M. Q., Stella, N. A., Arena, K. E. & Fender, J. E. Mutation of crp mediates *Serratia marcescens* serralysin and global secreted protein production. *Res Microbiol* **164**, 38–45 (2013).
466. Li, H. *et al.* Reactive Oxygen Species in Pathogen Clearance: The Killing Mechanisms, the Adaption Response, and the Side Effects. *Front Microbiol* **11**, 622534 (2021).
467. Stokes, J. M., Lopatkin, A. J., Lobritz, M. A. & Collins, J. J. Bacterial Metabolism and Antibiotic Efficacy. *Cell Metab* **30**, 251–259 (2019).
468. Shan, Y. *et al.* ATP-Dependent Persister Formation in *Escherichia coli*. *mBio* **8**, e02267-16 (2017).
469. Pu, Y. *et al.* ATP-Dependent Dynamic Protein Aggregation Regulates Bacterial Dormancy Depth Critical for Antibiotic Tolerance. *Mol Cell* **73**, 143-156.e4 (2019).
470. Lobritz, M. A. *et al.* Antibiotic efficacy is linked to bacterial cellular respiration. *Proceedings of the National Academy of Sciences* **112**, 8173–8180 (2015).
471. Høiby, N., Bjarnsholt, T., Givskov, M., Molin, S. & Ciofu, O. Antibiotic resistance of bacterial biofilms. *Int J Antimicrob Agents* **35**, 322–332 (2010).
472. Pamp, S. J., Gjermansen, M., Johansen, H. K. & Tolker-Nielsen, T. Tolerance to the antimicrobial peptide colistin in *Pseudomonas aeruginosa* biofilms is linked to metabolically active cells, and depends on the pmr and mexAB-oprM genes. *Mol Microbiol* **68**, 223–240 (2008).
473. Motamedi, H., Asghari, B., Tahmasebi, H. & Arabestani, M. R. Identification of Hemolysine Genes and their Association with Antimicrobial Resistance Pattern among Clinical Isolates of *Staphylococcus aureus* in West of Iran. *Adv Biomed Res* **7**, 153 (2018).

474. Lugtenberg, B., Peters, R., Bernheimer, H. & Berendsen, W. Influence of cultural conditions and mutations on the composition of the outer membrane proteins of *Escherichia coli*. *Mol Gen Genet* **147**, 251–262 (1976).
475. Alphen, W. V. & Lugtenberg, B. Influence of osmolarity of the growth medium on the outer membrane protein pattern of *Escherichia coli*. *J Bacteriol* **131**, 623–630 (1977).
476. Stokes, J. M. *et al.* Cold Stress Makes *Escherichia coli* Susceptible to Glycopeptide Antibiotics by Altering Outer Membrane Integrity. *Cell Chem Biol* **23**, 267–277 (2016).
477. Ray, C., Shenoy, A. T., Orihuela, C. J. & González-Juarbe, N. Killing of *Serratia marcescens* biofilms with chloramphenicol. *Ann Clin Microbiol Antimicrob* **16**, 19 (2017).
478. Matsumoto, K. Role of bacterial proteases in pseudomonal and *Serratia* keratitis. **385**, 1007–1016 (2004).
479. Günther, J. & Seyfert, H.-M. The first line of defence: insights into mechanisms and relevance of phagocytosis in epithelial cells. *Semin Immunopathol* **40**, 555–565 (2018).
480. Plotkowski, M. C. *et al. Pseudomonas aeruginosa* internalization by human epithelial respiratory cells depends on cell differentiation, polarity, and junctional complex integrity. *Am J Respir Cell Mol Biol* **20**, 880–890 (1999).
481. Palma Medina, L. M. *et al.* Metabolic Cross-talk Between Human Bronchial Epithelial Cells and Internalized *Staphylococcus aureus* as a Driver for Infection*. *Molecular & Cellular Proteomics* **18**, 892–908 (2019).
482. TRIBBLE, G. D. & LAMONT, R. J. Bacterial invasion of epithelial cells and spreading in periodontal tissue. *Periodontol 2000* **52**, 68–83 (2010).
483. Eick, S. & Pfister, W. Efficacy of antibiotics against periodontopathogenic bacteria within epithelial cells: an in vitro study. *J Periodontol* **75**, 1327–1334 (2004).

APPENDIX

I. Microscopic observation of samples from liquid co-culture (48 hours) of *L. plantarum* with Gram-negative bacteria *E. coli* and *P. aeruginosa*

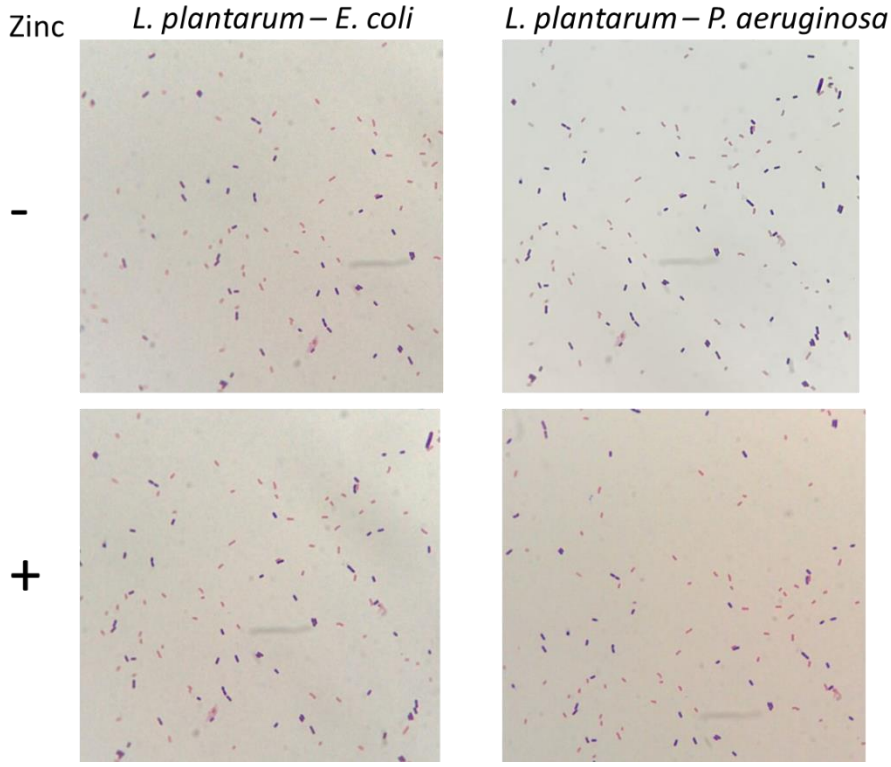

Appendix Figure 1: **Microscopical observation of bacterial cells from liquid co-culture of *L. plantarum* with Gram-negative bacteria**. Samples were collected from the liquid co-culture of *L. plantarum* and *E. coli* (left) or *L. plantarum* and *P. aeruginosa* (right) after 48 hours of growth at 37oC, 200 rpm with or without zinc. Gram-negative bacterial (*E. coli* or *P. aeruginosa*) are pink rods, while cells of the Gramp-positive *L. plantarum* are purple rods as a result of the Gram-staining colouration. Optical microscope: Nikon ECLIPSE E200 Microscope, 40x, 1.000x magnification.

II. Bacterial co-culture competition experiment results

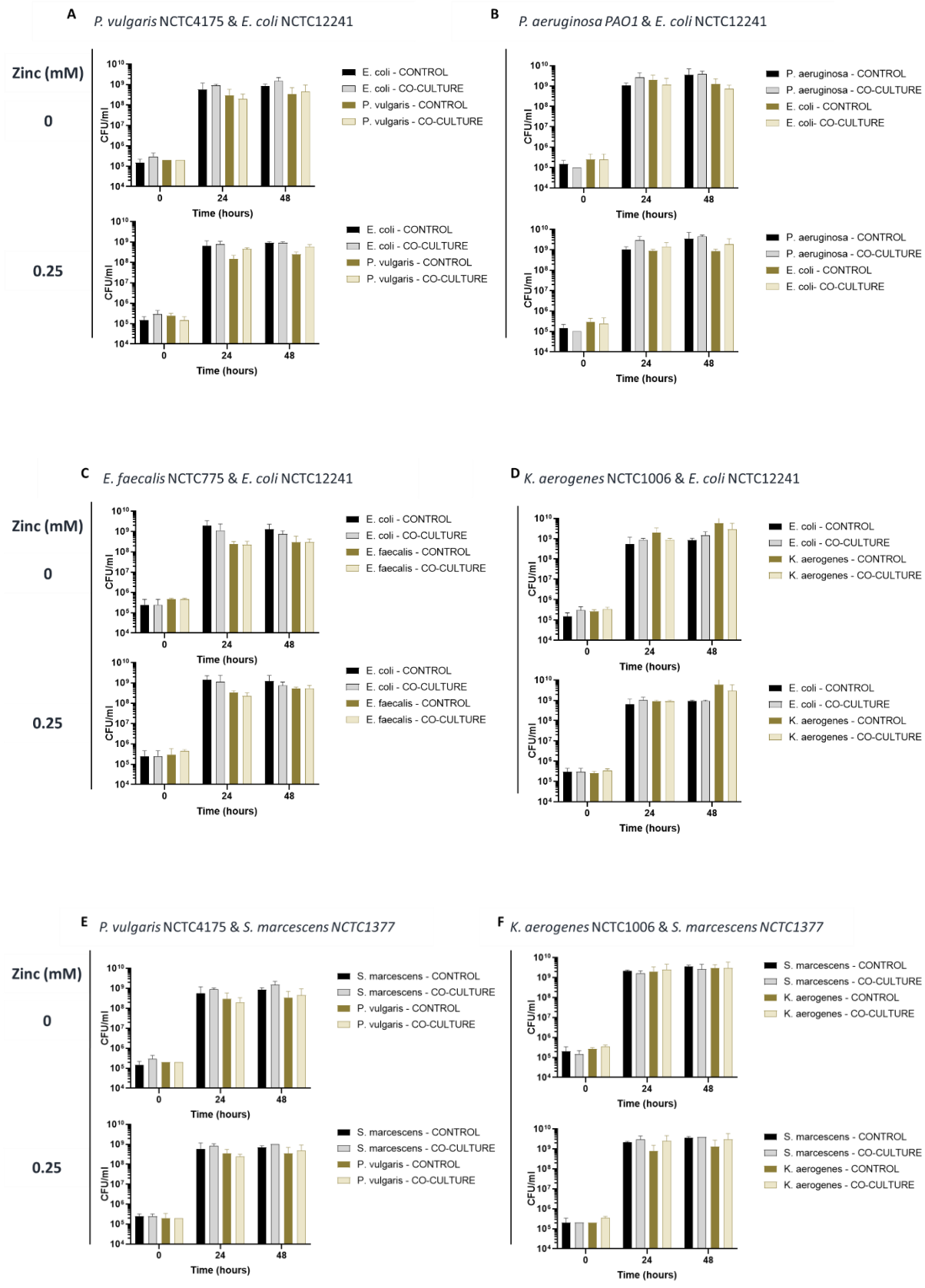

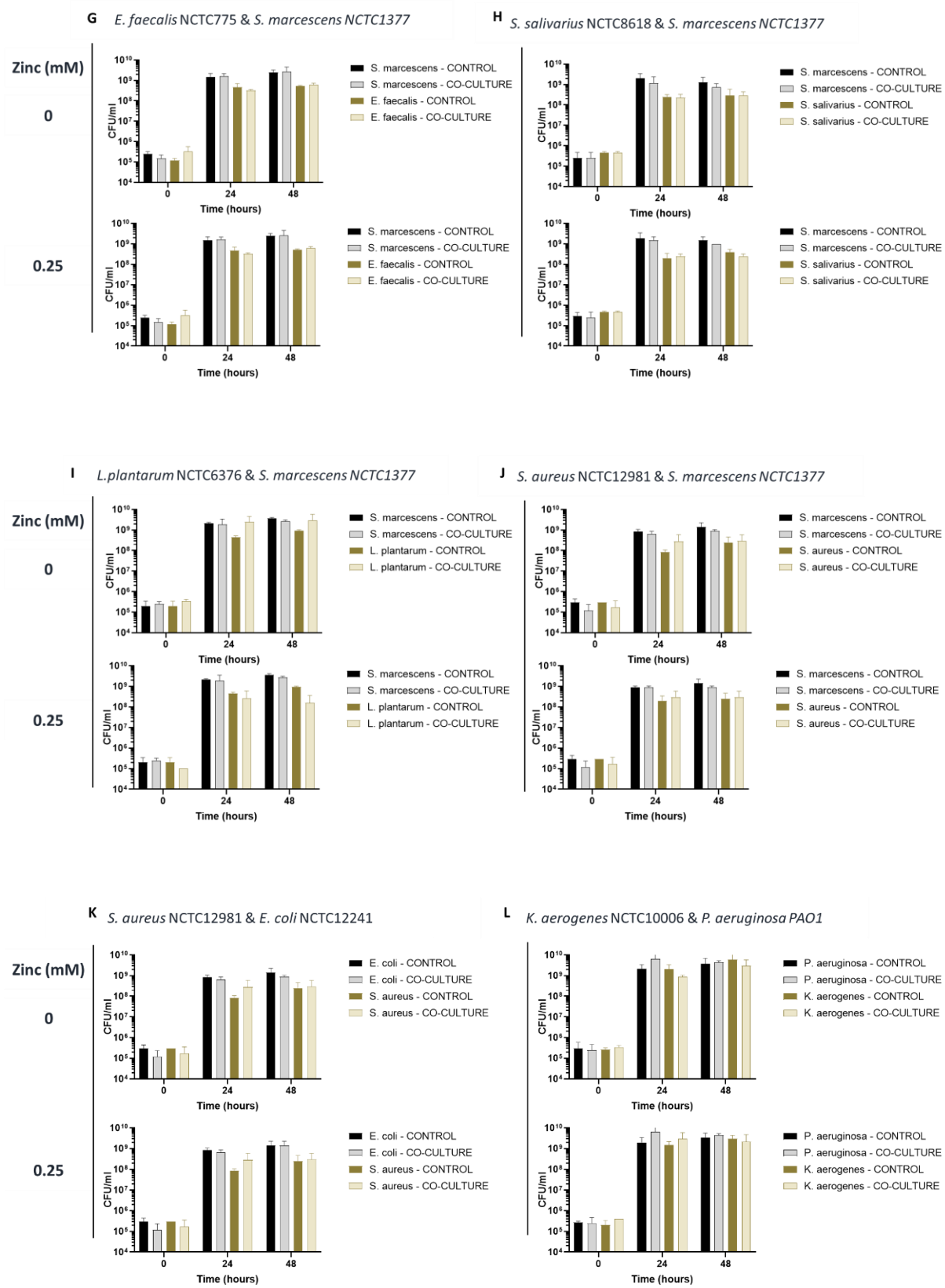
G E. faecalis NCTC775 & S. marcescens NCTC1377
H S. salivarius NCTC8618 & S. marcescens NCTC1377
I L.plantarum NCTC6376 & S. marcescens NCTC1377
J S. aureus NCTC12981 & S. marcescens NCTC1377
K S. aureus NCTC12981 & E. coli NCTC12241
L K. aerogenes NCTC10006 & P. aeruginosa PAO1
Zinc (mM)
0
0.25
CFU/ml
Time (hours)
S. marcescens - CONTROL
S. marcescens - CO-CULTURE
E. faecalis - CONTROL
E. faecalis - CO-CULTURE
S. salivarius - CONTROL
S. salivarius - CO-CULTURE
L. plantarum - CONTROL
L. plantarum - CO-CULTURE
S. aureus - CONTROL
S. aureus - CO-CULTURE
E. coli - CONTROL
E. coli - CO-CULTURE
P. aeruginosa - CONTROL
P. aeruginosa - CO-CULTURE
K. aerogenes - CONTROL
K. aerogenes - CO-CULTURE

M *E. faecalis* NCTC775 & *K. aerogenes NCTC1006*

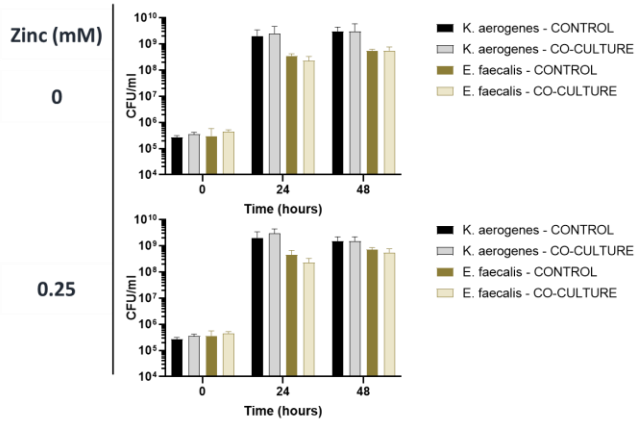

N *P. vulgaris* NCTC4175 & *K. aerogenes NCTC1006*

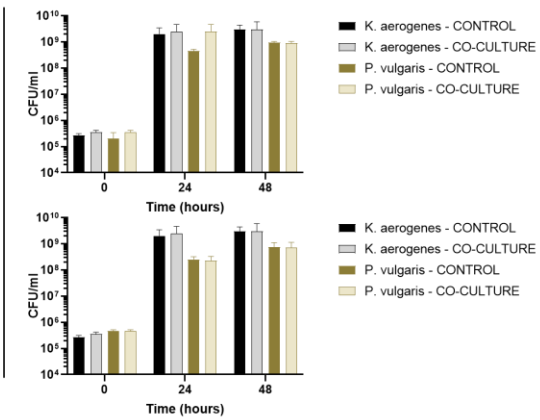

O *L. plantarum* NCTC6376 & *K. aerogenes NCTC1006*

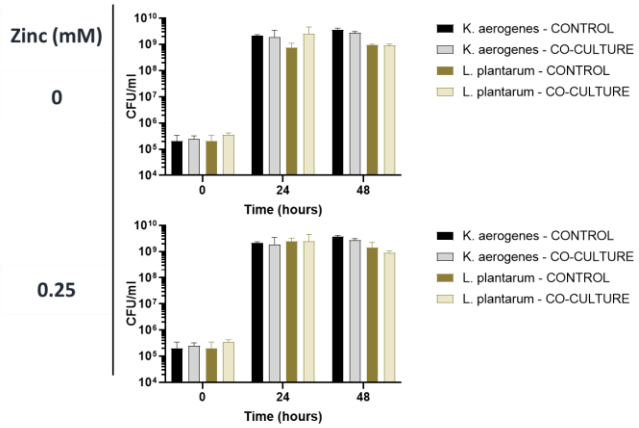

P *S. aureus* NCTC12981 & *K. aerogenes NCTC1006*

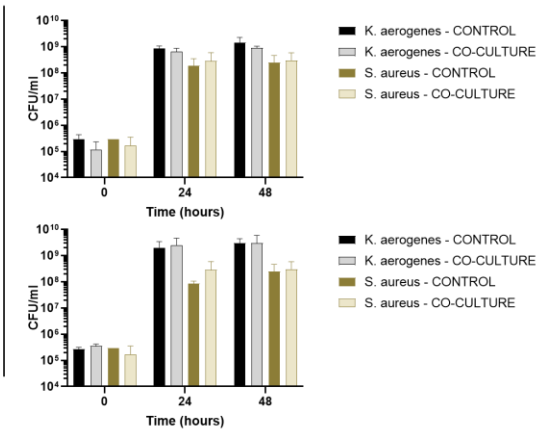

Q *E. faecalis* NCTC775 & *P. vulgaris* NCTC4175

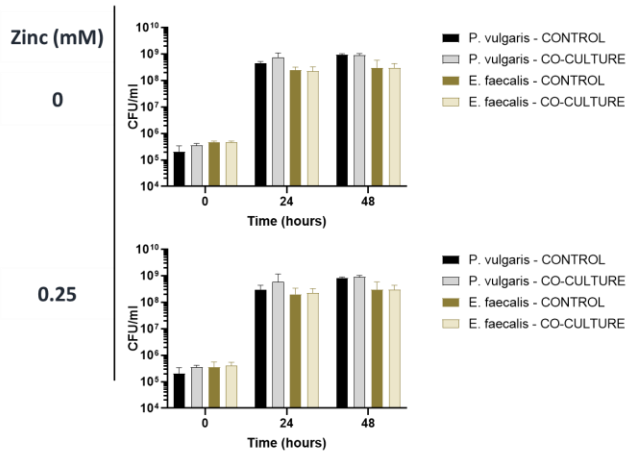

R *L. plantarum* NCTC6376 & *P. vulgaris* NCTC4175

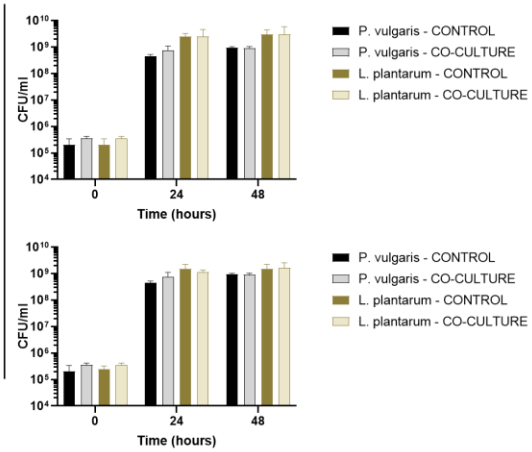

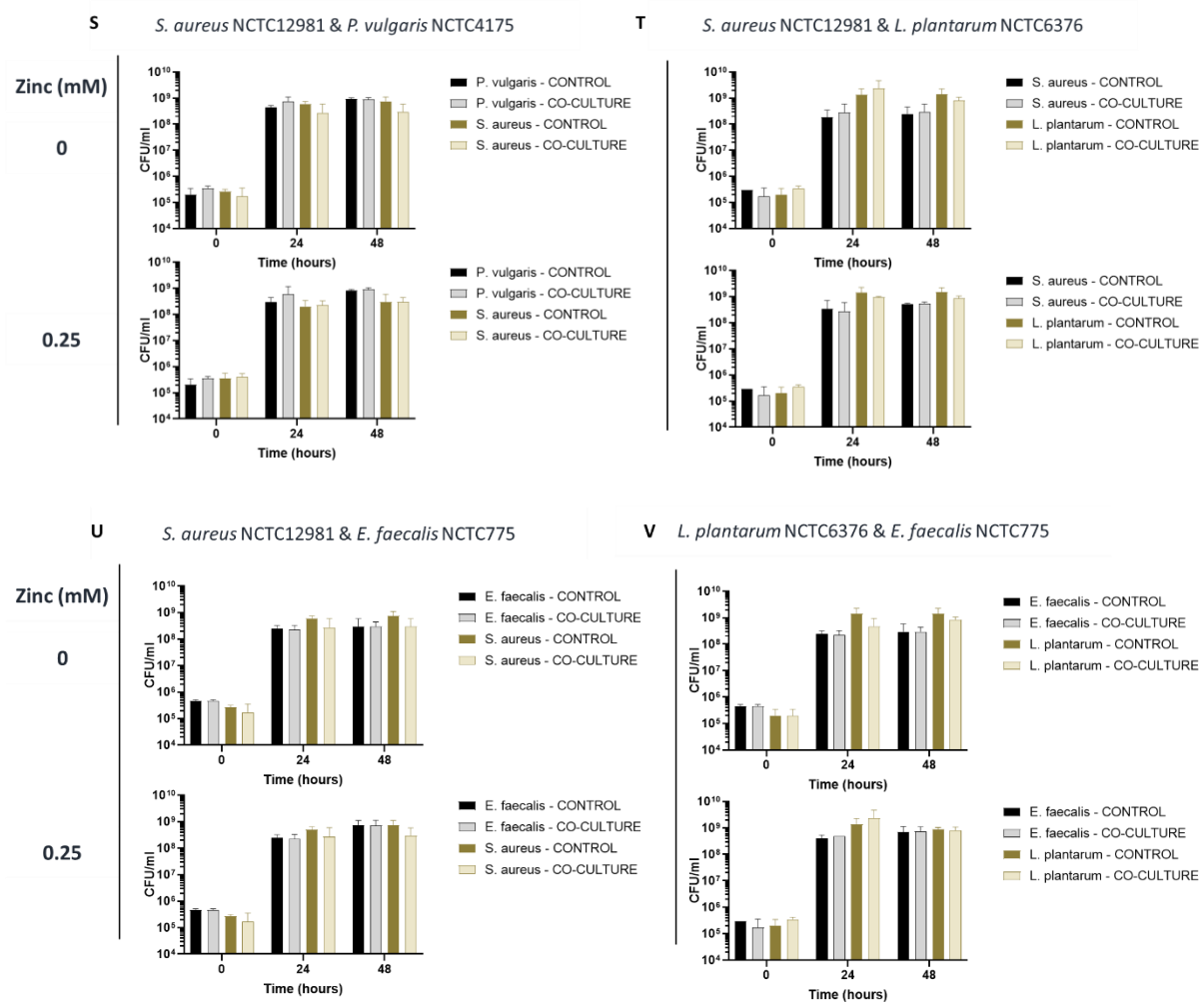

Appendix Figure 2: **Bacterial liquid co-cultures with or without Zn.** Bacterial liquid co-culture between **A**) *P. vulgaris* and *E. coli*; **B**) *E. coli* and *P. aeruginosa*; **C**) *E. faecalis* and *E. coli*; **D**) *K. aerogenes* and *E. coli*. **E**) *S. marcescens* and P. vulgaris; **F**) *K. aerogenes* and *S. marcescens*; **G**) *E. faecalis* and *S. marcescens*; **H**) *S. salivarius* and *S. marcescens*; **I**) *L. plantarum* and *S. marcescens*; **J**) *S. aureus* and *S. marcescens*; **K**) *S. aureus* and *E. coli*; **L**) *K. aerogenes* and *P. aeruginosa*; **M**) *E. faecalis* and *K. aerogenes*; **N**) *P. vulgaris* and *K. aerogenes*; **O**) *L. plantarum* and *K. aerogenes*; **P**) *S. aureus* and *K. aerogenes*; **Q**) *E. faecalis* and *P. vulgaris*; **R**) *L. plantarum* and *P. vulgaris*; **S**) *S. aureus* and *P. vulgaris*; **T**) *L. plantarum* and *S. aureus*; **U**) *E. faecalis* and *S. aureus*; **V**) *L. plantarum* and *E. faecalis*. Bacteria from independent exponential growing culture were co-cultured in LB with 0 (top) or 0.25 mM (bottom) $ZnCl_2$ and incubated at 37ºC, 200rpm. Sample for colony counting were collected at the time of inoculation (time 0), after 24 and 48 hours (X axis). Y axis indicates CFU/ml over time. Results and error bars indicate mean ± SD of three technical replicates. Graphs show representative data from three independent experiments. Data analysis was performed with a two-way analysis of variance (ANOVA) using Prism (GraphPad). P-values less than 0.05 were considered significant and indicated with asterisks.

III. Housekeeping genes and prodigiosin genes amplification

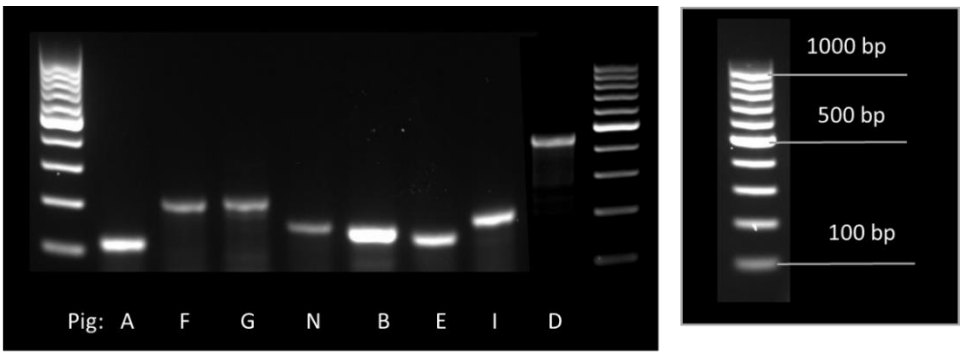

Gene name	PigA	PigF	PigG	PigN	PigB	PigE	PigI	PigD
Expected amplicon length	118	136	203	194	120	145	150	447

Appendix Figure 3: ***S. marcescens*** **prodigiosin genes amplicons obtained with standard PCR protol using primers built agains pordigiosin genes PigA – PigD.** 100 bp Gene Ruler and DNA Ladder were used. Name of the gene and expected length of the amplicon described in the figure.

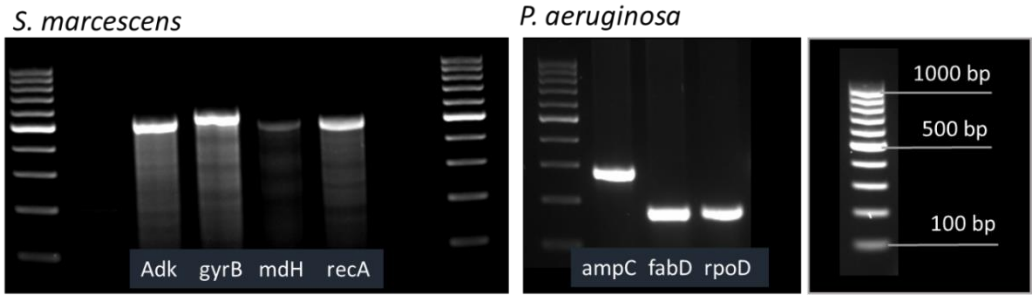

Gene name	Adk	gyB	mdH	RecA	ampC	fabD	rpoD
Exp amplicon length	118	136	203	194	120	145	150

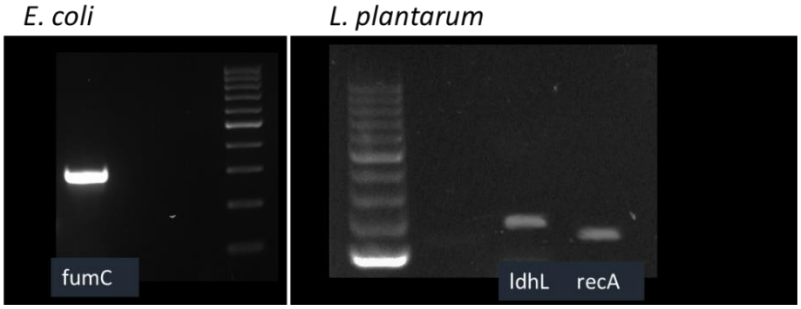

Gene name	274	ldhL	recA
Exp amplicon length	308	123	81

Appendix Figure 4: **Housekeeping genes amplicons obtained with standard PCR protol**. Target Housekeeping genes were the following: Adk, gyrB, mdH, recA for *S. marcescens*; ampC, fabD, rpoD for *P. aeruginosa*; fymC for *E. coli*; ldhL and recA *for L. plantarum*. 100 bp Gene Ruler and DNA Ladder were used. Name of the gene and expected length of the amplicon described in the figure.

IV. MetE 3D structure

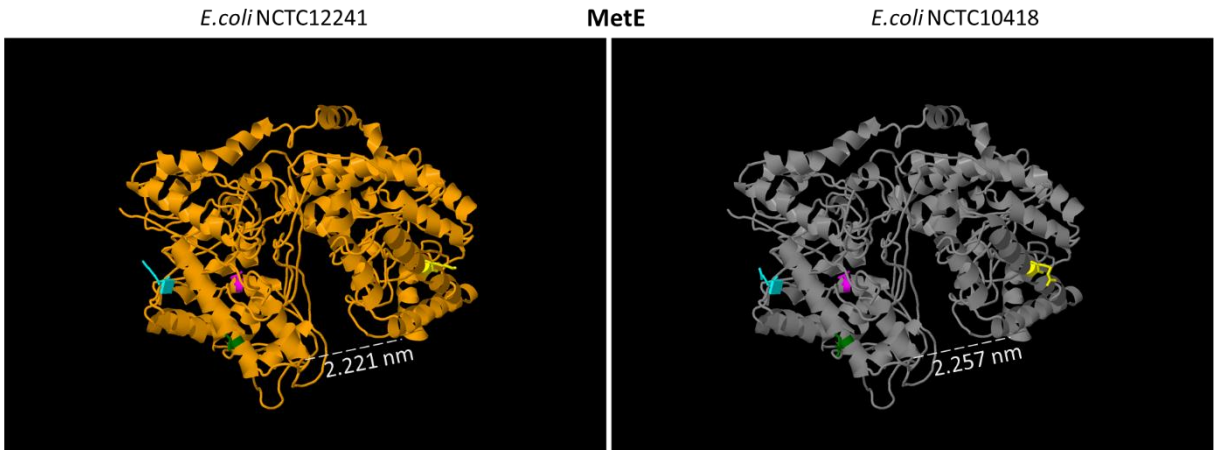

Appendix Figure 5: **Predicted 3D structure of MetE in *E. coli* NCTC12241 (left) and *E. coli* NCTC10418 (right).** The coloured chains in cyan and orange indicate the 2 homodimers. AAs that differ between MetR isolated from *E. coli* 12241, on the right, and from *E. coli* 10418 on the left, are highlighted in different colours, specifically: - for MetE *E. coli* NCTC12241: green for alanine, yellow for lysine (position 156), magenta for isoleucine and cyan for lysine (position 466) - for MetE *E. coli* NCTC10418: green for threonine, yellow for asparagine (position 156), magenta for valine and cyan for the arginine (position 466).

V. *E. coli* strains alignment

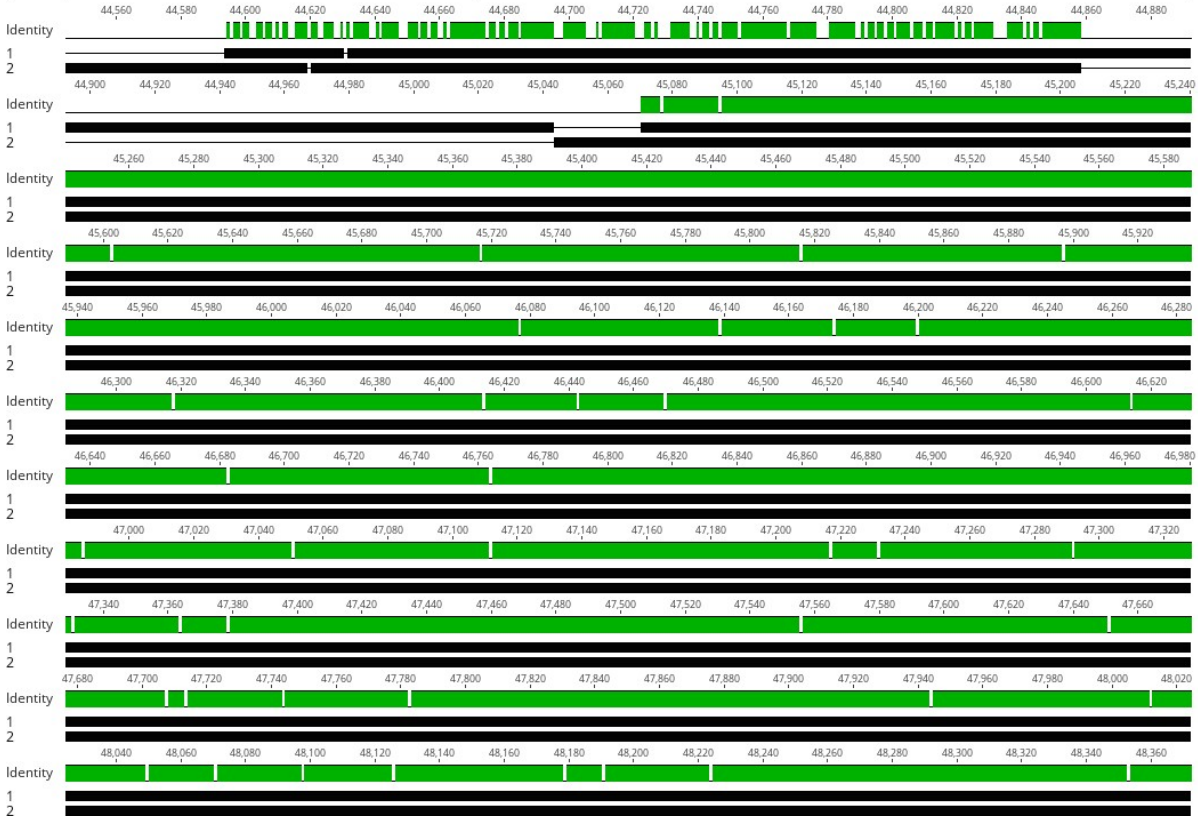

Appendix Figure 6: **Alignment of genomes of *E. coli NCTC12241* and *E. coli NCTC10418***. Sequences of *E. coli* NCTC12241 (1) and *E. coli* NCTC10418 (2) were downloaded from ATCC database and imported in Geneious Prime®2021.1.1. Comparative genome analyses of the two genomes were constructed through a Mauve alignment. Green sections indicate 100% , identity, while gaps indicate differences bases between the two genomes. The figure is a representation of a section (38,000 bases) of the full genomes.